



HAL
open science

Functional study of the MAGI1 scaffold protein and the Hippo pathway involvement in luminal breast and colorectal cancers

Diala Kantar

► **To cite this version:**

Diala Kantar. Functional study of the MAGI1 scaffold protein and the Hippo pathway involvement in luminal breast and colorectal cancers. Agricultural sciences. Université Montpellier, 2020. English. NNT : 2020MONTT050 . tel-03164571

HAL Id: tel-03164571

<https://theses.hal.science/tel-03164571>

Submitted on 10 Mar 2021

HAL is a multi-disciplinary open access archive for the deposit and dissemination of scientific research documents, whether they are published or not. The documents may come from teaching and research institutions in France or abroad, or from public or private research centers.

L'archive ouverte pluridisciplinaire **HAL**, est destinée au dépôt et à la diffusion de documents scientifiques de niveau recherche, publiés ou non, émanant des établissements d'enseignement et de recherche français ou étrangers, des laboratoires publics ou privés.

THÈSE POUR OBTENIR LE GRADE DE DOCTEUR DE L'UNIVERSITÉ DE MONTPELLIER

En Biologie Santé

École doctorale Sciences Chimiques et Biologiques pour la Santé - CBS2

Unité de recherche Institut de Recherche en Cancérologie de Montpellier (IRCM) - -INSERM U1194

Functional study of the MAGI1 scaffold protein and the Hippo pathway involvement in luminal breast and colorectal cancers

Présentée par Diala KANTAR

Le 27 Novembre 2020

Sous la direction de Alexandre DJIANE
et Lisa HERON-MILHAVET

Devant le jury composé de

Mme. Silvia FRE, DR, Institut Curie, Paris

Mme. Christine VARON, Pr, Bordeaux Research in translational oncology, Bordeaux

M. Jean-Paul BORG, PU/PH, Institut de recherche en cancérologie de Marseille, Marseille

M. Dominique HELMLINGER, CR, Centre de recherche en biologie cellulaire de Montpellier,
Montpellier

M. Alexandre DJIANE, CR, Institut de recherche en cancérologie de Montpellier, Montpellier

Mme. Lisa HERON-MILHAVET, CR, Institut de recherche en cancérologie de Montpellier, Montpellier

Rapporteure

Rapporteure

Examineur

Président/Examineur

Directeur

Co-Encadrante



UNIVERSITÉ
DE MONTPELLIER

Résumé

Au cours du développement, le comportement des cellules est étroitement régulé, ce qui assure un fonctionnement optimal des tissus épithéliaux sains. Les cellules épithéliales établissent ainsi des jonctions intercellulaires bien organisées, une polarité apico/basale, une architecture du cytosquelette et intègrent des entrées régulatrices et homéostatiques relayées par des voies de signalisation dédiées. Les altérations de ces processus sont le plus souvent associées au cancer.

Mon laboratoire s'intéresse au décryptage des mécanismes par lesquels les altérations de jonctions et de polarité sont capables d'induire une tumorigenèse. Les protéines d'échafaudage représentent des régulateurs importants de ces différents processus, et les altérations de plusieurs échafaudages épithéliaux clés ont été liées au cancer. Des travaux récents de l'équipe ont identifié Magi, un membre de la famille MAGUK, comme un régulateur des jonctions adhérentes à base d'E-Cadhérine pendant le développement de l'œil chez la drosophile. Le but principal de ma thèse était d'étudier la fonction de MAGI1, le membre le plus abondant de la famille MAGI dans les tissus humains, pendant le cancer, et plus spécifiquement ses rôles dans les cellules luminales A du cancer du sein. En utilisant principalement des approches de perte de fonction, nous avons pu identifier une fonction de suppression de tumeur de MAGI1 dans les cellules BCa luminales, aussi bien par des essais cellulaires *in vitro* que sur des souris nues xénogreffées. De plus, ces travaux ont révélé que MAGI1 inhibe un axe de signalisation AMOTL2/P38 qui est activé lors de la perte de MAGI1 et qui est ensuite responsable du phénotype de tumorigénicité accrue obtenu. Il est intéressant de noter que la perte de MAGI1 a induit une augmentation de l'activité de la myosine, des comportements de compression amplifiés et une tension élevée de la membrane plasmique associée, que nous proposons d'être l'un des activateurs de P38 en aval de la perte de MAGI1. Il est frappant de constater que, même si les cellules dépourvues de MAGI1 présentent une tumorigénicité élevée, l'activité de l'onco-protéine YAP est réduite dans les cellules du cancer du sein luminal dépourvues de MAGI1, ce qui suggère que la relation entre YAP et la tumorigenèse pourrait être plus complexe qu'on ne le pense généralement.

L'étude de la régulation de la voie d'Hippo est en effet un axe majeur de l'équipe. Un objectif secondaire de ma thèse était donc d'explorer l'implication de YAP/TAZ et de la voie Hippo lors de l'exposition à l'oxaliplatine dans les cellules cancéreuses du côlon. En tant que chimiothérapie de première ligne avec le 5 Fluorouracil, il est important de comprendre le mécanisme d'action de l'Oxaliplatine au-delà de son rôle majeur d'inducteur de cassures délétères des doubles brins d'ADN. Les cellules cancéreuses du côlon HCT116 traitées avec des doses relativement modestes d'oxaliplatine (à la IC50) ont présenté une translocation de YAP/TAZ vers le noyau accompagnée d'une augmentation de la transcription médiée par YAP/TAZ, comme en témoignent la RTqPCR et l'ARN-Seq. Cet effet a été couplé à une réorganisation du cytosquelette d'actine à l'intérieur de la cellule lors du traitement, et de nombreux gènes affectés par le traitement à l'oxaliplatine étaient des régulateurs d'actine (dont plusieurs qui sont également des cibles potentielles de YAP/TAZ). Cette étude implique YAP/TAZ dans la réponse HCT116 au traitement à l'oxaliplatine, et nous proposons qu'elle conduise à une réorganisation de l'actine.

Abstract

During development, the behaviour of cells is tightly regulated ensuring optimal functioning of healthy epithelial tissues. Epithelial cells thus establish well organized intercellular junctions, apico/basal polarity, cytoskeletal architecture, and integrate regulatory and homeostatic inputs relayed by dedicated signalling pathways. Alterations in these processes are most often associated with cancer.

My lab is interested in deciphering the mechanisms in which junctional and polarity alterations are able to induce tumorigenesis. Scaffold proteins represent important regulators of these different processes, and alterations to several key epithelial scaffolds have been linked to cancer. Recent work in the team identified Magi, a member of the MAGUK family, as a regulator of E-Cadherin-based Adherens Junctions during eye development in *Drosophila*. The main goal of my thesis was to study the function of MAGI1, the most abundant MAGI family member in human tissues, during cancer, and more specifically its roles in luminal A Breast Cancer cells. Using mainly loss-of-function approaches, we were able to identify a tumour suppressive function of MAGI1 in luminal BCa cells both in vitro cellular assays as well as in xenografted nude mice. Moreover, this work revealed that MAGI1 inhibits an AMOTL2/P38 signalling axis that is activated upon *MAGI1* loss and then responsible for the enhanced tumorigenicity phenotype obtained. Interestingly, the loss of MAGI1 induced increased myosin activity, increased compressive behaviours, and associated elevated plasma membrane tension, which we propose to be one of the activator of P38 downstream of MAGI1 loss. Strikingly, even though cells lacking MAGI1 showed increased tumorigenicity, the activity of the YAP onco-protein is lowered in MAGI1-deficient luminal breast cancer cells, suggesting that the relationship between YAP and tumorigenesis could be more complex than commonly assumed.

The study of Hippo pathway regulations is indeed a major axis of the team. A secondary objective of my thesis was thus to explore the involvement of YAP/TAZ and of the Hippo pathway during Oxaliplatin exposure in colon cancer cells. As first line chemotherapy along with 5 Fluorouracil, it is important to understand the mechanism of action of Oxaliplatin beyond its major role as inducer of deleterious DNA double strand breaks. HCT116 colon cancer cells treated with relatively modest doses of Oxaliplatin (at IC50), featured a translocation of YAP/TAZ to the nucleus accompanied with increased YAP/TAZ-mediated transcription, as judged by qPCR and RNA-Seq. This effect was coupled with a re-organization of the actin cytoskeleton inside the cell upon the treatment, and many genes affected by oxaliplatin treatment were actin regulators (including several that are also potential YAP/TAZ targets). This study involves YAP/TAZ in HCT116 response to Oxaliplatin treatment, and we propose that it leads to actin re-organization.

Acknowledgements

First of all, I would like to thank all my jury members for accepting to evaluate my work and for being part of my jury. Dr. **Silvia FRE**, Dr. **Christine VARON**, Dr. **Jean-Paul BORG** et Dr. **Dominique HELMLINGER**, thank you all, without you I sure can not accomplish this journey till its end. I hope that you could all be present in person the day of my defence.

I would also like to thank the member of my thesis comity, Dr. **Dominique HELMLINGER** and Dr. **Jean-Philippe HUGNOT**, you followed me for four years and helped me stay on the right track and progress during this journey.

Without you, I would never be there in the first place. Thank you **Alexandre DJIANE** for giving me the opportunity to be part of your team in 2016. I still remember the day of our meeting, when I still were in Master 2, I came to you asking for an internship and since then I am still here in this wonderful team. You were there in my ups and downs, always excited by new results and sure always being the optimistic person which was good because it kept me motivated and always moving forward. It is a pleasure working with you, it made me realize that actually, you are not just a boss but you are a leader. I will always be so gratefull.

Thank you **Lisa HERON-MILHAVET** for everything you did. When I needed to talk and when I was frustrated and so angry about weird experiments or results you were always there to calm me down. We had always interesting conversations, scientific and non-scientific too. And I will never forget you being here for me during my manuscript writing and always coming by my office and telling “Allée c’est la fin, c’est bon c’est fini!” thank you for your constant encouragements.

When I started you were not there, but it is as if I worked with you for a long time now. **Charles GEMINARD** and **Patrice LASSUS** I can never thank you enough, it is really so fun and awesome working with you two. Sorry, for the many questions, I asked you while you were working; you always knew what to tell me to not feel down anymore and to cheer me up. We had some many interesting conversations. I wish you all the best. Patrice thank you for all the times that I came by you asking you for advices. Charles you gave me a lot, a lot of stuff I learnt from you.

A big thank you for all the IRCM, the ones that I did not know and the ones I knew in the past and the present: **Toufic, Nour, Amanda, Rana, Mona, Emile, Rasha, Joelle, Benoit, Laetitia, Nabiya, Adrien, Gabriel, Celestine, Tristan, Valomanda, Hadjer, Alice, Diane, Habib, Valentin Antoine, Madi, Melanie, Mehdi, Ambre, Ander, Bilguun, Guillaume, Diane, Augusto, Isidora ...** I hope I did not forget anyone. A lot of you helped me integrate while I did not know anyone. Thank you all you made my journey special in this institut.

A special thanks for the gestion crew that I have been in touch with for several occasions. **Daniela, Nadia, Nadège**, thank you so much for your help.

MY team, **Brice, Cynthia, Benoit, Romain and Jean Daniel** you were my second team, I was always in your office. Thank you for all the good moment together the apéro and le tournoi de pétanque.

During these four years in the team, I witnessed the arrival and the departure of several people.

Elodie FOREST and **Remi LOGEAY**, when I arrived in the lab you were in your last years of PhD. When I saw you you two defending even though I was in my first year I felt like it was my own defence. It was cool working with you and I hope that you achieve all your goals in life.

Yeza, Yasser, Leslie, Katrin you were the best interns! It is always good to make good unexpected friends. We had our moments, our craziness together with the rest of the office. It was fun. I love you guys.

Florence FRAYSSINOX, it was a pleasure meeting you. Even though you left I will never forget our conversations in the lab whilst doing experiments and for sure our small talks outside the lab too. Merci d'avoir passé me voir de temps en temps dans mon bureau même après ton départ. Je ne t'oublierai pas c'est sur.

Sara BERNARDO, you were my best pal we were together since the Master 2. I am so grateful that I knew you, you are so sweet and you are on the right track. One day you will become the best researcher. I always enjoyed our scientific discussion together, they were the best. Good luck for the rest.

Toufic KASSOUF (aka toto), we miss you in here in the IRCM and in Montpellier. You are a wonderful person; I hope you become one of the best researcher. Thank you for helping me a little with the writing and finally “La2e7looooooooooooo” :D.

The people in my corridor (N1F3), **Charlotte GRIMAUD, Eric JULIEN, Alain THIERRY Corinne PREVOSTEL** thank you for your hello and good morning every day and for the small talks that we had.

My second floor friend, in cell culture and in the corridors. We had many conversations of hours it was nice having you in my life, you are so sweet and I love talking to you. **Catherine TEYSSIER**, once I am gone I will miss you.

The office people, it will be so difficult to express all what I want to say. The best people ever “Le bureau des étudiants” **Yannick, Julie and Miriam**. Guys I love you so much. **Yannick** you are the oldest among them, you were the weirdo who does not like to talk to people. Who knew that one day we can become best friends! You are the sweetest guy, I hope you get what you want in life and be happy. You deserve all best and I am sure that one day you will get your own (YP) because I know that you are capable of it! It is true that when you are stress you stress everyone with you, but we love you pd don't worry :D. **Julie “juju”**, I have never met such a sweet and sensitive girl. You help people when they need you without hesitations. Live your life to the fullest my dear, go and do whatever you want and do not let anything control what you want in life. You deserve everything good :*. **Miriamita “djudju”**, my office pal, my motivation each time I was down. I love you so much. You speak really well French stop staying no but it is cute, hahaha. Love our conversations together, all of them. I will miss when are we going to play badminton and do you want to buy bonbons and let's eat burger king and especially at what time we eat guys I am starving. **Maelys**, you just arrived but we consider you one of us. You knew directly your way inside our group, the cantine is good !! **Fatima**, I hope that you stay more with us because you became one of us too. I am so happy for having the chance to know you before the end of my PhD. Guys I love you so much and I hope that we will always stay in touch even if life and distances will separate us.

Outside the institute the Montpellier gang, hospital la colombière. Hardly I made my way through the group. You all achieved your goal in here and I guess from the old us I am the last one between you guys. **Dr. Joelle OBEID** we miss you here with us in France, **Dr. Jowelle NASSAR**, I love you girl even if I do not hang out a lot with you, you personality is awesome. **Dr. Husein GHAZALE**, it was pleasure knowing you and **Dr. William BAKHACHE**, you are one of the sweetest people I know and we used to have one of the best scientific discussions, it was cool. Hope

you all achieve your goals and you all deserve the best. **Jihad, Jamal** you are next, you are there you can do it. Jihad I will miss you passing by my office.

Rita and Zahra, you know that I will never know what to tell you. You guys are my sisters, I love you so much. You have been there for me for each and single moment in these 4 years. You were right across the corridor, I will miss going to your office when I want to see you and I will miss you being most of the time in my office. In the IRCM and outside the IRCM we were at some point inseparable. Zahra I will never forget the first day I met you when you were shocked it was the best! I really don't know what to say I will never forget you and I hope we stay in touch even after the end. I love you.

Ayman I am grateful to have known you. **Ziad** you were my youngest cousin that It was impossible to be friend with but when you came to Montpellier. Never assume things without proof, love you cousin I am so grateful that you came here. **Sansoun**, no word can describe how much I love you. You are so cute, fun, and caring. Stay like that do not change.

My lovely husband, Imad. It was hard for us all these years apart. You being here was the best part of this special year. Even though you don't show it but you were there each time I needed someone. During my ups and downs you were there. I love you so much and thank you for being here. Abasniiii habibi!!

My family in France, papa tu es le meilleur je t'aime beaucoup si ce n'est pour toi je serai jamais arrivée en France. Je n'oublierai jamais tes blagues de mouches . Allah ykhalili yek baba !! **Rouba**, j'espère que tu sais que je t'aime trop même si je te ne le dis pas trop. Pour tous les moments quand tu étais là pour moi quand j'avais besoin de toi Merci. **Jado et Dany**, mes frères, je vous aime trop. Vous étiez tous là quand j'avais besoin de soutiens.

My family in Lebanon, fatoun hebek ktir allah ykhalili yeki. **Manmoun** allah ykhalilna yeki ya rab bhebek ktir. Mes deux tantes les meilleures du monde! Je vous aime trop. Mes oncles tous sans exception **Ibrahim, Mhamad, abdlhamid, ahmad** je vous aime. Merci pour votre soutien durant toutes ces années.

Et finalement une speciale dédicace de cette thèse pour ma grand-mère, tu croyais toujours en moi et voilà le jour J arrive. J'espérais que tu sois là, tu me manques beaucoup !

Table of contents

Résumé	2
Abstract	3
Acknowledgements	4
List of abbreviations	10
List of Figures	16
List of Tables	18
Introduction	19
1. Epithelial tissues	19
1.1. Generalities on different types of epithelia.....	19
1.2. Examples.....	20
a. Breast tissue:	20
b. Colon tissue:	21
2. Epithelial cells:	22
2.1. Polarity :.....	22
a. Apical identity:	23
b. Basolateral identity:	25
2.2. Cellular Junctions:	27
a. Tight Junctions:.....	28
i) The Claudin family:	30
ii) The TAMPS: Occludins, Tricellulin and MarvelD3	32
iii) The JAMs family:	35
iv) Other families of proteins:	36
v) Protein associated with TJs:	36
• Members of the PDZ domain containing protein.....	36
• Members of the non PDZ containing proteins of the TJ plaque	38
b. Adherens junctions:	39
i) The core complex of the AJs.....	40
ii) The phospho-regulation of the cadherin-catenin complex association and levels	45
iii) Nectin/Afadin complex	45
c. Interplay between AJs and TJs and assembly of apical junctions:	46
2.3. Maintenance of cellular architecture (actin cytoskeleton):	47
a. Dynamic of the actin cytoskeleton:.....	49

b. Regulation and associated proteins:	50
i. Profilin:	51
ii. Nucleation proteins:	51
iii. Capping proteins (Cp):.....	52
iv. Severing proteins: Cofilin/ADF	53
3. Implication of junctions in signaling :	54
3.1. WNT/ β -catenin pathway:.....	54
3.2. MAP kinase pathways:	56
a. The ERK1/2 pathway:	57
b. The JNK pathway:	59
c. The p38 pathway:.....	60
3.3. The HIPPO pathway:	64
4. Cancers :	69
4.1. Carcinoma and epithelial polarity.....	70
4.2. Carcinoma and Junction regulation	71
4.3. Breast cancers:	74
4.4. Colon Cancers:.....	77
5. The MAGI scaffolds :	79
5.1. Structure and localization :	79
5.2. Function:	80
5.3. Role of MAGIs in non-mammalian species.....	82
5.4. Magi and cancer:.....	83
Thesis objectives	86
Results	88
1. Characterization of MAGI1 tumor suppressor effect in luminal A BCa.....	88
a) Work summary	88
b) Article	89
2. The implication of ECM stiffness in MAGI1 regulation of the Hippo pathway and the p38/AMOTL2 stress axis.	131
3. Characterization of the mechanism of action of the Oxaliplatin treatment in colorectal cancer cells (CCR).....	135
a) Oxaliplatin activates YAP/TAZ activity in HCT116:	135
b) Characterization of the mechanism of action of Oxaliplatin on Hippo pathway and TAZ: ...	137
c) Wider look at the effect of Oxaliplatin in HCT116:	138

Materials and Methods	142
Discussion and perspectives	150
REFERENCES	162
Other contributions	183

List of abbreviations

A

A/B: Apico/Basal
Abl: Abelson kinase
ABPs: Actin binding proteins
Ad9: Adenovirus type 9
ADF: Actin depolymerizing factor
ADP: Adenosine di-phosphate
AJs: Adherens junctions
AF-6: Afadin
AFM: Atomic force microscopy
AKT: Protein kinase B
ALL-1: Acute lymphoblastic leukemia 1
AMOT: Angiomotin
AMOTL1 - 2: Angiomotin protein like 1-2
AP1: Activator protein 1
APC: Adenomatous polyposis coli
aPKC: Atypical protein kinase C
ARC: Activity regulated cytoskeleton associated protein
AREG: Amphiregulin
ARHGAP29: Rho GTPases activating protein 29
ARM: Armadillo
ARP 2/3: Actin related protein 2/3
ASSP: Ankyrin repeat SH3 domain and proline rich region containing protein
ATF2: Cyclic AMP-dependent transcription factor
ATF6: Activating transcription factor 6
ATM: Ataxia telangiectasia mutated
ATP: Adenosine tri-phosphate

ATR: Ataxia telangiectasia and RAD3 related

AXL: AXL Receptor tyrosine kinase

B

BAI: Brain specific angiogenesis inhibitor
Baz: Bazooka
BC: Breast cancer
BCL9-2: B cell/ Lymphoma 9-2
bHLH: Basic helix loop helix
BIRC2: Baculoviral IAP repeat containing 2
BMP: Bone morphogenetic protein
BRCA: Breast Cancer gene
BSA: Bovine serum albumin
bZIP: Basic leucine zipper
B-TRCP: β transducing repeat containing protein

C

C. elegans : *Caenorabditis elegans*
CACO2: Adenocarcinoma of the Colon 2
CAR: Coxsackie virus and adenovirus receptor
CASK: Calcium/calmodulin dependent Serine protein kinase
CBD: Catenin binding domain
CCC: Cadherin catenin complex
CDC42: Cell division cycle 42
CDH1: Cadherin 1
CDK: Cyclin dependent kinase
CHEK: Check point kinase
ChIP: Chromatin immunoprecipitation
CK1-2: Casein kinase 1-2

CLDN: Claudin
CLMP: Coxsackie and adenovirus receptor-like membrane protein
Cobl: Cordon bleu
COXIB: Celecoxib
COXII: Cyclooxygenase II
Co-IP: co-Immunoprecipitate
Cp: Capping Proteins
CRB: Crumb
CRC: Colorectal cancer
CREB: Cyclic adenosine monophosphate responsive element binding protein
CRFR: Corticotropin releasing factor receptor
CRIB: CDC42 and Rac interactive binding
c-Src: Proto oncogene tyrosine kinase Src
CTGF: Connective tissue growthFactor
Ctrl: Control
c-Yes: Tyrosine protein kinase Yes
CYR61: Cysteine-rich, anigogenic inducer 61

D

DDR: DNA damage response
DIDO1: Death inducer obliterator 1
DKK: Dickkopf
DLG: Discs large
DLL: Delta like ligand
DMEM: Dulbecco's modified eagle medium
DMSO: Dimethyl sulfoxide
DNA: Deoxyribonucleic acid
Dsh: Dishevelled
DTT: Dithiothreitol

DUSP/MKP: Dual specificity phosphatase/MAPK phosphatase

E

EC: Extracellular cadherin
E-cadh: E-cadherin
ECM: Extracellular matrix
EDTA: Ethylenediaminetetraacetic acid
EGFR: Epidermal growth factor receptor
eIF-4E: Eukaryotic initiation factor 4E
EMT: Epithelial to mesenchymal transition
Ena/Vasp: Enabled/vasodilator-stimulated phosphoprotein
eNOS: Endothelial nitric acid synthase
Eph: Erythropoetine producing human hepatocellular receptor
EphA2: Ephrin type A receptor 2
ER: Endoplasmic reticulum
ER: Estrogen
ERE: Estrogen response element
ERK: Extracellular regulated kinase
ESAM: Endothelial cell-selective adhesion molecule
ESR: Estrogen receptor
Ex: Expanded

F

FA: Focal adhesion
F-actin: Filamentous actin
FAK: Focal adhesion kinase
FAP: Familial adenomatous polyposis
FBS: Fetal Bovine Serum
FERM domain: 4.1, Ezrin, Radixin, Moesin domain

FGFR: Fibroblast growth factor receptor

FH1-2: Formin Homology 1-2

FOSL2: Fos like 2

FOXO: Forkhead box O

Fz: Frizzled

G

G-actin: Globular actin

GAP: Guanosine triphosphate activating protein

GC: Gastric cancer

GLI: Glioma associated oncogene

GLT: Glutamate transporter

GPCR: G protein coupled receptor

GSEA: *Gene set enrichment analysis*

GSK3 β : Glycogen synthase beta

GTP: Guanine triphosphate

H

HBP1: HMG box transcription factor

HCC: Hepatocellular carcinoma

HCT116: Human colon cancer cells

HER2: Human epidermal growth factor receptor 2

HES1: Hairy and Enhancer off split 1

HH: Hedgehog

Hpo: Hippo

HPV: human papillomaviruses

I

IBD: Inflammatory bowel disease

IC50: Inhibitory median concentration

Ig: Immunoglobulin

IHC: Immunohistochemistry

IL-1: Interleukin 1

INF α : Interferon alpha

IQGAP: Ras GTPase-activating-like protein

J

JACOP: Junction associated coiled-coiled protein

JAG: Jagged

JAM: Junction adhesion molecule

JEAP: Junctional enriched and associated protein

JIP1-4: JNK interacting protein 1-4

JMD: Juxtamembrane domain

JNK: Jun N terminal kinase

K

K⁺: Potassium +

KD: Knock down

KIF7: Kinesin family protein 7

KO: Knock out

KPa: Kilo pascale

KSR: Kinase suppressor of RAS

L

LAP: LRR and PDZ

LATS: Large tumor suppressor kinase

LGL: Lethal giant larvae

LIMD1: LIM domain containing 1

LKB1: Live kinase B1

Lmod: Leiomodinn

LRP5/6: LDL Receptor related Protein 5/6

LRR: Leucine reach repeats

LSR: Lipolysis stimulated lipoprotein receptor

M

MAGI1: Membrane associated guanylate kinase with inverted structure 1

MAGUK: Membrane associated guanylate kinase
 MAL: Myelin and lymphocyte-associated protein
 MAPK: Mitogen activated protein kinase
 MAPKK: MAP kinase kinase
 MAPKKK: MAP kinase kinase kinase
 MCF7: Michigan cancer foundation-7 cells
 MDCK cells: Madin-darby canine kidney cells
 mm: Millimeter
 Mer: Merlin
 MET: Mesenchymal to Epithelial transition
 Mg²⁺: Magnesium 2+
 µg: Micrograms
 MINK1: Misshapen like kinase 1
 µM: Micro molar
 ml: Milliliter
 MLC: Myosin light chain
 MLCK: Myosin light chain kinase
 MNK: MAP kinase interacting serine/threonine kinase 1
 MOB: Monopolar spindle one binder proteins
 MOC: Microtubule organizing center
 MOS: Proto-oncogene serine/threonine-protein kinase mos
 MP1: MEK1 scaffolding protein
 MPED: Membrane proximal extracellular domain
 mRNA: Messenger ribonucleic acid
 MSI: Microsatellite instability
 MSK: Mitogen and stress activated kinase
 MST: Mammalian sterile 20 like kinase
 MTT: 3-(4, 5-dimethylthiazol-2-yl)-2, 5-diphenyltetrazolium bromide

MUPP1: Multi PDZ-domain Protein 1
N
 NFκB: Nuclear factor Kappa B
 NF2: Neurofibromatosis 2
 NFE2L1: Endoplasmic reticulum membrane sensor
 NGF: Nerve growth factor
 nm: Nanometer
 NPF: Nucleation promoting factor

O
 OD: Optical density
 OSM: Osmosensing scaffold

P
 P56lck: Lymphocyte specific tyrosine
 P90SK: P90 ribosomal S6 kinase
 PALS: Proteins Associated with Lin Seven
 PAR: Partitioning defective
 PARP: poly (ADP-ribose) polymerase
 PAR3-6: Partitioning defective homolog 3-6
 Pard : Drosophila partitioning defective
 PATJ: PALS-1 associated to tight junctions
 PCP: Planar cell polarity
 PDZ: PSD-95, Discs large and ZO-1
 PDZ-GEF2: Guanine exchange factor 2
 PEST: Proline, glutamate, serine, threonine
 PFA: Paraformaldehyde
 PI3K: Phosphatidylinositol-3 kinase
 PiP2: Phosphatidylinositol diphosphate
 PiP3: Phosphatidylinositol triphosphate
 PKA: Protein kinase A
 PKC: Protein kinase C

POSH: Plenty Of SH3

PP1: Protein phosphatase 1

PP2A: Protein phosphatase 2A

PR: Progesterone

PTEN: Phosphatase and tensin homolog

Q

qPCR: Quantitative polymerase chain reaction

R

Rac1: Ras-related C3 botulinum toxin substrate 1

Raf-1: Rapidly accelerated fibrosarcoma 1

RAPGEF6: Rap guanine nucleotide exchange factor 6

RAS: Reticular activating system

RASSF8: Ras associated domain family member 8

RB: Retinoblastoma

RET: Rearranged during transfection receptor

RhoA: Ras Homolog family member A

RNAi: Ribonucleotide acid interference

RNAseq: RNA sequencing

RNF146: Ring finger protein 146

ROCK1: Rho associated protein kinase 1

ROS: Reactive oxygen species

RUNT: Ribonuclease T

S

S/T: Serine/threonine

SAPK: Stress activated protein kinase

SAV: Salvador

SCF: Skp, Cullin, F-box

Scrib: Scribble

Sdt: Stardust

SFRP: Soluble frizzled related protein

shluc: Small hairpin RNA luciferase

shMAGI: Small hairpin RNA MAGI

siRNA: Small interfering RNA

SMAD: Small - mother against decapentaplegic

SMO: Smoothed

SNAI2: Snail 2

Sp1: Specificity protein 1

SRB: Sulforhodamin B

SRE: Serum response element dependent genes

STAT: Signal transducer and activator of transcription

SUFU: Suppressor of fused homolog

SYK: Spleen tyrosine kinase

Syx: Synectin-binding guanine exchange factor

T

TAMPS: Tight junctions associated marvel domain containing Proteins

TAO: Thousand and one amino acid protein kinase

TAZ: Transcriptional co activator with PDZ

TCA: Trichloroacid

TCF/Lef: T cell factor/ Lymphoid Enhancer binding protein

TDLU: Terminal ductal lobular unit

TEAD: Transcription enhanced associate domain

TEER: Transepithelial electric resistance

TFs: Transcription factor

TGF β : Transforming growth factor beta

TJs: Tight junctions

TNBC: Triple negative breast cancer

TNF α : Tumor necrosis factor alpha

TNKS1/2: Tankyrase1/2

TPL2: Tumor progression locus 2

TRIP6: Thyroid hormone receptor interactor 6

tTJs: Tricellular tight junctions

U

UV: Ultra violet

V

VAMP: Vesicle associated membrane protein

VAP-33: VAMP associated protein of 33 kDa

VGLL4: Vestigial like family member 4

W

WASP: Wiskott-Aldrich syndrome protein

WD40: Tryptophan-aspartate 40 amino acid repeats

WHO: World health organization

WIF: WNT inhibitor factor

WIP1: Wild Type p53 induced phosphatase 1

WNK1&4: With No lysin (K) 1 & 4

WNT: Wingless and integrated

Wts : Warts

X

XBP1: X-box binding protein

Y

Y: Tyrosine

YAP: Yes associated protein

Z

ZAK: ZO-associated kinase

ZAP70: ζ-chain associated protein kinase of 70 kDa

ZO-1/3: Zonula occludens 1/3

Zonab: ZO-1 associated Y-box factor

#

5-FU: 5 Fluorouracil

List of Figures

Figure 1: Different epithelial tissues, locations and functions.	19
Figure 2: Anatomy of the female Breast.....	20
Figure 3: A) The colon anatomy and B) histology.	21
Figure 4: Apico-basal polarity complexes in epithelial cells.	23
Figure 5: Interplay between the different polarity complexes in the cell.	27
Figure 6: Cellular junctions.	28
Figure 7: The structure of the TJs.	29
Figure 8: Different types of TJs.	30
Figure 9: Structure of the different transmembrane proteins constituting the TJs.	30
Figure 10: Summary of interactions between Occludin and TJs associated proteins.	34
Figure 11: The different PDZ containing domain proteins associated with the TJs.	38
Figure 12: Molecular architecture of adherens junctions.	40
Figure 13: β -catenin structure and binding partners.	43
Figure 14: Sequential formation and assembly of the AJs and the TJs.	46
<i>Figure 15: Cytoskeleton organization in cells.</i>	<i>47</i>
Figure 16: Schematic representation of a cell with different architecture.	49
Figure 17: Steps for F-actin formation: Nucleation, Elongation and steady state phase.	49
Figure 18: Summary of the different classes of actin nucleators and their mechanisms of action. ...	52
Figure 19: A non-exhaustive list of the different bundlers and crosslinkers of actin.	53
Figure 20: an overview of the WNT/Beta-catenin signaling pathway.	55
Figure 21: The MAPK signaling cascades.	58
Figure 22: p38 MAPK activation.	61
<i>Figure 23: Substrates and function of the p38α/β MAPKs.</i>	<i>62</i>
Figure 24: Simplified Hippo signaling pathway in Drosophila (Left) and mammals (Right).	64
Figure 25: Summary model for regulation of YAP by LIMD1.	67

Figure 26: Summary of non-exhaustive mechanisms able to regulate the Hippo pathway and/or the YAP/TAZ activity.....	69
Figure 27: Breast cancer in details. Origin, different classifications.....	75
Figure 28: CRCs progression in two different models.	78
Figure 29: The MAGI family members.....	79
Figure 30: Representation of MAGI1 protein and the associated interactors.	81
Figure 31: Schematic representation the effect of ECM stiffness on YAP/TAZ nuclear localization independently from the Hippo pathway components.	131
Figure 32: Effect of shRNA MAGI1 on MCF7 cells cultivated on soft matrix (0.5 KPa).....	132
Figure 33: Analysis of the effect of siRNA AMOTL2.....	133
Figure 34: Analysis of HCT116 cells after Oxaliplatin treatment.	136
Figure 35: Immunofluorescence of HCT116 cells after 48h of Oxaliplatin treatment.	138
Figure 36: Jvenn diagram showing the intersection between the upregulated genes obtained by RNAseq at different time point in Oxaliplatin treated HCT116 cells and the chIPsep list of gene of TEAD4 taken from Liu et al, 2016.	139
Figure 37: E-cadherin and contact inhibition.....	151
Figure 38: representation explaining the hypothesis supporting AMOTL2 accumulation in MCF7 cells upon MAGI1 removal.....	153
Figure 39: Scheme of RhoA signaling.....	156
Figure 40: Role of p38 α in tumorigenesis based on mouse modes.	158

List of Tables

Table 1: Knockout Mice models.....	31
Table 2: Summary of diseases and syndrome in which the canonical WNT pathway component are implicated.	56
Table 3: Frequency of mutations in the components of the ERK1/2 pathway across different tumors.....	59
Table 4: List of polarity genes disrupted in cancer.	70
Table 5: Diversity of adhesion genes are implicated in cancer.	72
Table 6: List of antibodies used for western blots analysis.	147
Table 7: List of antibodies used for Immunofluorescence analysis.....	147
Table 8: List of primers used for qPCR analysis	148
Table 9: Gene family analysis of the 200 genes of YAP/TAZ targets observed at the different Oxaliplatin treatment time points.	140

1. Epithelial tissues

In multicellular organisms, different types of cells enter in contact and communicate to create the different tissues and organs. In humans there are over 200 different cell types achieving a wide variety of functions, but one of the most ubiquitous cell architecture is that of epithelial cells, found as the basic building block of most internal organs. Through their adhesion, these cells will form cohesive sheets, epithelia, lining the interior of hollow organs or covering the surface of other tissues. They serve as barrier between the exterior and interior of the organism, and are the body first line protection. Epithelia serve as guardians of the body regulating the permeability and allowing limited passage of material over the physical boundaries made by them (OpenStax, 2013a). Changes in the integrity or the shape of these epithelia could disturb the organ function and lead to different diseases.

1.1. Generalities on different types of epithelia

Epithelial tissues are divided in different categories depending on shape and number of cells layers. Epithelia can be grouped by the rough shape of the constitutive cells: squamous (flat cells, with very small lateral membranes), cuboidal (cells as cubes), or columnar (tall rhomboid cells with extended lateral membranes) epithelia. Depending on the number of cells layers they are also classified as either simple or stratified. The main function of epithelial tissues, summarized in Figure 1, are: absorption and/or the secretion of different nutrients, waste and for some of them secretion of mucus. In addition, depending on their thickness, some of them play an important role in the protection of the organ lining.

Cells	Location	Function
Simple squamous epithelium 	Air sacs of lungs and the lining of the heart, blood vessels, and lymphatic vessels	Allows materials to pass through by diffusion and filtration, and secretes lubricating substance
Simple cuboidal epithelium 	In ducts and secretory portions of small glands and in kidney tubules	Secretes and absorbs
Simple columnar epithelium 	Ciliated tissues are in bronchi, uterine tubes, and uterus; smooth (nonciliated tissues) are in the digestive tract, bladder	Absorbs; it also secretes mucous and enzymes
Pseudostratified columnar epithelium 	Ciliated tissue lines the trachea and much of the upper respiratory tract	Secretes mucus; ciliated tissue moves mucus
Stratified squamous epithelium 	Lines the esophagus, mouth, and vagina	Protects against abrasion
Stratified cuboidal epithelium 	Sweat glands, salivary glands, and the mammary glands	Protective tissue
Stratified columnar epithelium 	The male urethra and the ducts of some glands	Secretes and protects

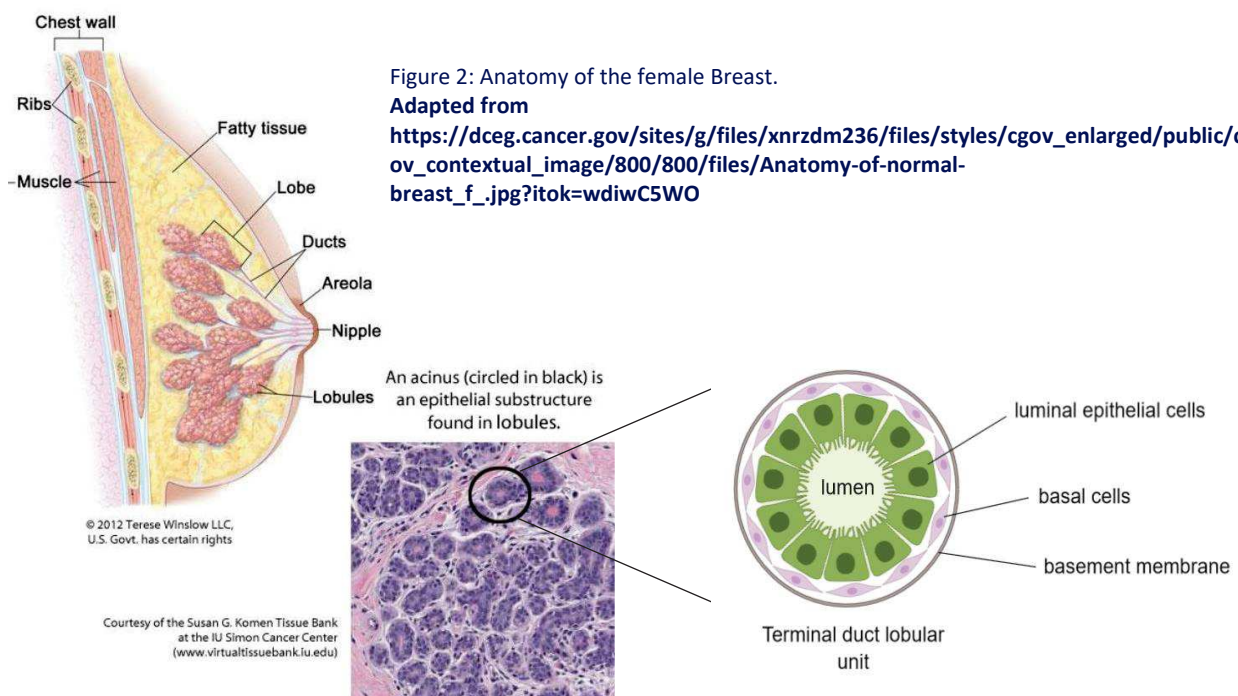
Figure 1: Different epithelial tissues, locations and functions.

Adapted from (OpenStax 2013)

1.2. Examples

a. Breast tissue:

The breast tissue has one specific function: produce milk. It is organized in glands in which nutrients coming from the blood are turned to milk, and ducts that collect and bring the milk to the nipples, a specialized feeding structure. The glands are constituted of 15 to 20 lobes separated by fat and each lobe is divided into lobules (Figure 2) also called Terminal ductal lobular unit or TDLU. Lobules are mainly composed of an epithelial structure called acinus; together all acini produce the milk from the blood (“Anatomy of the Female Breast,” n.d.).



The breast epithelium is a stratified epithelia constituted of two different types of epithelial cells: the internal luminal cells surrounded by the external basal myoepithelial cells. These cells are present lining the ducts and the terminal ductal lobular unit (Figure 2). The luminal cells are present in the inner layer of the ducts and the acini and have a simple columnar shape. They produce and help in the secretion and transport of the milk. The myoepithelial or basal cells are found on the outer part between the luminal cells and the basement membrane. Their function is to maintain the basement membrane and contract the lobules producing milk to favor its transport towards the collecting ducts. Basal cells also maintain the polarity of the luminal cells.

Basal cells are flat and organized resembling to a squamous epithelium (“Breast Development and Anatomy : Clinical Obstetrics and Gynecology,” n.d.).

Breast cancer originate in the breast epithelial cells, either in the lobules or in the ducts. It is thus a solid cancer of epithelial origin or carcinoma. This part will be detailed in section 4 of this thesis manuscript.

b. Colon tissue:

The colon is 150 cm long and divided into 5 main segments (Figure 3A). It is also called large intestine. It removes water salt and other nutrient leaving waste from food digestion. Muscles are lining the colon wall helping moving the stools towards the rectum, and billions of bacteria are living inside helping with food processing (Hoffman and MD, n.d.).

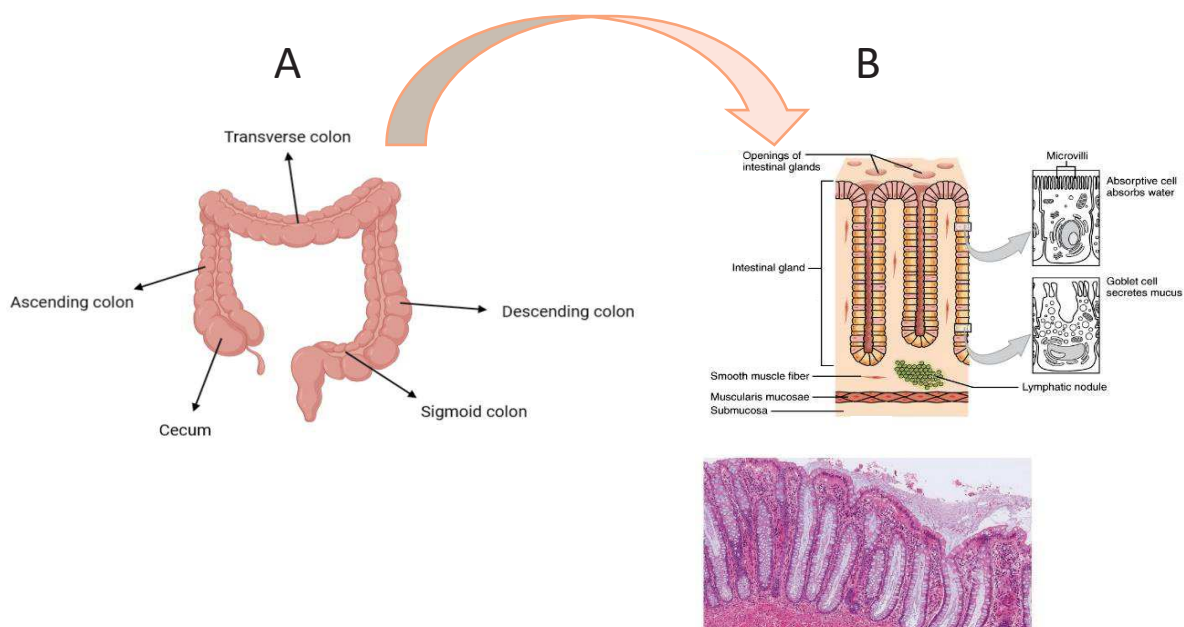


Figure 3: A) The colon anatomy and B) histology.

Adapted from <https://opentextbc.ca/anatomyandphysiology/chapter/23-5-the-small-and-large-intestines/>

The basic units of the colon are glands lining the wall of the colon, the intestine crypts also called crypts of Lieberkühn. These glands are covered by a simple columnar epithelium, the colon mucosa, composed mainly by enterocytes (absorptive cells) and goblet cells (Figure 3B) (OpenStax, 2013b), (“The Large Intestine | Boundless Anatomy and Physiology,” n.d.). Goblet cells secrete the mucus and Enterocytes absorb the water, salt and other nutrients produced by the intestinal bacteria.

There is always a renewing of the epithelium in the crypts, balancing the permanent shedding of damaged cells due to the continuous passage of food. Deep at the base of the crypts, multipotent stem cells, ensure this constant renewal and production of new epithelial cells.

Alterations in the proliferation control in the crypt are the primary cause of colorectal cancer; this part will be detailed in section 4 of this thesis manuscript.

2. Epithelial cells:

Epithelial cells are highly polarized cells, a feature that is essential for their function as barrier cells, ensuring thus polarized flow of molecules and information. Furthermore, epithelial cells develop several highly specialized intercellular junctions along the lateral membranes, which are critical for their adhesion, and for ensuring their function as barrier between the exterior and the interior of the organism (Knust and Bossinger, 2002). An important aspect for the formation of a tissue is that while the different components of polarity, adhesion molecules and cytoskeleton need to be asymmetrically distributed in each cell (to form the different axis of the cell), the organization of this asymmetry needs to be coordinated between all the cells in the epithelial sheet (Bryant and Mostov, 2008).

2.1. Polarity :

Different complexes orchestrate the asymmetric distribution of components and complexes (i.e. polarity) inside the cell. The polarity is established along the apico-basal (A/B) axis of the cell. In addition, some epithelial cells have a second axis of polarization, orthogonal to the A/B axis (the plane of the tissue) generally referred to as PCP or Planar Cell Polarity (Bryant and Mostov, 2008; Djiane et al., 2005).

The apical and basolateral membranes are usually associated with a set of proteins, transporters and enzymes responsible of the function of each membrane, but only a few play an essential role in the establishment and/or the maintenance of the polarity (Bazellières et al., 2018), which are evolutionarily conserved across the animal kingdom.

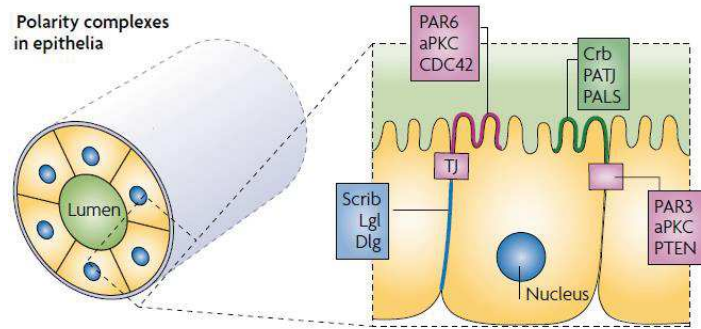


Figure 4: Apico-basal polarity complexes in epithelial cells.
Taken from Bryant et Mostov 2008.

a. Apical identity:

The apical domain of a cell is facing an external environment or a lumen if the cells are forming a tube. Two main complexes participate in the formation of the apical side of the cell: The PAR (CDC42, PAR6, PAR3 and aPKC) and Crumbs (CRB, PATJ/MUPP1 and PALS) complexes. The PAR complex can be subdivided in two: the apical complex composed of CDC42, PAR6 and aPKC and the Junctions associated complex with PAR3 and aPKC as main actors (Figure 4).

Using genetic screening in *Caenorabditis elegans* (*C.elegans*), Kempthues et al. identified the *Pard* genes (for Partitioning defective) which when mutated lead to a defect in the antero-posterior axis of the zygote (Kempthues et al., 1988). Six *Pard* genes were identified encoding for scaffold (such as PAR3 and PAR6), for serine threonine kinase (as Par1 and Par4), a member of the 14-3-3 family (Par5) and a ring finger protein implicated in the ubiquitin pathway (Par2). PAR6 and PAR3 have one and three PDZ domains (named for PSD-95, Discs Large and ZO-1) respectively promoting the formation of different protein complexes: PAR3 could bind aPKC (atypical Protein Kinase C) and these two proteins could also be found in a complex with PAR6 and CDC42, a small GTPase (Joberty et al., 2000; D. Lin et al., 2000) implicated in polarity from budding yeast to human (Pichaud, 2018). PAR6 binds Cdc42 through its CRIB domain (D. Lin et al., 2000).

In epithelial cells, despite its interaction with the Par complex, PAR3 is able to interact with other proteins including junctional proteins. PAR3 has thus early functions during polarity establishment and maintenance, but also during junctional biology in mature epithelia. There is evidence that PAR3 play an important role in recruiting the PAR6/aPKC complex through weak interactions to initiate and maintain the apical polarity (Laprise and Tepass, 2011). These complex interactions of PAR3 are regulated by its phosphorylation by aPKC (Izumi et al., 1998), (Hirose et al., 2002). Upon its phosphorylation, PAR3 detaches from the PAR6/aPKC complex and becomes relocalized at the levels of the Tight Junctions (Nagai-Tamai et al., 2002), (Suzuki et al., 2002), where it binds and

stabilizes for example the tumor-suppressor PTEN (for Phosphatase and Tensin homolog) to the Tight junctions. This PAR3-mediated PTEN stabilization is responsible for the transformation of the lipid PiP3 (phosphatidylinositol triphosphate) to PiP2 (phosphatidylinositol diphosphate), a critical step for plasma membrane compartmentalization and function (exo/endocytosis, cytoskeleton attachment... (Pichaud, 2018)). All these interactions highlight the critical role of PAR3 in epithelial cell biology, including in cytoskeleton dynamics. In addition to its phosphorylation by aPKC mentioned above, PAR3 is subjected to many regulations to ensure its good localization inside polarized cells. Par1 (a component of the basolateral membrane), after its activation by PAR4/LKB1, can phosphorylate Par3, creating a site for the 14-3-3 Par5 protein, leading thus to the disruption of its binding to the plasma membrane and its exclusion from the basolateral membrane (Benton and Johnston, 2003), (Hurov and Piwnica-Worms, 2007).

The main active component in the Par complex is the Serine Threonine kinase aPKC, which can phosphorylate many substrates such as PAR3 and PAR6 in the Par complex, but also proteins implicated in the establishment of the baso-lateral membrane identity such as LGL. This latter activity is essential for the exclusion of LGL from the apical membrane and the definition of the opposite basal identity (Bailey and Prehoda, 2015). Indeed, mutations that inactivate the aPKC in zebrafish lead to impairment of cellular polarity, mitotic spindle orientation and organogenesis (Plant et al., 2003), and the overexpression of a kinase dead isoform of aPKC blocks the formation of Tight Junctions (Suzuki et al., 2001).

While the Par complex regulates polarity in many cell types (including epithelia), the Crumbs polarity complex function is specific to epithelial cells. In 1990, the link between the epithelial polarity and Crumbs was uncovered in *Drosophila Melanogaster*. Using electron microscopy, it was clear that Crb is an essential apical determinants localized at the levels of the apical membrane and concentrated at the interface of the apical and the basolateral membrane where the junctions forms. There are three mammalian Crumbs homologues (Crb1-3). All three Crumbs have a conserved cytoplasmic tail, with a PDZ binding domain and a FERM domain. It seems that both domains are required for the correct activity of Crumbs (Klebes and Knust, 2000). The cytoplasmic tail of Crb binds the scaffold proteins Pals1 (associated with lin7) via its PDZ binding domain. Pals1 then will recruit Patj (Pals1 associated tight junction) to form the Crb complex (Assémat et al., 2008).

In *Drosophila Melanogaster*, loss of function mutations in *Crb* or *Sdt* (*Pals1* homologue) resulted in strong defects of epithelial polarity (Tepass et al., 1990),(Müller and Wieschaus, 1996) with a disappearance of the apical side, while the overexpression of Crumbs caused the expansion of the

apical domain (Makarova et al., 2003), highlighting the critical role of Crb in the apical side identity and size in *Drosophila* epithelial cells.

In mammalian epithelial cells, the Crb complex has been linked to Apical Junctions formation and biology. First, the overexpression of Crb in MDCK cells (Madin-Darby Canine Kidney cells) resulted in a delay in the formation of the tight junctions (Lemmers et al., 2004). Second, knockdown of *Pals1* in MDCK leads to a polarity defect and a severe disturbance of Tight Junctions but also Adherens junctions (Wang et al., 2006),(Straight et al., 2004). Finally, at Tight Junctions, Patj interacts with other TJ resident proteins such as ZO3 (Zonula Occludens 3) and Claudin1, and *Patj* knock-down results in the mis-localizations of ZO1, ZO3 and Occludins thus destabilizing Tight Junctions (Assémat et al., 2008).

b. Basolateral identity:

The complex specifying the basolateral identity in epithelial cells is constituted of three main protein: Scribble (SCRIB), Discs Large (DLG) and Lethal Giant Larvae (LGL) (Figure 4). Cells that lacks any of these proteins have polarity defects and have the ability to over proliferate (Bilder and Perrimon, 2000). It is shown in *Drosophila* that the main function of this complex is to restrain the apical protein from the lateral membrane. E-cadherin (Ecadh) mediated adhesion plays an important role on the localization the Scrib complex, and reciprocally, Scrib maintains Ecadh mediated adhesions to specify the basolateral membrane and oppose apical membrane identity (Bilder and Perrimon, 2000),(Navarro et al., 2005),(Qin et al., 2005).

The *scribble* gene was isolated in *Drosophila melanogaster* using a genetic screen for maternal mutations that could disrupt epithelial aspects such as adhesion, cell shape and polarity (Bilder and Perrimon, 2000). It encodes for a large protein with 16 leucine rich repeats (LRR) and four PDZ domains belonging to the LAP (LRR and PDZ) protein family (Bilder et al., 2000). Scrib is known for its role in maintaining the apico-basal polarity but also in tissue growth regulation in *Drosophila melanogaster* (Bonello and Peifer, 2019), *C.elegans* (Legouis et al., 2003) and human (Nagasaka et al., 2006). Depleting the LRR domain eliminated both function of Scrib (Zeitler et al., 2004). Recent discovery showed scribble controls polarity in the imaginal wing discs of *Drosophila* through the endocytosis of apical proteins on the basolateral membranes. More specifically, early endosomal internalization of cargos is not affected in *scribble* mutant cells, the transport from the endosome to the Golgi apparatus via retromer complex (a complex implicated in recycling) is disturbed. The apical protein Crumbs is one of the proteins cleared from basal through this pathway

(Vreede et al., 2014). Moreover in MDCK cells, removal of *Scrib* expression caused a delay in the formation of the Tight Junctions as evidence by de-novo junction reformation using the calcium switch model (Qin et al., 2005). Indeed, evidence suggest that SCRIB plays an important role in the assembly of the TJs, by regulating and stabilizing p120/E-Cadherin complexes at the levels of Adherens Junctions, ultimately regulating cell proliferation, migration and metastasis (Bonello and Peifer, 2019).

DLG belongs to the Membrane Associated Guanylate Kinase (MAGUK) family of scaffold proteins. Many studies in *Drosophila* have shown the important role of this gene in several key biological processes including epithelial polarity, asymmetric cell division and invasion. DLG mainly acts as a tumor suppressor. The list of its interactors is growing, and includes tumor suppressors such as APC (for Adenomatous Polyposis coli) and PTEN but also some oncogenes such as β -catenin (Roberts et al., 2012).

LGL is composed of repeated WD40 domains. These repeats act as a protein interacting modules for Scribble. LGL is a downstream target of the aPKC/PAR6 complex. This phosphorylation during the establishment of polarity causes the detachment of LGL from the complex and it prohibits its returning to the apical part of the cell (Plant et al., 2003), (Musch et al., 2002), (Chalmers et al., 2012). LGL regulates many biological processes including cell polarity and asymmetric division, through its interplay with other polarity proteins, regulating exocytosis, cytoskeleton dynamics and signaling pathways (Cao et al., 2015).

It is worth mentioning that the Scribble module regulates the PCP polarity axis (Cao et al., 2015).

Hence, it is clear that the Crumb and the Par complexes located at the apical region of the lateral membrane and the Scribble complex concentrated along the basal region of the lateral membrane, do not act alone to establish and maintain the identity of the different poles of the cell. The polarity of a cell is a complex phenomenon that requires intricate interactions between these different polarity molecules, such as the mutual exclusion of the apical and basal complexes. In addition to the example of the LGL and the PAR3 regulation by aPKC, similar reciprocal exclusion actions are performed to maintain the asymmetry of the cell (Figure 5).

Several cellular machinery cooperate with the different polarity complexes to form and maintain the apico-basal polarity:

- Adhesion between the different cells of the epithelia and between cells and the basement member.
- Polarized cytoskeleton that help and support the adhesion and traffic.

The establishment of the apico-basal polarity is essential for the right positioning of the junctions along the lateral membrane. Likewise, the expansion of the apical and basal membrane depends on the correct localization of the junctions.

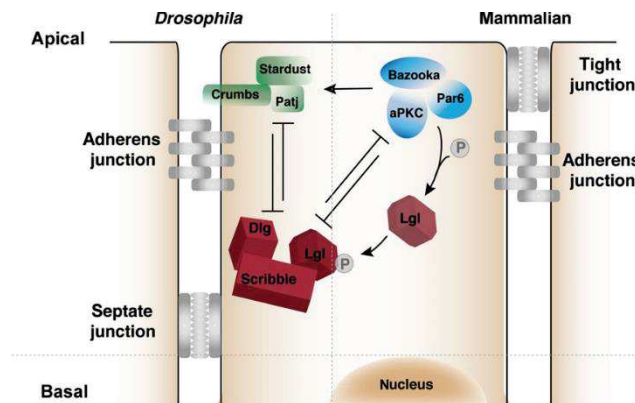


Figure 5: Interplay between the different polarity complexes in the cell.

The Par complex, composed of Bazooka (Par3 in mammalian cells), Par6 and aPKC and the Crumbs complex composed of Crumbs, Stardust (PALS1 in mammalian cells) and Patj act through mutual antagonistic interactions to maintain basolateral localization of the Scribble complex, which is composed of Scribble, Dlg and Lgl. **Adapted from Zeitler et al, 2004.**

2.2. Cellular Junctions:

Within an epithelium, cells establish intercellular junctions which fulfil different functions: epithelial cells need to be linked together and anchored tightly to the basement membrane. To that purpose, four different junction types are established between cells: Tight junctions (TJs), Adherens junctions (AJs), Gap junctions and Desmosomes. Other junctions are present to maintain interactions between cells and their basement membrane: Hemi desmosomes and focal adhesion (*Figure 6*). In the following part I am going to talk about the Tight and the Adherens junctions owing to its relevance for the project.

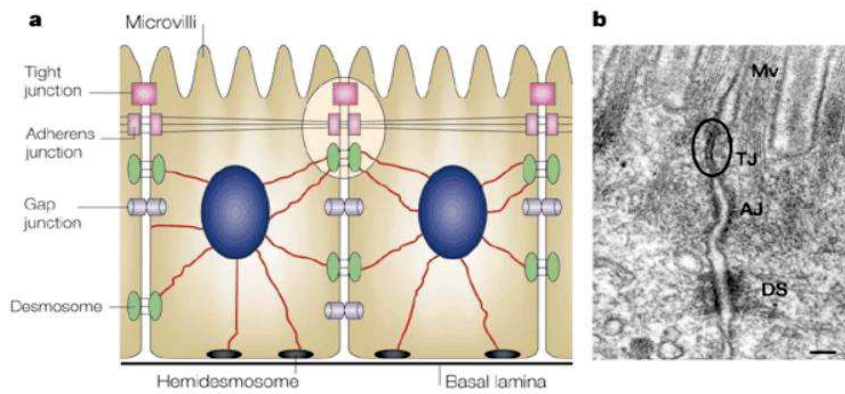


Figure 6: Cellular junctions. Representation of junctional complexes in intestinal epithelial cells (a). Electron micrograph in mouse intestinal epithelial cells. TJs are circled (b). Taken from Tsukita et al. 2001.

Nature Reviews | Molecular Cell Biology

A highly specialized adhesive belt present just below the apical membrane surrounds each cell. It is constituted of: the Tight Junctions (TJs) or the zonula occludens region and the Adherens Junctions (AJs) or the zonula adherens region followed by desmosomes. Gap junctions are present at the basal level of the lateral membrane and are specialized in communication through the exchange of small molecules (Figure 6).

a. Tight Junctions:

Fifty years ago, Farquhar et al described the ultrastructure of the TJs (Farquhar and Palade, 1963). The first protein associated with these structures was discovered in 1986 and called ZO-1 (for Zonula Occludens 1) (Stevenson et al., 1986). Following this characterization, other proteins were associated to the TJs such as ZO-2, ZO-3, cingulin and JACOP (for junction associated coiled-coil protein) (Ohnishi et al., 2004). However, the localization of these proteins at the periphery of the plasma membrane and their lacking of transmembrane domains suggested that they do not constitute the intermembrane strands linking adjacent cells. Using similar biochemical analyses, Tutsika's lab identified two transmembrane proteins at TJs: the Occludins and the Claudins (Furuse et al., 1993),(Furuse et al., 1998). At the same time, a member of the Immunoglobulin superfamily, Junction Adhesion Molecule (JAM) was identified as protein localized at the TJs (Martín-Padura et al., 1998).

TJs are composed by a mesh of strands constituted by intramembranous particles, which are linearly polymerized (Figure 7a). The complexity of the TJs network and the number of parallel strands are

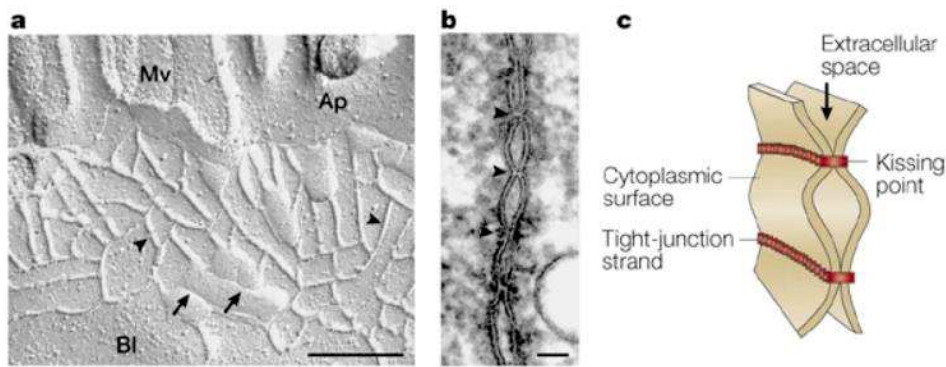


Figure 7: The structure of the TJs.

Freeze-Fracture Electron microscopy of mouse intestinal TJs (a) (Ap:apical side, Bl: Basolateral side, Mv: microvilli, arrows show strands on the protoplasmic side, arrow heads represent grooves at the extraplasmic side). Thin layer view of the TJs. The kissing point (arrowhead) where the passage is blocked with specific permeability (b). A three dimensional scheme for TJs between two cells (c). **Taken from Tsukita et al. 2001.**

different between the different epithelia. Its density and tightness are correlated with the trans-epithelial electric resistance (TEER) even though some exceptions exist (Møllgård et al., 1976),(Martinez-Palomo and Eriij, 1975).

The transport between epithelial cells occurs through two pathways: the transcellular (through the cell) and the paracellular (between the cells) which depends on the TJs (Frömter and Diamond, 1972). Dysfunction in the TJs function can then be related to many pathological conditions (Sawada, 2013).

In addition to its role as a gate keeper and its selective permeability to ions and solutes, TJs have an important role acting as a fence, preventing the mixing between the different lipid and protein components of the apical and the basolateral membranes (Hartsock and Nelson, 2008).

TJs are associated with a group of cytoplasmic proteins called the TJs protein plaque, among which many contain PDZ domains and/or act as molecular scaffolds, able to establish macromolecular complexes linking TJs with the actin cytoskeleton, the closely localized AJs and different signaling pathways (Schneeberger and Lynch, 2004).

When three adjacent cells meet, it is called tricellular junctions (tTJs) (Figure 8). At the interface, the TJs expand along the lateral membrane and a central tube is formed, which is thought to be permeable to higher molecular weight solutes (Schulzke et al., 2012).

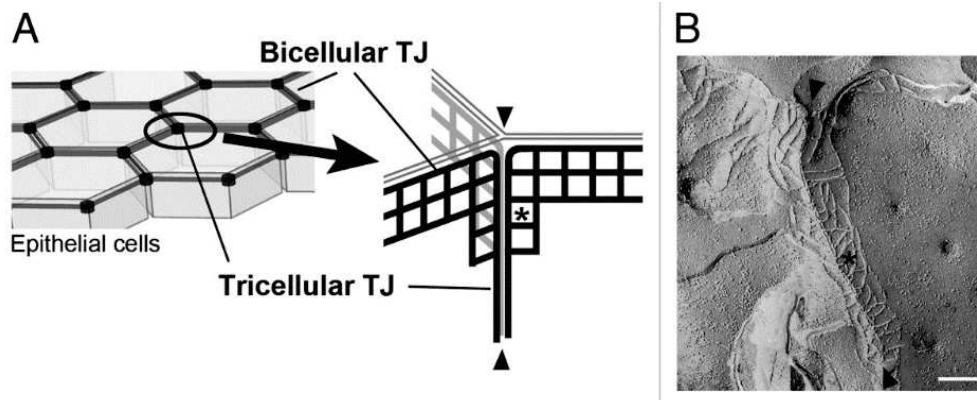
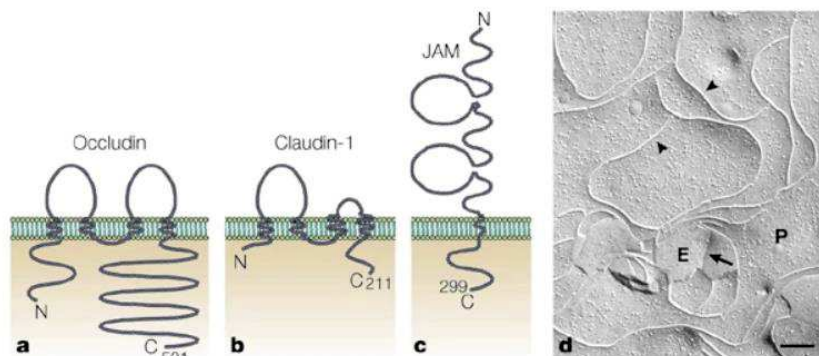


Figure 8: Different types of TJs. Representation of the different types of TJs (a). Freeze-Fracture Electron microscopy for TJs in MDCK cells (b). Taken from Higashi et Chiba 2020.

i) The Claudin family:

Claudins are tetraspan proteins with short cytoplasmic tails (Figure 9b) localized at the level of the TJs strands. The C-terminal part of all Claudins (27 members have been identified so far), except the Claudin-12, ends with PDZ binding sites. These motifs mediate the interactions between Claudins and different proteins such as ZO-1, ZO-2, ZO-3, MUPP1 and PATJ (Hamazaki et al., 2002; Itoh et al., 1999; Müller et al., 2003; Roh et al., 2002). All these interactions act like a bridge to link the actin cytoskeleton and to recruit other proteins to the TJs.



Nature Reviews | Molecular Cell Biology

Figure 9: Structure of the different transmembrane proteins constituting the TJs. FFEM of L mouse fibroblasts expressing Claudin-1 (d). Taken from Tsukita et al. 2001

Exogenous Claudin expression triggered TJs-like structures in mice fibroblasts (Figure 9d) (Furuse et al., 1998),(Tsukita et al., 2001), suggesting that Claudins alone are sufficient to build TJs strands. However overexpressing a mutant form of Claudin-1 unable to bind to the cytoskeleton lead to the formation of aberrant TJs strands in MDCK cells (Kobayashi et al., 2002),(McCarthy et al., 2000), suggesting that the cytoskeleton plays an important role in the formation, maturation and regulation

of the TJs. The Claudins polymerize in the TJs strands through cis (side to side) or trans (head to head) interactions (Tsukita et al., 2019).

All KO mice models support the idea that Claudins are important for TJs functions (*Table 1*) and in particular for ion permeability. Indeed, most Claudins (1, 4, 5, 8, 11 and 14) are known to increase the TER of the cell by decreasing cation permeability while others act as cations pores and two of them are known to act as anion pores (Angelow et al., 2008),(Tsukita et al., 2019). These different ions permeability capacities are conferred by their first extracellular loop (Colegio et al., 2003),(Colegio et al., 2002). It is worth mentioning that the function of Claudins goes far beyond the regulation of the barrier and adhesion. (Claude and Goodenough, 1973) observed that some Claudin molecules were present along the basolateral membrane of stomach epithelial cells. This observation was further confirmed in other tissues such as epidermis, lung, kidney, intestine and others (Hagen, 2017). Finally, some Claudins were detected in the nucleus (Dhawan et al., 2005), even though the functional relevance of this nuclear localization remains to be established.

<i>Knockout model</i>	<i>Affected organs</i>	<i>Impaired function</i>	<i>Citation</i>
Cldn1 ^{-/-}	Skin	Barrier	7
Cldn2 ^{-/-}	Kidney, liver	Barrier	13, 35
Cldn4 ^{-/-}	Kidney	Barrier	15
Cldn5 ^{-/-}	Blood-brain barrier	Barrier	12
Cldn7 ^{-/-}	Intestine	Adhesion	19
Cldn10 ^{-/-}	Kidney	Na ⁺ absorption	49
Cldn11 ^{-/-}	Inner ear	Barrier	21
Cldn14 ^{-/-}	Kidney	Regulation	22
Cldn15 ^{-/-}	Small intestine	Mucosal differentiation	14
Cldn16 ^{-/-}	Kidney	Barrier	23
Cldn18 ^{-/-}	Bone	Bone resorption and osteoclast differentiation	17

Table 1: Knockout Mice models. Taken from Markov et al. 2015.

The Claudins are tissue and organ specific. They are expressed in epithelia with different barrier properties which suggests that a wide range of interactions between Claudins exists and could confer specific properties unique for each tissue (Markov et al., 2015). Generally, more than two different Claudins are expressed inside the cell, and having multiple Claudins that could interact with each other as homodimers or heterodimers could explain, at least in part, the functional diversity of the TJs (Furuse et al., 1999).

Claudins at the TJs are tightly regulated ensuring their correct localization and functions (reviewed in (Angelow et al., 2008)). Their cytoplasmic tail is subjected to phosphorylation by serine/threonine kinases and also to other post translational modifications such as palmitoylation (e.g. palmitoylation of Claudin-14 controlling routing to TJs (Van Itallie et al., 2005)). Claudins are the substrate of different kinases such as PKA (Protein Kinase A), PKC (Protein Kinase C), WNK1&4 (With No lysine [K] 1&4), Rho Kinase, MAP kinase, and EphA2, all modulating Claudins' functions. Finally, Claudins are also regulated at the transcriptional level. For example, an important physiological process associated with regulation of Claudins expression is the epithelial to mesenchymal transition (EMT). Several Claudin genes have E box motifs in their promoters, which can bind and thus be silenced by Snail, a transcription factor associated with EMT.

ii) The TAMPS: Occludins, Tricellulin and MarvelD3

If Claudins are responsible for the paracellular transport of ions and water between two cells, the TAMPs or Tight Junction-Associated Marvel domain-containing proteins are known to regulate the macromolecules barrier formation: the “leaky pathway” (Shen et al., 2011). Moreover, while Claudins alone were sufficient to create TJs strands in fibroblasts, the introduction of any of the three TAMPs along with Claudins is able to change the morphology of the strands suggesting that the TAMPs affect the organization of the TJs but not their formation (Cording et al., 2013). These data suggest that Claudins and TAMPs complement each other to form functional TJs.

TAMPs are characterized by four transmembrane domains with a long C-terminal tail. They share homology with the MAL protein (Myelin and lymphocyte-associated protein) and are known to play important role in vesicle trafficking between Golgi and apical plasma membrane.

TAMPS show some level of redundancy and could compensate for each other. For instance in Occludin-deficient mice, Tricellulin spread along the bicellular TJs even though in wild-type it is more abundant at the tricellular TJs (Ikenouchi et al., 2008).

Occludins:

Occludins are localized at the levels of the TJs strands along with the Claudins. Introduction of Occludin in fibroblasts expressing Claudins resulted in their colocalization at the TJs suggesting that Claudin play a role in the correct localization of Occludins (Furuse et al., 1998). Using

truncated forms of Occludin identified the second extracellular loop as necessary for its correct localization at the TJs (Medina et al., 2000).

Occludin knockout mice were viable without drastic effect on the TJs structure. However, after birth, these KO mice showed growth retardation and chronic inflammation at the level of the gastric epithelium along with other abnormalities in other tissues (Saitou et al., 2000),(Schulzke et al., 2005) suggesting that Occludins are required for the correct functions of several tissues.

Overexpression of Occludins in MDCK cells enhanced macromolecules permeability such as mannitol (Balda et al., 1996), but this might actually represent a dominant-negative effect since a similar increased permeability to macromolecules up to 70kDa was reported after Occludin knockdown in CaCo-2 cells or in ex-vivo intestinal murine tissues (Al-Sadi et al., 2011). A debate still exists on whether or not the Occludin could affect the ion permeability and the TER of the TJs. Hence, Occludins appear to be important for the barrier role of the TJs, and even though it does not affect the TER, their disturbance changes the TJs properties and therefore may lead to damages. Occludins are often targets of pathogens during infections (Nava et al., 2004; Raleigh et al., 2010), suggesting that barrier loosening against macromolecules is a process used by pathogens to enter inside tissues.

Occludins have many binding partners, among which most of them are implicated in junctional regulation. ZO-1, ZO-2 and ZO-3 can bind to Occludins and constitute a bridge between TJs and F-actin. Occludin itself could bind F-actin, a unique property among TJs transmembrane proteins (González-Mariscal et al., 2003). JAMs (see later) also bind Occludins. When co-transfected with Occludin, JAMs cause its accumulation at TJs suggesting that JAMs recruit and/or stabilize Occludins at TJs. Occludins belong the MAL family implicated in vesicle traffic. VAP-33 (VAMP associated protein of 33 kDa), a protein involved in vesicle fusion and docking (Skehel et al., 1995), is a binding partner of Occludins in human liver cells (Lapierre et al., 1999), suggesting that VAP-33 could be using Occludin as an anchor for directional vesicle trafficking (Feldman et al., 2005). Finally, other partners for Occludins include CLMP (coxsackie- and adenovirus receptor-like membrane protein), JEAP (junction enriched and -associated protein) or AMOTL1 (Angiomotin protein like 1) and ZAK (ZO-associated kinase). A summary of the different Occludin binding partners is shown in *Figure 10*.

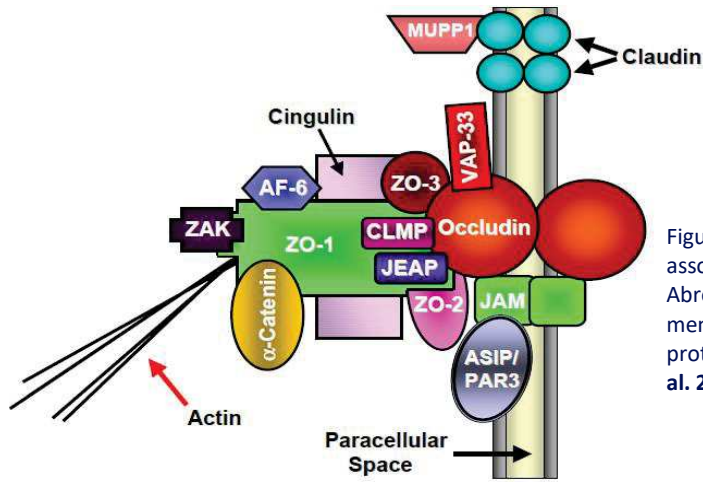


Figure 10: Summary of interactions between Occludin and TJs associated proteins. Abbreviations: CLMP, coxsackie- and adenovirus receptor-like membrane protein, JEAP, junction enriched and -associated protein, ZAK, ZO-associated kinase. **Adapted from Feldman et al. 2005.**

Phosphorylation on Serine/Threonine (S/T) residues represents the key factor for the regulation of Occludins function (Seth et al., 2007; Wong, 1997). After TJs disruption by treating cells with low calcium, Occludins are dephosphorylated, suggesting that the S/T phosphorylation could play a critical role in the maintenance of TJs integrity. Since aPKC (part of the apical polarity complex) is found at TJs, it was suggested that this kinase is able to phosphorylate Occludins. PP2A (protein phosphatase 2) and PP1 are implicated in the regulation of Occludin in MDCK and in CaCo-2 cells (Nunbhakdi-Craig et al., 2002; Seth et al., 2007), and Knockdown of any of these two phosphatases enhanced TJs stability. Surprisingly, S/T dephosphorylation associated with disruption of TJs is coupled with tyrosine (Y) phosphorylation, and Y kinases inhibitors prevented the disassembly of junctions following hydrogen peroxide treatment (Basuroy et al., 2003; Rao et al., 2002; Sheth et al., 2003). Many kinases have been reported to induce Y phosphorylation of Occludin including c-Src (proto-oncogene tyrosine kinase Src) (Basuroy et al., 2003), c-Yes (tyrosine protein kinase Yes) (Chen et al., 2002) and PI3K (phosphatidylinositol-3 kinase) (Sheth et al., 2003). The Y phosphorylation of Occludin is associated with a loss of interaction with ZO-1. Thus, the balance between S/T and Y kinases and phosphatases regulates the phosphorylation status of Occludins and therefore regulates the TJs assembly/disassembly.

Finally, Occludins can also be regulated by small GTPases such as RhoA, Rac1 (Jou et al., 1998), Raf-1 (Li and Mrsny, 2000) and PAR6 with its binding partner CDC42 (Gao et al., 2002), as well as by proteases secreted by viruses (Wu et al., 2000) and cytokines like Interferon alpha (INF- α) (Lechner et al., 1999).

Tricellulin and MARVELD3

Tricellulin is concentrated at the levels of the tricellular TJs while weaker presence at bicellular junctions is observed.

Knockdown of Tricellulin in cell lines induced a discontinuity of the TJs and the bicellular TJs were thinner with abnormal pattern of Occludin. Furthermore, the paracellular barrier was highly affected and the TER was compromised (Ikenouchi et al., 2005). Introduction of Tricellulin in L Fibroblast expressing Claudin-1 changed the shape of the TJs strands by increasing the number of crosslinks and Claudin oligomerization (Cording et al., 2013). Moreover, Tricellulin knockdown in CaCo-2 cells induced a delay in barrier development (Raleigh et al., 2010). Despite all these cellular phenotypes caused by the deregulation of Tricellulin, the only obvious phenotype in the KO animals was deafness (Riazuddin et al., 2006).

A limited number of partners are described for this protein. Giving the 32% similarity of its C-terminal tail with that of Occludin, it is known to bind ZO-1. Tricellulin also binds MARVELD3 but not Occludin (Furuse et al., 2014).

iii) The JAMs family:

Unlike the Claudins and the TAMPs, the JAMs (Junctional Adhesion Molecule; JAM-A/B/C) have only one transmembrane domain (*Figure 9c*). They belong to the immunoglobulin superfamily of adhesion molecules (with JAM-4, coxsackievirus and adenovirus receptor (CAR) and endothelial cell-selective adhesion molecule (ESAM), and mediate adhesion through cis-dimerization and trans interactions (González-Mariscal et al., 2003).

When JAM-A is transfected into L-fibroblasts, cells do not exhibit strand-like structure as when transfected with Claudins, suggesting that JAMs do not participate directly in the formation of the TJs strands (Itoh et al., 2001). Supporting this notion, JAMs are expressed in a variety of cells lacking stable junctions such as leucocytes and platelets.

JAM-A depletion by RNAi, increased the paracellular barrier permeability (Luissint et al., 2014). In addition, MDCK cells lacking JAM-A were not able to form 3D polarized spheroids in collagen, suggesting that it participates to the establishment of the apico-basal polarity (Rehder et al., 2006), a function likely linked to its interaction with PAR-3 (a protein involved in polarity). The JAMs family have also been reported to regulate many other processes such as leucocyte trans-epithelial

and trans-endothelial migration, inflammation, epithelial proliferation and wound healing (González-Mariscal et al., 2003).

Through a PDZ binding motif at the level of their cytoplasmic C-terminal part, JAMs interact with many proteins associated with the TJs such as ZO-1 and ZO-2, Afadin, MUPP1, PAR-3, and MAGI-1 (Membrane Associated Guanylate kinase with Inverted domain structure 1) but also PDZ-GEF2 (guanine exchange factor 2) and CASK (calcium/Calmodulin-dependent serine protein kinase).

aPKC is able to phosphorylate JAM-A, and this phosphorylation is important for the maturation of TJs and the maintenance of its gate function (Ebnet, 2013).

iv) Other families of proteins:

Recently, a family of monospan proteins was identified and associated with tTJs. Angulins, known before as lipolysis-stimulated lipoprotein receptor (LSR), regulate the paracellular permeability of the TJs barrier. Interestingly, in Angulin knockdown cells, the localization of tricellulin is impaired but not the other way around (Masuda et al., 2011), suggesting that Angulin is recruiting the tricellulin at the levels of the tTJs.

CRUMB3 is a single-pass transmembrane protein localized at the TJs that was described and developed earlier in this manuscript (polarity determinants section (2.1.a)). Despite their role in polarity determination, CRUMBS also control TJs biology.

v) Protein associated with TJs:

A protein plaque is associated to the transmembrane proteins at the levels of the TJs. This plaque is connected to the actomyosin cytoskeleton. Proteins constituting this plaque can be divided in two groups: proteins containing PDZ domains and proteins lacking PDZ domains.

- Members of the PDZ domain containing protein

Constituted of the ZO proteins (ZO-1, ZO-2 and ZO-3), the membrane associated guanylate kinase inverted proteins (MAGIs), the multi PDZ protein (MUPP1), the Ras target protein Afadin (AF-6), PAR-3, PAR6, PALS1 and PATJ (*Figure 11*).

The ZO proteins belong to the MAGUK (Membrane Associated Guanylate Kinase) family. They are considered as a network interaction hub (Guillemot et al., 2008). Through its PDZ domains ZO-1 interacts with:

Claudins. This interaction is essential for the correct formation of TJs (Umeda et al., 2006). Accordingly, mammary epithelial cells which do not have ZO-1 and ZO-2 fail to assemble TJ strands. Introduction of a ZO-1 mutant unable to localize to the junctions but to the lateral membrane leads to the formation of ectopic TJ strands (Umeda et al., 2006) suggesting that the assembly of ZO proteins is necessary and sufficient for TJ strands formation. It is noteworthy that cells lacking the three ZO proteins have normal apico-basal polarity.

Other ZO proteins. This dimerization is crucial for ZO-1 because cells with dimerization mutant ZO-1 were not able to recruit Claudins to the junctions (Umeda et al., 2006).

Connexins, components of the gap junctions. Considering the increasing number of this family described to interact with the ZO proteins, ZOs emerge as playing a role in organizing the gap junctions and signaling pathway related to it (Umeda et al., 2006).

JAMs. Since JAMs interact with PAR-3, ZO-1 establish a link between the polarity components and the Claudin-based TJs strands (Itoh et al., 2001).

The interaction with p120-catenin (a component of the AJs) is unique to ZO-3. But targeted deletion of ZO-3, to date, is not linked to any detectable phenotypic effect.

Through other domains than the PDZs, ZO-1 and ZO-2 interact with Occludins, Afadin, ZONAB (ZO-1 associated Y-box factor), actin and many others (Guillemot et al., 2008). Accordingly, ZO-1 and ZO-2 regulates directly the cytoskeleton organization by binding to actin but also indirectly by affecting protein Rac-1 activity (a small GTPase known to regulate actin) (Guillemot et al., 2008).

PAR-3, PAR-6, PALS1 and PATJ, proteins part of the apico-basal polarity machinery were detailed in section 2.1.

MUPP1 has 13 PDZ domains, allowing it to scaffold and regroup protein complexes along the lateral membrane alongside the TJs. It binds to Claudins, JAM-1, CAR, Crumbs-1 and the angiomin (AMOT) family.

AF-6 (Afadin) was originally identified as a fusion protein of the acute lymphoblastic leukemia-1 (ALL-1). It is concentrated at the levels of the TJs but also the AJs. It could bind to the JAMs and the Eph (Erythropoietin-Producing human Hepatocellular receptors) family of tyrosine kinase receptors. It interacts with profilin, a major remodeler of actin filaments. AF-6 appears to play a critical role for early polarization of the apical junctional complex (Huang et al., 2012).

The MAGI family. This family will be detail in chapter 5 of this thesis manuscript.

Hence, the PDZ containing domain proteins of the TJs plaque regroup many proteins, involved in signaling, adhesion and maintenance of the TJs.

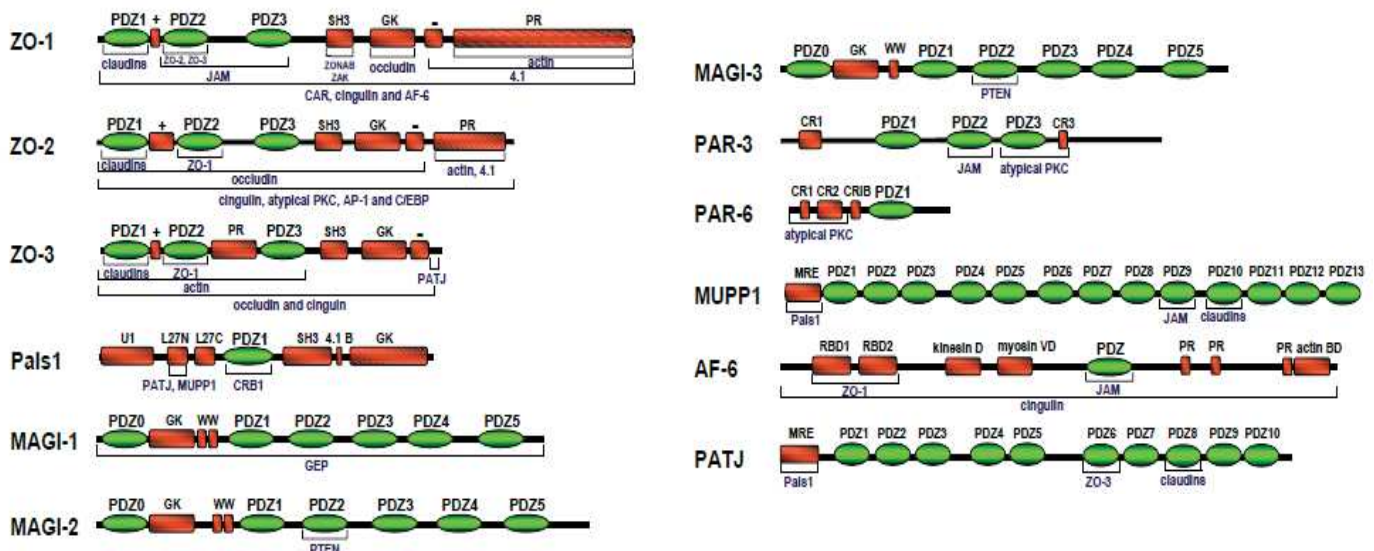


Figure 11: The different PDZ containing domain proteins associated with the TJs. Their potential interactors are represented. Taken from Gonzalez-Mariscal et al, 2003

- Members of the non PDZ containing proteins of the TJ plaque

Cingulin and Paracingulin. Unlike Cingulin, a TJs specific protein, Paracingulin is found at TJs and AJs. They both associate with the actin and microtubule cytoskeletons. Cingulin interacts with Myosin and is recruited to the TJs by ZO-1 (Gonzalez-Mariscal et al., 2016). Both proteins can regulate RhoA activity (a small GTPase molecule able to regulate the dynamic of Actin). Cingulin is characterized by a globular head and forms a parallel homodimer with two subunits. The head

interacts with several protein, such as Actin but also the ZO protein family, Occludin. Its knock-down or upregulation do not affect the TJs formation and the barrier function but affects the expression of a wide range of genes, including several genes coding for the TJs components Claudin and Occludin (Guillemot et al., 2004).

AMOT family. This family will be presented in the future section 3.3 of this manuscript.

The protein plaque is composed of many other proteins implicated in signaling and the maintenance of cellular architecture.

b. Adherens junctions:

AJs are found directly below the TJs (Figure 6). They connect neighboring cells together by initiating and stabilizing the cell-cell adhesion. These junctions contribute to the establishment and maintenance of the apico-basal polarity of the epithelial cells (Coopman and Djiane, 2016) but also to mechanical sensor functions and to signaling pathways that are essential for survival, growth and development, proliferation and differentiation (Collinet and Lecuit, 2013).

They were first referred to as stable structures at the cellular membrane (Farquhar and Palade, 1963) but a dynamic view of these junctions has emerged in the recent years. Even though cells need stable adhesion to sustain a robust entity and polarized epithelia, cell-cell contact remodeling occurs in a variety of physiological processes such as development and wound healing (Collinet and Lecuit, 2013). The remodeling of AJs is associated with adjustment of cell size, structure and activity (Coopman and Djiane, 2016). Plasticity of the AJs is not just the product of adhesion molecules recycling, it is also due to active pulling forces that are caused by the interaction between actin filaments and AJs components (Takeichi, 2014). The core of the AJs is composed of the cadherin superfamily such as E-cadherin and catenin family members' p120, α -catenin and β -catenin (Figure 12).

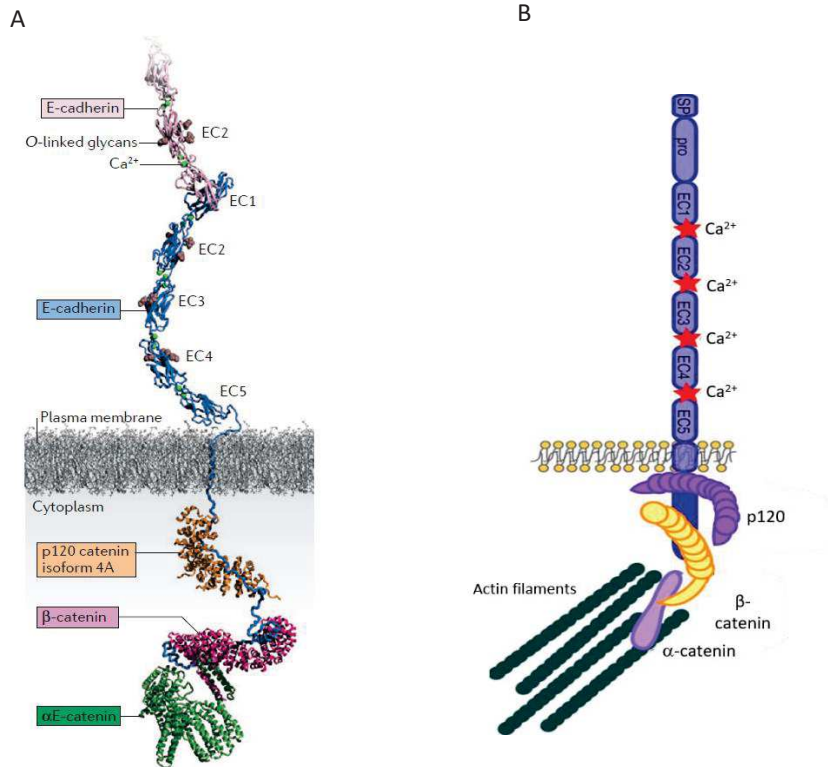


Figure 12: Molecular architecture of adherens junctions.

a) A model for the E-cadherin and the catenin family complex based on crystal structure: pink and blue domains (the ectodomain) of the E-cadherin is bound to divalent Ca^{2+} ion (green) and O-linked glycans (brown). The p120 catenin (orange) binds to the juxtamembrane domain of E-cadherin. The β -catenin (dark pink) and the α -catenin bind the E-cadherin-catenin binding domain found in the cytoplasmic domain of E-cadherin. **Taken from Masatoshi Takeichi 2014**

b) A schematic model of the interaction between the E-cadherin and the catenin family proteins. The extracellular domain of the E-cadherin contains five repetitions (EC1-5). The combination of three calcium ions between each EC domain enables the formation of rigid homophilic interactions in trans (by its EC1) with other E-cadherin molecules present on the neighbouring cells. The cytoplasmic domain allows the interaction with the catenin family proteins that play an important role in anchoring the F-actin at the levels of the AJs. **Adapted from Wheelock et al, 2008.**

i) The core complex of the AJs

E-cadherin:

Cadherins, a name derived from "Calcium dependent ADHESion", constitute a superfamily of transmembrane glycoproteins, which may interact in trans with other cadherin molecules, in a calcium dependent manner through their extracellular domain, and which play a key role in their adhesion function (Takeichi, 1977).

The E (epithelial)-cadherin is considered as the main protein in the classical cadherin family along with the N (neural), the P (Placental), the R (Retina) and the VE (vascular endothelial) cadherin. It is a transmembrane glycoprotein with one single-pass (Hartsock and Nelson, 2008).

The extracellular domain or ectodomain of E-cadherin is formed by five repetitions of extracellular cadherin repeats (EC1-5) in tandem. EC1-4 are highly conserved between species whereas the EC5,

also known as MPED (Membrane Proximal Extracellular Domain), is the least conserved. Then, the hydrophobic membrane domain is followed by a short cytosolic domain (Figure 12). The latter enables the interaction of E-cadherin with other proteins implicated in endocytosis, recycling, degradation, signaling, transcription and the regulation of the actin cytoskeleton (Hartsock and Nelson, 2008). This domain has two binding regions: the JMD (for juxtamembrane domain) binding to p120-catenin and the CBD (for catenin binding domain) associated with β -catenin. The anchoring of E-cadherin to the actin cytoskeleton is processed through α -catenin which is able to bind to β -catenin.

The total knockout of E-cadherin is lethal in mouse embryos which show defects in cell junctions and in the organization of the cytoskeleton, which in turn lead to the failure of formation of the trophectoderm, the first polarized epithelial layer in the embryo (Larue et al., 1994). Moreover, conditional knockouts (removing the gene in a specific tissue) confirm the important role of the E-cadherin not just in establishing cell-cell adhesion but also in the formation of the TJs (Tunggal et al., 2005).

E-cadherin is tightly regulated in cells and cadherin-mediated cell-cell adhesion is highly dynamic. For example, during epithelial to mesenchymal transition in normal and cancer cells, the expression of E-cadherin is downregulated while other members of the cadherin superfamily are taking over. The regulation of the cadherin switch and the implication of E-cadherin in cancer will be further detailed in chapter 4.2 of the introduction.

p120-catenin:

p120 was initially identified as a substrate for Src kinase. Its tyrosine phosphorylation mediated by Src correlated with cellular transformation (Reynolds et al., 1989) and then later assigned to the catenin family due to its sequence homology with β -catenin. p120-catenin is ubiquitously expressed.

It has 10 armadillo repeats allowing it to interact with the JMD of E-cadherin and mutations in this domain have shown that it is necessary and sufficient to recruit p120 to the AJs (Thoreson et al., 2000). This binding stabilizes E-cadherin by preventing its endocytosis. This was demonstrated by conducting downregulation experiments of p120 in human cells; the downregulation causes the loss

of membranous E-cadherin, its internalization and its trafficking to the lysosomes for degradation (reviewed in (Xiao et al., 2007)). p120 is not required for the correct distribution of E-cadherin at the plasma membrane but once it is there its stabilization depends on the presence of p120. Different studies have highlighted several mechanisms to better understand the stabilization of E-cadherin by p120. It was demonstrated that p120 is in competition with Presenilin 1 and Hakai to bind the JMD of E-cadherin. Presenilin 1 binds to E-cadherin and mediates its proteolytic cleavage (Kouchi et al., 2009) whereas Hakai is an E3 ubiquitin ligase able to bind phosphorylated E-cadherin and target it to degradation (Fujita et al., 2002). Other evidences suggest the presence of a di-leucine motif next to the JMD important for the clathrin-dependent E-cadherin endocytosis, which is hidden by the binding of p120 hide this motif (Chiasson et al., 2009).

Another important role of p120 is the regulation of Rho family of small GTPases (RhoA, Rac1 and Cdc42). This family of proteins regulates cell migration and the actomyosin cytoskeleton dynamic. p120 inhibits RhoA and activates Rac1 and Cdc42. It can directly bind and inhibit RhoA activity. Moreover, at newly formed AJs, p120 can activate Rac1 and Cdc42 to promote actin cytoskeleton remodeling and at the same time recruit 190RhoGap which is a mediator of Rac-dependent inhibition of RhoA activity. Finally, p120 associates and links directly the Rho associated protein kinase 1 (ROCK1) to the plasma membrane (Kourtidis et al., 2013) and it can also regulate the stability and the association of microtubules at the AJs.

β-catenin:

β-catenin has 12 armadillo repeats mediating protein-protein interactions and was first discovered as an adhesion molecule present at the level of AJs linking E-cadherin to F-actin via α-catenin (Kemler, 1993). It binds E-cadherin through its armadillo repeats in a phospho-regulated manner while its N-terminal part binds α-catenin.

In vivo, the knockout of β-catenin is lethal at the embryonic stage, 5.5 days after mating: the absence of the β-catenin leads to a defect in the ectoderm formation and a failure in the establishment of the A/B polarity axis (Huelsenken et al., 2000).

It plays a dual role depending on its localization in the cell:

- a. Part of the AJs core complex to stabilize the complex.
- b. A key nuclear effector associated with the WNT canonical pathway (detailed in section 3.1 of the manuscript).

How can the β -catenin mediate both adhesive and signaling functions separately?

Its structure has the answer. Most of the β -catenin binding proteins have overlapping sites at the levels of the ARM repeats: E-cadherin, APC (for adenomatous polyposis coli, an important partner in the destruction complex) and TCF/Lef (for T Cell Factor/ Lymphoid Enhancer binding protein, its main partner in the nucleus) (Valenta et al., 2012) (Figure 13). Moreover, depending on its conformation, β -catenin will be committed to a specific role. To date, the switch between the two pools of β -catenin is still not entirely clear. Brembeck et al. have characterized BCL9 (B-cell CLL/lymphoma 9 protein)-2 and shown that its binding domain overlaps with the α -catenin binding domain. They identified a tyrosine that needs to be phosphorylated within this region enhancing its binding to BCL9-2 and inducing its translocation into the nucleus and thus enabling its transcriptional activity (Brembeck et al., 2004). siRNA directed against BCL9-2 in SW480 fibroblast-like cells enhanced their epithelial morphology by keeping the β -catenin at the level of the membrane and stabilizing the core complex of the AJs whereas the expression of BCL9-2 in MDCK cells (epithelial cells) induced EMT.

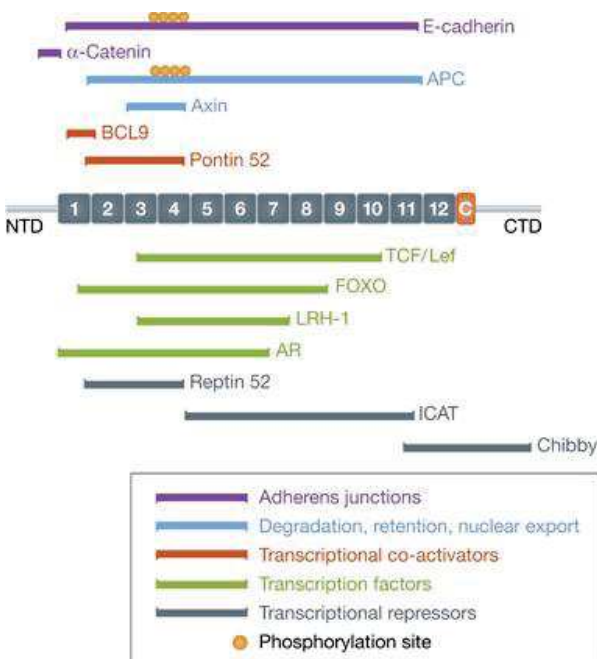


Figure 13: β -catenin structure and binding partners.

The β -catenin protein is composed of 12 armadillo repeats represented by boxes flanked by the N and the C terminal domains. The different binding proteins based on the bibliography are represented. All of these partners have overlapping binding domains. The one in purple represents the protein related to AJs, in blue are related to the β -catenin destruction complex, in red are activators of the β -catenin transcription function, in green are the different transcription factor bound by β -catenin the nucleus and finally in grey are proteins able to repress the transcription activity of β -catenin. Orange circles represent phosphorylation sites known to enhance the binding to β -catenin. APC, Adenoma Polyposis Coli; TCF/Lef, T-cell factor/Lymphoid enhancer factor; AR, Androgen Receptor; LRH-1, Liver Receptor Homologue-1; ICAT, Inhibitor of b-catenin and TCF; BCL9, B-cell lymphoma-9. **Taken from Valenta et al, 2012.**

The interaction between β -catenin and the newly synthesized E-cadherin occurs in the endoplasmic reticulum (ER). This interaction provides a mutual protection of both proteins. The binding of β -catenin to E-cadherin covers the PEST (for proline, glutamate, serine, threonine) domain of E-cadherin recognized by the E3 ubiquitin ligase thereby protecting it from degradation. Simultaneously, E-cadherin association to β -catenin protects it from degradation mediated by its destruction complex in the cytoplasm (Valenta et al., 2012).

β -catenin can also associate with several proteins implicated in the actin cytoskeleton regulation such as Fascin, IQGAP and α -actinin (see section 2.3 for more details about these proteins).

α -catenin:

α -catenin has three different isoforms: α E (epithelial)-catenin, α N (neural)-catenin and α T (heart and testicles) catenin. It has three domains, the N-terminal, the middle and the C-terminal and each domain has a different set of interactors. For example, the N-terminal part binds β -catenin, the middle part can associate with vinculin, an actin binding protein closely related to α -catenin, and the C-terminal domain can link F-actin (Takeichi, 2018).

α -catenin is needed to strengthen the cadherin-catenin complex adhesiveness by linking it to the actin cytoskeleton under force and tension. Cells lacking α -catenin display a deficiency in cell-cell adhesion, and even though they do have the rest of the core complex, they fail to concentrate it at the cell surface suggesting that α -catenin plays an important role in maintaining the cadherin /catenin complex at the level of the membrane (reviewed in Scott and Yap, 2006).

Interestingly, α -catenin is detected as a homodimer in the cytosol. This homodimer binds F-actin in a cadherin-catenin independent manner to regulate the F-actin dynamic suggesting that α -catenin has other roles than cell-cell adhesion. The association with β -catenin masks its homo-dimerization domain concluding that α -catenin is in its monomeric form when associated to the AJs. It can also translocate to the nucleus and interfere with the transcriptional activity of β -catenin. (Takeichi, 2018).

α -catenin possesses other binding partners such as α -actinin, afadin and formin (actin binding proteins), zevatin which binds the non-muscular myosin at the same time linking the AJs to actin and tension forces and finally ZO-1 (component of the TJs) (Kobielak and Fuchs, 2004).

ii) The phospho-regulation of the cadherin-catenin complex association and levels

The structural and functional integrity of the E-cadherin/catenin/actin complexes is largely regulated by phosphorylation and de-phosphorylation processes, respectively dependent on protein kinases and phosphatases. The phosphorylation of these proteins can affect them either by increasing their affinity to bind other proteins or by inhibiting their protein interactions or by affecting their amount in cells (Bertocchi et al., 2012).

A main kinase family implicated in the regulation of the core complex interaction is the Src family of tyrosine kinases (reviewed in (Coopman and Djiane, 2016) and this by:

- i. Phosphorylation of E-cadherin on two different residues (Y753/754) enabling thus its degradation through the proteasome
- ii. Phosphorylation of β -catenin on Y86 and Y654 thus decreasing its affinity for E-cadherin
- iii. Phosphorylation of α -catenin on Y177 thus inhibiting cell adhesion
- iv. Phosphorylation of p120-catenin on Y112 thereby destabilizing the AJs

Other kinases can affect the establishment and the levels of the core AJs complex:

- i. The RET receptor kinase can phosphorylate β -catenin and impair its binding E-cadherin
- ii. The tyrosine kinases such as EGFR FGFR2-3 are able to phosphorylate β -catenin thus causing its dissociation from the membrane and its cytoplasmic accumulation finally activating the WNT/ β -catenin canonical pathway.
- iii. CK1, a serine/threonine kinase, phosphorylates E-cadherin. This phosphorylation inhibits its localization at the membrane weakening its binding to β -catenin.
- iv. JNK phosphorylates β -catenin disturbing its cellular contacts

While many phosphorylations have negative effect on the AJs complex, others promote its stabilization. The SYK kinase, CK2 and PKC ensure the correct localization of the different components at the cell membrane and the enhancement of cell-cell adhesion.

iii) Nectin/Afadin complex

The Nectin/Afadin complex is also essential for intercellular adhesion at the level of the AJs. From a structural point of view, Nectin is an adhesion molecule related to the immunoglobulin

(Ig)/Calcium-independent superfamily and containing three Ig domains in its extracellular part. The family of nectins is composed of four members which form homodimers in cis on the same cell. They share the same general structure, defined by three extracellular Ig type domains, one transmembrane domain and an intracellular domain capable of interacting with the actin-binding protein, Afadin/AF-6.

Loss of Afadin delays the E-cadherin localization at the cell membrane but also weakens the AJs. Nectin/Afadin interacts with Par3 and controls its' correct spatio-temporal localization, and thus A/B polarity establishment. (Campbell et al., 2017).

c. Interplay between AJs and TJs and assembly of apical junctions:

The TJs and the AJs are not independent structures; they communicate and are physically linked. During the assembly of the apical junctions of the cells, the assembly of the AJs enables the formation of TJs. Below, the assembly of apical junctions reviewed in (Campbell et al., 2017; Coopman and Djiane, 2016) Figure 14 is detailed :

1. Actin protrusions are formed in order to get adjacent membranes for two different cells.
2. The Nectin/Afadin complex is set up and forms an homophilic interaction in trans. Afadin recruits ZO-1
3. The cadherin complex assembles and α -catenin binds ZO-1.
4. Once the AJs matured, the occludins and other TJs proteins are recruited.
5. Occludins bind ZO-1 and as TJs matured, ZO-1 dissociates from the AJs and binds exclusively the TJs.

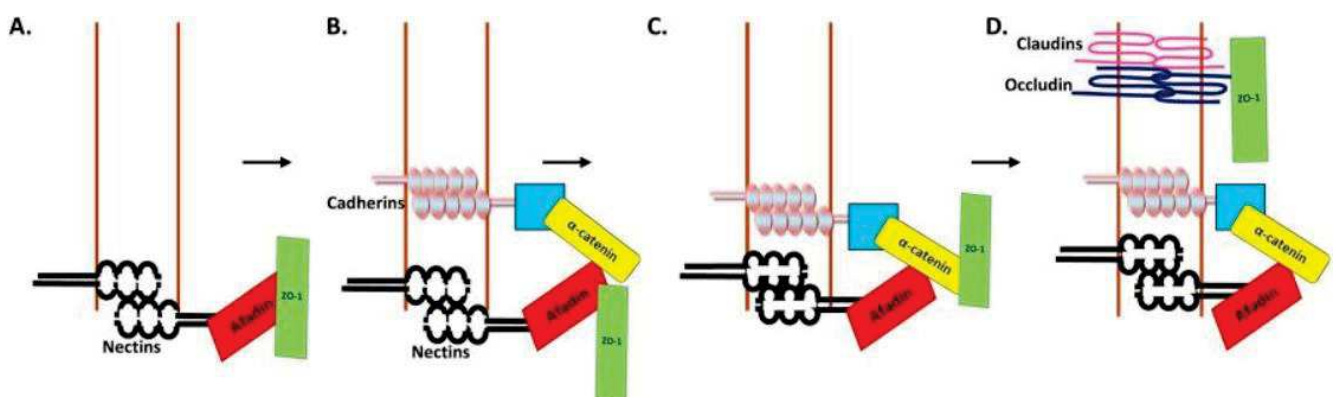


Figure 14: Sequential formation and assembly of the AJs and the TJs.

Once membranes of adjacent cells meet, a nectin/Afadin complex based trans interaction is established. Afadin (in red) recruits ZO-1 to the membrane and the cadherin complex starts to assemble (Cadherin in pink, α -catenin in yellow and β -catenin in blue). The α -catenin binds ZO-1 and the AJs starts to mature. As the AJs mature, occludins and claudins (proteins of the TJs core) are recruited and ZO-1 switches partners and associates with occludin). **Taken from Campbell et al, 2017**

This model of junctional assembly is not exclusive and many studies suggest the implication of other protein complexes. Moreover, ZO-1 is shown to have other binding proteins at the levels of the AJs such as vinculin, proteins implicated in the regulation of F-actin dynamic suggesting that ZO-1 modulates the actin cytoskeleton at the levels of the apical junction promoting maturation and assembly of its different components.

2.3. Maintenance of cellular architecture (actin cytoskeleton):

The cytoskeleton is constituted of cytoplasmic proteins forming a robust structure inside the cell Figure 15. It has three main role (Pollard and Goldman, 2018):

- Spatially organize the intracellular space.
- Connect the cell physically and biochemically to its surrounding environment.
- Maintain mechanical integrity and generate coordinated force that enable the cell to move, divide and change shape.

In Eukaryotic cell, the cytoskeleton is composed of three polymers, the actin filament (F-actin), the intermediate filament and the microtubules. The structure of these polymers is different and each one of them has its own function inside the cell. Immunofluorescence images (cf Figure 15) show that one pool of actin (in blue) is concentrated around the periphery of the cell (cortical actin) and another pool is present in bundles (stress fibers) and is anchored to the plasma membrane at

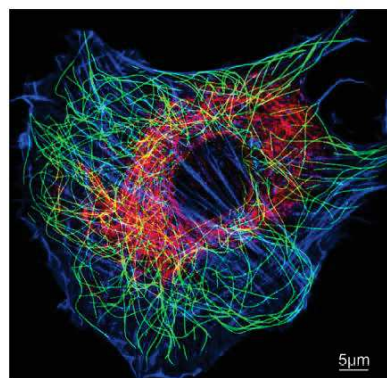
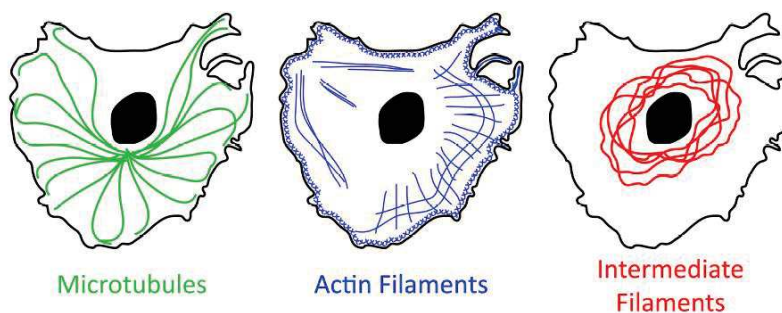


Figure 15: Cytoskeleton organization in cells. Fluorescence of a cultured fibroblast stained with fluorescent phalloidin (blue) and antibodies to microtubules (green) and intermediate filaments (red). **Adapted from Pollard and Goldman, 2018.**



adhesion sites (Svitkina, 2018). In contrast, the intermediate filaments (in red) are present in the cytoplasm around the nucleus and they propagate to the periphery to anchor the desmosomes and the hemi-desmosomes (Jones et al., 2017) (mentioned in section 2.2.a and 2.2.b). Finally, the microtubules which are dense, long and stiff polymers (in green) all start from one specific point inside the cell: the Microtubule Organizing Center (MOC), and radiate to the edge of the cell.

These three filaments assemble spontaneously inside the cell under physiological conditions. The microtubules and the F-actin are dynamic features and they require energy (GTP (guanine triphosphate) and ATP (adenosine tri-phosphate) respectively) for their polymerization/depolymerization (reviewed in (Pollard and Goldman, 2018)). The components of the cytoskeleton are linked together; this link provides a robust mechanosensation web in the cell.

In the section below, I will mainly detail the actin cytoskeleton because of its relevance to my project.

Cells are able to change their shape and adapt to their environment, to divide, to migrate in order to pass through narrow spaces and to activate endo and exocytosis. The main mechanism by which these cells modify their shape is by assembling actin. Actin are monomers of proteins assembled into a variety of architecture (cf Figure 16) that fulfill a multitude of functions.

At the front of the cell, the branched and cross-linked actin (lamellipodia) acts as an engine for cell movement and its polymerization pushes the cell membrane forward. Filopodia help the cell determine the direction in which it will be going. Cortical actin maintain cell shape and Stress fibers connect the cell to the ECM via focal adhesions sites acting as tension sensors (shown in Figure 16). The myosin superfamily, a well-known actin molecular motor, assembles in filaments and once incorporated in F-actin causes its contraction and tension (Blanchoin et al., 2014).

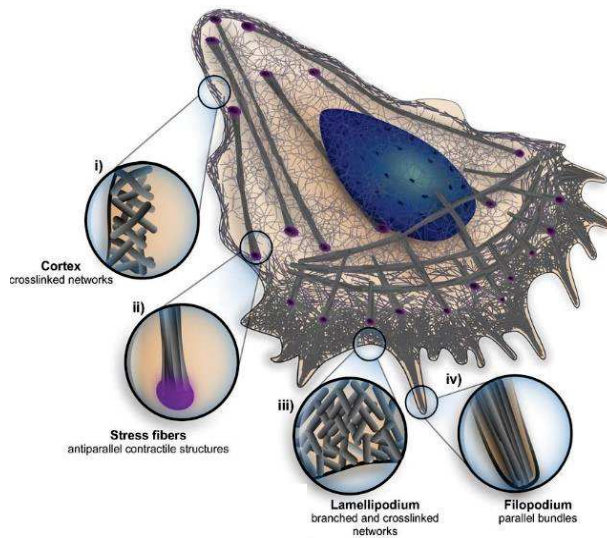


Figure 16: Schematic representation of a cell with different architecture.

i) cell cortex, ii) an example of contractile fibers: the stress fibers, iii) lamellipodium, vi) filopodium.
Adapted from Blanchoin et al, 2014.

How this diversity of actin structures is generated inside the cell?

a. Dynamic of the actin cytoskeleton:

The core component of actin filaments is G-actin or globular actin. It will assemble into double helical filaments called F-actin. The assembly is composed of three main steps: nucleation, elongation and steady states (summarized in Figure 17).

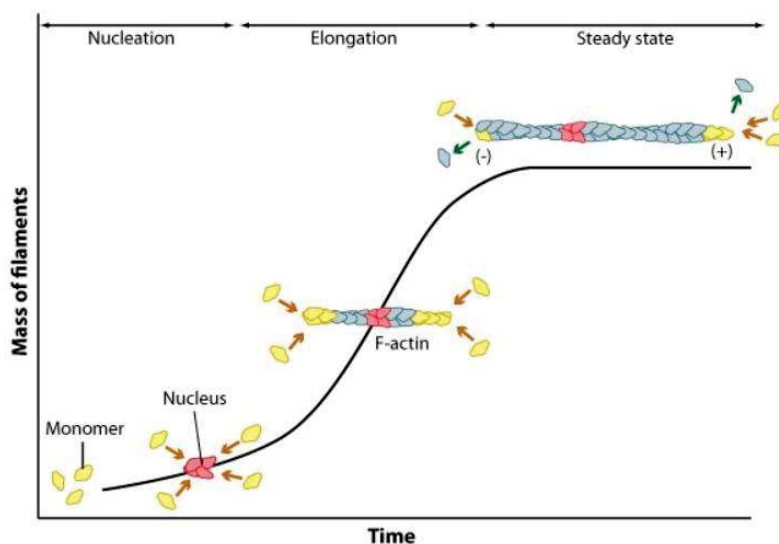


Figure 17: Steps for F-actin formation: Nucleation, Elongation and steady state phase.
Taken from <https://www.mechanobio.info/cytoskeleton-dynamics/what-is-the-cytoskeleton/what-are-actin-filaments/how-do-actin-filaments-grow/>.

One monomer of G-actin has binding sites for two additional monomers. Binding an ATP molecule and an Mg^{2+} bivalent ion, the monomer is active and ready for the nucleation step. The nucleation step is the formation of a trimer of G-actin. Once the trimer is formed the elongation occurs. This step consists in the addition of monomers from both sides of the trimer. The actin filament has two distinguishable ends: the positive (barbed) and the negative (pointed) end. It is noteworthy that the positive end polymerizes five to ten times faster than the negative end. The polarity of the F-actin is important for the assembly but also for the myosin filament movement relative to the actin (Cooper, 2000).

The ATP is hydrolyzed upon the incorporation of the monomer inside the filament.

The last step (steady state) is the step in which the concentration of G-actin is low and an equilibrium between the G-actin and the F-actin occurs in the cell: the association of actin-ATP is compensated by the dissociation of actin-ADP.

After each dissociation, the ADP is exchanged with an ATP and the monomer is integrated again in the filament. This phenomenon of polymerization at the positive side, the hydrolysis of ATP, the dissociation of actin-ADP at the negative end and the exchange of nucleotides is called treadmilling of the F-actin (Gressin, 2016).

Hence, the formation of actin filaments in the cell is a dynamic mechanism. It is regulated by the concentration of salt at the physiological state, the concentration of ATP, and the concentration or the availability of G-actin.

But having different structures of F-actin inside the cell implies the need to have regulators able of guiding the cell toward each type to meet its needs. Thus, the next part will deal with the actin regulation and regulators.

b. Regulation and associated proteins:

In vivo, cells tightly control the turnover of actin and this is done by:

1. Maintaining G-actin stores
2. Triggering the formation of new filaments and forming specific structures
3. Inhibiting when needed the polymerization of the minus end (preventing shortage of G-actin)

4. Accelerating the disassembly of old F-actin to maintain a high concentration of G-actin inside the cell

This is regulated by actin binding proteins (ABPs). ABPs include Profilin, nucleation proteins, capping proteins and Cofilin or ADF (for actin depolymerizing factor) (summarized in (Pollard, 2016)).

i. Profilin:

The G-actin located in the cell is not stable; it needs to be associated to Profilin, a step essential for cell survival since its knockdown abolishes the formation of all lamellipodia in *Drosophila* (Rogers et al., 2003). Profilin has high affinity for ATP bound G-actin, and binds the barbed end of the monomers inhibiting their spontaneous nucleation thus promoting polymerization only at the barbed (+) end of the filaments. Once the monomer is associated to the filament, Profilin dissociates freeing the barbed end for extra polymerization.

Another important role of Profilin is to dissociate ADP from newly freed actin monomers thus favoring the exchange with ATP priming actin monomers to be integrated in F-actin.

ii. Nucleation proteins:

(Figure 18) Nucleation proteins include the ARP (actin related protein) 2/3 complex, responsible for branched/cross-linked Composed of actin formation, this complex is poised in cells and activated by a nucleation promoting factor (NPF) such as N-WASP (Wiskott-Aldrich syndrome protein). It catalyzes the polymerization of de novo filaments recycling older filaments (Chesarone and Goode, 2009).

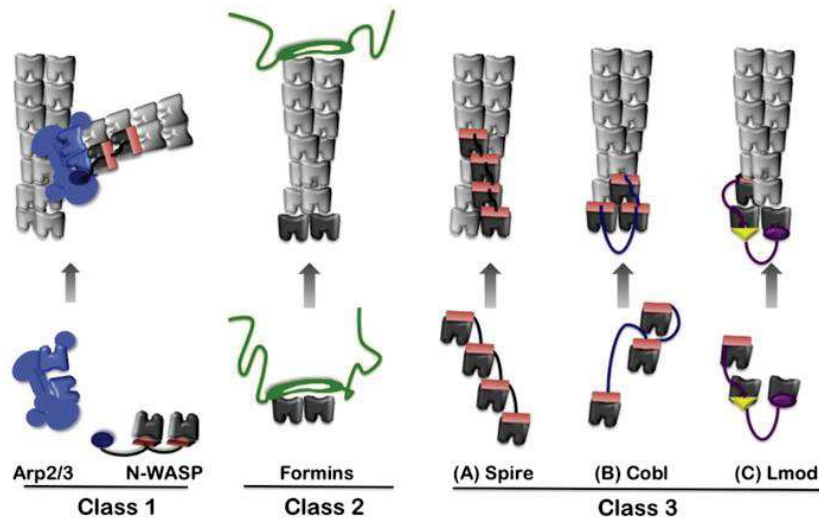


Figure 18: Summary of the different classes of actin nucleators and their mechanisms of action. ARP2/3 is recruited on a pre-existing actin filament and acts simultaneously with its N-WASP activator. ARP2/3 contains two actin-related subunits, in addition to those present on N-WASP, allow the nucleation of a new filament. The formin dimerizes in a round shape and is capable of stabilizing two actin monomers to initiate elongation of a filament. Formin remains associated with the barbed end of the actin filament to promote elongation. Spire, Cobl, Lmod, interact with three or four actin monomers via the WH2 domain or other domains as is the case for Lmod. They are then able to form a stable nucleus to initiate the elongation of the filament. Adapted from Chesarone and Goode 2009.

Other proteins in this family include the Formins, nucleators of bundled actin implicated in stress fibers, filopodia, cytokinesis, polarized cell growth, cell motility and vesicle transport (Edwards et al., 2014). This family of protein is characterized by the presence of two well-defined domains called FH1 and FH2 essential for the nucleation. While FH2 can dimerize and form a circle around and stabilize the barbed extremity for further polymerization, the FH1 domain binds Profilin linked to ATP-actin thus bringing actin monomers closer to the nucleation area and facilitating the elongation process (Chesarone and Goode, 2009). The Ena/Vasp family of nucleators has similar functions as Formins.

WH2 domain containing proteins also include Spire, Cordon bleu (Cobl) and Leiomodinn (Lmod) (Quinlan et al., 2005; Ahuja et al., 2007; Chereau et al., 2008). These proteins bind and cluster G-actin monomers, a step sufficient to create a stable nucleus and initiate F-actin elongation (Chesarone and Goode, 2009).

iii. Capping proteins (Cp):

These proteins inhibit the elongation of F-actin. Indeed, uncontrolled actin filaments elongation is toxic in part because actin pushing toward the cell membrane generates pressure that might lead to

plasma membrane breakage. Cp proteins compete with nucleation proteins such as profilin to bind the barbed end of F-actin (Dang, 2014) thus ensuring tight regulation and recycling of actin monomers.

Cross linker proteins such as Filamin, α -actinin, Fascin, Fimbrin, Spectrin and Dystrophin further stabilize the different F-actin architectures (Figure 19). They affect the dynamics of the actin cytoskeleton by cross-linking actin filaments and other cytoskeleton components thus creating a scaffold that provides cellular stability and integrates the inputs from different signaling pathways such as the Hippo pathway.

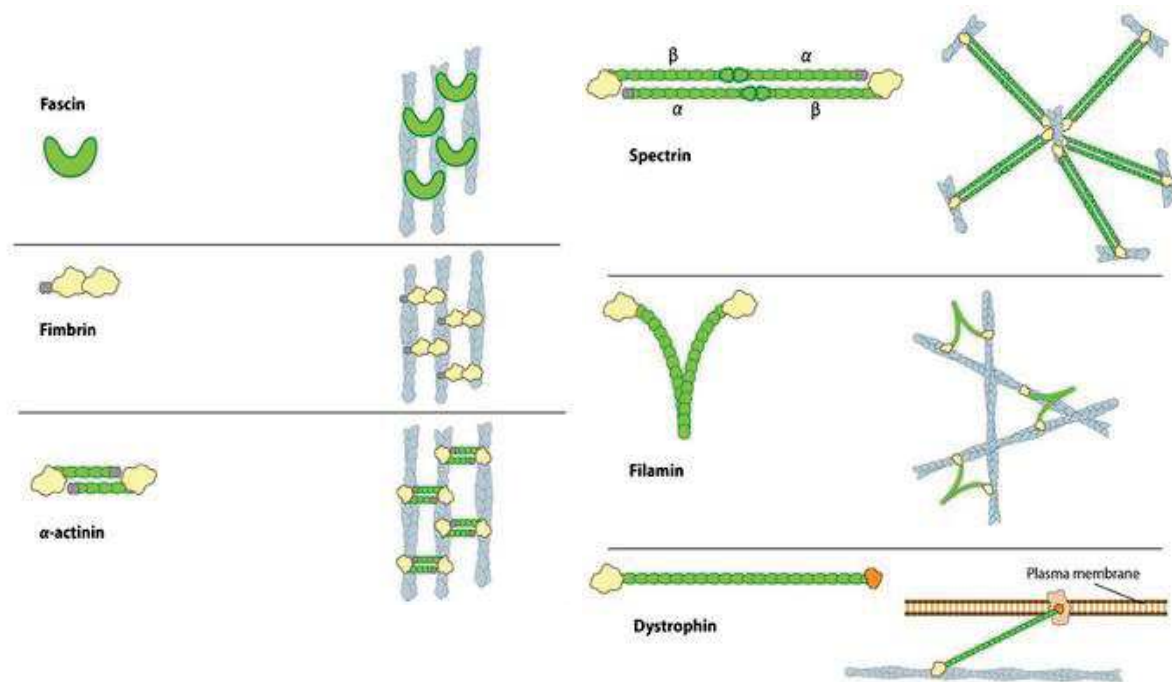


Figure 19: A non-exhaustive list of the different bundlers and crosslinkers of actin. Small proteins such as fascin, fimbrin and α -actinin form actin bundles. Others that are larger such as Spectrin, filamin and dystrophin create larger spaces between the different F-actin and thereby form actin networks. Taken from <https://www.mechanobio.info/cytoskeleton-dynamics/actin-crosslinking/>.

iv. Severing proteins: Cofilin/ADF

They control the depolymerization, the disassembly and the fragmentation of F-actin. Five members have been characterized: ADF, Cofilin, Actophorin, Depactin and Destrin.

These proteins are able to bind G- and F-actin. For instance, Cofilin binds preferentially to ADP-conjugated G-actin monomers preventing the ATP nucleotide exchange, thus preventing polymerization. Cofilin also binds the ADP-actin of old F-actin causing twisting and rendering it more suited for depolymerization (Gressin, 2016).

Small GTPases such as Rho, Rac and Cdc42 are the main regulators of ABPs and thereby of actin cytoskeleton organization and remodeling.

The actin cytoskeleton is therefore a highly dynamic multi-protein polymer that is tightly regulated and involved in many physiological processes.

3. Implication of junctions in signaling :

Many components of the different signaling pathways are located and concentrated at the level of cellular junctions and are regulated by the polarity machinery. In this chapter, I will give few noteworthy examples relevant to the project.

3.1. WNT/ β -catenin pathway:

The β -catenin protein is essential both for the structure and function of the AJs and the WNT/ β -catenin signaling pathway.

While the membrane pool of β -catenin is highly stable, the cytoplasmic pool is not. In the absence of WNT signaling, the cytoplasmic pool is destroyed (Bienz, 2005). It is worth mentioning that the membrane pool of β -catenin is tightly bound to E-cadherin and this interaction is regulated by phosphorylation events (Nelson and Nusse, 2004).

WNT stands for *Wingless* (the segment polarity gene in *Drosophila melanogaster*) and its homolog in vertebrates *integrated* (*int-1*) (Komiya and Habas, 2008). They are secreted glycoproteins that regulates many cellular processes such as cell fate determination, cell migration, proliferation stem cell renewal, neuronal patterning but also organogenesis during embryonic development and playing a key roles during adult tissues homeostasis in multicellular organisms (Steinhart and Angers, 2018).

When WNT is OFF (cf. Figure 20), the destruction complex is active in the cytoplasm. It is composed of the scaffold proteins Axin, and Adenomatosis Polyposis Coli (APC), and of the enzymes protein phosphatase 2A (PP2A), glycogen synthase kinase β (GSK3 β) and casein kinase 1 α (CK1 α). The β -catenin is phosphorylated by CK1 α and GSK3. This phosphorylation is

important for the recruitment of the SCF E3 ubiquitin ligase which will target β -catenin to the proteasome for degradation (Komiya and Habas, 2008).

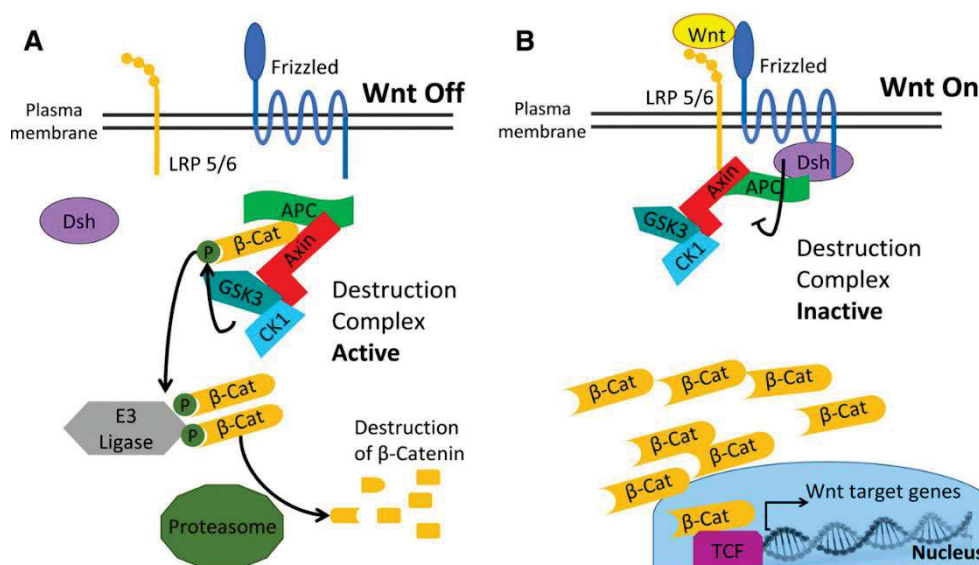


Figure 20: an overview of the WNT/Beta-catenin signaling pathway.
Taken from Schaefer et al, 2019

The binding of Wnt to the receptor Frizzled (Fz) and its co-receptor LRP5/6 (LDL Receptor related proteins 5/6) turns the pathway ON and induces first the recruitment of Dishevelled (Dsh) via its interaction with Fz. Secondly, Axin and GSK3 β are recruited by Dsh enabling the phosphorylation of the LRP5/6. This phosphorylation recruits CSK1 α which will phosphorylate LRP5/6. Finally, phosphorylated LRP5/6 binds Axin and promotes its degradation thus inhibiting the assembly of the destruction complex and stabilizing the cytoplasmic pool of β -catenin in the cell (Tolwinski and Wieschaus, 2004). However, studies (Cselenyi et al., 2008), (Piao et al., 2008) and (Stamos et al., 2014) have claimed that these phosphorylations directly block the degradation of β -catenin by inhibiting the kinase activity of the GSK3 β .

The accumulation of the β -catenin in the cytoplasm is then followed by its translocation to the nucleus where it acts as a transcription co-activator factor and modulates the Tcf (T Cell Factor)/Lef (Lymphoid Enhancer binding protein) family of DNA binding protein activity.

In the extracellular medium, secreted factors have been identified to be able to antagonize the interaction between WNT and FZ or LRP5/6. This includes Dickkopf (DKK) (Glinka et al., 1998), WNT inhibitor protein (WIF) (Hsieh et al., 1999), soluble Frizzled related protein (SFRP) (Hoang et al., 1998), Cerebrus (Bouwmeester et al., 1996) and others summarized in (Komiya and Habas,

2008). The canonical WNT signaling is implicated in many human diseases and in cancer. A summary of the implication of each component of the WNT signaling in diseases and cancer can be found in Table 2.

Gene	Condition/disease	Mutation or activity/ expression change	Reference
<i>WNT1</i>	Schizophrenia	Elevated	24
<i>WNT3</i>	Tetra-amelia	LOF	13
<i>WNT4</i>	Intersex	GOF	14
<i>WNT4</i>	Kidney damage	Elevated	16,17
<i>WNT4</i>	Polycystic kidney disease	Variable	18
<i>WNT5a</i>	Leukaemia	LOF; reduced	21
<i>WNT5a</i>	Metastasis	Elevated	22
<i>sFRP3</i>	Osteoarthritis	SNP; reduced	28
<i>FZ4</i>	FEVR	LOF	30
<i>LRP5</i>	FEVR, low bone mass	LOF	31,40
<i>LRP5</i>	High bone mass	GOF	37,38
<i>DSH/DVL</i>	Lung cancer	Elevated	47
<i>APC</i>	Cancer	LOF	46
<i>AXIN</i>	Cancer	LOF	45
<i>AXIN2</i>	Cancer, tooth agenesis	LOF	53
<i>β-catenin</i>	Cancer	GOF	45
<i>β-catenin</i>	Aggressive fibromatosis	Elevated	61
<i>β-catenin</i>	Pulmonary fibrosis	Elevated	65

APC, adenomatous polyposis coli; *DSH/DVL*, Dishevelled; FEVR, familial exudative vitreoretinopathy; *FZ*, Frizzled; GOF, gain of function; LOF, loss of function; *LRP*, LDL-receptor-related protein; *sFRP*, secreted Frizzled-related protein.

Table 2: Summary of diseases and syndrome in which the canonical WNT pathway component are implicated.

Taken from Moon et al, 2004

3.2. MAP kinase pathways:

The Mitogen Activated Protein Kinase (MAPK) pathways convey, enhance and integrate signals from a variety of stimuli such as growth factors and stress and mediate an appropriate cellular response including cellular proliferation, differentiation, apoptosis and inflammatory responses in mammalian cells (Qi and Elion, 2005; Zhang and Liu, 2002). This is achieved by phosphorylating different downstream targets such as Transcription Factors, cytoskeletal proteins and kinases that will play a role in gene expression, metabolism, cellular division and morphology as well as survival.

Till now, four classical branches have been characterized: The Extracellular Regulated Kinase 1/2 (ERK1/2), Jun N-terminal Kinase (JNK1, JNK2), P38 kinase isozymes (p38 α , p38 β , p38 γ and p38 δ) and ERK5 (Qi and Elion, 2005). The first three are the most characterized and I have chosen to detail the p38 pathway the most.

The MAPK pathways contain a kinase cascade comprising a MAP kinase kinase kinase (MAPKKK), a MAP kinase kinase (MAPKK) and a MAP kinase (MAPK). Most of the time, the

signal is sent by small GTPases anchored to the membrane. These GTPases are regulators of junctions assembly and stability and of the cytoskeleton (Citi et al., 2014) .

The MAPKKK are activated by relief of auto-inhibition and oligomerization or through binding to the small GTPases. This activation leads to the MAPKK activation by a dual phosphorylation of Serine threonine residues. Interestingly the MAPKK exhibit great specificity for their MAPK(Cargnello and Roux, 2011). Upon their phosphorylation, they phosphorylate the MAPKs on double residues (threonine and tyrosine) enabling thus their activity.

For all the pathways, scaffold molecules have been identified (Good et al., 2011). These proteins are able to tether at least two kinases from the cascade. The purpose of this, similarly to all scaffold proteins, is to enhance the signaling by concentrating the MAPKs together, providing thus a spatial and temporal regulation of the cascade and localizing the complex in a specific cellular site(Morrison, 2012). Specific scaffolds exist for each pathway: KSR (Kinase suppressor of RAS) and MP1 (MEK1 scaffolding protein) for ERK1/2, JIP1-4 (JNK interacting proteins) and POSH (Plenty of SH3s) for JNK and JIP1-2 and OSM (osmosensing scaffold for MEKK3) for p38(Morrison, 2012).

a. The ERK1/2 pathway:

ERK was the first MAPK that was cloned and characterized (Cargnello and Roux, 2011). It is a serine threonine kinase that transmits mainly mitogenic signals. It is located in the cytoplasm and translocates to the nucleus upon activation to regulate transcription factor activity and gene expression(Guo et al., 2020). The Ras-Raf/MEK/ERK pathway is one of the best MAPK signaling characterized so far.

The ERK module is activated by growth factors such as Platelet-Derived growth factor (PDGF), Epidermal growth factor (EGF), Nerve growth factor (NGF) and Insulin (Boulton et al., 1990). Moreover, it can be activated by G protein coupled receptors (GPCRs), cytokines, microtubules disorganization and osmotic stress (Raman et al., 2007).

The RAF family of proteins are the main MAPKKK composing this pathway (Figure 21). In contrast, MOS et TPL2 are utilized in a more restricted cell type and stimulus specific matter (Gotoh and Nishida, 1995),(Salmeron et al., 1996).

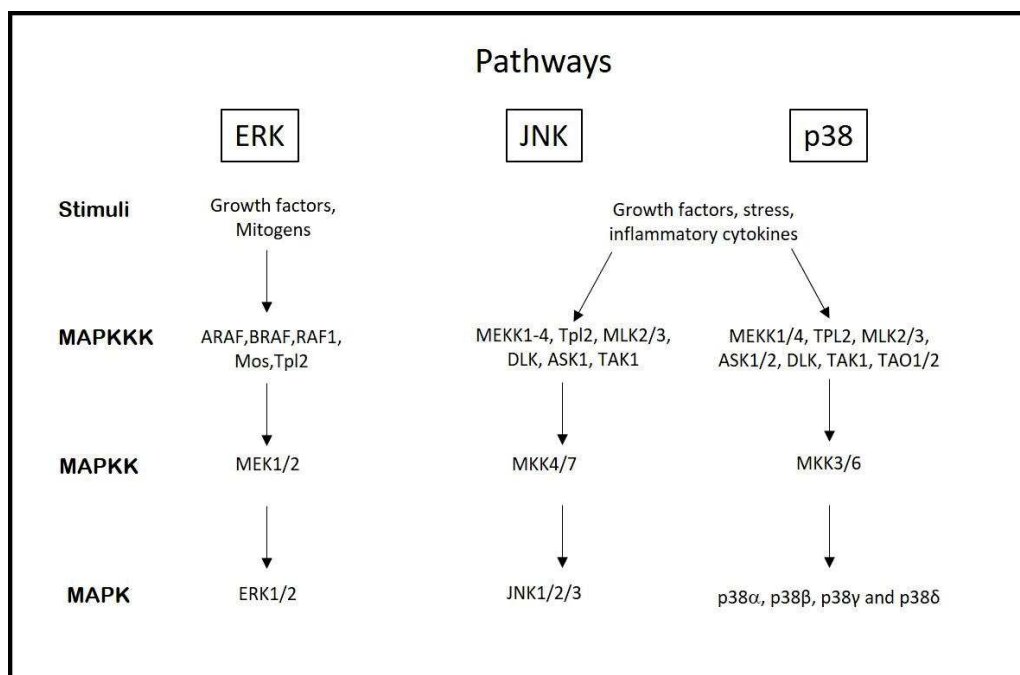


Figure 21: The MAPK signaling cascades.

ARAF: Serine-threonine protein kinase ARAF, BRAF: Serine-threonine protein kinase BRAF, RAF1: CRAF or Serine-threonine protein kinase CRAF, Mos: Serine-threonine protein kinase mos, Tpl2: MAP3K8 or Mitogen-activated protein kinase kinase 8, MEKK: Mitogen Activated protein kinase kinase 1, MLK: Mitogen Activated protein kinase kinase 11, DLK: Mitogen-Activated Protein Kinase Kinase 12, ASK: Apoptosis signal regulating kinase 1, TAK1: Mitogen-Activated Protein Kinase Kinase Kinase 7, TAO: serine threonine protein kinase TAO1, MEK1: Mitogen Activated protein kinase 1, MKK: Mitogen activated protein Kinase Kinase, ERK: Extracellular regulated kinase, JNK: Jun N-terminal kinase.

ERK kinase has many targets (reviewed in (Yoon and Seger, 2006)): some of them are localized in the cytoplasm like MLCK (Myosin light chain kinase) and RAF while others can be found in the nucleus such as ATF2 (Cyclic AMP-dependent transcription factor), cMYC (myc proto-oncogene protein), cFOS (fos proto-oncogene protein), STAT3 (signal transducer and activator of transcription) and SMAD2/3 (mother against decapentaplegic homolog 2/3). Interestingly, some targets are located at the level of the plasma membrane like SYK (tyrosine protein kinase syk) and EGFR or are part of the cytoskeleton such as Paxillin, Tau (microtubule associated protein tau), and Dystrophin.

The ERK pathway plays a critical role in the regulation of the cellular proliferation via several mechanisms (reviewed in (Meloche and Pouysségur, 2007)). As an example, Cyclin D1 which is crucial for the progression into the G1 phase of the cell cycle, has AP-1 (Activator Protein 1)

binding motifs at the levels of its promoter. ERK1/2 phosphorylates and stabilizes C-FOS and thereby its ability to bind to C-JUN and form a transcriptionally active AP-1 complex able to bind Cyclin D1 promoter and activate its transcription thus favoring the progression into the cell cycle.

Most players in the ERK pathway are frequently mutated in cancers (summarized in Table 3), leading to sustained activation of the pathway with typical pro-tumoral and anti-apoptosis effects(Guo et al., 2020).

Author, year	Tumour type	KRAS	NRAS	HRAS	BRAF	MEK	ERK	(Refs.)
Colombino <i>et al</i> , 2012; Edlundh-Rose <i>et al</i> , 2006; Namba <i>et al</i> , 2003; Davies <i>et al</i> , 2002; Murugan <i>et al</i> , 2009; Nikolaev <i>et al</i> , 2011; Wang <i>et al</i> , 2007; Jänne <i>et al</i> , 2017	Melanoma	15-29%	20%	N/A	90%	3-8%	67-90%	(51-58)
Nikolaev <i>et al</i> , 2011; Seo <i>et al</i> , 2012; Cardarella <i>et al</i> , 2013	NSCLC	35%	N/A	N/A	4%	N/A	N/A	(56,59,60)
Davies <i>et al</i> , 2002; Tol <i>et al</i> , 2009; Jones <i>et al</i> , 2017	Colorectal	40%	N/A	N/A	5-20%	<3%	N/A	(54,61,62)
Sieben <i>et al</i> , 2004	HGSOC	0-12%	N/A	N/A	N/A	N/A	N/A	(63)
Bell, 2005; Singer <i>et al</i> , 2003	LGSOC	27-36%	N/A	N/A	33-50%	N/A	N/A	(64,65)
Cardarella <i>et al</i> , 2013; Bansal <i>et al</i> , 2013; Paik <i>et al</i> , 2011	THCA	9-27%	9-27%	9-27%	10-70%	N/A	N/A	(60,66,67)
Bansal <i>et al</i> , 2013; Xing <i>et al</i> , 2013	PTC	20%	N/A	N/A	N/A	N/A	N/A	(66,68)
Singer <i>et al</i> , 2003; Bansal <i>et al</i> , 2013	ATC/FTC	N/A	15%	N/A	N/A	N/A	N/A	(65,66)
Tiacci <i>et al</i> , 2011	Hairy Cell	N/A	N/A	N/A	79-100%	N/A	N/A	(69)
Namba <i>et al</i> , 2003	PDA's	70%	N/A	N/A	N/A	N/A	N/A	(53)
Jones <i>et al</i> , 2017; Xi <i>et al</i> , 2012	AML/ALL	10%	N/A	N/A	N/A	N/A	N/A	(63,70)
Cardarella <i>et al</i> , 2013	BLCA	N/A	N/A	20%	N/A	N/A	N/A	(60)
Paik <i>et al</i> , 2011	RCCs	N/A	N/A	2%	N/A	N/A	N/A	(67)
Davies <i>et al</i> , 2002; Chao <i>et al</i> , 1999; Cheng <i>et al</i> , 2005; Sun <i>et al</i> , 2001	BC	<5%	N/A	N/A	1.2%	7-9%	N/A	(54,71-73)

NSCLC, non-small cell lung carcinoma; HGSOC, high-grade serous ovarian cancer; LGSOC, low-grade serous ovarian cancer; THCA, thyroid carcinoma; PTC, papillary thyroid cancers; ATC, anaplastic thyroid cancers; FTC, follicular thyroid cancers; PDA's, pancreatic ductal adenocarcinomas; AML, acute myeloid leukaemia; ALL, acute lymphoblastic leukaemia; BLCA, bladder urothelial carcinomas; RCCs, renal cell carcinomas; BC, breast cancer.

Table 3: Frequency of mutations in the components of the ERK1/2 pathway across different tumors.
Taken from Guo et al, 2020

b. The JNK pathway:

The Jun N-terminal kinase (JNK) also known as stress activated protein kinase (SAPK) is activated by stress stimuli in response to heat shock, ionizing radiation, oxidative stress, DNA damage, cytokines, UV and growth factor deprivation(Cargnello and Roux, 2011). The JNK kinases have three different isoforms JNK1, JNK2 and JNK3. The JNK1 and 2 are ubiquitously expressed. The MAPKK activating the JNK kinases are MKK4 and MKK7 (see Figure 21).

About hundred substrates have been documented for JNK (Zeke et al., 2016). Most of its targets are implicated in proliferation, cell death and cell movement. For example, diverse families of transcription factors are targeted by JNK such as the bZIP (for Basic Leucine Zipper) family (Jun and ATF2), the bHLH (for basic Helix-loop-Helix) family (HES1 (Hairy and Enhancer off split 1) and Twist1), the zinc finger family (Sp1 (Specificity Protein 1)), Forkhead (FOXO3, FOXO4 (for Forkhead box O3 and O4)) and RUNT (p53), as well as some nuclear receptors and the co-activator of transcription such as YAP1 (for YES associated protein 1) (reviewed in (Zeke et al., 2016)).

One of the main targets of this pathway is the JUN proto-oncogene. Being part of the AP-1 complex, JNK indirectly controls the transcription of genes related to cell cycle, metalloproteinases and genes related to tumor development (Wagner and Nebreda, 2009).

Not all JNK targets are nuclear, some other targets are related to cytoskeleton such as paxillin or to vesicle trafficking and exocytosis (reviewed in (Zeke et al., 2016)).

JNK has been implicated in different pathological stresses including the oncogenic transformation (Wu et al., 2019), the insulin resistance and the excitotoxicity (when nerve cells are damaged due to high levels of neurotransmitters).

c. The p38 pathway:

p38 was simultaneously discovered by three different teams in 1994 (Han et al., 1994; Lee et al., 1994; Rouse et al., 1994). The four p38 isoforms (p38 α , p38 β , p38 γ and p38 δ) are all activated by stress stimuli including oxidative stress, UV, hypoxia, lipopolysaccharide, interleukin-1 (IL-1) and tumor necrosis factor alpha (TNF α). They can also be activated by the Rho GTPases (RAC and CDC42) (reviewed in (Cargnello and Roux, 2011)). The p38 isoforms are phosphorylated by the MKK3/6 (Figure 21). Despite the redundancy between the p38 and the JNK pathways, some differences can be observed and their implication in the cellular physiology depends on cell type, tissue and organism (Martínez-Limón et al., 2020).

p38 α is the most abundant isoform in cells and it shows functional redundancy with p38 β . The other two isoforms are less abundant and their targets are different than those of the α and the β isoforms (Cuenda and Rousseau, 2007). Genetically engineered mice targeting the different p38 isoforms have been made; in contrast to p38 α KO, in which mice die in the embryonic stage, the

p38 β , p38 γ and p38 δ KO mice do not have any developmental defects (Adams et al., 2000),(Mudgett et al., 2000).

p38 is activated by phosphorylation mediated by its specific upstream MAPKK (Figure 21). Interestingly p38 α can also be activated by MAPKK independent mechanisms (Figure 22); for instance, the activation of T lymphocytes induces the phosphorylation of the p38 α by the ZAP70 (ζ -chain associated protein kinase of 70 KDa) / P56lck (for lymphocyte specific tyrosine) kinases. This phosphorylation promotes p38 α auto-phosphorylation and thereby its activation (Salvador et al., 2005).

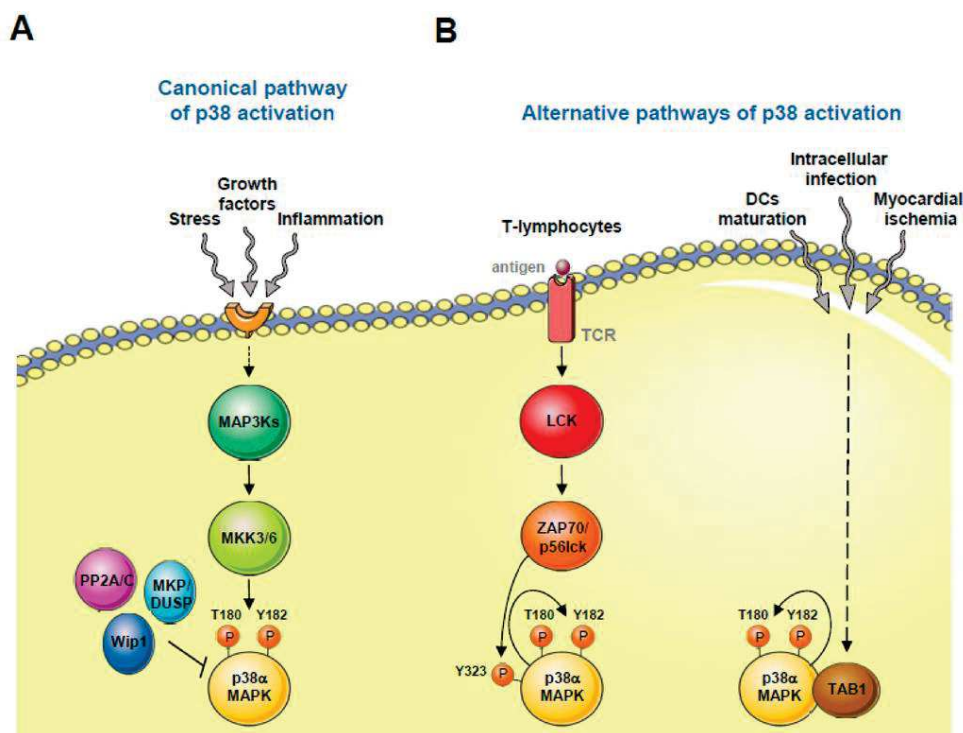


Figure 22: p38 MAPK activation.

(A) Canonical pathway: Several environmental stimuli activate p38 by phosphorylation of Thr180 and Tyr182 through MAPKKs and MAPKKs MKK3/6. Phosphatases PP2A/C, Wip1 and MKP/DUSP inhibit p38 activation. (B) Non-canonical p38 activation occurs in T-lymphocytes upon antigen presentation (TCR: antigen T cell receptor) and involves phosphorylation of Tyr323, which promotes an auto-phosphorylation loop. In addition, p38 can be activated by the presence of other stimuli such as intracellular infection, myocardial ischemia or dendritic cells (DCs) maturation signals. In these cases, TAB1 associates with p38 (TAB1: TGF β associated kinase 1-binding protein 1), promoting its auto-phosphorylation. **Taken from Martinez-Limon et al, 2020.**

WIP1 (for Wild-type P53 induced phosphatase 1) is upregulated by p53 upon UV. This phosphatase is able to downregulate the activity of p38 allowing cells to recover from stress (Takekawa et al., 2000). Similarly, as part of a negative feed-back loop, p38 activates indirectly the transcription of members of the DUSP/MKP (dual specificity phosphatase/MAPK phosphatase) family which dephosphorylate p38 thus inhibiting its activity (Ferreiro et al., 2010).

Studies based on the targeted deletion of each isoform allowed to identify the different substrates of p38 kinases. p38 α has many very diverse substrates. Some of these substrates include transcription factors, regulators of chromatin remodeling, regulators of protein degradation and localization, mRNA stability, endocytosis, apoptosis, cytoskeleton dynamic and cell migration (Cuadrado and Nebreda, 2010) (Figure 23). For instance, p38 α/β phosphorylate MSK (mitogen and stress activated kinase) 1 and 2 which can then activate CREB (for cyclic adenosine monophosphate responsive element binding protein), ATF1 and STAT1 and 3. p38 α/β also activate the MNK1/2 kinases regulating eIF-4E (eukaryotic initiation factor 4E) thus regulating protein synthesis.

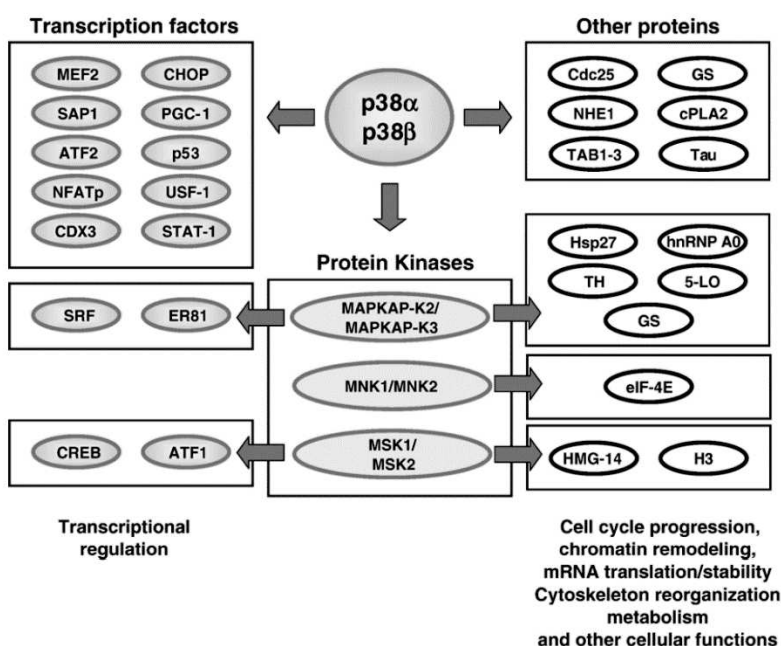


Figure 23: Substrates and function of the p38 α/β MAPKs. The list of substrates indicated in this figure is not complete but shows the many important substrates and physiological roles described for these kinases to date. CHOP, CCAAT/enhancer-binding protein-homologous protein; MEF, myocyte enhancing factor; PGC, peroxisome proliferators activated receptor γ coactivator; SAP, serum response factor accessory protein; HBP, high mobility group-box transcription factor; NFAT, nuclear factor of activated T-cells; ATF, activating transcription factor; MAPKAP-K, mitogen activated protein kinase activated protein kinase; MSK, mitogen and stress activated protein kinase; MNK, mitogen activated protein kinase-interacting protein; TAK, transforming growth factor- β -activated kinase. Taken from **Cuenda et al, 2007**.

Pathological implication of the p38 MAPK pathway is well established. It plays a role in promoting inflammation but also in cancer, cardiovascular dysfunction and Alzheimer disease (Cuenda and Rousseau, 2007). In cancer, a dual role of p38 has been observed. Indeed, some studies have demonstrated that p38 acts as an anti-tumorigenic factor in cells while others have claimed that this kinase could be a tumor promoter (Martínez-Limón et al., 2020).

The tumor suppressive role of p38 is supported by the following observations. The hyper-activation of RAS in the cell is able to activate the p38 MAPK pathway. This activation is able to inhibit RAS-dependent gene expression (AP-1 and SRE (Serum response element dependent genes) and cell growth (Chen et al., 2000). Moreover, p38 is able to sense ROS (reactive oxygen species) excessive production upon the oncogenic RAS activate and thereby triggering apoptosis in these cells (Dolado

et al., 2007). Mice lacking the p38 upstream kinases MKK3/6 are more keen to develop tumors (Wagner and Nebreda, 2009). p38 is able to induce a cell cycle arrest by inducing the G1/S and the G2/M checkpoints by activating and stabilizing the HBP1 (for HMG box transcription factor). This transcription factor is known to be a negative regulator of the cell cycle through direct binding to the promoters of different cyclins (Bollaert et al., 2019). It can control the cell cycle by direct or indirect effect on p53 and can also phosphorylate the retinoblastoma (RB) protein rendering it less sensitive to the phosphorylation by the cyclin/CDK complex thus stopping the progression of the cell cycle (Joaquin et al., 2017).

On the other hand, p38 α is found to be required for breast cancer progression in mouse models. Indeed, targeting p38 α abolished the DNA repair response and induced chromosomal instability. (Cánovas et al., 2018) have shown that upon deletion of the p38 α gene (in vivo and after tumor development), the tumor volume was reduced due to the decreased ability of cells to repair DNA damage as a consequence of impaired ATR (for Ataxia Telangiectasia and RAD3 related) signaling, one of the DNA damage response (DDR) in the cell. In lung cancer models, p38 protein expression was found to be elevated in lung resected tumors when compared to normal tissues (Greenberg et al., 2002). There are also evidence that p38 α inhibition suppresses proliferation in some cancer cell lines (Campbell et al., 2014), (Chen et al., 2009).

Because cancer is a complex and highly heterogeneous pathology with genetic and metabolic rearrangements / adaptations happening at each step of the progression, tumors evolve as cancer progresses. Evidences have shown that low activity of p38 impairs the tumor formation and initiation (early stages) while advanced stages could profit from a higher activation of this kinase (Igea and Nebreda, 2015). Therefore, compared to other genes frequently mutated in cancer, the mutation frequency of the p38 gene is lower than 1% (Martínez-Limón et al., 2020). This pathway is therefore highly pleiotropic, and its action depends on the nature of the stimuli (mitogens or acute cellular stress), the duration and the intensity of its activation, cell and tissue type, and on potential crosstalks with the other pathways. So despite its initial implication as a tumor suppressor, accumulating evidences suggest that some cancer cells might also use this pathway to their advantage.

3.3. The HIPPO pathway:

The Hippo pathway is an evolutionary conserved pathway involved in the regulation of many biological processes including cell growth, fate decision, organ size control, regeneration and tumorigenesis (Davis and Tapon, 2019). It was first characterized in *Drosophila melanogaster*: genetic mosaic screens for genes implicated in tissue growth led to the discovery of the Hippo pathway core components. It consists of a kinase cascade (Figure 24) starting with the Ste-20 family kinase Hippo (Hpo, mammalian sterile 20 like kinase 1/2 (MST1/2) as orthologue) which with the scaffolding of its binding partner Salvador (Sav/ SAV1), phosphorylates and activates the NDR family kinase member Warts (Wts/ Large tumor suppressor kinase 1/2 (LAST1/2)) and the associated scaffold Mats (Mob as tumor suppressor/ MOB1A/B). Activated LATS then phosphorylates (on Ser127) and inhibits the transcriptional co-activator YAP (Yki in *Drosophila*), in part through its cytoplasmic sequestration by 14-3-3 proteins. In mammals, TAZ represents a redundant factor to YAP similarly regulated by the LATS kinases. There are five different sites phosphorylated by LATS in YAP. Another important phosphorylation is on Ser397. This phosphorylation primes phosphorylation by casein kinase 1 (CK1) unleashing a phosphodegron on YAP. This phosphodegron recognized by the β -TRCP (β -transducin repeat containing protein) complex which mediates YAP ubiquitination and its subsequent proteasomal degradation in the cytoplasm (B. Zhao et al., 2010).

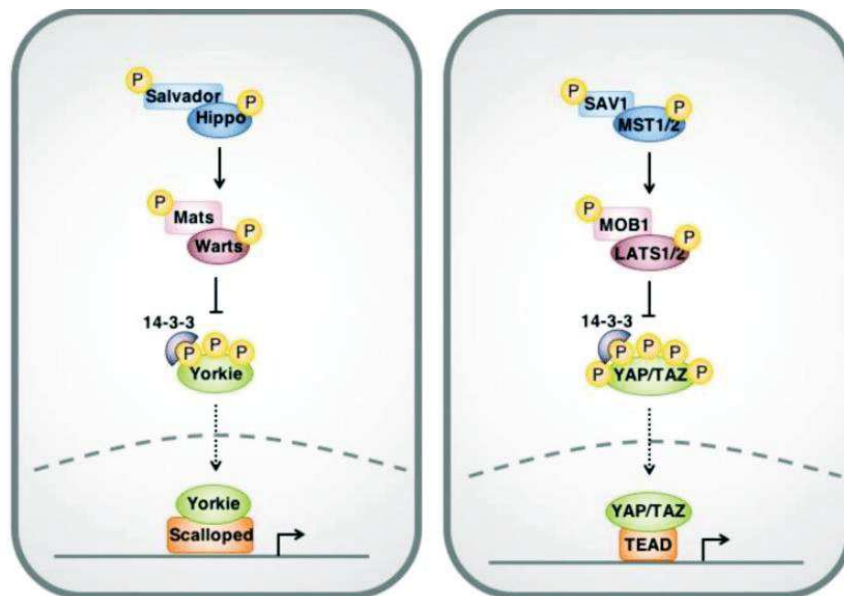


Figure 24: Simplified Hippo signaling pathway in *Drosophila* (Left) and mammals (Right).

Hippo signaling is initiated by a variety of upstream stimuli. Activation of Hippo (MST1/2) leads to subsequent phosphorylation of Warts (LATS1/2). Warts negatively regulates the Hippo pathway effector Yorkie (YAP/TAZ). Unphosphorylated Yorkie translocates into the nucleus where it interacts with its Scalloped (TEAD) transcription factors to upregulate the transcription of a variety of genes. In contrast, phosphorylation of Yorkie by Wts lead to its cytoplasmic sequestration by 14-3-3 proteins and degradation. Taken from Taha et al, 2018.

When the Hippo pathway is off, the kinase cascade does not occur leading to the translocation of YAP/TAZ to the nucleus where it interacts with the TEAD1-4 transcription factors (Scalloped in *Drosophila*), activating the transcription of target genes involved in cell proliferation and growth including genes responsible of the G1/S transition in the cell cycle, DNA replication, repair, mitosis. Interestingly, it also regulates genes of the Hippo pathway as part of a negative feedback loop (e.g. Expanded in *Drosophila* or Amotl2 in mammals), genes implicated in cytoskeleton dynamic, apoptosis, or components of other signaling pathways such as WNT and Notch (Pocaterra et al., 2020). It should be noted that TEAD default function consists in a transcription co-repressor with VGLL4 (Vg) (Guo et al., 2013), that is converted to an activator by translocated YAP/TAZ/Yki.

YAP/TAZ are considered, as oncogenes and promoter of organ growth. Since the Hippo cascade is an inhibitor of YAP/TAZ activity, MST1/2 (with their partner SAV) and LATS1/2 (with their partner MOB) are thus considered as tumor suppressors.

Other kinases can also phosphorylate LATS1/2 including the MAP4Ks family MAP4K1/2/3/5 (orthologues of Happyhour in *Drosophila*), the MAP4K 4/6/7 (orthologues of Misshappen) (Meng et al., 2015), and the TAO kinases (MAP3K responsible of the activation of the p38 kinase) (Plouffe et al., 2016). (Meng et al., 2015; Plouffe et al., 2016) have shown that these additional kinases work in parallel of MST1/2 to activate LATS, and that MST1/2 invalidation in cells was not able to totally suppress YAP phosphorylation.

Subsequent findings have identified other mechanisms directly or indirectly involved in the regulation of the Hippo pathway providing more complexity to this pathway.

In *Drosophila*, it was suggested that the apical membrane-associated FERM-domain proteins Merlin (Mer) and Expanded (Ex) could influence the Hippo pathway (Hamaratoglu et al., 2006). It was not clear how until the discovery of the C2 and WW domain containing protein Kibra that functions along with Mer and Ex, binding directly the Hpo-Sav complex and activating the Hippo pathway (Yu et al., 2010). (Zhang et al., 2010) confirmed these results in mammals. They demonstrated that NF2 (Neurofibromatosis 2) is required for YAP activity inhibition by working in synergy with KIBRA and SAV and inducing the phosphorylation of LATS. Notably, Mer and Ex have independent functions in regulating the Hippo pathway. Merlin is able to bind Hpo/Mst leading to its activation (Yu et al., 2010), while Expanded traps partially Yki in the cytoplasm thus limiting its translocation to the nucleus (Badouel et al., 2009).

Cell density is one of the main regulators of the Hippo pathway. A fundamental aspect of normal cells is to stop proliferating upon reaching confluency (contact inhibition phenomenon) and one important hallmark of transformation is losing this aspect (Hanahan and Weinberg, 2000). At high cell density, the YAP pool is shifted to the cytoplasm through the Hippo kinase cascade and cells stop proliferating (Bin Zhao et al., 2010) suggesting that Hippo could play a role in contact inhibition in normal cells. How the confluency activates the Hippo cascades was a hot field of study, one potential mechanism suggested is the regulation by the Angiomotin family of protein.

The Angiomotin family of proteins is constituted of AMOT, AMOTL1 and AMOTL2 in mammalian. The AMOTs can be found at the apical junctions in cells and they are known for their ability to bind the F-actin. The role of the AMOTs is mainly to negatively regulate YAP activity by different mechanisms:

1. AMOT binds directly YAP and traps it in the cytoplasm regardless of its phosphorylation status by the LATS1/2 kinases (B. Zhao et al., 2011).
2. AMOT triggers the activation of LATS (B. Zhao et al., 2011). The phosphorylation of AMOT by LATS causes the dissociation of AMOT from F-actin where it could bind NF2. This interaction activates NF2 which in return binds LATS and triggers its phosphorylation and the activation of the Hippo pathway (Li et al., 2015).

In 2011, the lab of Gumbiner demonstrated in human cells that E-cadherin-mediated contact inhibition occurs through Hippo components. The downregulation of MER, LATS1/2 and KIBRA caused the loss of contact inhibition induced by E-cadherin trans-dimerization. In cells lacking E-cadherin, high cell density did not cause the accumulation of YAP in the cytoplasm, while E-Cad re-expression did, strongly suggesting that E-cadherin triggers contact inhibition of proliferation by modulating the activity of YAP (Kim et al., 2011).

It is well established now that high cell density activates the Hippo core cascade through proteins presents at the levels of the apical junctions. α -catenin is considered as a major sensor of the forces created upon cell/cell contact (Yonemura et al., 2010). It transmits this information to the cytoplasm through conformational changes. When unfolded (under tension/low cell density) (Figure 25), α -catenin reveals a binding site to a protein called AJUBA, a family member of the LIM domain containing 1 (LIMD1). Ajuba in *Drosophila* as well as in mammals is a repressor of the activity of Wts/LATS upon cytoskeletal tension (Rauskolb et al., 2014),(Ibar et al., 2018). Upon the recruitment of AJUBA to the membrane, it traps LATS at the junctions and thereby YAP could translocate to the nucleus.

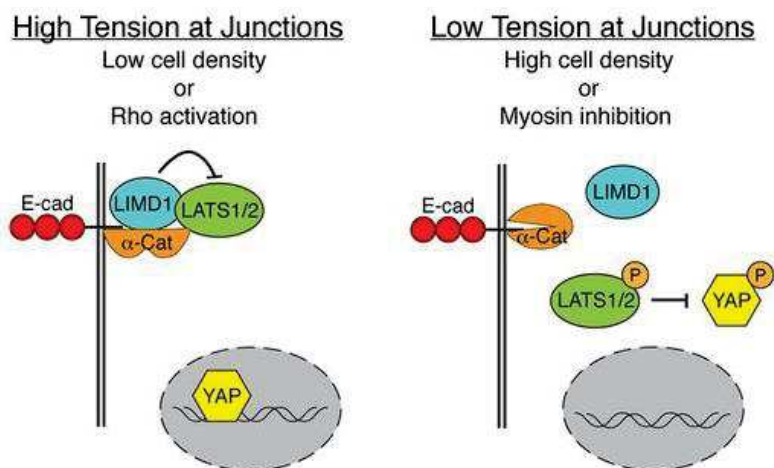


Figure 25: Summary model for regulation of YAP by LIMD1.

When the cells are under high tension (left, e.g. cell low density or Rho activation), LIMD1 is associated with adherens junctions through α -catenin, where it recruits and inhibits LATS. This allows YAP to go to the nucleus and activate transcription. When cells are under low tension (right, e.g. high density or myosin inhibition), the α -catenin conformation is altered, LIMD1 and LATS are released from junctions, and LATS can be activated. Activated (phosphorylated) LATS phosphorylates and inhibits YAP by promoting its cytoplasmic localization and degradation. **Taken from Ibar et al, 2018.**

There is a correlation between cell density and cell morphology. In a high cell density environment, cells are compact and round due to the restricted growth area. On the contrary, when cells are flat and spread this correlates with a low cell density environment. This correlation led to the discovery of the cell morphology as a regulator of the Hippo pathway and YAP activity. Wada et al (Wada et al., 2011) confirmed that cellular morphology, independently from cell/cell contact, regulates the localization of YAP in the cell. The actomyosin cytoskeleton is an important regulator of the cell morphology. Cells become flat and spread in response to external stretches forces or the forces generated by the cell periphery stress fibers which are produced to counterbalance (internally) the external stretch forces generated. The use of anti F-actin drugs, such as cytochalasin D or latrunculin A, or anti-myosin drugs, such as blebbistatin or Y27632 (inhibiting the activation of the myosin light chain (MLC) or the Rho associated kinase (ROCK) respectively), was able to modulate YAP localization reducing stress fibers formation. It is worth mentioning that this phenomenon was independent from the microtubule cytoskeleton. This regulation of YAP localization by the actomyosin cytoskeleton goes through LATS1/2 phosphorylation of YAP.

YAP and TAZ are considered as sensors of the extracellular matrix (ECM) stiffness. When cells are growing on a soft matrix, they are round with no cytoskeleton tension and when they are grown on hard matrix they are spread and flat. (Dupont et al., 2011) showed, similarly to what was proposed by Wada et al, that when the ECM is soft YAP and TAZ activities are inhibited, while they are activated on hard ECM. Interestingly, they suggest that this regulation of YAP might be independent from the core Hippo pathway kinases, even though this remains debated.

Focal adhesions are hubs of different regulators of YAP/TAZ activity. They are formed by integrins complexes that bind the ECM and a group of adaptor proteins. Their role is to integrate extracellular

stimuli and relay them inside the cell. Focal adhesions thus link ECM and the cell cytoskeleton. When focal adhesion kinase (FAK) is activated, it recruits the SRC kinase. It was shown in many studies (summarized in (Dasgupta and McCollum, 2019)) that FAK and SRC are able to regulate YAP/TAZ activity by direct or indirect mechanisms:

1. FAK phosphorylates YAP (on Y357) and MOB1. The phosphorylation of YAP is proposed to enhance its binding to its transcription factor TEAD in the nucleus. The tyrosine phosphorylation of MOB prevents its binding to LATS, thus preventing LATS activity.
2. SRC is able to phosphorylate YAP on three different sites to enhance its activity.
3. FAK acts through CDC42 to recruit a phosphatase (protein phosphatase 1A) able to limit the Ser397 phosphorylation of YAP by LATS, thus preventing its degradation.

Components of the A/B cell polarity complexes are able to regulate the Hippo pathway. SCRIB, a protein of the DLG-SCRIB-LLG complex responsible of the baso-lateral identity of the cell, is considered as a negative regulator of the YAP/TAZ activity. SCRIB assembles a complex containing MST, LATS and TAZ at the membrane, mediating the activation of LATS and the phosphorylation of TAZ. Moreover, CRUMBS, an apical identity determinant of the cell present at the levels of the TJs, is able to bind YAP/TAZ and to sequester them in the cytoplasm (Varelas et al., 2010). However the exact mechanism of Crumb effect on YAP/TAZ is not clear yet.

At physiological states, cells need nutrients and growth factors for growth and survival. It was demonstrated that some extracellular molecules such as hormones might regulate the Hippo pathway and the YAP/TAZ activity through their G protein coupled receptors (GPCRs) (reviewed in (Meng et al., 2016)). GPCR receptors once activated transduce the signal through a wide variety of cytoplasmic relays. Some activate RhoGTPases, which in turn can inactivate LATS1/2 by a mechanism that is dependent of F-actin. Conversely other GPCRs, through protein kinase A (PKA) or cAMPK-dependent mechanisms increase LATS activity, thus inhibiting YAP/TAZ activity.

Although the main kinases responsible of the cytoplasmic retention and regulation of YAP/TAZ activity are LATS1/2, many studies have shown that YAP/TAZ could be phosphorylated by other Serine/threonine kinases and by tyrosine kinases (see before and reviewed in (Piccolo et al., 2014)). AKT can phosphorylate YAP on the same residue of LATS1/2 (Ser127) (Basu et al., 2003) therefore inducing its recognition by the 14-3-3 protein and its cytoplasmic retention. YES, SRC and cAbl tyrosine kinases can phosphorylate YAP (Y357), an activating phosphorylation of YAP activity.

Besides posttranslational modifications, the interaction of YAP/TAZ with different proteins can also contribute to its retention in a specific compartment inside the cell. As an example, when the WNT pathway is OFF, the destruction complex of the β -catenin is active in the cytoplasm. It was shown by the lab of Stefano Piccolo (in 2014) that YAP/TAZ are strongly associated to this destruction complex thus retained in the cytoplasm independently of their phosphorylated state (Azzolin et al., 2014).

Altogether, these observations suggest that the regulation of the YAP/TAZ localization and activity is the result of the integration of different inputs inside the cell. It is clearly dependent on cell and tissue type, and on the different stimuli received by the cell (summarized in Figure 26). This pathway and its effectors are under complex and tight regulation. Misregulations of YAP/TAZ could affect several key cellular processes contributing to carcinogenesis such as proliferation, cell plasticity, drug resistance and survival, which is why they are frequently hijacked by cancer cells.

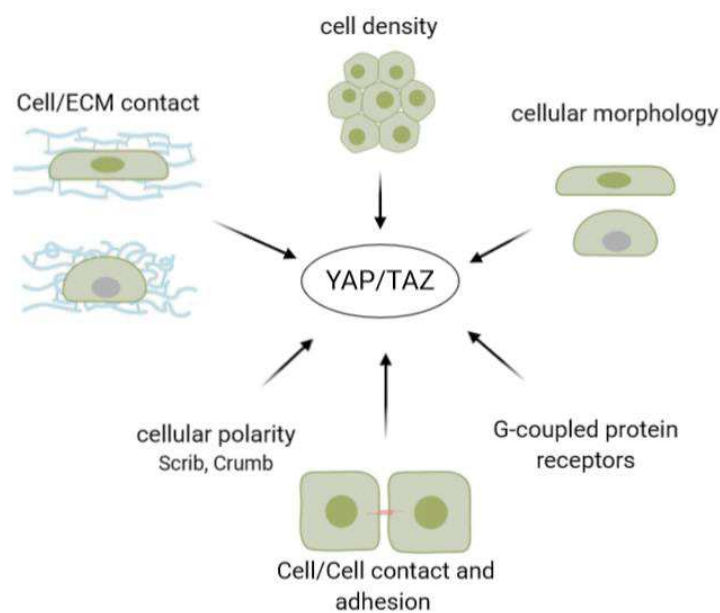


Figure 26: Summary of non-exhaustive mechanisms able to regulate the Hippo pathway and/or the YAP/TAZ activity. Cf text for mere details about each category.

4. Cancers :

The human body is composed of billions of cells that live in harmony. It constitutes a dynamic system that needs to be highly regulated so it does not lose its balance (cell proliferation versus cell death). In case the balance favors local cell accumulation and uncontrolled proliferation, a cancer will arise. This correct balance is lost when cells lose their breaks and identity.

Based on the WHO (World Health Organization) database, cancer was considered the second leading cause of mortality worldwide in 2018. There are five major types of cancer, classified depending on their cellular origin: Carcinoma (originating from epithelial cells), Sarcoma (connective tissues), lymphoma (immune cells affecting the lymph nodes), melanoma (skin cells) and leukemia (blood and bone marrow cells).

4.1. Carcinoma and epithelial polarity

Epithelial cells need to have a well-established polarity and highly organized junctions for their proper biology and achieve their different functions. Most of the polarity proteins are known to be proto-oncogenes or tumor suppressors. Moreover, oncogenic signaling often targets cellular polarity and the loss of polarity is known to be an early event in epithelial cancers. As described in the table below (Table 4), some polarity proteins such as Par, Scrib or Dlg exhibit altered expression (gene amplification, deletion, epigenetic alteration etc...) (Halaoui and McCaffrey, 2015).

Common name	Gene name	Alteration	Types of cancer	Phenotype	References
Par3	PARD3	Gene deletion or downregulation Overexpression	Esophageal squamous carcinoma, breast, glioblastoma, head and neck and lung cancers Renal cancer	Disrupted cell junctions, promotes tumorigenesis and metastasis (breast). Poor prognosis	41, 90, 123, 152 153
Par6	Par6 (protein)	Phosphorylation	BRCA1-associated tumor tissues	Protein phosphorylation, lumen filling, cell junction disruption, increased metastasis	135
	Par6 (protein)	Overexpression	Lung (NSCLC)	Stroma: good prognosis	142
	PARD6B	Amplification or overexpression	Breast cancer	Cell hyperproliferation. Amplification in luminal subtypes	154, 155
aPKC ζ	PRKCZ	Deletion	Adrenal and lung cancers		41
		Overexpression	Hepatocellular carcinoma, bladder, squamous cell carcinoma, head and neck, pancreatic, breast and prostate cancers	Invasion, poor prognosis, increased proliferation	155-161
aPKC δ	PRKCI	Downregulation	Colorectal and bladder cancers	Poor prognosis, increased recurrence	84, 162, 163
		Mislocalization	Ovarian cancer		
aPKC δ /A	PRKCI	Amplification or overexpression	Hepatocellular carcinoma, lung (NSCLC), pancreatic, ovarian, esophageal, breast and skin (basal cell carcinoma) cancers	Protein phosphorylation, metastasis and invasion, cell transformation, poor prognosis, prognostic marker, low survival, invasion, metastasis	36, 164-169
Scrib	SCRIB	Downregulation or mislocalization	Colon adenocarcinoma, cervical, endometrial, breast and prostate cancers	Neoplastic colon, intraepithelial lesions, invasion (cervical), associated with clinical stage and lymph node metastasis	40, 49, 170-172
		Overexpression	Breast cancer	Invasive phenotype, correlates with relapse and decreased survival	86
Dlg	DLG1	Downregulation or mislocalization	Cervical, colon adenocarcinoma and kidney cancers	Protein targeted for degradation by HPV E6	170, 173-176
	DLG2	Overexpression	Kidney (oncocytoma, benign tumor)		177
	DLG3	Deletion	Cervical and lung cancers		41
Lgl	LLGL1	Downregulation	Colorectal cancer	Promotor methylation	178
	LLGL1	Exon deletion	Hepatocellular carcinoma		179-181
	LLGL2	Downregulation	Breast cancer	Malignant phenotype	182
Patj	INADL	Downregulation or mislocalization	Gastric, endometrial	EMT	38, 183-185
		Downregulation	Colon, breast, cervical	EMT, target of viral protein E6	120, 186
Lkb1	STK11	Inactivating mutation, deletion or downregulation	Gastrointestinal, colorectal, esophageal, head and neck, hepatocellular carcinoma, pancreatic, kidney, lung (NSCLC), ovarian, cervical, breast, testicular, melanoma and brain cancers	Peutz-Jeghers syndrome, proliferation, high grade, poorly differentiated, poor prognosis, loss of cell polarity	67, 69, 187-210

Table 4: list of polarity genes disrupted in cancer.

Taken from Halaoui et McCaffrey 2015.

The fact that polarity defect is one the main hallmarks of cancer was evidenced by experiments done in *Drosophila* in which the invalidation of proteins part of the basolateral complex (dlg, lgl and scrib) showed some neoplastic transformations in the developing wing imaginal discs in larvae (Zeitler et al., 2004), (Bilder, 2004). Consistent with these findings, studies in human patients showed a decrease in the expression of polarity proteins (Lee and Vasioukhin, 2008). More evidences came from mice models supporting the fact that a loss of polarity contributes to tumor growth. For example, the loss of Scrib in prostate was sufficient to cause hyperproliferation and prostate neoplasia (Pearson et al., 2011) and in a similar manner, the loss of Lgl was able to induce overgrowth and dysplasia in neuronal progenitors issued from KO mice (Klezovitch et al., 2004).

Hence, cell polarity is implicated in the regulation of many signaling pathways and inputs in the cell(Halaoui and McCaffrey, 2015):

- Growth control by regulating Ras, Myc, MAPK signaling
- Cell density-epithelial proliferation control by regulating the Hippo pathway
- Metabolism, invasion and metastasis

Polarity is thus considered as a primary target for the oncogenic machinery.

4.2. Carcinoma and Junction regulation

Junctions are tightly regulated by the polarity machinery for their localization and size. Accordingly, other studies have shown that the dysregulation of junctions was involved in malignancy transformation and metastasis (Morris et al., 2008),(Talbot et al., 2012). Junctions are highly regulated to adjust adhesions for many physiological processes. EMT being one of these processes, it is known to be implicated in early development (type I EMT) and wound healing (Type II EMT), in which cells need to lose their junctions in order to leave their cohesive epithelial sheet and migrate. It is tightly controlled and implicates genes that functions to decrease the adhesion and increase the migratory phenotype of the cells. Most of cancer metastasis is thought to be due to cells undergoing uncontrolled EMT (type III EMT) (Knights et al., 2012).

Deregulation of junctions is widely documented in many cancers (Jaggi et al., 2005; Kinugasa et al., 2012; Kurrey et al., 2005; Martin et al., 2010; Orbán et al., 2008; Soini, 2012; Tobioka et al., 2004) (summarized in Table 5), affecting AJs, TJs and desmosomes.

Cell junction genes and cancer

Cancer	Upregulated genes	Downregulated genes	References
Breast	<i>SNAI1, SIP1, CLDN4</i>	<i>OCN, CDH1, CLDN1,2,7</i>	[6, 30, 33, 44-48]
Colorectal	<i>CLDN1, CTNNB</i>	<i>CDH1</i>	[5]
Endometrial		<i>OCN</i>	[7]
Liver	<i>CLDN1, PKP2</i>	<i>TJP1, OCN, PKP1,3</i>	[5, 9, 13]
Lung	<i>CLDN1-5, 7</i>	<i>DSP, PKP3CLDN2</i>	[3, 11, 39]
Oral		<i>CDH1, KRT8</i>	[25, 49]
Ovarian	<i>SNAI1, SIP1, SNAI2</i>	<i>CDH1, CTNNB, OCN, TJP1, DSG2</i>	[8, 30]
Pancreatic	<i>SNAI1</i>	<i>CDH1</i>	[29]
Prostate	<i>PKP3, PKP1</i>	<i>PKP3, PKP2, CTNNA, CTNNB, CTNND, CDH1</i>	[13, 32, 33, 36, 38]

Table 5: Diversity of adhesion genes are implicated in cancer.
Taken from Knights et al 2012.

The main hallmark of EMT is the “cadherin switching”, which consists on the switch of E-cadherin to N-cadherin. Moreover, the TGF β pathway is one of the master regulators of this process along with some Transcription Factors (TFs) such as Slug, Snail and Twist (Gravdal et al., 2007; Krisanaprakornkit and Iamaroon, 2012; von Burstin et al., 2009). Changes in the expression of these TFs causes the deregulation of components of the different junctional complexes (TJs, AJs and desmosomes).

The switch of cadherin has been studied extensively in order to better understand its regulation and the associated mechanisms. Two different studies have revealed that:

1. The shift was associated with an aberrant DNA methylation of the CDH1 gene promoter in breast and prostate carcinomas (Graff et al., 1995; Strathdee, 2002). The CDH1 promoter is CpG island rich, and its hyper-methylation causes the downregulation of its expression leading thus to initiation of EMT program.
2. At the post-transcriptional level, it is known that there is a di-leucine motif in the cytoplasmic domain of E-cadherin, binding to p120-catenin, stabilizing it at the membrane preventing its endocytosis. Knock-Down of p120-catenin results in the degradation of E-cadherin thus abolishing its tumor suppressive activity. The downregulation of p120 is frequent in most cancers (Davis et al., 2003; Kawauchi, 2012).

Even though downregulation of AJs expression is associated with poor prognosis in some cancers, in small cell lung cancer the expression of β -catenin is upregulated and associated with poor prognosis. Probably because of its nuclear accumulation and its activation of the Wnt signaling pathway, a pro-proliferation pathway (Yang et al., 2012). The deregulation of AJs has different outcomes depending on the type of cancer.

The deregulation of the TJs was also associated with tumoral behavior. Truncated forms of occludins were detected in cancer cell lines and in patients samples, and it correlated with increased progression and metastasis in a variety of cancer (Martin et al., 2010; Orbán et al., 2008; Tobioka et al., 2004). These truncated forms impaired the traffic to the plasma membrane and the interaction of occludins with ZO-1 and with the cytoskeleton. Moreover, claudins were also associated with cancer. TFs implicated in EMT could deregulate the expression of the different claudins in the cell (Ikenouchi et al., 2003; Martínez-Estrada et al., 2006). For instance, decreased expression of CLDN1, 2 and 7 correlated with high malignancies in breast carcinomas. Paradoxically, increased expression of CLDN4 was also described to be implicated in breast cancer aggressiveness (Lanigan et al., 2009), probably associated with increased “stemness” capacities. In summary, this differential expression of claudins in cancer highlights the important role of TJs in tumorigenesis and disease progression.

Nevertheless, studies have shown that the regulation of junctions during carcinogenesis is not that simple. The loss of junctional proteins is indeed a crucial step in metastatic spread of a malignant cell; however, tumorigenesis is a multi-step process: initiation, promotion and progression. So what about the status of the junctions in the other steps and the other types of migration? During expansive growth of the tumor and the increase volume of a tissue, cells tend to push others to the outside so they could fit, resulting in a multicellular aggregation with intact cell-cell adhesion. This process of pushing cells causes their movements. Moreover, if it is coupled with migration, collective migration occurs (Irina et al., 2011). This latter is proven to promote cell survival by protecting the tumor from chemotherapy (Gillett et al., 2001). Harigopal et al. have shown that the metastatic lymph nodes cells in breast cancer have high levels of E-cadherin (Harigopal et al., 2005). Concomitantly, another study proved that cells at the metastatic site of breast and lung cancer have more E-cadherin and that the microenvironment of these sites is able to induce the re-expression of E-cadherin in the cells promoting thus Mesenchymal to Epithelial transition (MET) (Chao et al., 2010). Padmanaban et al, study revealed that E-cadherin could be a survival factor for cancer cells during metastasis, because the loss of this latter induces high levels of stress and

increases apoptosis (Padmanaban et al., 2019). Taking together, junctional regulation is not a black and white process during tumorigenesis and its outputs are versatile.

Carcinomas are the most diagnosed cancers, given the abundance of the epithelial cells inside the body. It develops in breast, digestive tract, respiratory tract, skin and other tissues. The most common carcinoma subtypes are: squamous cell carcinomas, renal cell carcinomas, adenocarcinomas, basal carcinomas and transitional carcinomas. They could be in situ, invasive or metastatic. Below I will be talking further about breast and colon carcinomas due to their relevance to my PhD projects.

4.3. Breast cancers:

Breast cancer is the most frequent disease in women and the global incidence is rising each year. Almost all of breast cancer cases are carcinomas, with tumors arising from the terminal duct lobular unit. Breast cancer can be inherited (10% of the cases) and associated to family history of some predisposition genes (the BRCA1 and 2 genes implicated in DNA repair) or it could be sporadic (Harbeck et al., 2019). Germline mutations related to DNA repair and genome integrity are also shown to be related to hereditary breast cancer such as mutation linked to the BRCA genes (BRCA1 and 2), TP53, CHEK2, ATM and others (Taylor et al., 2018). For sporadic cancer, hormone receptors are the main drivers, thus the drugs blocking its effect on the mammary gland or inhibiting its production play an important role in the treatment of breast cancer.

In order to classify breast cancers for better clinical evaluation and personalized treatments, physicians assess the histological grade (with four different grades) and type of the tumor by immunohistochemistry (IHC). Histological subtypes can be divided in two big groups: pre-invasive and invasive. The pre-invasive includes the ductal and the lobular carcinomas in situ, meaning it is not invasive but could become. On the other hand, there is the ductal and the lobular invasive breast cancer. The ductal is the most common type of breast cancer. Both invasive types have different molecular and genetic characteristics and different treatments (Feng et al., 2018). Other less common breast cancer subtypes exist such as inflammatory breast cancer, breast cancer in men, Paget disease, papillary carcinoma and angiosarcoma.

Together with the histological classification, physicians also assess the expression status of three receptors: estrogen (ER) and progesterone receptors (PR) as well as the status of the HER2 receptor. 60 to 70% of patients are hormone receptor positive (ER+/PR+) and approximately 10 to 15%

are HER2 positive. Finally, 10 to 20% are HER2 negative and ER, PR negative and called triple negative (TNBC). TNBC are extensively studied since there is to date a lack of treatments options for them (Dawson et al., 2013). Based on the two classification above, there are six breast cancer subtypes: luminal A (ER and PR +), luminal B (ER +, PR + and HER2 + or -), HER2-enriched (non-luminal) and basal-like (or TNBC) that could be further separated in two subgroups according to cytokeratin and EGFR expression. Additional biomarkers were proposed including the Ki-67 as a marker of cell proliferation (Vuong et al., 2014). It is a nuclear protein present in the nucleus during the active phases of the cell cycle. High Ki-67 is associated with high proliferation rates thus it is associated with low overall patient survival in breast cancer (de Azambuja et al., 2007). All these markers together gave rise to the surrogate intrinsic subtypes (Figure 27). On the other hand, the next generation sequencing helped us to better understand this disease, as an attempt to diagnose it earlier and to have better chances of higher relapse free survival in the patients. The PAM50 is a classification based of fifty different gene expression and it came up with five different subtypes in which specific amplification of some genes were associated to each one (Figure 27).

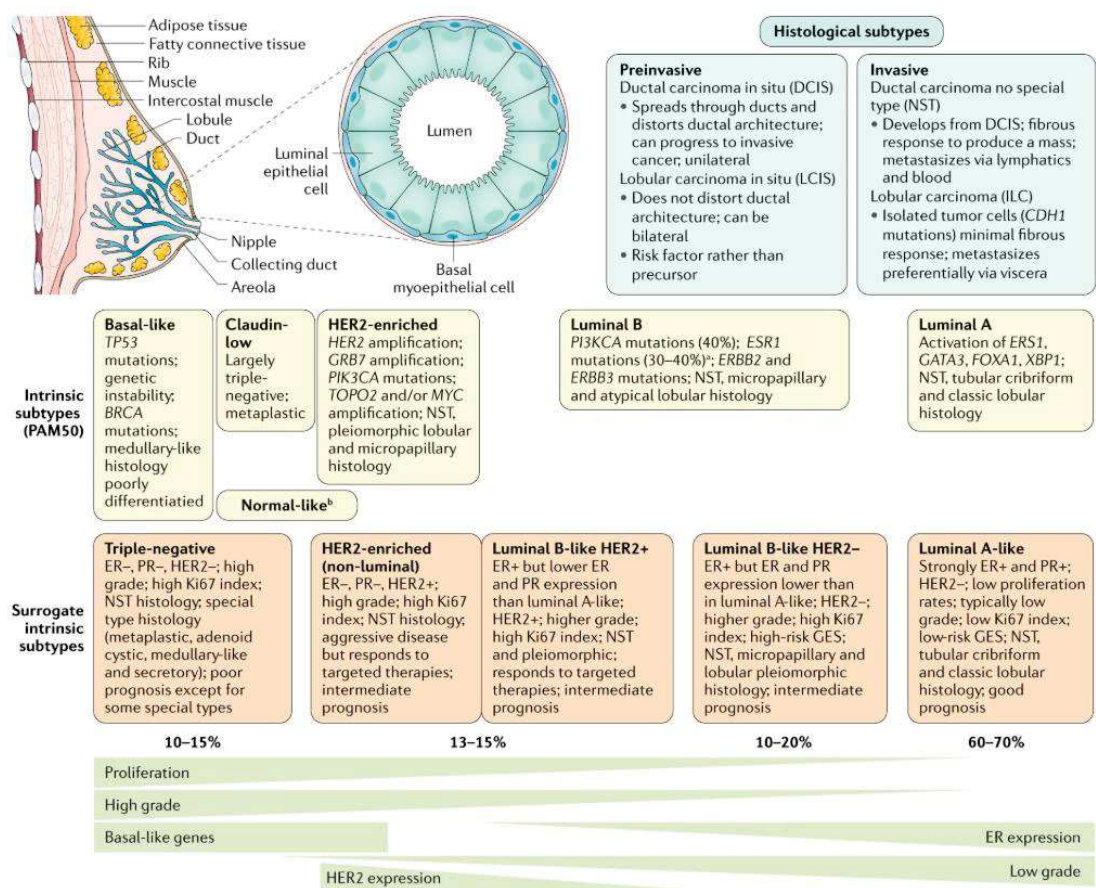


Figure 27: Breast cancer in details. Origin, different classifications.

NST is for no special type. The PAM50 intrinsic classification is based on Perou and Sorlie classification in which they used 50 genes expression signature. The surrogate intrinsic subtypes are usually used in clinic based on histological and IHC expression of some markers. GES is for gene expression signature. Taken from Harbeck et al. 2019.

A diversity of treatments exist for breast cancers: locoregional (surgery followed by radiation) for early breast cancer and other methodical strategies that include the use of endocrine therapy against hormone receptors for luminal A and luminal B subtypes, anti HER2, chemotherapy, inhibitors of BRCA mutations carriers and immunotherapy (Harbeck et al., 2019).

The TNBC are the most aggressive ones and usually associated with poor prognosis. They are susceptible for early recurrences and they tend to metastasize in the lungs and brains (Harbeck et al., 2019). Luminal A tumors as well as the luminal B relapse late and tend to metastasize to the bones and the lymph nodes (Harbeck et al., 2019). Even though luminal A and luminal B subtypes seems to be the less aggressive tumors, after relapse they tend to progress rapidly and because of the lack of personalized treatment other than chemotherapy, they are difficult to treat.

Many signaling pathways are implicated in the formation and the progression of breast cancer, such as:

- The estrogen pathway in the hormone receptor positives subtypes. As said above, the estrogen receptor (encoded by the ESR1 gene) is a driver of the breast cancer, due to its binding to the ERE (Estrogen Response Element) in the nucleus. This binding initiate the transcription of many genes implicated in the proliferation, survival and migration of the cell (Cyclin D1 (Said et al., 1997) important for the transition from G1 to S phase of the cell cycle). Moreover the estrogen is able to work independently from the ERE by activating the expression of many genes including BRAC1.
- The HER2 pathway in the HER2 positive subtypes. HER2 is part of the human epidermal growth factors family. It is a tyrosine kinase receptor able to activate many downstream signaling pathway including PI3K/AKT and MAPK pathway (Arteaga and Engelman, 2014).
- WNT pathway. Mutations in this pathway are not that common in breast cancer, but 50% of patients are known to have a constitutively active WNT pathway due to their high levels of stabilized β catenin. This latter is the main actor of this pathway, it will translocate to the nucleus and activate the transcription of a wide range of pro-proliferative and pro-survival genes. The accumulation of the β catenin is associated with poor prognosis (Khramtsov et al., 2010), (S. Y. Lin et al., 2000).
- Notch pathway. It is implicated in breast carcinogenesis and constituting a novel therapeutic target. This pathway consist on the recognition between the ligand (Jagged or Delta) on one cell and the receptor (Notch 1-4) on the other cell. After the recognition, the receptor will undergo a series of proteolytic cleavages and the Notch intracellular domain will be released and will translocate to the nucleus to activate the target genes. High levels of NOTCH1 and JAG1 are associated with poor prognosis, and might reflect stemness potential (Reedijk et al., 2005).

And other pathways such as TGF β (de Kruijf et al., 2013), NF κ B (Vlahopoulos, 2017) and PI3/AKT/mTOR pathway (Costa et al., 2018).

It is clear now that breast cancer goes beyond the histological markers and that there are many genes, susceptible of being targeted, implicated in the formation and the progression of cancer. Thus the need to study in details the different inputs and pathways causing the relapse and target them.

4.4.Colon Cancers:

Colorectal cancer (CRC) is the third most common malignancy in the world, with 50% of diagnosed patients presenting metastases. Due to the extreme conditions inside the colon (chemicals, enzymes, bacteria...), the replacement of the epithelial wall is done each 5 days (Xue et al., 2018). The colon stem cells present in the bottom of the Lieberkühn crypts are responsible for the development of the colon and its different cell types. Because of this highly dynamic structure, under physiological conditions the balance between stem cells, their progeny and the microenvironment need to be tightly controlled (Medema and Vermeulen, 2011).

Many signaling pathways act to maintain the homeostasis of the crypt. The WNT and the Notch pathways maintain the proliferation status of the cells (Fre et al., 2005; van Es et al., 2010, 2005). The BMP pathway acts as a brake for proliferation and stemness, it is activated at the top of the crypt while it is inactivated at the bottom by the expression of BMPs inhibitors like noggin. BMPs are large class of TGF β family of ligands, expressed in many tissues under physiological conditions. Upon reception by specific receptors, they act through the phosphorylation of the SMADs TF which translocate to the nucleus and activate the transcription of target genes. And finally, the hedgehog pathway (HH). Its role is still not entirely clear but there is evidence that it nullifies the WNT-mediated epithelial proliferation through BMP (van Dop et al., 2009). The protein HH initiates the signaling by binding to the canonical PATCHED receptor. This binding will result in the derepression of a GPCR protein like Smoothened (SMO), its accumulation and its phosphorylation. SMO mediates the release of GLI (the main effector of the HH signaling) from the kinesin family protein (KIF7) and SUFU its main intracellular regulator. GLI are transcriptional activators that activate the transcription of the HH pathway targets.

CRC develops due to accumulation of different genetic mutations with time. Some predisposition factors also are found such as familial adenomatous polyposis (FAP) or the hereditary non polyposis CRC (lynch syndrome or HNPCC).

It is known that CRC arises from polyps (small abnormal tissue growth). Two different models of CRC are presented in Figure 28.

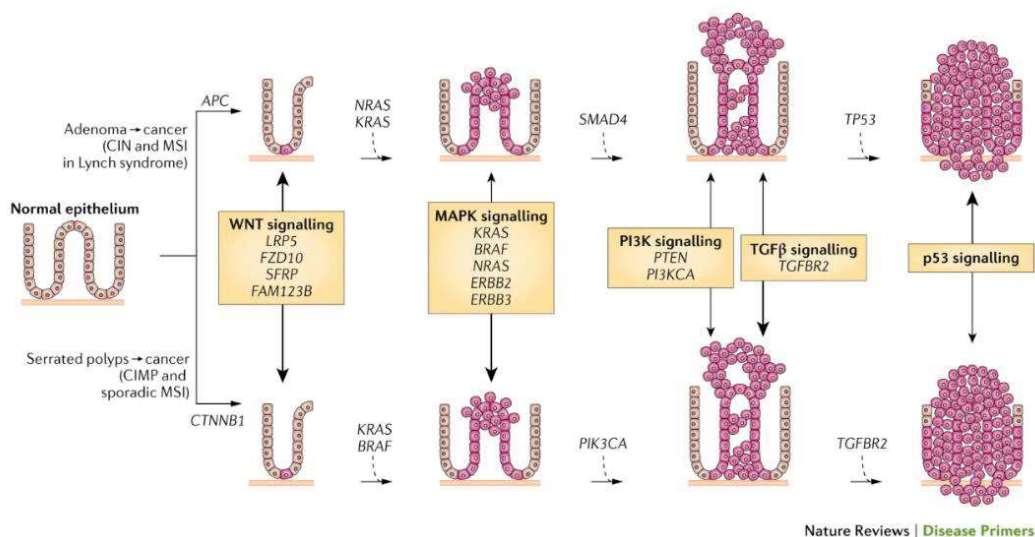


Figure 28: CRCs progression in two different models. Some genes are the same in the models but others are specific of each model. The width of the arrows shows the implication of this pathway in tumor formation. Taken from Kuipers et al. 2015

The top row represents the classical model, which starts with aberrant crypts and progress to early adenomas (tubular adenomas) then advanced adenomas to finally become CRC. It progresses fast in patients with Lynch Syndrome. The bottom row represents an alternative model discovered 10 years ago predicting that CRC could arise from polyps called sessile serrated polyps histologically and molecularly different from the tubular adenomas. They are characterized by microsatellite instability (MSI) and excessive methylation of CpG islands (CIMP) (Kuipers et al., 2015).

Even though high heterogeneity is observed between the different tumors in CRCs, genetic mutations can be grouped. Most common mutations are APC, β -catenin from the WNT pathway, KRAS and BRAF, SMAD4 from the TGF β pathway, P53, PI3K-AKT kinase, mismatch repair gene and others listed as proto-oncogenes or tumor suppressors.

The TNM system (T: primary tumor, N: regional lymph nodes, M: distant metastasis) is a good grading system for CRCs but it does not allow precise prediction and personalized treatments for patients. Since there is no clear classification for colorectal cancer, many potential markers have been described: chromosomal or microsatellite instabilities and hyper-methylation of DNA and the different mutations described above, but they are not yet applicable in clinic (Weitz et al., 2005). DNA array could be more suitable for CRCs.

Treatments options depend on the grade on the CRCs, there is surgery, chemotherapy and immunotherapy. Surgery could be an option of early stages of CRCs, and even it could be used to remove oligometastasis of stage IV patients. Chemotherapy such as FOLFOX (5-fluorouracil and oxaliplatin) or the FOLFIRI (5-fluorouracil and irinotecan), basic treatments in CRCs, are used in combination with EGFR and VEGF inhibitors in metastatic stage of CRCs. BRAF and MEK inhibitors could also be used. Last, immunotherapy concerns 5% of CRCs patients that have high MSI and do not respond to conventional chemotherapy.

Hence, it is clear that CRCs is a heterogeneous disease that despite the different treatment options is still one of the deadliest cancers and needs further characterization for more personalized treatments.

5. The MAGI scaffolds :

5.1. Structure and localization :

The Membrane Associated Guanylate kinase with Inverted arrangement of protein-protein interaction domains (MAGUK Inverted or MAGI) family are scaffold proteins associated to the membrane at the levels of TJs (Laura et al., 2002) and AJs (Feng et al., 2014) . Among the three MAGI proteins (MAGI1, 2 and 3), MAGI1 and MAGI3 are ubiquitously expressed. They all have six PDZ domains and one or two WW domains mediating interactions with a variety of proteins (Figure 29). MAGIs also have an inactive pseudo-kinase GUK domain, which may mediate interactions with other proteins.

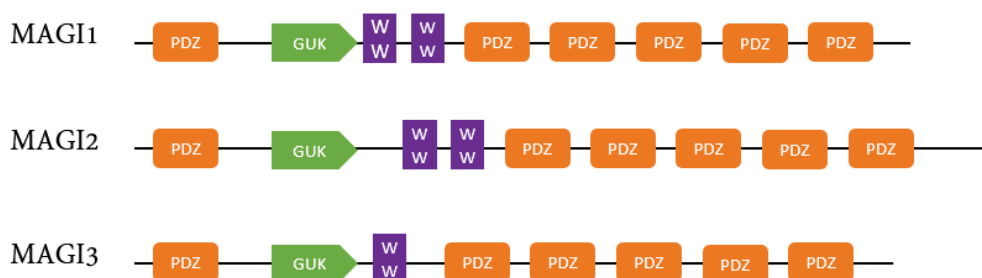


Figure 29: The MAGI family members.

PDZ domains are represented in orange, the GUK domain in green and the WW domains in purple. MAGI1 is the most expressed one at the levels of the apical junctions along with MAGI3, the MAGI2 is mainly expressed in the nervous system at the levels of synapses. MAGI3 is the shortest isoform displaying one WW domain.

For the rest of chapter 5, I will focus on MAGI1 due to its relevance to my project.

MAGI1 was the first MAGI member to be cloned in 1998 by (Shiratsuchi et al., 1998) when they were trying to identify interactors of BAI1 (for Brain-specific angiogenesis inhibitor 1) using yeast two hybrid.

The MAGI1 protein has three different isoforms generated by alternative splicing: MAGI1-a/b/c. The MAGI-b isoform localizes at TJs and apical junctions of epithelial cells whereas the two other isoforms are expressed mainly in non-epithelial cells.

5.2. Function:

MAGI1 is a scaffold protein present mainly at the plasma membrane and involved both in signal transduction and in the assembly of multi-protein signaling complexes. As shown in Figure 30, many interactors of MAGI1 have been identified (reviewed in (Gonzalez-Mariscal et al., 2016)) and the list is not exhaustive.

MAGI1 is able to form complexes responsible for the assembly the TJs but also for the modulation of the AJs through its binding to β -catenin and PTEN (Laura et al., 2002),(Ide et al., 1999),(Dobrosotskaya and James, 2000). Overexpression of MAGI1 in CRC cells increased the recruitment of β -catenin and E-cadherin at the levels of the AJs therefore maximizing their stability. Conversely, MAGI1 silencing in CRC cells caused E-cadherin dissociation from cell-cell junction, stress fibers disruption with reduced paxillin staining in immunofluorescence, anchorage independent growth and elevated activity of the WNT signaling pathway (Zaric et al., 2012) . Interestingly, reducing MAGI1 expression in glomerular podocytes (renal cells lining the Bowman's capsule able to filter the blood), altered TJs which were performing less robustly their impermeable fence function as evidenced by an increased passage of fluorescent albumin over time (Ni et al., 2016). Hence, MAGI1 is important for cell-cell adhesion and stabilization of junctions in epithelial cells.

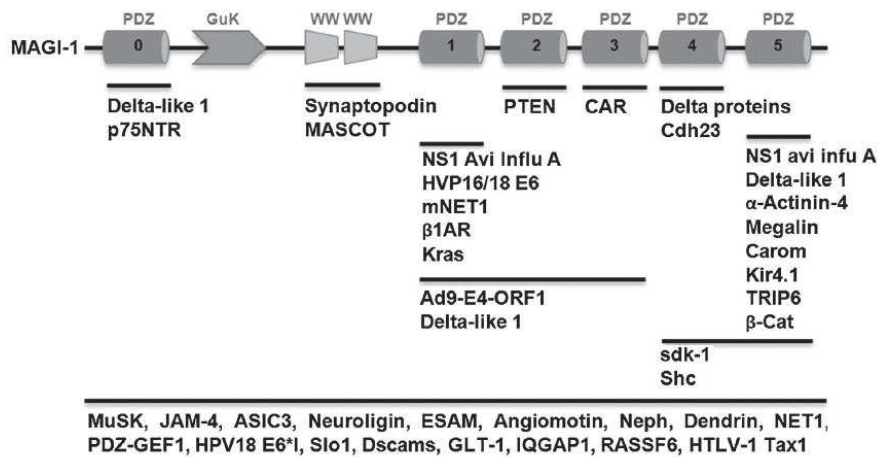


Figure 30: Representation of MAGI1 protein and the associated interactors.
Taken from Gonzalez-Mariscal et al. 2016

One of the most studied function of the MAGI protein is its role during signaling in glomerular injured podocytes. Rap1 is a small GTPase essential for integrin activation in podocytes (cells lining the Bowman's capsule able to filter the blood) and its downregulation is associated with glomerular diseases in mice and humans. The downregulation of MAGI1 or Nephhrin induces glomerulosclerosis, in part due to the aberrant activation of Rap1 (Ni et al., 2016), suggesting that MAGI1 in combination with other genetic alterations is important for the normal function of podocytes.

(Tanemoto et al., 2008) showed that MAGI1 regulates salt homeostasis in distal renal tubules. They demonstrated that a phosphorylation affecting the PDZ binding motif of the K⁺ channel subunit Kir4.1, and mediating its' binding to MAGI1, alters the correct localization of the K⁺ channels thus leading to disrupted fluid and electrolytes homeostasis. Such role as anchor is also reported for MAGI1 in other tissues. In the hippocampus, MAGI1 is able to regulate the GLT-1 surface expression (Glutamate Transporter subtype 1, a sodium dependent glutamate transporter) and the levels of glutamate (Zou et al., 2011). In the central nervous system, regulates the traffic of CRFR1 (Corticotropin-releasing factor receptor 1) (Hammad et al., 2016). This receptor is implicated in some psychiatric illness and used as a target for anxiety and depression treatments. Altered expression of MAGI1 caused a defect in CRFR1 endocytosis by interfering with β -arrestin membrane recruitment (a major endocytosis pathway for protein G coupled receptors). In the developing spinal cord of mice, MAGI1 recruits DLL1 (delta like 1 ligand) at the AJs, a well-known ligand for the Notch receptor, this result was further confirmed in cultured fibroblasts (Mizuhara et al., 2005).

Non-canonical roles for MAGI1 have also been suggested, where MAGI1 function is not restricted to the plasma membrane or to the apical junctions. Many studies have linked the *MAGI1* locus to chronic inflammatory diseases such as inflammatory bowel disease (IBD), psoriasis and Crohn disease (Alonso et al., 2015; Camilleri et al., 2016; Julià et al., 2015). For instance, mRNA expression of MAGI1 is elevated in the intestine mucosa of IBD patients suggesting that MAGI1 could play an important role in the endothelial activation upon inflammation. One recent study has shown that MAGI1 could be phosphorylated by the p90 ribosomal S6 kinase (P90RSK) and thus activating the inflammatory response of endothelial cells in blood vessels upon disturbed flow (Abe et al., 2019). This phosphorylation triggers deSUMOylation of MAGI1 and its translocation to the nucleus along with the p90RSK enzyme. This study also show that MAGI1 activates XBP1 (X-box binding protein1), a protein related to ER stress, via its association to the cleaved form of ATF6 (Activating Transcription factor 6) which translocates from ER and Golgi to the nucleus and binds the ER stress response element to activate the transcription of *XBPI*. This indicates that MAGI1 is essential for the regulation of the endothelial activation. MAGI1 also mediates (through PKA signaling) the phosphorylation of eNOS (endothelial Nitric Oxide Synthase) leading to NO (Nitric Oxide) production under shear stress in endothelial cells(Ghimire et al., 2019).

Finally, the tumor suppressive function of MAGI1 (reviewed in (Feng et al., 2014)) will be further detailed in section 5.d.

5.3. Role of MAGIs in non-mammalian species

- *Danio rerio* (Zebrafish):

The interaction between *magi1* and the Notch ligand Delta was studied extensively in zebrafish embryos. This physical interaction is independent of the Delta-Notch interaction and is associated with the migration of the Rohon-Beard sensory neurons in zebrafish(Wright et al., 2004).

- *Caenorhabditis elegans* (Nematode):

To understand the modulation of the cadherin complexes, (Lynch et al., 2012) conducted a genome wide RNAi screen in *C.elegans* embryos and discovered *magi1* as a key player. They demonstrated that MAGI1 is essential for embryos segregation and the maintenance of stable apical junction during morphogenesis. Moreover, depletion of *magi1* leads to disorganized actin cytoskeleton

through its partner Afadin (AFD-1) at the junctions and to increased rates of membrane protein movement at the levels of the apical junctions, leading to the conclusion that magi1 regulates the actin cytoskeleton and is able to stabilize proteins once recruited and assembled at the apical junctions.

Furthermore, another study showed that the knockdown of magi1 resulted in the mixing of the different components of the CCC (Cadherin-Catenin complex) and the DAC (AJM-1/DLG-1 complex) complexes constituting the different junctions in *C. elegans* (Stetak and Hajnal, 2011), suggesting that magi1 is important for the correct compartmentalization of the different complexes and acts as a spatial separation between the two.

- *Drosophila Melanogaster* (fruit fly):

Magi null mutants were viable despite its important role in mammals in maintaining the stability of the apical junctions. Overexpression studies showed that elevated levels of Magi affect the apical polarity complex localization (Bazooka/PAR3, Par6 and aPKC) (Barmchi et al., 2016). In this study, authors also suggested a model of competition between Baz and Magi where the level of expression of one could lower the level of the other.

My team has a long interest in Magi and its functions. Before my arrival, Zaessinger et al. showed that Magi regulates E-cadherin belt integrity by assembling a multi-protein complex in the developing eye of the *Drosophila* (Zaessinger et al., 2015). My lab showed that Magi is able to recruit and interact with RASSF8 (Ras associated domain family member 8)/ASSP (Ankyrin repeat, SH3-domain, and proline-rich-region containing protein) during the AJs remodeling, thus stabilizing the E-cadherin complexes at the levels of the AJs. Moreover, they showed that this interaction is important for the correct recruitment of Baz/PAR3 protein to the membrane.

Taken together, these studies in non-mammalian organisms, show that Magi scaffolds are important for the stabilization of the apical junctions and the maintenance of the epithelial morphology.

5.4. Magi and cancer:

MAGI1 is targeted by certain oncogenic viruses. Indeed, human adenovirus type 9 (Ad9) and the high risk human papillomaviruses (HPV) are two families of viruses containing onco-proteins

which can induce tumors and in particular cervical cancer in the case of HPV. These viruses contain onco-proteins able to bind PDZ-containing proteins such as DLG (Kiyono et al., 1997; Lee et al., 1997), MAGI1 (Glaunsinger et al., 2000; Kranjec and Banks, 2011) proteins thus sequestering them in the cytoplasm or targeting them for degradation. It is noteworthy that in transformation defective Ad9, the ability to bind MAGI1 was weakened (Glaunsinger et al., 2000). Moreover, during HPV infection, the knockdown of its onco-protein restores two pools of MAGI1 in the cell, a membrane pool and a nuclear pool (Lee et al., 1997), suggesting that the removal of MAGI1 might represent an advantage for the HPV mediated transformation. These findings were the first hints for a tumor suppressor role of MAGI1 in cells.

Then, it was proven that MAGI1 was able to abolish the Src/AKT invasiveness phenotype in MDCK cells when performing a gain of function experiment. This rescue was dependent on the interaction between MAGI1 and β -catenin on one hand and on the interaction between MAGI1 and PTEN on the other hand (Kotelevets et al., 2005). While the recruitment on MAGI1 at the junctions reversed the Src-mediated invasiveness, this study suggested that MAGI1 stabilizes E-cadherin and cooperates with PTEN to suppress invasion phenotype.

In 2008, two groups conducted different genome wide approaches to identify potential new candidates that could be dysregulated in cancer. A genetic profile on Egyptian hepatocellular carcinomas (HCC) associated with hepatitis C showed that 134 genes were down regulated ; 19% were implicated in signaling and MAGI1 was one of them (Zekri et al., 2008). Meanwhile, a genome wide analysis of promoters associated with CpG islands showed that MAGI1 promoter is highly methylated in Acute lymphoblastic leukemia (ALL) and, along with other genes, was associated with poor prognosis in patients (Kuang et al., 2008).

Overexpression of MAGI1 in the HepG2 HCC cell line reduced their migratory and invasive behavior. In addition, this overexpression correlated with the upregulation of PTEN in cells, suggesting that MAGI1 could be a potential tumor suppressor in HCC playing its role through regulating PTEN in cells (Zhang and Wang, 2011). Further research determined that low levels of MAGI1 in HCC patients correlates with multiple nodules formation and shortened overall survival (Zhang et al., 2012).

In colorectal cancer (CRC), cyclooxygenase II (COXII) is overexpressed and enhances tumor progression. The use of the COXII inhibitory enzymes such as celecoxib (COXIB) is considered as complementary treatment for patients with familial adenomatous polyposis with high risk for CRC. Zaric et al, demonstrated that upon COXIB treatment, MAGI1 is upregulated. To assess the function

of MAGI1 in CRC, they overexpressed it in colon cancer cells and found that cells exhibit more epithelial cells morphology with increased levels of E-cadherin and β -catenin at the junctions. Moreover, cells were less migratory and invasive compared to the control ones. While its downregulation led to the converse, they concluded that MAGI1 is a potential tumor suppressor in CRCs and is able to regulate the WNT pathway, a crucial and critical pathway for cancer initiation (Zaric et al., 2012).

Likewise, in gastric cancer (GC), weak levels of MAGI1 were detected and correlated with elevated levels of distant metastasis. Jia et al, showed that the downregulation of MAGI1 in GC cell lines enhanced cell proliferation, migration and invasion. This phenotype was associated with elevated ERK activity and upregulation of metalloproteases expression and EMT markers such as N-cadherin (Jia et al., 2017).

Hence, MAGI1 has been proven to be a potential tumor suppressor in a variety of different cancers, HCC, ALL, CRC and GC but also renal cell carcinomas (Wang et al., 2019) and gliomas (Li et al., 2019; Lu et al., 2019).

It is worth mentioning that MAGI2 and MAGI3 have been recently implicated in cancer. Genomic sequencing of seven different prostate patients samples showed that four of them have rearrangements in the MAGI2 locus predicted to inactivate this latter, claiming that MAGI2 could be a tumor suppressor in prostate cancer (Berger et al., 2011). However, Goldstein et al, showed immunohistochemistry analyses on seventy eight different samples of prostate cancer patients that higher abundancy of MAGI2 was observed in high-grade prostatic intraepithelial neoplasia and adenocarcinomas compared to benign tumors suggesting that MAGI2 play a role in prostate carcinogenesis (Goldstein et al., 2016). MAGI2 overexpression stabilizes the PTEN protein via decreasing its degradation and PTEN is a known tumor suppressor able to block the AKT signaling activation and the focal adhesion formation by inhibiting the FAK (Focal adhesion kinase) phosphorylation. The MAGI2-PTEN complex blocks the proliferation and the migration in human hepatocellular carcinomas cell lines (Hu et al., 2007). MAGI3 as well is implicated in cancer. whole genome analyses showed a fusion between the MAGI3 protein and the AKT3 resulting in a constitutively active AKT signaling in breast cancer samples (“CBFB Mutations and MAGI3–AKT3 Fusions Recur In Breast Cancer,” 2012).

Thesis objectives

Junctional disturbance and cellular polarity alterations are often associated with epithelial cancer initiation and progression (see Introduction). The biology of Junctions, Polarity, but also signaling is controlled by scaffold proteins, amongst many other regulators. Previous work in the team uncovered the role of Magi, the sole *Drosophila* member of a family of MAGUK scaffolds, in the remodeling of AJs during eye development (Zaessinger et al., 2015). I thus wanted to explore the function of MAGIs apical scaffolds in Cancer.

MAGI1, the most widely expressed MAGI in humans, is poorly studied in the context of mammary development and breast cancer. Given its important role in orchestrating many processes (see chapter 5 of the introduction), my main thesis project consisted in focusing on MAGI1 and studying its function in breast cancer cells.

Among all breast cancer subtypes, MAGI1 is almost only expressed in luminal A breast cancer (BC) cell lines. Even though luminal breast cancer patients have the best prognosis among all breast cancer patients, unfortunately some do relapse. When luminal tumors relapse, they are really hard to treat. Herein, the importance to better understand the progression of this disease. Till 2019, MAGI1 was poorly studied in BCs and no article was published in this area. In early 2020, the group of Dr Ruëgg published a possible implication of MAGI1 in estrogen receptor positive breast cancer cells (Alday-Parejo et al., 2020). While they report a cancer-opposing role for MAGI1, similarly to my own discoveries, my results do not support the mechanisms they proposed. This article will be further discussed in the discussion chapter of this manuscript. My work on MAGI1 uncovered a potential link with the Hippo pathway and thus my PhD thesis includes work on:

1. The characterization of the MAGI1 tumor suppressor effect in luminal A BCs.

In this first part, I will be presenting the work I have been doing that led to an article currently under review, in which I am first author. Interesting results obtained in this project made us explore another aspect of MAGI1 that I will detail in the second part.

2. The implication of ECM stiffness in MAGI1 regulation of the Hippo pathway and the p38/AMOTL2 stress axis.

In this section, I will first explore the effect of the extracellular matrix stiffness on MAGI1 regulation of the Hippo pathway and YAP activity and I will also provide some results concerning the potential mechanisms by which MAGI1 controls the p38/AMOTL2 stress axis.

3. Characterization of the mechanism of action of Oxaliplatin treatment in colorectal cancer (CRC) cells.

In a third part, I will be presenting the results that I obtained on a second project I was working on during my PhD, and exploring the potential role of the Hippo/YAP/TAZ pathway during Oxaliplatin treatment, which is represent the first line of treatment for most CRC patients. This project is still ongoing and its results will be part of a future publication for which I will be part of the authors.

1. Characterization of MAGI1 tumor suppressor effect in luminal A BCa.

a) Work summary

In this work, we show that the loss of MAGI1 promotes 2D cell growth, anchorage-independent cell growth, clonal mammosphere formation, increased cellular stiffness, and tumor growth in xenografted nude mice validating thereby the tumor suppressor effect of MAGI1 described in the literature for other tumors and cancers. This phenotype is associated with subtle alterations of specific junctional proteins, such as increased levels of the adhesive E-Cadherin and of the Actin binding scaffold AMOTL2, and with elevated activity of the Stress Activated Protein Kinase p38. Importantly, we further show that the increased tumorigenicity of *MAGI1* deficient breast luminal cells is suppressed in the absence of AMOTL2 or after inhibition of p38, leading us to propose that MAGI1 acts as a tumor-suppressor by inhibiting an AMOTL2/p38 tumorigenic stress pathway. Interestingly, none of the classical proliferative pathway, such as canonical WNT pathway, ERK and the AKT pathway, were implicated after the loss of MAGI1. Furthermore, upon MAGI1 loss we could demonstrate elevated levels of p-YAP and a clear downregulation of the different YAP targets. This inhibition of YAP signaling has almost never been associated with increased tumorigenicity, thus opening a new field of discussion, maybe specific to luminal A BC, which calls for further investigations and a reassessment of the link between YAP signaling and breast cancers.

b) Article

MAGI1 inhibits the AMOTL2/p38 stress pathway and prevents luminal breast tumorigenesis

Diala Kantar ¹, Emilie Bousquet Mur ^{1,+}, Vera Slaninova ^{1,+}, Yezza Ben Salah ¹, Luca Costa ³, Elodie Forest ¹, Patrice Lassus ¹, Charles Géminard ¹, Marion Larroque ^{1,2}, Florence Boissière-Michot ^{1,2}, Béatrice Orsetti ¹, Charles Theillet ¹, Jacques Colinge ¹, Christine Benistant ³, Antonio Maraver ¹, Lisa Heron-Milhavet ^{1,*}, and Alexandre Djiane ^{1,*}

¹ IRCM, Univ Montpellier, Inserm, ICM, Montpellier, France. ² Translational Research Unit, ICM, Montpellier, France. ³ CBS, Univ Montpellier, CNRS, Inserm, Montpellier, France.

⁺ Co-second authors: E.B. and V.S.

^{*} Co-last authors and co-corresponding authors: L.H.M. and A.D.

^{*} Authors to whom all correspondence and material requests should be addressed: L.H.M. and A.D. (Emails: lisa.heron-milhavet@inserm.fr / alexandre.djiane@inserm.fr)

ABSTRACT

Alterations to cell polarization or to intercellular junctions are often associated with epithelial cancer progression, including breast cancers (BCa). We show here that the loss of the junctional scaffold protein MAGI1 is associated with bad prognosis in luminal BCa, and promotes tumorigenesis. E-cadherin and the actin binding scaffold AMOTL2 accumulate in *MAGI1* deficient cells which are subjected to increased stiffness. These alterations are associated with low YAP activity, the terminal Hippo-pathway effector, but with an elevated ROCK and p38 Stress Activated Protein Kinase activities. Blocking ROCK prevented p38 activation, suggesting that MAGI1 limits p38 activity in part through releasing actin strength. Importantly, the increased tumorigenicity of *MAGI1* deficient cells is rescued in the absence of AMOTL2 or after inhibition of p38, demonstrating that MAGI1 acts as a tumor-suppressor in luminal BCa by inhibiting an AMOTL2/p38 stress pathway.

INTRODUCTION

Breast cancers (BCa) arise from mammary epithelial cells, and show tremendous diversity. Based on transcriptome, BCa are typically divided into five main subtypes: luminal A, luminal B, HER2-enriched, normal-like, and basal (reviewed in (Holliday and Speirs, 2011) (Guedj et al., 2012)), partly overlapping with previous classifications (such as ER/PR/HER2 receptors expression status). Basal tumors, overlapping strongly with triple-negative breast cancers, are the most aggressive and present the worst prognosis. However, even though luminal A and B subtypes (typically ER/PR positives) usually respond well to current treatments, when “luminal” tumors relapse, they become very difficult to treat with very poor outcome.

The apico-basal (A/B) polarity of mammary epithelial cells is established and maintained by the asymmetric segregation of evolutionarily conserved protein complexes (Knust and Bossinger, 2002b). A/B polarity governs the correct position of different intercellular junctions that ensure the integrity of the epithelial sheet. Adherens Junctions (AJs) constitute apical adhesive structures mediated by the homophilic trans-interactions of E-cadherin/catenin complexes (Coopman and Djiane, 2016) (Jeanes et al., 2008). At the very apical part of epithelial cells, Tight junctions (TJs) ensure the impermeability of tissues in part through the action of Claudins/Zonula Occludens proteins complexes (Balda and Matter, 2016). The transmembrane proteins of these different junctions (E-cadherin, Claudins...) are coupled and anchored to the actin cytoskeleton via adaptor scaffold proteins, thus coupling adhesion and cell contacts to actin dynamics. As such AJs represent mechano-sensory structures, where tensile or compressive forces, arising from internal or external sources, will be sensed to promote short term responses such as changes in adhesion and actomyosin dynamics, but also long term responses to control cell density, in particular through the mechano-sensitive Hippo pathway (Charras and Yap, 2018; Pinheiro and Bellaïche, 2018). In epithelial cells, the compressive forces exerted by the cortical actin cytoskeleton or by cell packing, sensed at AJs, antagonize the proliferative and anti-apoptotic effects of YAP/TAZ in part through α -catenin conformational change, or through the release of Merlin/NF2 (Benham-Pyle et al., 2015; Furukawa et al., 2017; Hirata et al., 2017; N.-G Kim et al., 2011; Schlegelmilch et al., 2011; Silvis et al., 2011). Other signaling pathways such as β -catenin, ERK, or JNK/SAPK stress pathways can also be influenced by polarity and forces sensed at junctions (Aoki et al., 2017; Hall et al., 2019; Hirata et al., 2017; Pereira et al., 2011; Wagner and Nebreda, 2009). BCa are derived from transformed mammary epithelia where frequent alterations in TJs and/or AJs composition and structure, and the associated abnormal mechano-sensory responses have been linked to cell dysfunction such as uncontrolled cell proliferation and metastasis (Beavon, 2000; Bosch-Fortea and Martín-Belmonte, 2018).

At apical junctions, cortical scaffold proteins such as MAGI (MAGUKs with Inverted domain structure), assemble large and dynamic molecular complexes. In humans, among the three MAGI proteins (MAGI1-3), MAGI1 is the most widely expressed and contains several protein-protein interaction domains including six PDZ and two WW domains (Laura et al., 2002) mediating interactions with TJ proteins (Hirabayashi et al., 2003). In *Drosophila*, we have demonstrated that Magi, the sole fly MAGI homolog, is required for E-cadherin belt integrity and AJ dynamics ultimately restricting cell numbers in the developing eye (Padash Barmchi et al., 2016; Zaessinger et al., 2015). The regulation of Cadherin complexes by MAGIs, is evolutionarily conserved from *C. elegans* (Allison M. Lynch et al., 2012), to vertebrates, and in particular vertebrate endothelial cells where MAGI1 links VE-cadherin

complexes with the underlying cortical actin cytoskeleton (Hultin et al., 2014). A tumor suppressive role of MAGI1 (reviewed by (Feng et al., 2014)) is suggested by the correlation between low *MAGI1* expression and poor prognosis in various cancers, such as hepatocellular carcinoma (Zhang et al., 2012). The anti-tumoral activity of MAGI1 is further supported by its ability to bind the tumor-suppressor PTEN (Kozakai et al., 2018; Zhang and Wang, 2011; Zmajkovicova et al., 2013), the fact that it is often targeted by viral oncoproteins (Kranjec et al., 2014; Makokha et al., 2013), and by the observation that in colorectal cancer cells, MAGI1 was upregulated in response to cyclooxygenase-2 inhibitor and prevented metastasis (Zaric et al., 2012). Thus it appeared that the apical junction-localized MAGI1 scaffold protein participates in multiple complexes to fine-tune adhesion and signaling, and may therefore be considered as a tumor suppressor.

The angiomin (AMOT) family of membrane-associated scaffold proteins is composed of three members: AMOT, AMOTL1, and AMOTL2, playing important roles in the regulation of intercellular junctions (Hildebrand et al., 2017). In endothelial cells and in Zebrafish developing embryos, AMOTL2 has been shown to link cadherins and the actin cytoskeleton. In particular, AMOTL2 is required for the maintenance of tension (mainly arising from compressive forces) at the level of cadherin junctions to properly shape strong blood vessels (Hultin et al., 2014, 2017). Moreover, AMOTs are also known to control the Hippo tumor-suppressor signaling pathway. Canonical Hippo pathway, through sequential activation of the Hippo/MST and Wts/LATS kinases, promotes the phosphorylation and cytoplasmic retention of the transcriptional co-activators Yki/YAP/TAZ (reviewed by (Maugeri-Saccà and De Maria, 2018)). Specific PPxY motifs found in AMOTs interact with the WW domains of YAP and TAZ (B. Zhao et al., 2011) and AMOTs act thus as negative regulators of YAP/TAZ mediated transcription by trapping YAP (Yu and Guan, 2013; B. Zhao et al., 2011) and TAZ (Chan et al., 2011) in the cytoplasm. Recent studies identified interactions between MAGI1 and AMOTs, in particular in the regulation of intercellular junctions (Wang et al., 2014) (Bratt et al., 2005; Patrie, 2005).

We report here that low levels of *MAGI1* are associated with bad prognosis in luminal ER+ BCa. Impairing MAGI1 expression in luminal BCa cells promoted their growth in 2D, and their ability to grow in low attachment conditions in-vitro and in subcutaneously grafted nude mice. We further document that *MAGI1* deficient cells accumulate specific junctional proteins, including E-cadherin and AMOTL2. Mechanistically, we show that all *MAGI1* deficient phenotypes are suppressed by down-regulating *AMOTL2* suggesting that AMOTL2 and its effects on junctions is the primary cause of the increased tumorigenicity after MAGI1 loss. Consistent with these observations, we could further show that *MAGI1* deficient luminal BCa cells experience higher stiffness as evidenced by increased Young's modulus, and ROCK activity as evidenced by increased ROCK-specific Ser19 phosphorylation of the regulatory Myosin Light Chain 2. They activate the p38 stress signaling pathway while YAP activity is antagonized. Finally, we provide evidence that releasing actin cytoskeletal strength, or impairing p38 activity can revert the effects of MAGI1 loss, supporting a model by which, in response to MAGI1 loss, elevated AMOTL2/E-cadherin and junction dysfunction, together with actin cytoskeletal tension activate the p38 stress pathway fueling tumorigenicity.

MATERIALS & METHODS

Plasmids, mutant constructs and shRNA cloning

All expression plasmids were generated with the Gateway system (Invitrogen). The Entry vector *pDONR223-MAGII* was a gift from William Hahn (Addgene plasmid #23523) (Johannessen et al., 2010) and it was used to introduce the different point mutations in *MAGII* by mutagenesis PCR using PfuTurbo (Agilent). All the Gateway destination vectors that were generated are listed as follows : *pCMV10 3xFlag RfB-MAGII*, *pCMV10 3xFlag RfB-MAGII P331A*, *pCMV10 3xFlag RfB-MAGII P390A* and *pCMV10 3xFlag RfB-MAGII-P331/390A*. *pEZY-EGFP-MAGII* was constructed by Gateway recombination between the *pDONR223-MAGII* and the *pEZY-EGFP* destination vector that was a gift from Zu-Zhu Zhang (Addgene plasmid #18671) (Guo et al., 2008). *pcDNA3 HA-AMOT*, *pcDNA3 HA-AMOT Y242A*, *pcDNA3 HA-AMOT Y287A* and *pcDNA3 HA-AMOT Y242/287A* were gifts from Kunliang Guan (Addgene plasmids #32821, #32823, #32824 and #32822 respectively) (B. Zhao et al., 2011).

shRNA directed against human *MAGII* and *AMOTL2* were constructed and cloned in the pSIREN-RetroQ vector (TaKaRa) according to the manufacturer's conditions between BamHI and EcoRI cloning sites as previously described for other genes (Marzi et al., 2016). Targeted sequences were:

shRNA-MAGII(1-1): CACCTATGAAGGAAACTATT

shRNA-MAGII(3-1): GATCTCATAGTGGAAGTTAA

shRNA-AMOTL2(1416): GGAACAAGATGGACAGTGA

shRNA-AMOTL2(3667): GAGATGTCTTGTAGCATA

All hairpins were validated (<http://cancan.cshl.edu/cgi-bin/Codex/Codex.cgi>). The shRNA targeting Luciferase as a control was kindly provided by Celine Gongora (IRCM). Retroviral particles were produced in HEK293 cells and used to infect MCF7 and T47D (and HCT116) cell lines that were then selected with 1 µg/ml puromycin.

Cell culture and cell transfection

MCF7, T47D and HCT116 human cell lines originated from the *TumoroteK* bank (SIRIC Montpellier Cancer) and have been authenticated by STR (Short-tandem repeat) profiling and certified mycoplasma-free. MCF7 cell lines were grown respectively in DMEM:HAM F12 or DMEM medium supplemented with penicillin and streptomycin antibiotics (1%) and fetal calf serum (2% or 10%). T47D and HCT116 were grown in RPMI medium supplemented with antibiotics (1%) and fetal calf serum (2 % or 10%). MCF7, T47D and HCT116 shRNA cell lines were grown in their respective medium in the presence of puromycin (1 µg/mL) for selection of cells expressing shRNAs.

Plasmid transfections were performed in MCF7 cells using Lipofectamine2000 reagent (Invitrogen) according to the manufacturer's directions. Cell extracts were assayed for protein expression 24-48 hours post-transfection. Concerning *AMOTL2*siRNA transfection

(Dharmacon siGENOME #M-01323200-0005), a final concentration of 100 nM was used using Lipofectamine2000 reagent as well.

Western blotting

Proteins issued from transfected MCF7, MCF7shRNA, T47DshRNA or HCT116shRNA cell lines were extracted, analyzed by SDS-PAGE. Antibodies used were mouse anti-MAG1 (1/250; Santa Cruz #sc100326), rabbit anti-MAGI1 (1/1000; Sigma #HPA031853), rabbit anti-MAGI2 (1/250; Santa Cruz #sc25664), rabbit anti-MAGI3 (1/250; Santa Cruz discontinued), mouse anti-tubulin (1/10000; Sigma-Aldrich #T6074), mouse anti-AMOT (1/250; Santa Cruz #sc166924), rabbit AMOTL2 (1/600; Proteintech #23351-1-AP), mouse M2 anti-Flag (1/2000; Sigma-Aldrich #F1804), mouse anti-HA (1/2000; BioLegend #901501), rabbit anti-GFP (1/2000; Torrey Pines Laboratories #TP401), rabbit anti-YAP/TAZ (1/1000; Cell Signaling Technology #8418), rabbit anti YAP (1/1000; Cell Signaling Technology #14074), p-YAP (S127) (1/1000; Cell Signaling Technology #13008) and p-YAP (S397) (1/1000; Cell Signaling Technology #13619), rabbit anti LATS1 (1/1000; Cell Signaling Technology #3477), p-LATS1 (1/1000; Cell Signaling Technology #8654), p-Mob1 (1/1000; Cell Signaling Technology #8699)-mouse anti-actin (1/250; Developmental Studies Hybridoma Bank #JLA20), goat anti-SCRIB (1/250; Santa Cruz #sc11049), rabbit anti-Claudin-1 (1/1000; Cell Signaling Technology #13255), anti-Claudin-3 (1/1000; Genetex #15102), anti-ZO-1 (1/1000; Cell Signaling Technology #8193), anti- β -catenin (1/1000; Cell Signaling Technology #8480), anti-PARD3 (1/1000; Millipore #07-330), anti-E-cadherin (1/1000; Cell Signaling Technology #3195), anti-p-p38 (Cell Signaling Technology #4511), anti-p38 (Cell Signaling Technology #8690), anti-p-JNK/SAPK (Cell Signaling Technology #9251), anti-JNK/SAPK (Cell Signaling Technology #9252), anti-p-MLC Ser19 (Cell Signaling Technology #3675), anti-MLC (Cell Signaling Technology #3672), anti-p-Akt (Cell Signaling Technology #4060), anti-Akt (Cell Signaling Technology #4691), anti-p-ERK1/2 (Cell Signaling Technology #4370) and anti-ERK1/2 (Cell Signaling Technology #4695).

RNA extraction, reverse transcription and real time RT-qPCR

RNAs were extracted from cells using RNeasy plus kit (Qiagen) and cDNAs were prepared starting from 1 μ g of RNAs using the Superscript III reverse transcriptase (Invitrogen) and following manufacturer's directions. Real time quantitative PCR was then performed on cDNAs using SYBR Green I Mastermix (Roche) according to the manufacturer's conditions on a Light Cycler 480 device (Roche). All primers used are listed as follows, 5' to 3':

MAGI1_For: CGTAAAGTGGTTTTTGCGGTGC

MAGI1_Rev: TCTCCACGTCGTAGGGCTGC

MAGI2_For: ATCATTGGTGGAGACGAGCC

MAGI2-Rev: TAGCCACGACACAACACCAG

MAGI3_For: CTGCACTTTTCAGTCTTCTTTTGAC

MAGI3_Rev: CTGAACCAAATTACGTGGCCC
AMOTL2_For: CCAAGTCGGTGCCATCTGTT
AMOTL2_Rev: CCATCTCTGCTCCCGTGTTT
CTGF_For: TTCCAAGACCTGTGGGAT
CTGF_Rev: GTGCAGCCAGAAAGCTC
CYR61_For: ACCAAGAAATCCCCGAACC
CYR61_Rev: CGGGCAGTTGTAGTTGCATT
BIRC2_For: GTCAGAACACCGGAGGCATT
BIRC2_Rev: TGACATCATCATTGCGACCCA
AREG_For: CGAAGGACCAATGAGAGCCC
AREG_Rev: AGGCATTTCACTCACAGGGG
HPRT_For: CTGACCTGCTGGATTACA
HPRT_Rev: GCGACCTTGACCATCTTT

Patients and TMA construction

Breast cancer samples were retrospectively selected from the Institut régional du Cancer de Montpellier (ICM) pathology database using the following inclusion criteria: chemotherapy-naïve at the time of surgery and estrogen (ER), progesterone (PR) receptor and HER2 status available. The tissue micro-array (TMA) was constructed to encompass the four subtypes of breast cancer. Fifty samples were identified: 14 with hormone receptor positive expression (>10% of tumor cells expressing ER and PR) and HER2-negative (scored 0 by immunohistochemistry), 12 with hormone receptor positive but HER2-positive (scored 3+ by immunohistochemistry), 10 hormone receptor negative HER2 positive and 14 triple negative samples (ER-,PR- and HER2-negative). Tumor samples were collected following French laws under the supervision of an investigator and declared to the French Ministry of Higher Education and Research (Biobanque BB-0033-00059; declaration number DC-2008–695). All patients were informed about the use of their tissue samples for biological research and the study was approved by the local translational research committee.

Tissue blocks with enough material upon gross inspection were initially selected and then the presence of breast carcinoma was evaluated on hematoxylin–eosin-stained sections. The areas to be used for the construction of the TMA were marked on the slide and on the donor block. Samples corresponding to the selected areas were extracted using a manual arraying instrument (Manual Tissue Arrayer 1, Beecher Instruments, Sun Prairie, WI, USA). To take into account the tumor heterogeneity, tumor sampling consisted of two cores (1 mm in diameter) from different tumor areas from a single specimen, and placed at the specified coordinates.

Immunohistochemistry

Four μm thin sections of the TMA were mounted on Flex microscope slides (Dako) and allowed to dry overnight at room temperature before immunohistochemistry (IHC) processing. PT-Link® system (Dako) was used for pre-treatment, allowing simultaneous deparaffinization and antigen retrieval. Heat-induced antigen retrieval was executed for 15 minutes in High pH Buffer (Dako) at 95°C. Immunohistochemistry procedure was performed using the Dako Autostainer Link48 platform. Briefly, endogenous peroxidase was quenched using Flex Peroxidase Block (Dako) for 5 min at room temperature. TMA sections were incubated with rabbit polyclonal antibodies against MAGI1 (1/50; Sigma Aldrich #HPA0311853) and YAP (1/100; Santa Cruz #15407) at room temperature. Following an amplification step with a rabbit linker (Dako) and two rinses in buffer, the slides were incubated with a horseradish peroxidase-labeled polymer coupled to secondary anti-mouse and anti-rabbit antibodies for 20 min, followed by appliance of 3,3'-Diaminobenzidine for 10 min as substrate. Counterstaining was performed using Flex Hematoxylin (Dako) followed by washing the slides under tap water for 5 min. Finally, slides were mounted with a coverslip after dehydration. MCF7 cell line transfected with Flag-MAGI1 expression vector was used as positive control for MAGI1 IHC.

Staining intensity of each marker was performed in a blinded fashion by two trained observers with the following criteria: 0 (negative), 1 (weak), 2 (moderate), 3 (strong). When both spots were assessable, data were consolidated into a single score as the mean of the duplicate.

Immunofluorescence

Cells seeded on glass coverslips were fixed 10 min in paraformaldehyde (4 %), before being permeabilized in PBS / 0.1% TritonX-100 for 10 min. After blocking in PBS / 0.5% BSA, cells were incubated with primary antibodies overnight at 4°C. Antibodies used were mouse anti-MAGI1 (1/100; Sigma Aldrich #HPA031853), rabbit anti-AMOT (1/100; Proteintech #24550-I-AP), rabbit anti AMOTL2 (1/100; Atlas Antibodies #HPA063027), rabbit anti-E-cadherin (1/100; Cell Signaling Technology #3195), mouse anti-E-cadherin (1/200; BD Transduction Lab #610182), phalloidin (1/200; Sigma-Aldrich #P1951), rabbit anti- β -catenin (1/1000; Cell Signaling Technology #8480), rabbit anti-Claudin-3 (1/100; Genetex #GTX15102), anti-PARD3 (1/1000; Millipore #07-330) and anti-ZO-1 (1/100; Cell Signaling Technology #8193). Secondary Alexa Fluor Antibodies (1/200; Invitrogen) were used as described previously (Zaessinger et al., 2015) for 1 hour at room temperature before mounting the coverslips with Vectashield (Vector Laboratories #H-1200) and imaging on a Zeiss Apotome microscope.

Atomic Force Microscopy (AFM) measurements

Cells were plated on glass 35mm fluorodish at intermediate (1/3) dilution density, grown overnight, and placed in 2% serum medium before AFM experiments. Cells grew as clusters of cells. AFM Force Spectroscopy (AFM-FS) experiments (Saavedra V et al., 2020) on living cell clusters were performed on a JPK Nanowizard 4 microscope equipped with a CellHesion stage (JPK). The AFM is mounted on an inverted Axiovert 200M microscope system (Carl Zeiss) equipped with a 100x (1.5NA, plan-Apochromat) objective lens (Carl Zeiss). We

employed a heating module (JPK) placed at the sample level to maintain cells at the physiological temperature of 37°C during measurements. We used CP-CONT-SIO-D cantilevers with 10µm colloidal beads as tip (NanoAndMore). Cantilever stiffness and optical lever sensitivities were both calibrated in liquid environment using the Contact-Free-Method provided by JPK AFM, and based on a mix of a thermal and Sader (Fernandes et al., 2020) calibration methods. Calibrated springs constant for cantilevers were evaluated in the range of 0.15-0.24 N/m. AFM-FS indentation cycles were performed using a 5-10nN force threshold to induce 2-3µm (approx. 20% of cell height) maximal indentation lengths. A squared grid of 4x4 pixels covering a region of 50µm X 50µm was fixed at the center of cell cluster monolayers, defining a force map constituted by 16 indentation curves. At least 5 force maps were acquired in each experiment on each cell category and 3 separated experiments were performed. Analyses were carried out using the JPK AFM data processing software. The elastic Young's modulus (E; Pa) was evaluated by fitting each force versus tip-cell distance curve with the Hertz contact model for indenting an infinite isotropic elastic half space with a solid sphere as described in (Cartagena-Rivera et al., 2017).

Cell cycle analysis

MCF7shRNA cell lines were fixed with ethanol and stained with propidium iodide for cell cycle analysis according to the on-line technical protocol (BioLegend http://www.biolegend.com/media_assets/support_protocol) and analyzed using a Gallios Flow cytometer (Beckman Coulter).

Mammosphere culture

MCF7sh*Luc* and MCF7sh*MAGII* cell suspensions were obtained by trypsinization and then filtered using 30µm cell strainer (Miltenyi). Filtered cells were immediately seeded in 96 well plates coated with 1% Poly (2-hydroxyethyl methacrylate; Sigma Aldrich) at a density of 200 or 50 cells per well. Cells were grown in MEBM basal medium supplemented with B27 without vitamin A (50X), 20 ng/mL EGF, 20 ng/mL bFGF and 4 µg/mL heparin. Cells were incubated at 37 °C with 5% CO₂ during 5 days.

Mammosphere acquisition and analysis

At day 5, mammospheres were labeled using 0.2 nM Calcein-AM (PromoCell GmbH) and incubated 30 minutes at room temperature. Data acquisition was done using Incucyte® (Essen Bioscience, Sartorius) for brightfield and green fluorescence. Image analysis was processed with IncuCyteS3 ®Software using the following parameters: Segmentation [Top Hat, Radius (100µm), Threshold (2 GCU)], Edge split [on, edge sensitivity -55], Hole fill [100µm²].

Immunoprecipitation and co-immunoprecipitation

Protein extracts were prepared in lysis buffer (NaCl 150 mM, Tris pH 7.4 10 mM, EDTA 1 mM, Triton X-100 1%, NP-40 0.5%, cOmplete, EDTA-free protease inhibitors (Roche #11873580001) for 30 min on ice before centrifugation. Immunoprecipitations were

performed overnight at 4°C on a rocking wheel using either mouse anti-MAGI1 antibody for endogenous immunoprecipitations or anti-HA antibody and EZview Red anti-FLAG M2 affinity gel (Sigma-Aldrich #F1804) for co-immunoprecipitations. Protein G sepharose was then added to the MAGI1- or HA- immunoprecipitates for 1 hour at 4°C before extensive washes. Concerning the FLAG immunoprecipitation, washes were performed followed by protein elution by competition with 3XFLAG peptide (150 ng/μL final concentration) during 1 hour at 4°C. The different immunoprecipitates were then submitted to Western blotting for detection of protein complexes.

Subcellular fractionation - Isolation of cytoplasmic, nuclear and membrane protein fractions.

Subcellular fractionation of cultured human cell lines was performed as previously described; samples, buffers and centrifugations were kept and performed at 4°C at all time. For more details, the protocol is available on-line (<http://www.bio-protocol.org/e754>).

Cell growth assay

2D cell growth assay was analyzed using MTT (Thiazolyl Blue Tetrazolium Bromide (Sigma Aldrich #M2128)). Briefly, cells seeded in 96 well plates were stopped from day 0 to day 7 by incubation with MTT solution (0.5 mg/mL final concentration) during 4 hours at 37 °C. Before reading OD at 570 nm, cells were incubated with DMSO to solubilize the formazan crystals formed in the presence of MTT.

3D Spheroid formation and measures

10 000 cells were seeded in Ultra-Low Attachment 96 well plates (Costar) cultured in their regular medium supplemented with 15 % FCS. After 3 days, all cells formed 3D spheroids that can be further analyzed by perimeter and circularity measurements. Pictures of spheroids were taken 3 days after seeding cells to assay the ability of cell lines to form spheroids and both the perimeters and the circularity of spheroids were calculated. Circularity was calculated ($4\pi \times (\text{area}/(\text{perimeter})^2)$) where 1 is considered as a perfect circle.

p38 MAPK inhibitor treatment

The different MCF7*shRNA* cell lines were plated at 3×10^6 cells per 60mm plates. The day after, 10 μM of Ralimetinib (LY2228020; Selleckchem #S1494) was added and 24 h later cells were collected and counted to be plated for the different experiments (Ralimetinib treatment is maintained throughout the experiments). For proliferation assay, 3000 cells were plated in 96-well plates and plates were stopped at Day 0, Day 2, Day 5 and Day 8 using 10 % of Trichloroacetic acid (TCA; Sigma Aldrich #T4885) for 10 min, then washed 3 times with PBS and stored at 4°C until the end of the experiment. Once the experiment is finished, 50 μl of Sulforhodamine B (SRB; Sigma Aldrich #230162) 0.04% diluted in acetic acid 1% were added for 30 min before extensive washes with acetic acid 1% and drying step overnight at room temperature. Before reading OD at 540 nm, cells were incubated with Tris 10 mM pH 10.5. For Soft agar assay, 10 000 cells were plated in 12-well plates before proceeding to the

assay detailed below. The same experiments were conducted with another p38 inhibitor using 10 μ M of Pexmetinib (ARRY-614; Selleckchem #S7799).

ROCK inhibitors treatment

The treatments of MCF7*shRNA* cell lines with either Blebbistatin (Selleckchem #7099) or Y-27632 (Selleckchem #S1049) were both performed at a final concentration of 10 μ M and cells were treated during 2 hours before being lysed for Western blot analyses.

Soft Agar assay

To assess anchorage independent growth, soft agar assays were performed. A first layer of 0.8% Noble agar (Sigma Aldrich #A5431) was prepared in 12-well plates and left at 4C during 1 hour for the agar to solidify gently. The plate was kept at 37C before the cell-containing agar layer was prepared. 5,000 or 10,000 cells were imbedded in the second layer containing 0.4% Noble agar on top of the first layer. When the second layer was solidified, fresh medium was added on top of the cells. MCF7 cell lines were cultured during 14 to 21 days before Crystal violet coloration (0.01% final concentration; Sigma Aldrich #C0775) or MTT assay (1 mg/mL final concentration).

Primary tumor growth assay

MCF7*shRNA* and HCT116*shRNA* cell lines were injected subcutaneously in six-week-old female athymic Nude-Foxn1 mice (Envigo). Both flanks of each mouse were injected with cells mixed with Matrigel (10⁶ cells injected for HCT116; 10x10⁶ cells injected for MCF7). Mice injected with MCF7 cells were subjected to neck dropping with 50 μ l of α -estradiol (1.5 mg/mL diluted in ethanol) to stimulate MCF7 cell growth. Animal procedures were performed according to protocols approved by the French national committee on animal care.

RESULTS

The loss of MAGI1 enhances tumorigenicity of luminal breast cancer (BCa) cells

In order to study the role of the apical scaffold MAGI1 during breast carcinogenesis, we first analyzed the expression of MAGI1 by western blot in both luminal and basal BCa cell lines: MAGI1 expression was restricted to luminal ER+ lineages (T47D and MCF7 luminal A, and to a lesser extent in ZR75 luminal B), while no expression could be detected in basal ER-lineages (immortalized MCF10A and triple negative MDA-MB-468 and BT549; Supplemental Fig. 1A). Moreover, public database mining (<http://www.kmplot>) (Györfy et al., 2010), indicated that low *MAGI1* RNA expression levels were associated with worse prognosis in relapse-free survival for BCa patients, but only in ER+ (mainly luminal) molecular BCa subtypes (Kaplan Meier curve; Supplemental Fig. 1B).

We thus decided to investigate the functional role of MAGI1 and the consequence of MAGI1 knockdown in luminal BCa, and generated MCF7 and T47D cell lines in which *MAGI1* was targeted by constitutive shRNA. Two independent shRNA constructs targeting different parts of the *MAGI1* transcript were used, *shMAGI1(3-1)* and *shMAGI1(1-1)*, which led respectively to more than 90% and around 50% MAGI1 knockdown at the protein level as shown by western blot and immunofluorescence analyses (Supplemental Fig. 1D&E). The knockdown was specific for MAGI1 and did not induce compensatory up-regulation of MAGI2 and MAGI3, the two remaining MAGI family members (Supplemental Fig. 1D&F). *shMAGI1(3-1)* was the most potent resulting in almost knock-out like down-regulation, and was therefore used in all subsequent studies and referred to as *shMAGI1* thereafter.

First, *MAGI1* knockdown increased 2D cell growth of MCF7 cells (25% increase at day 7) as assayed by MTT cell growth assay (Fig. 1A). It was associated with a weak increase in the proportion of cells in the S phase of the cell cycle from 21% in control MCF7*shLuc* to 29% in MCF7*shMAGI1* cells (Fig. 1B). More importantly, in anchorage-independent soft agar cell growth conditions, MCF7*shMAGI1* cell lines formed circa twice as many colonies compared to *shLuc* controls (Fig. 1C). Similarly, MCF7*shMAGI1* cells showed enhanced clonal mammosphere capacities which were correlated with an expanded area occupied by the spheres (60% increase; Fig. 1D). Significantly, when MCF7*shMAGI1* cells were injected subcutaneously in nude mice, they grew as a tumor mass much more rapidly and extensively than control MCF7*shLuc* cells (Fig. 1E). Together, these results show that the loss of MAGI1 in MCF7 cells promotes tumorigenicity (Fig. 1A-E). Similar results were obtained in T47D, a second luminal A BCa cell line, in which MAGI1 knockdown (*shMAGI1*) led to elevated 2D and anchorage-independent cell growth (Supplemental Fig. 2A&B). Even though BCa was the prime focus of this study, the effects of *MAGI1* knockdown appeared not restricted to mammary cells, and similar observations on anchorage-free growth in soft agar, and orthotopic tumor growth in nude mice were also observed using HCT116 colon cancer cells (Supplemental Fig. 2E&F) extending earlier reports (Zaric et al., 2012). Altogether, our results show that the loss of MAGI1 in luminal A BCa cells enhances their tumorigenic behaviors.

The loss of MAGI1 promotes the accumulation of epithelial junctions components

In order to further investigate the role of MAGI1 in breast tissue, we sought to determine its localization in mammary epithelial cells. Immunohistochemistry on BCa patient tissue microarray revealed that in normal breast cells, MAGI1 was expressed only in the luminal epithelial cells and not in the underlying basal myo-epithelial layer, consistent with MAGI1 expression exclusively in luminal-type BCa cell lines (Supplemental Fig. 1A). At the sub-cellular level, MAGI1 was localized at the apical pole of luminal breast cells (Supplemental Fig. 1C, arrows). Using MCF7 cancer cells, immortalized hMEC (human mammary epithelial cells), and polarized canine MDCK cells, we further confirmed by immunofluorescence that MAGI1 localized near the plasma membrane, overlapping with junction components such as E-cadherin (AJ), ZO1, and Claudin3 (TJ), suggesting that MAGI1 is a TJ and/or AJ resident protein (Fig. 2A, arrows and data not shown).

The localization of MAGI1 at apical junctions prompted us to explore whether MAGI1 could control their biology. Performing western-blot analyses on whole protein extracts, the loss of MAGI1 did not affect the total protein abundance of the typical TJs component ZO-1 nor of the AJs component PARD3 (Fig. 2B). However, in MCF7*shMAGI1* we observed increases in the junctional proteins β -catenin (x1.25), E-cadherin (x1.6) and AMOTL2 (x1.8) (Fig. 2B). Consistently, performing immunofluorescence on fixed MCF7*shMAGI1* cells, the membrane levels and localization of ZO-1 and PARD3 were unchanged, while E-cadherin staining was increased, and less tightly restricted to the plasma membrane (Fig. 2C). The altered distribution of E-cadherin in *shMAGI1* cells is reminiscent of the role of Magi in *Drosophila* where we showed that it controls E-cadherin belt at AJs in epithelial cells of the developing eye (Zaessinger et al., 2015).

In epithelial cells, the increase in E-cadherin material is often associated with increased strength of the junctions, and through the linkage to the underlying actin to increases in tension and overall compressive forces (reviewed by (Charras and Yap, 2018)). While we did not observe obvious changes in the intensity or morphology of F-actin upon MAGI1 knockdown (Supplemental Fig. 3A&B), MCF7*shMAGI1* cells exhibited behaviors compatible with increased compressive forces. First, when cultured as spheroids, MCF7*shMAGI1* cells grew as round masses of cells, rounder than MCF7*shLuc* controls with circa 30% smaller perimeter (Fig. 3A&B) and better circularity (0.95 vs 0.62 respectively; Fig. 3C), a sign that MCF7*shMAGI1* cells aggregates were more compact, even though composed of the same number of cells as MCF7*shLuc* controls. This compaction was also observed in T47D *shMAGI1* cells (Supplemental Fig. 2C&D). Second, using Atomic Force Microscopy (AFM), we showed that MCF7*shMAGI1* cells were stiffer than controls (higher Young's modulus factor; Fig. 3D), strongly suggesting that MCF7*shMAGI1* cells may have a stronger cytoskeleton and might experience higher internal pressure. Since AFM was performed on small MCF7 cells clusters, our data indicate that the increased compressive forces were generated from within the cells, likely through increased actin contractility. Indeed, elevated ROCK activity was detected in MAGI1 deficient cells as shown by the increase in ROCK-specific serine 19 phosphorylation of the regulatory myosin light chain MLC2 (Fig. 3E&F), suggesting that the actin cytoskeleton was under higher tension. Furthermore, treating MCF7*shMAGI1* cells with ROCK inhibitors completely abolished the increased cell stiffness

and the Young's modulus factors measured by AFM after inhibitors treatment reached similarly low levels in *shMAG11* and *shLuc* controls (Supplemental Fig. 3C).

MAG11 loss does not promote YAP nor β -catenin signaling

In epithelial cells, E-cadherin-based AJs regulate the activity of mechanosensitive pathways, and in particular the Hippo and Wnt/ β -catenin pathways, two major pathways controlling cell proliferation and frequently mis-regulated during carcinogenesis (Nusse and Clevers, 2017; Pinheiro and Bellaïche, 2018). We thus explored whether these two pathways could be affected following MAG11 depletion.

Monitoring Hippo pathway and YAP activity in stable MCF7*shMAG11* showed that in the absence of *MAG11*, total YAP and phosphorylated YAP (on both serine residues S127 and S397) accumulated in the cells while TAZ levels remained unchanged (Western blot analyses; Fig. 4A). By immunofluorescence, we then showed that unlike what was observed for control cells grown at similar confluence, YAP did not accumulate in the nuclei of MCF7*shMAG11* cells (Fig. 4B). These findings were further confirmed in luminal BCa patients TMA, where we observed a strong correlation in ER+ tumors between MAG11 apical membrane localization and YAP nuclear localization: only 27 % of the patients with no MAG11 expression or mis-localized MAG11 (no membrane staining) showed YAP nuclear localization while 92% of patients with membranous MAG11 showed nuclear YAP (Figure 4C). Accordingly, *MAG11* knockdown in MCF7 cells resulted in impaired YAP transcriptional activity with decreased expression of canonical YAP target genes such as *CTGF*, *CYR61*, *BIRC2*, and *AREG* (Figure 4D). Surprisingly, even though YAP phosphorylations on S127 and S397 are mediated by LATS kinases (Reviewed in (Furth and Aylon, 2017; Misra and Irvine, 2018)), the loss of MAG11 did not promote a higher activity of the Hippo pathway and the levels of phosphorylated activated LATS1 kinase and of phosphorylated MOB1 were unaffected (Figure 4A). This suggests that the elevated phosphorylated YAP were not the consequence of increased upstream Hippo pathway activity (MST kinases), but might reflect higher p-YAP stability, either because it is protected from destruction, or because it is not dephosphorylated as efficiently, or a combination of the two. These results are in agreement with earlier studies showing that E-cadherin junctional tension in epithelial cells promote YAP/TAZ nuclear exclusion either through α -catenin conformational change (N.-G Kim et al., 2011; Schlegelmilch et al., 2011; Silvis et al., 2011), or through Merlin/NF2-mediated cytoplasmic retention (Furukawa et al., 2017). Together, these results show that the junctional MAG11 scaffold prevents the accumulation of phosphorylated YAP in the cytoplasm of luminal BCa cells.

Similarly, even though higher overall protein levels of β -catenin could be observed in MCF7*shMAG11* cells compared to controls, this was not reflected by an increase in the active unphosphorylated β -catenin pool (Figure 4A). These results are in agreement with studies showing that increased compression transduced by apical junctions in epithelial cells prevent β -catenin nuclear accumulation (Hall et al., 2019; Hirata et al., 2017). These results thus show

that the loss of MAGI1 does not promote YAP nor β -catenin signaling, and suggest that these pathways do not mediate the increased tumorigenicity of *MAGI1* deficient cells.

p38 Stress Activated Protein Kinase mediates tumorigenicity of MAGI1 deficient cells

We thus asked which mechanisms mediate the increase in 2D cell proliferation and in anchorage-independent cell growth observed upon MAGI1 loss (see Fig. 1), focusing on other known oncogenic pathways. The ERK/MAP Kinase and JNK stress kinase pathways could be influenced by junctions and the forces they sense (Aoki et al., 2017; Pereira et al., 2011; Wagner and Nebreda, 2009). In response to MAGI1 loss, we did not detect any alterations of the main oncogenic pathways: Akt, ERK1/2, and JNK pathways (Fig. 5A&B). Interestingly, the p38 stress kinase was strongly activated in MCF7*shMAGI1* compared to MCF7*shLuc*, and the amount of phosphorylated p38, normalized to total p38 protein level, was increased 2 fold (Fig. 5A&4B). The p38 pathway is activated in response to a wide variety of cellular stresses and has been implicated either as a tumor-suppressor or as an oncogene in various cancers, including BCa (Cánovas et al., 2018b; Gupta et al., 2014; Gupta and Nebreda, 2015; Hardwick et al., 2001; Maik-Rachline et al., 2018). Using p38 specific inhibitors, we then tested whether the p38 pathway could mediate, at least in part, the increased tumorigenicity of MCF7 luminal cells. In 2D cell growth, MCF7*shMAGI1* treated with LY2228820 p38 α/β inhibitor (also named Ralimetinib) grew less than untreated cells (2 fold suppression at 8 days of growth; Figure 5C). It should be noted that p38 inhibition also slowed the growth of MCF7*shLuc* control cells, but the effect was far less pronounced than for MCF7*shMAGI1* cells. In soft agar, LY2228820 treatment suppressed strongly the anchorage-independent cell growth of MCF7*shMAGI1* (2.5 fold decrease) as compared to its effect on MCF7*shLuc* control cells (Figure 5D). Similar effects were obtained using a second independent p38 inhibitor, ARRY-614 (p38 and Tie2 inhibitor), even though we observed higher toxicity (data not shown), strongly supporting that the effects observed were the consequence of p38 inhibition and not any unspecific action of the drugs. Taken together, our results demonstrate the essential role of the p38 signaling pathway for MAGI1-deficient MCF7 luminal BCa cells tumorigenicity, consistent with previous report identifying the critical role of p38 α in mammary tumorigenesis using mouse BCa models (Cánovas et al., 2018b).

Strikingly, treating MCF7*shMAGI1* cells with the Rho Kinase (ROCK) inhibitors Y-27632 or Blebbistatin that prevent Myosin-mediated F-actin tension, abolished p38 activation (Fig. 5E&F) and largely decreased elastic cell Young's modulus (Supplemental Fig. 3C), showing that increased ROCK activity and actin strength represent critical events to activate p38 signaling. However, due to their cell toxicity, these ROCK inhibitors treatments could only be maintained for short periods, preventing us to assay formally, whether releasing actin tension in MAGI1 deficient cells could suppress their tumorigenicity as would be expected from their effects on p38.

MAGI1 interacts with the angiomin family members AMOT and AMOTL2 at the junctions

In order to better understand how the loss of MAGI1 and the associated alterations in ROCK activity and in E-cadherin-based junctions could lead to p38 stress-kinase activation, we decided to focus our studies on the junctional MAGI1 molecular complexes. Several studies, including proteomic approaches, have described a physical association between MAGI1 and AMOT or AMOTL2, two members of the angiomin family of apical scaffolds, acting both as junctions/actin linkers as well as negative regulators of YAP transcriptional activity (Bratt et al., 2005; Couzens et al., 2013; Hildebrand et al., 2017; Patrie, 2005; Wang et al., 2014). We thus, investigated whether AMOTs could mediate the effects of MAGI1 to restrict tumorigenesis in breast luminal cells.

First, using co-immunoprecipitation experiments, we confirmed that overexpressed Flag-tagged MAGI1 or endogenous MAGI1 interacted with endogenous AMOT and AMOTL2 in MCF7 luminal BCa cells (Fig. 6A&B). Building on the availability of numerous constructs generated by the group of KL. Guan (B. Zhao et al., 2011), we have then used AMOT as a paradigm to study the interaction between MAGI1 and AMOTs through co-immunoprecipitation experiments between Flag-tagged MAGI1 and HA-tagged AMOT constructs. Using point mutations affecting key structural Proline residues in the first and second WW motifs of MAGI1, we showed that the second WW motif was required for the interaction with AMOT, since co-immunoprecipitation was abolished by a point mutation on Proline residue 390 (mutated to Alanine MAGI1 P390A; Fig. 6C&D). The first WW domain appeared dispensable as no change in binding was observed when mutating Proline 331 (MAGI1 P331A). Similar results were obtained performing co-immunoprecipitations on endogenous AMOTL2 (Fig. 6E), showing that as for AMOT, the second WW domain of MAGI1 was required for AMOTL2 binding, confirming earlier findings (Patrie, 2005). The N-terminus part of AMOT contains two PPXY motifs, which represent canonical WW domains interactors. Using HA-tagged AMOT point mutants, we then determined that the interaction between MAGI1 and AMOT occurred through the second PPXY motif (Fig. 6F&G) since co-immunoprecipitation was lost in AMOT Y287A (Tyrosine 287 mutated to Alanine; the mutation AMOT Y242A did not show any effect). Together these results confirm using precise point mutations that MAGI1 binds to AMOT and AMOTL2 through its second WW domain, and at the level of the conserved second PPXY motifs of the N-terminal domains of AMOT family scaffolds.

Then, using immunofluorescence on MCF7 fixed cells, MAGI1, AMOT, and AMOTL2 localized in overlapping membrane domains corresponding to cellular junctions (Fig. 6H; the AMOT nuclear staining is non-specific). Even though, MAGI1 colocalized with AMOTL2 and AMOT (Fig. 6H, arrows), it was not required for their proper membrane localizations as they were unaffected in *shMAGI1*, suggesting that even though they physically interact once in proximity, they must reach their membrane localization independently (Fig. 6I). Nevertheless, even though MAGI1 was not required for AMOTL2 localization, it did however control AMOTL2 levels, and AMOTL2 accumulated 1.8 fold in MCF7*shMAGI1* compared to controls as measured by western blots on whole protein extracts (Supplemental Fig. 3A&B). These results suggest that MAGI1 regulates the stability and/or degradation of AMOTL2, but using classic drugging approaches, we were unable to identify the mechanisms involved.

Together our results confirm the physical interaction between MAGI1 and AMOTs and show that MAGI1 restricts the total AMOTL2 protein levels, through a mechanism that remains to be established.

AMOTL2 mediates the increased tumorigenicity of MAGI1-deficient luminal BCa cells

We observed that in luminal BCa cells, the loss of MAGI1 triggered both i) an accumulation of AJs material including its binding partner AMOTL2, and ii) an activation of the p38 pathway driving an increase in tumorigenicity. We thus studied next whether these two different aspects were linked or independent consequences of MAGI1 loss. Generating double knockdown MCF7 cells for *MAGI1* and *AMOTL2*, we could show that the increased 2D growth and anchorage-independent growth after MAGI1 loss were suppressed by the knockdown of *AMOTL2* (Fig. 7A&B). Consistently, *AMOTL2* knockdown abolished the accumulation of E-cadherin and the activation of the p38 stress kinase (phospho-p38 levels; Fig. 7C&D). These results identify AMOTL2 accumulation as a critical mediator in the p38 activation and tumorigenesis induced by impaired *MAGI1*.

Together, these results show that both AMOTL2 and ROCK activity are required for p38 activation in MAGI1 deficient luminal BCa cells. They support a model in which, the AMOTL2 accumulation in MAGI1 deficient cells governs an increase of E-cadherin-based junctions, which together with ROCK activity and cortical actin tension, activates the tumorigenic activity of the p38 signaling pathway (Fig.7E).

DISCUSSION

In this study, we explored the function of the junctional component MAGI1 in breast carcinogenesis and showed that the loss of MAGI1 in luminal BCa cell lines promoted tumorigenesis. At the cellular level, we showed that the loss of MAGI1 induced an accumulation of AJ components and increased cell compression behaviors. Importantly, we showed that the increased tumorigenicity of MAGI1 deficient luminal BCa cells was mediated by p38 stress signaling. Molecularly, we confirmed that MAGI1 interacted with the AMOT family of apical scaffolds and actin linkers, and showed that decreasing *AMOTL2* levels, completely suppressed the effect of *MAGI1* loss on the activation of p38 and on tumorigenicity. Finally, we provided evidence that inhibiting ROCK activity could alleviate the p38 activation, supporting a model in which MAGI1 suppresses luminal BCa by preventing both ROCK and AMOTL2-mediated Junction dysfunction, and subsequent p38 stress signaling.

The loss of MAGI1 led to an increase in tumorigenicity, and an accumulation of AJ material, in particular E-cadherin, reminiscent to the role we described previously for the unique MAGI homologue in *Drosophila* (Zaessinger et al., 2015). This correlation could appear counterintuitive as E-cadherin knockdown promotes invasion and migration in cultured cells (Frixen et al., 1991), and is critical during EMT and for aggressiveness (recently reviewed in (Yang et al., 2020)). However, in several cancers including some BCa, E-cadherin expression is maintained with a proposed tumor supporting role (Kleer et al., 2001; Rodriguez et al.,

2012) and recent mouse models of luminal and basal invasive ductal carcinomas have demonstrated that mammary cancer cells proliferation, resistance to apoptosis, and distant metastatic seeding potential, require E-cadherin (Padmanaban et al., 2019). These observations reconcile the high E-cadherin levels and increased tumorigenicity observed upon *MAGI1* loss, and suggest that at least in specific phases of tumorigenesis (e.g. mass proliferation, colony formation), E-cadherin could play a positive role during BCa.

One striking feature of *MAGI1* depleted cells is the protein accumulation of *AMOTL2*. Even though the exact mechanisms remain to be described, the stability of the related *AMOT* is controlled by the activity of the *RNF146/Tankyrase* pathway (Campbell et al., 2016; Wang et al., 2015), and by phosphorylation by the Hippo pathway core kinase *LATS1* (reviewed by (Maugeri-Saccà and De Maria, 2018)). Importantly *AMOTL2*, a binding partner of *MAGI1*, is required for the increased tumorigenicity of *MAGI1*-depleted luminal BCa cells, showing that *AMOTL2* is a critical mediator in this context. *AMOTs* are apical scaffolds playing important roles in cadherin-based junction regulations and its linkage to the actin cytoskeleton (Hildebrand et al., 2017; Hultin et al., 2014, 2017). Previous reports have shown that *AMOTL1* is overexpressed in invasive ductal carcinomas, leading to invasive behaviors. However, this effect of *AMOTL1* appears specific to ER-negative subtypes (Couderc et al., 2016). *AMOTL1* is not expressed in breast luminal lineages, in which *AMOTL2* is the most abundant (twice more abundant than *AMOT* in MCF7 cells; our unpublished observation). We propose thus that in ER-positive luminal breast lineages, *AMOTL2* overexpression could play similar roles as marker and mediator of tumorigenesis. Interestingly, a short isoform of *AMOTL2* (*AMOTL2* p60 in contrast to the long *AMOTL2* p100) was reported overexpressed in *in situ* and invasive ductal carcinoma cells (Mojallal et al., 2014). The *AMOTL2* p60 isoform lacks the PPxY domain critical for its interaction with *MAGI1*, and it is possible this isoform is thus insensitive to *MAGI1*-dependent destabilization, even though this remains to be studied. Hypoxia and Fos signaling govern the specific expression of *AMOTL2* p60 (Mojallal et al., 2014), and the accumulation of *AMOTL2* in the context of *MAGI1* mutation could thus represent an alternative mechanism for *AMOTL2* expression, extending the relevance of *AMOTL2* up-regulation during carcinogenesis.

AMOTL2 couples adhesion complexes to the actin cytoskeleton to allow F-actin tension and thus morphogenesis in endothelial cells (coupling with VE-cadherin (Hultin et al., 2014)) and in epithelial cell during embryogenesis (E-cadherin (Hildebrand et al., 2017)). Importantly, the specific cellular morphology defects in *AMOTL2* knockdown could be mimicked by inhibiting ROCK kinase and Myosin phosphorylation showing that *AMOTL2* and actin tension are linked (Hildebrand et al., 2017). Relaxing actin tension using two ROCK inhibitors (Y-27632 and Blebbistatin), or preventing *AMOTL2* accumulation (siRNA), both robustly suppressed p38 activation, a key feature mediating tumorigenesis after *MAGI1* loss. So how could *AMOTL2* and ROCK interact to mediate the effects of *MAGI1* loss? They could either (i) be two independent consequences of *MAGI1* loss or (ii) they could be linked causally. Due to the toxicity of long term exposures to ROCK inhibitors, we were unable to study whether *AMOTL2* stability could be a consequence of ROCK activity. Preliminary results would indicate that *AMOTL2* does not control ROCK activity (data not shown), suggesting that ROCK might act upstream, or in parallel to *AMOTL2*, but more experiments are needed to better determine how *MAGI1* controls ROCK activity, and how ROCK and *AMOTL2* regulate p38 activity.

p38 signaling is activated by many upstream signals including a wide variety of environmental stresses such as UV, genotoxic agents, heat shock, or hyperosmotic conditions (Wagner and Nebreda, 2009). During osmotic shock, the cellular cortex is subjected to external pressure reminiscent to compressive forces, and we propose therefore that E-cadherin and AMOTL2 enrichment, together with increased ROCK activity and actin tension result in similar compressive forces that could represent a new stress signal activating p38. Amongst the four different p38 kinases (p38 α , β , δ), P38 α is the most ubiquitously expressed. p38 signaling has been implicated either as a tumor suppressor or as an oncogene depending on cancer type and stage (Gupta et al., 2014; Hardwick et al., 2001; Maik-Rachline et al., 2018; Wagner and Nebreda, 2009). In BCa, targeting p38 δ resulted in a reduced rate of cell proliferation and enhanced cell-matrix adhesion (Wada et al., 2017). More importantly, BCa mouse models, demonstrated the critical role of p38 α (Mapk14) during the initiation, and proliferation of mammary tumors. The tumor promoting role of p38 α involves a protective role against deleterious DNA damage in the mammary epithelial cancer cells (Cánovas et al., 2018b). We observed in *MAGI1*-deficient cells an increased proportion of cells in S-phase, indicating that these cells might have a slower S-phase. Slow S-phase is classically observed when cells have to overcome a high level of DNA damage. These results highlight the need for further studies to better understand the link between *MAGI1* loss, p38 activation, DNA damage, and breast tumorigenesis.

Besides elevated p38 signaling, *MAGI1*-deficient cells exhibited low YAP nuclear activity, consistent with earlier reports showing that in epithelial cells with high E-cadherin and/or under compressive forces α -Catenin and NF2/Merlin act to exclude YAP from the nucleus (Furukawa et al., 2017). Here we demonstrated the critical role of AMOTL2 downstream of *MAGI1* to mediate E-cadherin accumulation. Since AMOTs have been shown to trap YAP in the cytoplasm (B. Zhao et al., 2011), further studies are thus required to better understand the interactions between *MAGI1*/AMOTL2 and α -Cat/NF2 in the control of YAP localization and activity. This low YAP signaling could appear surprising since the oncogenic role of nuclear YAP is well established (Zanconato et al., 2016). However, the oncogenic role of YAP in luminal BCa remains debated. While elevated YAP/TAZ activity gene signatures have been reported to correlate with more aggressive BCa (Bartucci et al., 2015; Cordenonsi et al., 2011; Di Agostino et al., 2016), aggressive BCa are enriched in basal/triple negative sub-types. Furthermore, several studies report conflicting or no correlation between YAP staining levels and clinical outcomes in BCa patients (reviewed in (Zanconato et al., 2016)) suggesting that YAP/TAZ levels and nucleo/cytoplasmic distributions in luminal BCa could be re-examined.

ACKNOWLEDGEMENTS

We acknowledge the contribution of G. Froment, D. Nègre and C. Costa from lentivectors' production facility of SFR Biosciences (UMS3444/CNRS, US8/Inserm, ENS Lyon, UCBL, France). We thank the ABIC (IRCM), MRI (IRCM), MGC (IGMM) platforms, and the URT (IRCM, Montpellier, France). We thank V. Chambon and T. Soirat for technical help with the mammosphere formation assay and PE Milhiet (CBS, Montpellier, France) for helpful discussion and AFM set up. All plasmids obtained from Addgene are detailed in the Material

and Methods section and all references have been included. We also thank Drs C. Gongora, L. Holmgren, N. Tapon, and B. Zhao for discussion, tools and advice. This work was supported by grants from Fondation ARC and Ligue Régionale Contre le Cancer (34) to LHM and AD. DK is supported by Ligue Nationale Contre le Cancer. VS and EB were supported by Fondation de France.

AUTHOR CONTRIBUTIONS

DK, VS, EB, YBS, EF, ML, FBM, CB, LC, BO, and LHM performed experiments. LHM and AD designed the experiments. DK, JC, BO, LHM, and AD analyzed the data. DK, PL, CG, JC, CT, AM, LHM, and AD interpreted the data. LHM and AD wrote the manuscript.

FIGURES

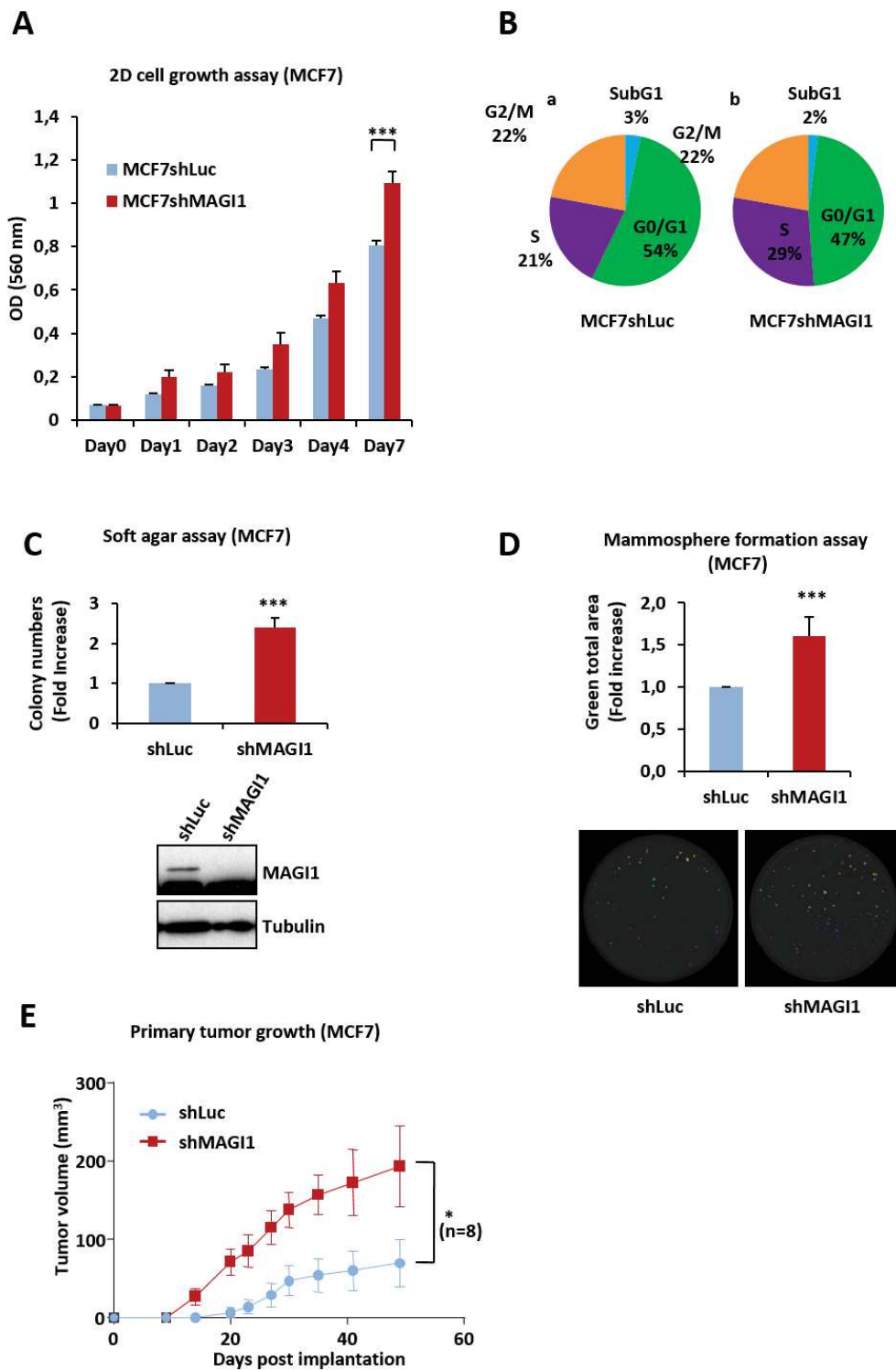


Figure 1: MAGI1 impairment induces tumorigenic phenotypes in epithelial cells

(A) MTT assay (OD 560 nm) representing 2D cell growth of MCF7shMAGI1 as compared to MCF7shLuc cells. Bars represent mean \pm Standard Deviation (SD; n=10 wells as replicates) of a representative experiment (out of 3). Unpaired two-tailed Student's t-test; *** p < 0.001.

(B) Cell cycle phases of MCF7shLuc (a) and MCF7shMAGI1 (b) cells labeled with propidium iodide and analyzed by Flow cytometry, showing a slight increased proportion of cells in S phase at the expense of G0/G1 after MAGI1 invalidation.

(C) Top: quantification of colony numbers of MCF7shMAG1 cells grown in anchorage independent conditions (soft agar assay) and represented as fold increase compared to MCF7shLuc cells. Data are presented as the means \pm SD (n=3). Unpaired two-tailed Student's t-test; *** p < 0.001. Bottom: western blot analysis of whole protein extracts issued from the cells used in the soft agar assays and showing the relative amounts of MAG1 in the different cell lines; Tubulin was used as a loading control.

(D) Top: quantification of mammospheres represented as total area issued from MCF7shMAG1 cells and shown as fold increase compared to MCF7shLuc cells, starting from 200 cells. Data are presented as the means \pm SD (n=4). Unpaired two-tailed Student's t-test; *** p < 0.001. Bottom: images of mammosphere formation assay showing a representative experiment.

(E) Primary tumor growth of MCF7shLuc and MCF7shMAG1 cells injected subcutaneously in nude mice. Primary tumor growth was assessed by measuring the tumor volume over time until the tumors were too big and the mice had to be euthanized. Bars correspond to the mean \pm Standard Error to the Mean (n=8 mice per group). Unpaired two-tailed Student's t-test; * p < 0.05.

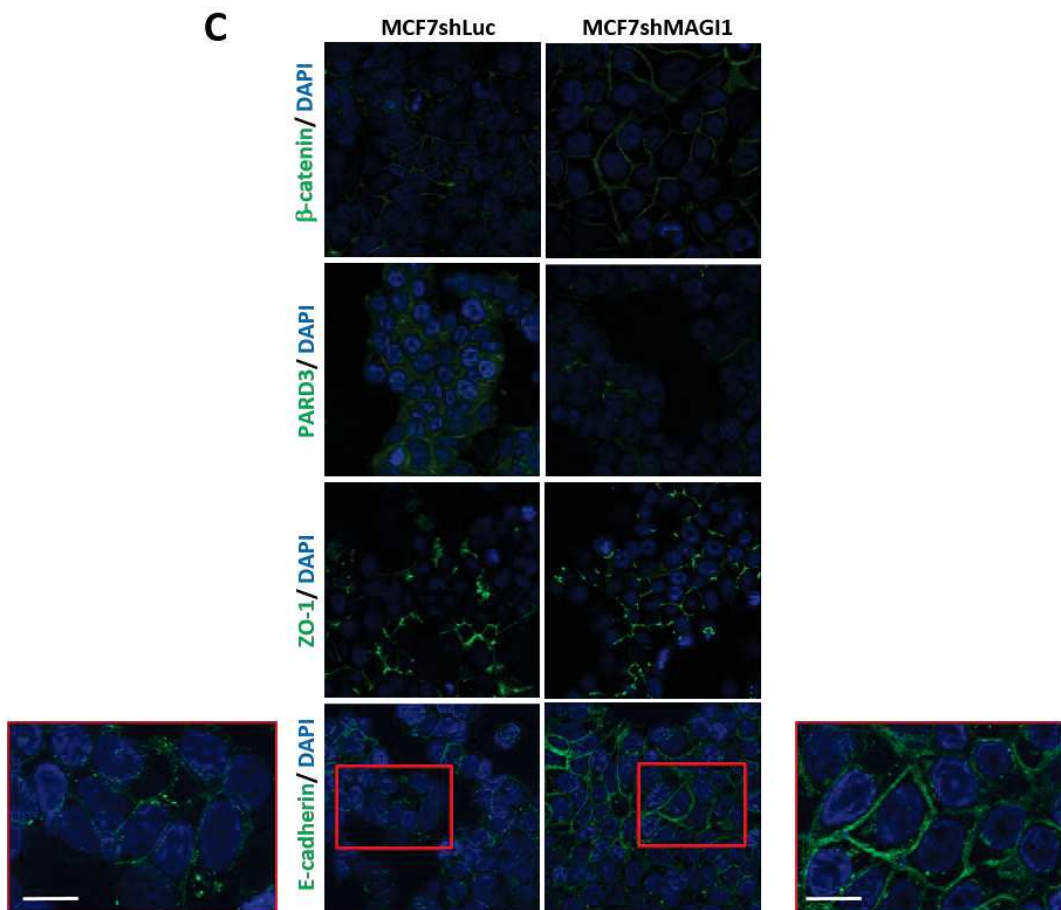
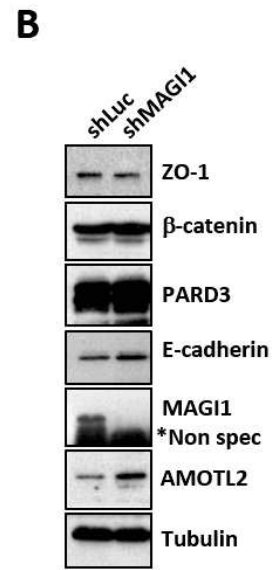
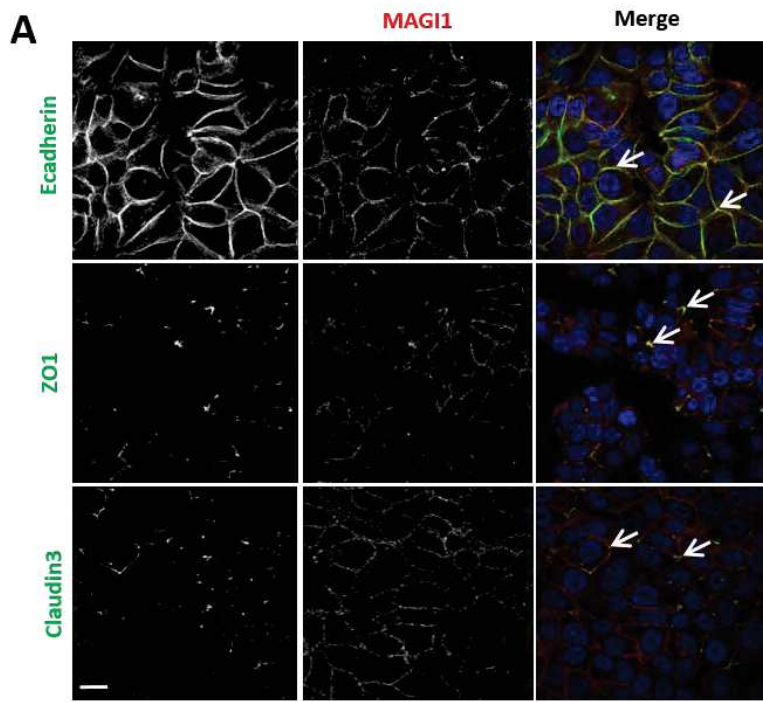


Figure 2: The loss of MAGI1 affects E-cadherin levels and localization in MCF7 cells

(A) Representative immunofluorescence experiments performed in MCF7 cells monitoring MAGI1 localization (red) compared to E-cadherin, ZO1, and Claudin3 (green). DAPI (blue) was used to stain DNA and the nuclei. White arrows indicate staining overlap. Scale bar=10 μ m.

(B) Western blot analysis of whole protein extracts (n=4) monitoring the expression the junctional components Claudin-1, ZO-1, β -catenin, PARD3, E-cadherin and AMOTL2 in MCF7*shMAGI1* cell lines compared to MCF7*shLuc*. Tubulin was used as a loading control. Note the increase in E-cadherin levels. Western blot experiments have been repeated at least four times. Protein expression levels were quantified as compared to Tubulin (not shown).

(C) Representative immunofluorescence experiments (n=3) were performed on MCF7*shMAGI1* compared to MCF7*shLuc* cells monitoring the localization of β -catenin, PARD3, Claudin-3, ZO-1 and E-cadherin (green). DAPI (blue) was used to stain DNA and the nuclei. Scale bar=10 μ m. Note the slight sub-cortical accumulation of E-cadherin shown in the high magnification images.

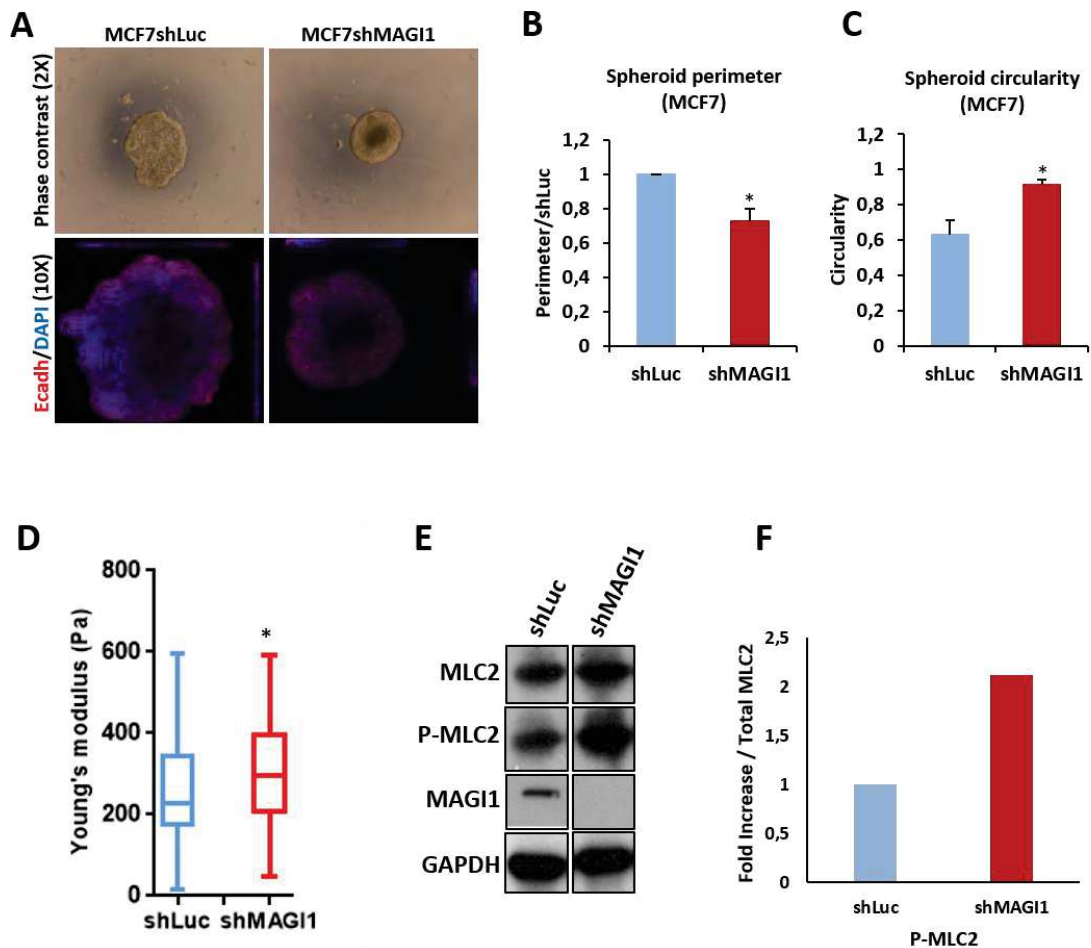


Figure 3: The loss of MAGI1 affects MCF7 cell compaction, ROCK activity, and compressive forces

(A) Representative phase contrast and fluorescence images of MCF7shLuc and MCF7shMAGI1 cells grown in 3D spheroid cultures and stained with E-cadherin (red) and DAPI (blue).

(B) Calculated perimeters for 3D spheroid cultures of MCF7shMAGI1 normalized by the perimeter of MCF7shLuc cells. Bars represent mean \pm SD (n=10 spheroids) of five independent experiments. Unpaired two-tailed Student's t-test; * $p < 0.05$.

(C) Calculated circularity for 3D spheroid cultures of MCF7shLuc and MCF7shMAGI1 (calculations were done with the ImageJ software where a value of 1 is considered as a perfect circle). Bars represent mean \pm SD (n=10 spheroids) of five independent experiments. Unpaired two-tailed Student's t-test; * $p < 0.05$.

(D) Elastic Young's modulus (EYM) of cells: Hertz contact mechanics model for spherical indenters was used. In MCF7shMAGI1 cells, the apical surface EYM is significantly elevated when compared to control MCF7shLuc cells. Data are represented as mean \pm standard deviation: shLuc EYM= 258.8 \pm 101, shMAGI1 EYM= 302.4 \pm 91. Unpaired two-tailed Student's t-test; * $p < 0.05$ (n=132 and 94 for shLuc and shMAGI1 respectively).

(E) Western blot analysis on whole protein extracts (n=3) of ROCK-specific ser19 phosphorylation of Myosin Light Chain 2, total MLC2 and MAGI1 in MCF7shMAGI1 cell lines compared to MCF7shLuc. GAPDH was used as a loading control.

(F) Quantification of the representative Western blot showing protein expression represented in panel E. Phosphorylated proteins were quantified as compared to their total protein counterparts to evaluate their activation.

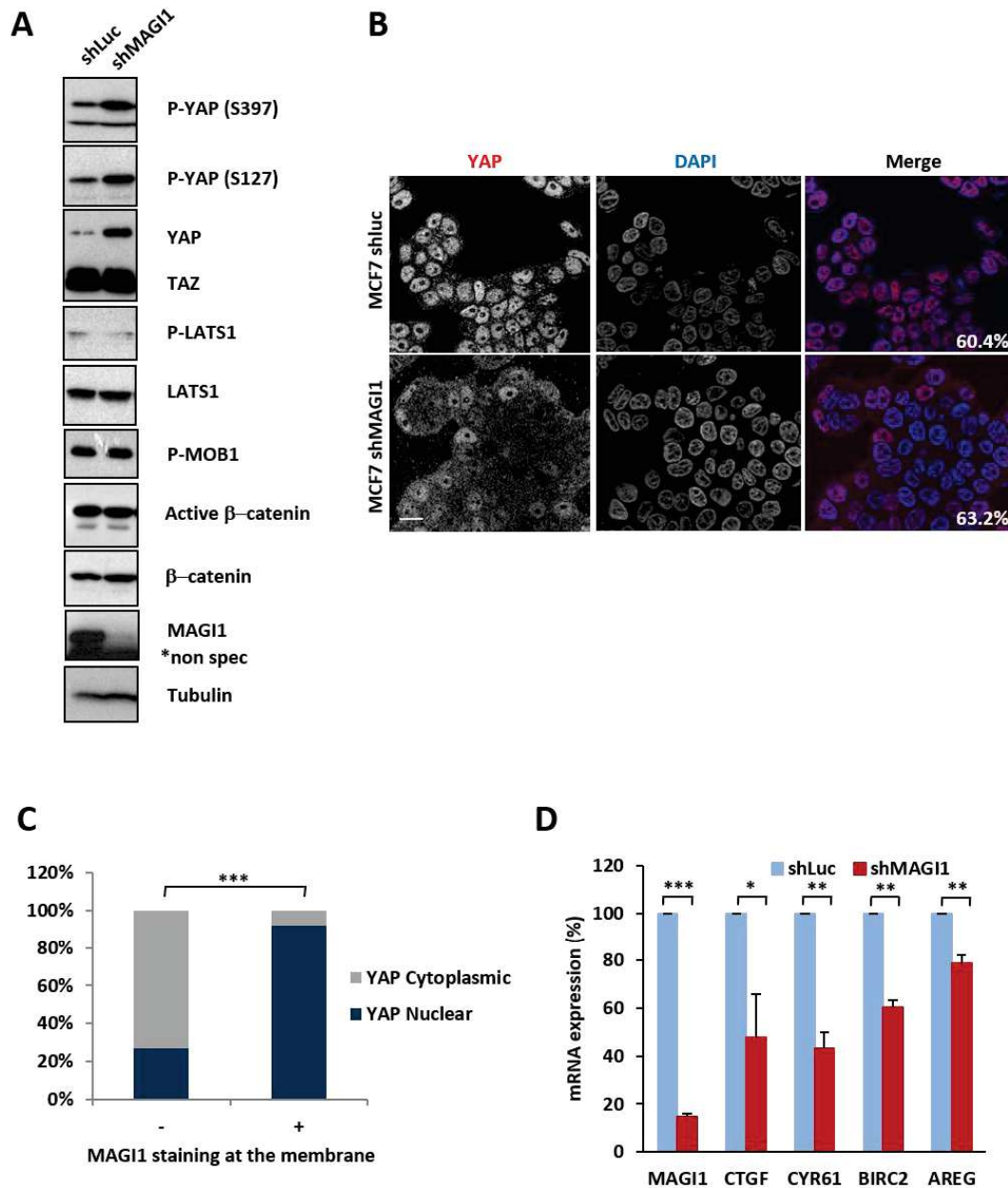


Figure 4: The loss of MAGI1 tumorigenic phenotypes are not associated with active YAP

(A) Western blot analysis on whole protein extracts (n=3) of phosphorylated YAP (S397 & S127), total YAP and TAZ, phosphorylated LATS1, total LATS1, phosphorylated MOB1, non-phosphorylated (active) β -catenin, total β -catenin and MAGI1 in MCF7shMAGI1 cell lines compared to MCF7shLuc. Tubulin was used as a loading control.

(B) Representative immunofluorescence images (n=3) of endogenous MAGI1 and YAP protein expression in MCF7shLuc and MCF7shMAGI1 cells cultured to similar confluence (60.4 % and 63.2 % respectively). Scale bar=10 μ m.

(C) Quantification of MAGI1 and YAP staining in a tissue micro-array (TMA) from luminal breast cancer patients in a cohort of 28 patients, showing the strong correlation between MAGI1 membranous and YAP nuclear localizations; Fisher exact test, *** p<0.001. Histogram shows the percentages of patients having a nuclear or a cytoplasmic YAP staining according to the absence or the presence of MAGI1 membranous staining.

(D) Real-time qRT-PCR showing the expression of canonical Hippo pathway target genes (CTGF, CYR61, BIRC2 and AREG) in MCF7shMAGI1 compared to the control MCF7shLuc cells and normalized with GAPDH expression. Data are presented as the means \pm SD (n=3). Unpaired two-tailed Student's t-test; * p < 0.05; ** p < 0.01; *** p < 0.001.

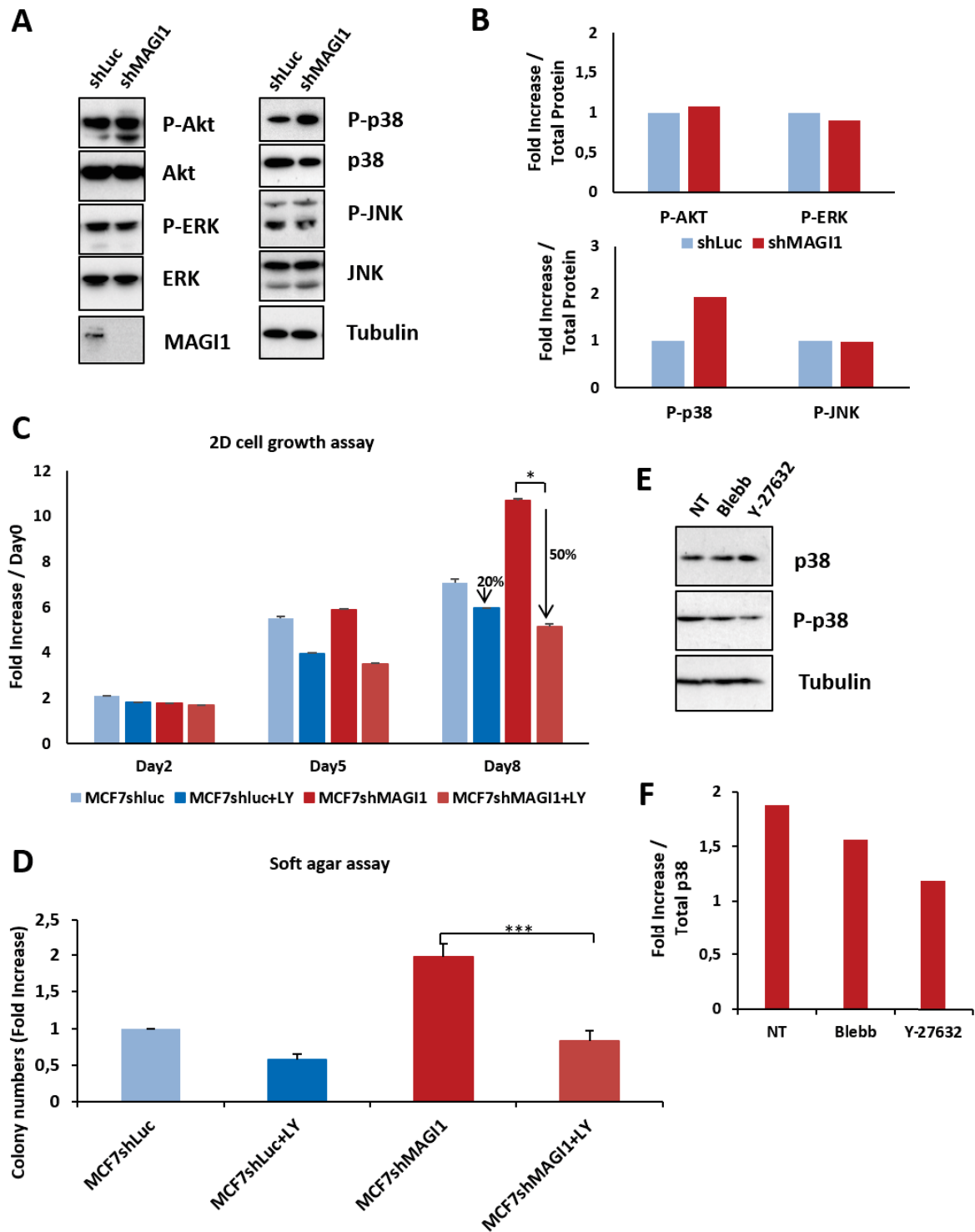


Figure 5: The loss of MAGI1 tumorigenic phenotypes are associated with p38 stress signaling pathway activation

(A) Western blot analysis showing protein expression and/or activation of Akt and MAPK proliferation signaling pathways as well as p38 and JNK stress signaling pathways in MCF7shMAGI1 compared to MCF7shLuc cells. Tubulin was used as a loading control. Western blot experiments have been repeated at least three times.

(B) Quantification of the representative Western blot showing protein expression represented in panel A. Phosphorylated proteins were quantified as compared to their total protein counterparts to evaluate their activation. (C) 2D cell growth assay of MCF7shMAGI1 treated, or not, with the p38 MAPK inhibitor LY2228820 (LY in the figure) compared to MCF7shLuc.

Bars represent mean \pm SD (n=6 wells as replicates) of a representative experiment (n=3). Unpaired two-tailed Student's t-test; * p<0.05. Note the increased percentage of drop for MCF7*shMAG1* cells at day 8.

(D) Quantification of colony numbers of MCF7*shMAG1* cells non treated or treated with LY2228820 grown in anchorage independent conditions (soft agar assay) and represented as fold increase compared to MCF7*shLuc* cells non treated or treated with the p38 inhibitor (LY in the figure). Data are presented as the means \pm SD (n=3). Unpaired two-tailed Student's t-test; *** p < 0.001.

(E) Western blot analysis showing protein levels of phosphorylated p38 and total p38 in MCF7*shMAG1* cells treated or non-treated (NT) with Blebbistatin (Blebb) or Y-27632. Both inhibitors were used at 10 μ M during 2 h and Tubulin that was used as a loading control.

(F) Quantification of the representative Western blot showing protein expression and represented in panel E. Phosphorylated p38 was quantified as compared to total p38 to evaluate its activation.

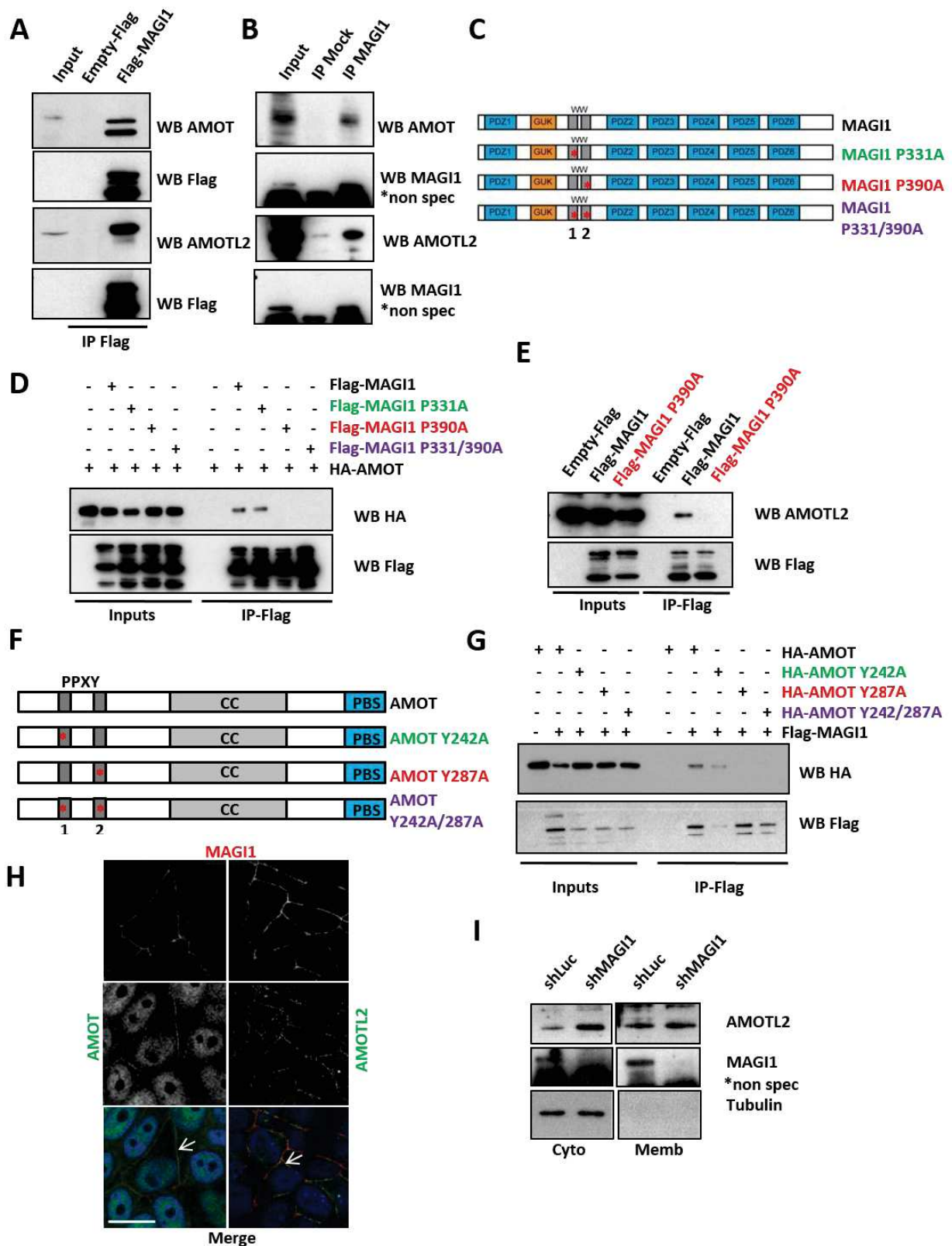


Figure 6. MAGI1 interacts with AMOT and AMOTL2

(A) Western blot of Flag-MAGI1 immunoprecipitates: Flag-MAGI1 transfections were performed in MCF7 cells and endogenous AMOT (upper panels) and AMOTL2 (lower panels) were revealed; Flag blotting was used as the immunoprecipitation control. Note that we could hardly detect Flag-MAGI1 by Western blot in the inputs, even though

MAGI1 was well immunoprecipitated, due to sensitivity issues associated with single Flag tag in Flag-MAGI1 used in this typical experiment.

(B) Western blot analysis of endogenous MAGI1 immunoprecipitates revealing the presence of endogenous AMOT (upper panels) and AMOTL2 (lower panels). MAGI1 blotting was used as the immunoprecipitation control (*shows non-specific bands with the anti-MAGI1 antibody).

(C) Schematic of full length MAGI1 and of the point MAGI1 WW domain mutants used (P331A & P390A).

(D) Western blot analysis of Flag-MAGI1 immunoprecipitates on protein extracts from MCF7 cells transfected with HA-AMOT and different Flag tagged MAGI1 constructs, showing that the interaction with AMOT occurred through the second WW domain of MAGI1 (interaction lost in P390A; red).

(E) Western blot analysis of Flag-MAGI1 immunoprecipitates on protein extracts from MCF7 cells transfected with Flag-MAGI1 or Flag-MAGI1 P390A mutant, revealing the interaction of endogenous AMOTL2 with Flag-MAGI1 but not Flag-MAGI1 P390A (red).

(F) Schematic of full-length AMOT and of the point AMOT PPXY mutants used (Y242A & Y287A).

(G) Western-blot analysis of Flag-MAGI1 immunoprecipitates on protein extracts from MCF7 cells transfected with Flag-MAGI1 and different HA-AMOT constructs, showing that the interaction occurs through the second PPXY domain of AMOT (interaction lost in Y287A; red). Similar levels of interaction were obtained for HA-AMOT/Flag-MAGI1 and HA-AMOT Y242A/Flag-MAGI1 complexes (quantified using the ImageJ software).

(H) Representative immunofluorescence images of endogenous staining for MAGI1 (red; top panels) co-localizing at the plasma membrane (white arrows) with AMOT (green; left) or AMOTL2 (green; right) in MCF7 cells. Note the non-specific nuclear staining for AMOT. Scale bar=10 μ m.

(I) Western blot analysis after subcellular fractionation showing the relative amount of AMOTL2 protein in the cytoplasmic and membrane fractions in MCF7*shMAGI1* compared to MCF7*shLuc* cells. Tubulin was used as a cytoplasmic control for the fractionation and for normalization.

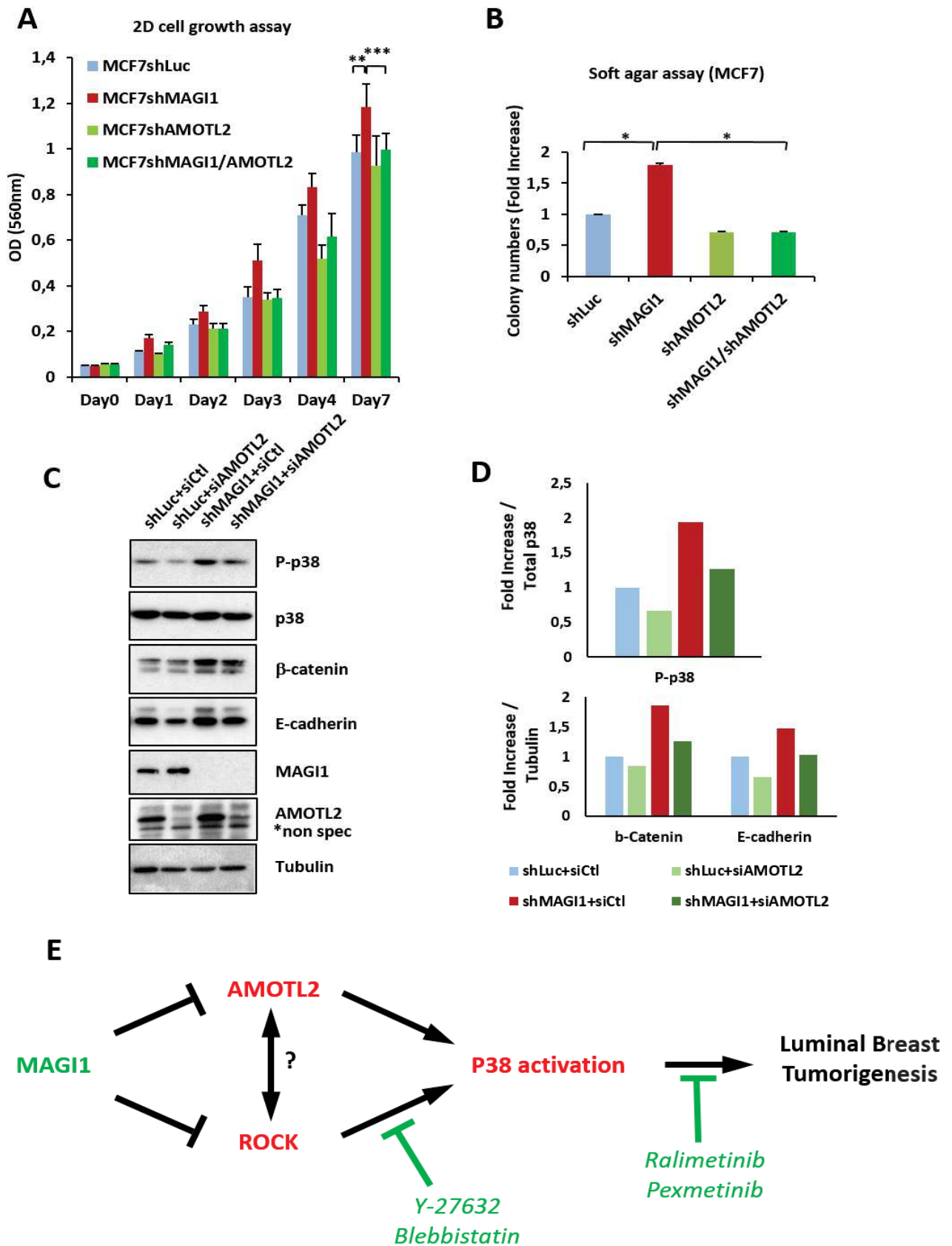


Figure 7. AMOTL2 mediates the effects of MAGI1 on junctions and on p38 signalling

(A) MTT assay (OD 560 nm) representing 2D cell growth of MCF7*shMAG1*, MCF7*shAMOTL2* and MCF7*shMAG1/shAMOTL2* cells as compared to MCF7*shLuc*. Bars represent mean \pm SD (n=10 wells as replicates) of a representative experiment (n=3). Unpaired two-tailed Student's t-test; ** p<0.01; *** p < 0.001.

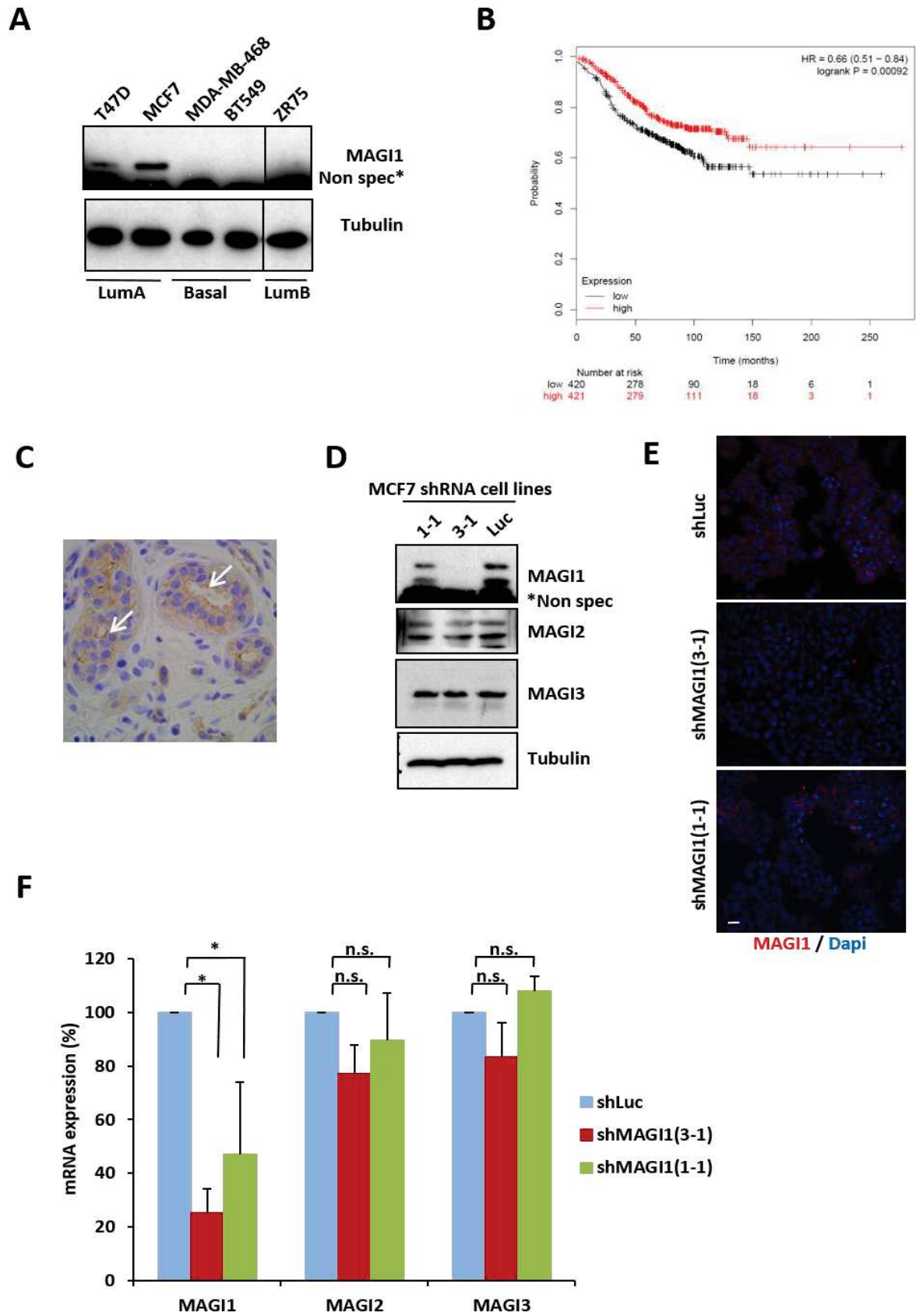
(B) Quantification of colony numbers of MCF7 cells (*shMAG1*, *shAMOTL2* & *shMAG1/shAMOTL2*) grown in anchorage independent conditions (soft agar assay) and represented as fold increase compared to MCF7*shLuc* cells. Data are presented as the means \pm SD (n=3). Unpaired two-tailed Student's t-test; * p < 0.05. Western blot analyses confirmed the 90 % knockdown for MAG1 in MCF7*shMAG1* and MCF7*shMAG1/shAMOTL2* and QPCR data confirmed the 50 to 60 % knockdown for AMOTL2 in MCF7*shAMOTL2* and MCF7*shMAG1/shAMOTL2* respectively (determined by RT-qPCR and/or Western Blot ; Data not shown).

(C) Western blot analysis showing protein expression and/or phosphorylation (activation) of p38 and JNK stress signaling pathways as well as junctions' components in MCF7*shMAG1* as compared to MCF7*shLuc* cells when *AMOTL2*siRNA were transfected. Tubulin was used as a loading control. Western blot experiments have been repeated at least three times.

(D) Quantification of the representative Western blot showing protein expression and represented in panel C. Phosphorylated proteins were quantified as compared to their total protein counterparts to evaluate their activation and junctions' proteins were quantified as compared to tubulin that was used as a loading control. Upper: Phosphorylated p38 / Total p38 protein quantification and Lower: protein / Tubulin quantification.

(E) Model for the role of MAG1 during Luminal BCa. MAG1 prevents the accumulation of junctional AMOTL2 and E-cadherin as well as ROCK activity thus releasing cellular stiffness. Increased AMOTL2 and ROCK then activate p38 stress signaling responsible for the increased tumorigenicity of MAG1-deficient cells. Anti and Pro tumorigenic events are highlighted in green and red respectively.

SUPPLEMENTAL FIGURE LEGENDE



Suppl Figure 1

(A) Western blot showing MAGI1 expression in different breast cancer cell lines (T47D and MCF7 from the luminal A sub-type, MDA-MB-468 and BT549 from basal sub-type and ZR75 from luminal B sub-type). Tubulin was used as loading control.

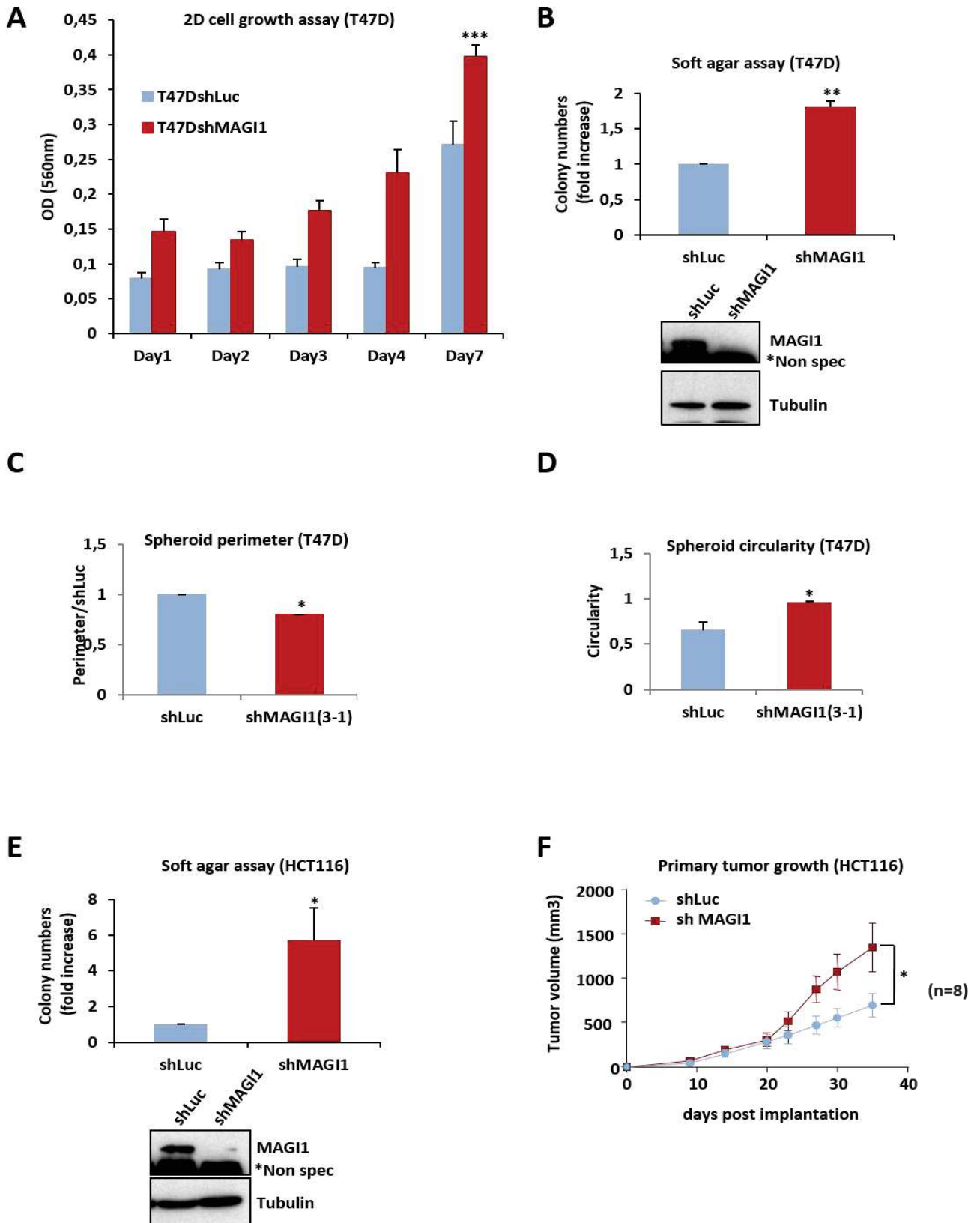
(B) Kaplan-Meier survival curves and log-rank analysis. Relapse-free survival (RFS) curves for 841 ER positive breast cancer patients as a function of MAGI1 expression. Patients were split according to median expression. Data for MAGI1 (225474_at) were obtained using the KM plotter website at <http://kmplot.com> (Gyorffy B, Lanczky A, et al, Breast Cancer Res Treatment, 2010).

(C) Representative immunohistochemical staining of MAGI1 performed in normal human breast samples. Brown staining indicates positive immunoreactivity and arrows show MAGI1 staining.

(D) Western blot analysis of MAGI1, MAGI2 and MAGI3 expression in MCF7*shMAGI1(1-1)* and MCF7*shMAGI1(3-1)* showing respectively 50% and 100% knockdown as compared to MCF7*shLuc* control cell line. Tubulin was used as a loading control.

(E) Representative immunofluorescence images showing MAGI1 staining (red) in the MCF7*shMAGI1 (1-1)* and (3-1) and in MCF7*shLuc* cell lines. Scale bar=10 μ m.

(F) Real-time qRT-PCR showing the expression of *MAGI1*, *MAGI2* and *MAGI3* mRNA in MCF7*shMAGI1(1-1)* and in MCF7*shMAGI1(3-1)* compared to the control MCF7*shLuc* cell line. Data are presented as the means \pm SD. Three independent experiments; unpaired two-tailed Student's t-test (* $p < 0.05$; n.s. not significant).



Suppl Figure 2

(A) MTT assay (OD 560 nm) representing 2D cell growth of T47DshMAGI1 as compared to T47DshLuc cells. Bars represent mean \pm SD (n=10 wells as replicates) of a representative experiment (n=3), showing similar increased cell growth as observed for MCF7 cells. Unpaired two-tailed Student's t-test; *** p < 0.001.

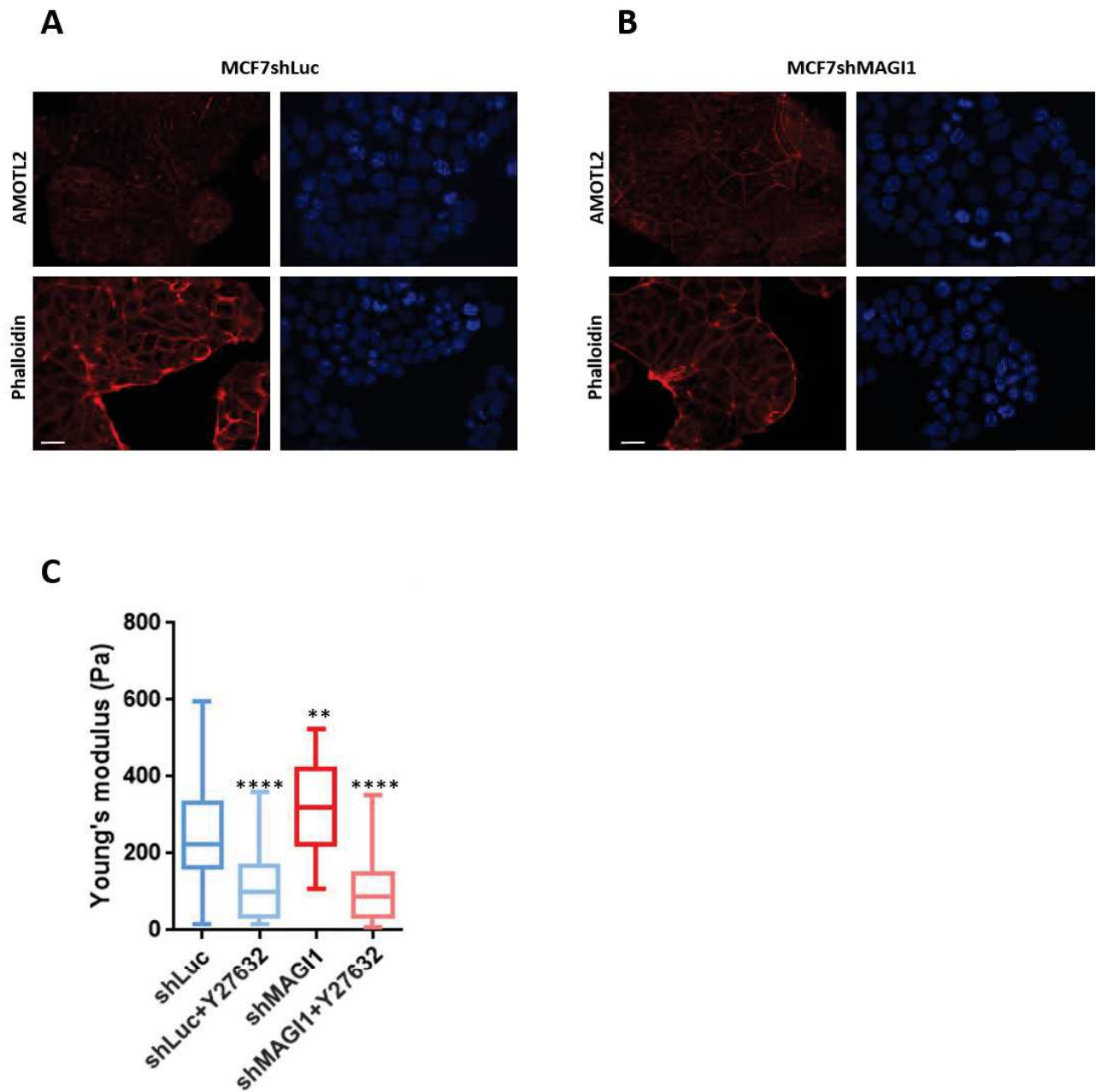
(B) Upper: quantification of the number of colonies of T47D*shMAG1* grown in anchorage independent conditions (soft agar assay) represented as fold increase compared to T47D*shLuc* cells. Data are presented as the means (n=3) ± Standard Deviation. Unpaired two-tailed Student's t-test; ** p < 0.01. Below: western blot analysis on whole protein extracts from cells used on the left showing the efficient MAG1 protein knockdown; Tubulin was used as a loading control.

(C) Calculated perimeters for 3D spheroids cultures of T47D*shMAG1* (shMAG1(3-1) cell line only) normalized by the perimeter of T47D*shLuc* cells. Bars represent mean ± SD (n=10 spheroids) of three independent experiments. Unpaired two-tailed Student's t-test; * p < 0.05.

(D) Calculated circularity for 3D spheroid cultures of T47D*shLuc* and T47D*shMAG1* (shMAG1(3-1) cell line only). Calculations were done with the ImageJ software where a value of 1 is considered as a perfect circle. Bars represent mean ± SD (n=10 spheroids) of three independent experiments. Unpaired two-tailed Student's t-test; * p < 0.05.

(E) Upper: quantification of the number of colonies of HCT116*shMAG1* grown in anchorage independent conditions (soft agar assay) represented as fold increase compared to HCT116*shLuc*. Data are presented as the means (n=3) ± Standard Deviation. Unpaired two-tailed Student's t-test; * p < 0.05. Below: analysis on whole protein extracts from cells used on the left showing the efficient MAG1 protein knockdown; Tubulin was used as a loading control.

(F) Primary tumor growth of HCT116*shLuc* and HCT116*shMAG1* cells injected subcutaneously in nude mice. Primary tumor growth was assessed by measuring the tumor volume over time until the tumors were too big and the mice had to be euthanized. Bars correspond to the average ± SEM (n=8 mice). Unpaired two-tailed Student's t-test (* p < 0.05).



Suppl Figure 3

(A&B) Representative immunofluorescence images of endogenous AMOTL2 and actin (phalloidin red staining) in MCF7shLuc (A) and MCF7shMAGI1 (B) showing unaffected localisation at the plasma membrane. Scale bar=10 μ m.

(C) Elastic Young's modulus (EYM) of cells treated, or not, with Y-27632 (10 μ M for 45 min): Hertz contact mechanics model for spherical indenters was used. In treated cells, the apical surface EYM is significantly decreased when compared to untreated cells. Data are represented as mean +/- standard deviation: shLuc untreated EYM= 248.4 +/- 133.5, treated with Y-27632 EYM= 112.0 +/- 81.5, shMAGI1 untreated EYM= 321.1 +/- 107.1 and shMAGI1 treated with Y-27632 EYM= 103.3 +/-79.9. Anova and unpaired two-tailed student's *t*-test; * p <0.05 (n=67, 49, 57 and 63 for untreated and treated control shLuc and shMAGI1, respectively).

REFERENCES

1. Holliday, D. L. & Speirs, V. Choosing the right cell line for breast cancer research. *Breast Cancer Res. BCR* 13, 215 (2011).
2. Guedj, M. *et al.* A refined molecular taxonomy of breast cancer. *Oncogene* 31, 1196–1206 (2012).
3. Knust, E. & Bossinger, O. Composition and formation of intercellular junctions in epithelial cells. *Science* 298, 1955–1959 (2002).
4. Coopman, P. & Djiane, A. Adherens Junction and E-Cadherin complex regulation by epithelial polarity. *Cell. Mol. Life Sci. CMLS* 73, 3535–3553 (2016).
5. Jeanes, A., Gottardi, C. J. & Yap, A. S. Cadherins and cancer: how does cadherin dysfunction promote tumor progression? *Oncogene* 27, 6920–6929 (2008).
6. Balda, M. S. & Matter, K. Tight junctions as regulators of tissue remodelling. *Curr. Opin. Cell Biol.* 42, 94–101 (2016).
7. Charras, G. & Yap, A. S. Tensile Forces and Mechanotransduction at Cell-Cell Junctions. *Curr. Biol. CB* 28, R445–R457 (2018).
8. Pinheiro, D. & Bellaïche, Y. Mechanical Force-Driven Adherens Junction Remodeling and Epithelial Dynamics. *Dev. Cell* 47, 3–19 (2018).
9. Benham-Pyle, B. W., Pruitt, B. L. & Nelson, W. J. Cell adhesion. Mechanical strain induces E-cadherin-dependent Yap1 and β -catenin activation to drive cell cycle entry. *Science* 348, 1024–1027 (2015).
10. Furukawa, K. T., Yamashita, K., Sakurai, N. & Ohno, S. The Epithelial Circumferential Actin Belt Regulates YAP/TAZ through Nucleocytoplasmic Shuttling of Merlin. *Cell Rep.* 20, 1435–1447 (2017).
11. Hirata, H., Samsonov, M. & Sokabe, M. Actomyosin contractility provokes contact inhibition in E-cadherin-ligated keratinocytes. *Sci. Rep.* 7, 46326 (2017).
12. Kim, N.-G., Koh, E., Chen, X. & Gumbiner, B. M. E-cadherin mediates contact inhibition of proliferation through Hippo signaling-pathway components. *Proc. Natl. Acad. Sci. U. S. A.* 108, 11930–11935 (2011).
13. Schlegelmilch, K. *et al.* Yap1 acts downstream of α -catenin to control epidermal proliferation. *Cell* 144, 782–795 (2011).
14. Silvis, M. R. *et al.* α -catenin is a tumor suppressor that controls cell accumulation by regulating the localization and activity of the transcriptional coactivator Yap1. *Sci. Signal.* 4, ra33 (2011).
15. Aoki, K. *et al.* Propagating Wave of ERK Activation Orients Collective Cell Migration. *Dev. Cell* 43, 305–317.e5 (2017).
16. Hall, E. T., Hoelsing, E., Sinkovics, E. & Verheyen, E. M. Actomyosin contractility modulates Wnt signaling through adherens junction stability. *Mol. Biol. Cell* 30, 411–426 (2019).
17. Pereira, A. M., Tudor, C., Kanger, J. S., Subramaniam, V. & Martin-Blanco, E. Integrin-dependent activation of the JNK signaling pathway by mechanical stress. *PloS One* 6, e26182 (2011).

18. Wagner, E. F. & Nebreda, A. R. Signal integration by JNK and p38 MAPK pathways in cancer development. *Nat. Rev. Cancer* 9, 537–549 (2009).
19. Beavon, I. R. The E-cadherin-catenin complex in tumour metastasis: structure, function and regulation. *Eur. J. Cancer Oxf. Engl.* 1990 36, 1607–1620 (2000).
20. Bosch-Fortea, M. & Martín-Belmonte, F. Mechanosensitive adhesion complexes in epithelial architecture and cancer onset. *Curr. Opin. Cell Biol.* 50, 42–49 (2018).
21. Laura, R. P., Ross, S., Koeppen, H. & Lasky, L. A. MAGI-1: a widely expressed, alternatively spliced tight junction protein. *Exp. Cell Res.* 275, 155–170 (2002).
22. Hirabayashi, S. *et al.* JAM4, a junctional cell adhesion molecule interacting with a tight junction protein, MAGI-1. *Mol. Cell. Biol.* 23, 4267–4282 (2003).
23. Padash Barmchi, M., Samarasekera, G., Gilbert, M., Auld, V. J. & Zhang, B. Magi Is Associated with the Par Complex and Functions Antagonistically with Bazooka to Regulate the Apical Polarity Complex. *PLoS One* 11, e0153259 (2016).
24. Zaessinger, S., Zhou, Y., Bray, S. J., Tapon, N. & Djiane, A. Drosophila MAGI interacts with RASSF8 to regulate E-Cadherin-based adherens junctions in the developing eye. *Dev. Camb. Engl.* 142, 1102–1112 (2015).
25. Lynch, A. M. *et al.* A genome-wide functional screen shows MAGI-1 is an L1CAM-dependent stabilizer of apical junctions in *C. elegans*. *Curr. Biol. CB* 22, 1891–1899 (2012).
26. Hultin, S. *et al.* AmotL2 links VE-cadherin to contractile actin fibres necessary for aortic lumen expansion. *Nat. Commun.* 5, 3743 (2014).
27. Feng, X., Jia, S., Martin, T. A. & Jiang, W. G. Regulation and involvement in cancer and pathological conditions of MAGI1, a tight junction protein. *Anticancer Res.* 34, 3251–3256 (2014).
28. Zhang, G., Liu, T. & Wang, Z. Downregulation of MAGI1 associates with poor prognosis of hepatocellular carcinoma. *J. Invest. Surg. Off. J. Acad. Surg. Res.* 25, 93–99 (2012).
29. Kozakai, T. *et al.* MAGI-1 expression is decreased in several types of human T-cell leukemia cell lines, including adult T-cell leukemia. *Int. J. Hematol.* 107, 337–344 (2018).
30. Zhang, G. & Wang, Z. MAGI1 inhibits cancer cell migration and invasion of hepatocellular carcinoma via regulating PTEN. *Zhong Nan Da Xue Xue Bao Yi Xue Ban* 36, 381–385 (2011).
31. Zmajkovicova, K. *et al.* MEK1 is required for PTEN membrane recruitment, AKT regulation, and the maintenance of peripheral tolerance. *Mol. Cell* 50, 43–55 (2013).
32. Kranjec, C., Massimi, P. & Banks, L. Restoration of MAGI-1 expression in human papillomavirus-positive tumor cells induces cell growth arrest and apoptosis. *J. Virol.* 88, 7155–7169 (2014).
33. Makokha, G. N. *et al.* Human T-cell leukemia virus type 1 Tax protein interacts with and mislocalizes the PDZ domain protein MAGI-1. *Cancer Sci.* 104, 313–320 (2013).
34. Zaric, J. *et al.* Identification of MAGI1 as a tumor-suppressor protein induced by cyclooxygenase-2 inhibitors in colorectal cancer cells. *Oncogene* 31, 48–59 (2012).
35. Hildebrand, S. *et al.* The E-cadherin/AmotL2 complex organizes actin filaments required for epithelial hexagonal packing and blastocyst hatching. *Sci. Rep.* 7, 9540 (2017).
36. Hultin, S. *et al.* AmotL2 integrates polarity and junctional cues to modulate cell shape. *Sci. Rep.* 7, 7548 (2017).

37. Maugeri-Saccà, M. & De Maria, R. The Hippo pathway in normal development and cancer. *Pharmacol. Ther.* 186, 60–72 (2018).
38. Zhao, B. *et al.* Angiomotin is a novel Hippo pathway component that inhibits YAP oncoprotein. *Genes Dev.* 25, 51–63 (2011).
39. Yu, F.-X. & Guan, K.-L. The Hippo pathway: regulators and regulations. *Genes Dev.* 27, 355–371 (2013).
40. Chan, S. W. *et al.* Hippo pathway-independent restriction of TAZ and YAP by angiomotin. *J. Biol. Chem.* 286, 7018–7026 (2011).
41. Wang, W. *et al.* Defining the protein-protein interaction network of the human hippo pathway. *Mol. Cell. Proteomics MCP* 13, 119–131 (2014).
42. Bratt, A. *et al.* Angiomotin regulates endothelial cell-cell junctions and cell motility. *J. Biol. Chem.* 280, 34859–34869 (2005).
43. Patrie, K. M. Identification and characterization of a novel tight junction-associated family of proteins that interacts with a WW domain of MAGI-1. *Biochim. Biophys. Acta* 1745, 131–144 (2005).
44. Johannessen, C. M. *et al.* COT drives resistance to RAF inhibition through MAP kinase pathway reactivation. *Nature* 468, 968–972 (2010).
45. Guo, F., Chiang, M.-Y., Wang, Y. & Zhang, Y.-Z. An in vitro recombination method to convert restriction- and ligation-independent expression vectors. *Biotechnol. J.* 3, 370–377 (2008).
46. Marzi, L. *et al.* FOXO3a and the MAPK p38 are activated by cetuximab to induce cell death and inhibit cell proliferation and their expression predicts cetuximab efficacy in colorectal cancer. *Br. J. Cancer* 115, 1223–1233 (2016).
47. Saavedra V, O., Fernandes, T. F. D., Milhiet, P.-E. & Costa, L. Compression, Rupture, and Puncture of Model Membranes at the Molecular Scale. *Langmuir ACS J. Surf. Colloids* 36, 5709–5716 (2020).
48. Fernandes, T. F. D., Saavedra, O., Margeat, E., Milhiet, P.-E. & Costa, L. Synchronous, Crosstalk-free Correlative AFM and Confocal Microscopies/Spectroscopies. *Sci. Rep.* 10, 7098 (2020).
49. Cartagena-Rivera, A. X., Van Itallie, C. M., Anderson, J. M. & Chadwick, R. S. Apical surface supracellular mechanical properties in polarized epithelium using noninvasive acoustic force spectroscopy. *Nat. Commun.* 8, 1030 (2017).
50. Györfy, B. *et al.* An online survival analysis tool to rapidly assess the effect of 22,277 genes on breast cancer prognosis using microarray data of 1,809 patients. *Breast Cancer Res. Treat.* 123, 725–731 (2010).
51. Nusse, R. & Clevers, H. Wnt/ β -Catenin Signaling, Disease, and Emerging Therapeutic Modalities. *Cell* 169, 985–999 (2017).
52. Furth, N. & Aylon, Y. The LATS1 and LATS2 tumor suppressors: beyond the Hippo pathway. *Cell Death Differ.* 24, 1488–1501 (2017).
53. Misra, J. R. & Irvine, K. D. The Hippo Signaling Network and Its Biological Functions. *Annu. Rev. Genet.* 52, 65–87 (2018).
54. Cánovas, B. *et al.* Targeting p38 α Increases DNA Damage, Chromosome Instability, and the Anti-tumoral Response to Taxanes in Breast Cancer Cells. *Cancer Cell* 33, 1094–1110.e8 (2018).

55. Gupta, J. & Nebreda, A. R. Roles of p38 α mitogen-activated protein kinase in mouse models of inflammatory diseases and cancer. *FEBS J.* 282, 1841–1857 (2015).
56. Gupta, J. *et al.* Dual function of p38 α MAPK in colon cancer: suppression of colitis-associated tumor initiation but requirement for cancer cell survival. *Cancer Cell* 25, 484–500 (2014).
57. Hardwick, J. C., van den Brink, G. R., Offerhaus, G. J., van Deventer, S. J. & Peppelenbosch, M. P. NF-kappaB, p38 MAPK and JNK are highly expressed and active in the stroma of human colonic adenomatous polyps. *Oncogene* 20, 819–827 (2001).
58. Maik-Rachline, G., Zehorai, E., Hanoch, T., Blenis, J. & Seger, R. The nuclear translocation of the kinases p38 and JNK promotes inflammation-induced cancer. *Sci. Signal.* 11, (2018).
59. Hildebrand, S. *et al.* The E-cadherin/AmotL2 complex organizes actin filaments required for epithelial hexagonal packing and blastocyst hatching. *Sci. Rep.* 7, 9540 (2017).
60. Couzens, A. L. *et al.* Protein interaction network of the mammalian Hippo pathway reveals mechanisms of kinase-phosphatase interactions. *Sci. Signal.* 6, rs15 (2013).
61. Zhao, B. *et al.* Angiomotin is a novel Hippo pathway component that inhibits YAP oncoprotein. *Genes Dev.* 25, 51–63 (2011).
62. Frixen, U. H. *et al.* E-cadherin-mediated cell-cell adhesion prevents invasiveness of human carcinoma cells. *J. Cell Biol.* 113, 173–185 (1991).
63. Yang, J. *et al.* Guidelines and definitions for research on epithelial-mesenchymal transition. *Nat. Rev. Mol. Cell Biol.* (2020) doi:10.1038/s41580-020-0237-9.
64. Kleer, C. G., van Golen, K. L., Braun, T. & Merajver, S. D. Persistent E-cadherin expression in inflammatory breast cancer. *Mod. Pathol. Off. J. U. S. Can. Acad. Pathol. Inc* 14, 458–464 (2001).
65. Rodriguez, F. J., Lewis-Tuffin, L. J. & Anastasiadis, P. Z. E-cadherin's dark side: possible role in tumor progression. *Biochim. Biophys. Acta* 1826, 23–31 (2012).
66. Padmanaban, V. *et al.* E-cadherin is required for metastasis in multiple models of breast cancer. *Nature* 573, 439–444 (2019).
67. Campbell, C. I. *et al.* The RNF146 and tankyrase pathway maintains the junctional Crumbs complex through regulation of angiomotin. *J. Cell Sci.* 129, 3396–3411 (2016).
68. Wang, W. *et al.* Tankyrase Inhibitors Target YAP by Stabilizing Angiomotin Family Proteins. *Cell Rep.* 13, 524–532 (2015).
69. Couderc, C. *et al.* AMOTL1 Promotes Breast Cancer Progression and Is Antagonized by Merlin. *Neoplasia N. Y. N* 18, 10–24 (2016).
70. Mojallal, M. *et al.* AmotL2 disrupts apical-basal cell polarity and promotes tumour invasion. *Nat. Commun.* 5, 4557 (2014).
71. Hultin, S. *et al.* AmotL2 links VE-cadherin to contractile actin fibres necessary for aortic lumen expansion. *Nat. Commun.* 5, 3743 (2014).
72. Wada, M. *et al.* P38 delta MAPK promotes breast cancer progression and lung metastasis by enhancing cell proliferation and cell detachment. *Oncogene* 36, 6649–6657 (2017).
73. Zanconato, F., Cordenonsi, M. & Piccolo, S. YAP/TAZ at the Roots of Cancer. *Cancer Cell* 29, 783–803 (2016).

74. Bartucci, M. *et al.* TAZ is required for metastatic activity and chemoresistance of breast cancer stem cells. *Oncogene* 34, 681–690 (2015).
75. Cordenonsi, M. *et al.* The Hippo transducer TAZ confers cancer stem cell-related traits on breast cancer cells. *Cell* 147, 759–772 (2011).
76. Di Agostino, S. *et al.* YAP enhances the pro-proliferative transcriptional activity of mutant p53 proteins. *EMBO Rep.* 17, 188–201 (2016).

c) Conclusion

MAGI1 has tumor suppressive effect in luminal A BCa and this is reflected by its ability to control cell proliferation, anchorage independent cell growth and tumor growth in vivo. MAGI1 acts through p38 MAPK stress pathway to control the aggressiveness of the luminal A BCa cells. More importantly, AMOTL2 a binding partner of MAGI1 is required for this phenotype. The implication of AMOTL2, an F-actin binding protein, and the slight increase of E-cadherin levels are associated with an increased cell stiffness and increased ROCK activity as shown by elevated levels of p-MLC.

2. The implication of ECM stiffness in MAGI1 regulation of the Hippo pathway and the p38/AMOTL2 stress axis.

When attached to a stiff matrix, isolated and non-confluent cells are flat and spread; when attached to a soft matrix they are rounder. Cells sense the ECM stiffness through a macromolecular complex called the Focal Adhesion (FA). Components of the FA transduce the ECM state into the cell: that is called mechano-transduction. One of the main pathway involved in mechano-transduction by FA is the Hippo pathway. Although mechanisms dependent of the Hippo core kinase LATS have been described as regulators of YAP/TAZ in response to ECM changes (see Introduction, FAK phosphorylating YAP or MOB), other independent mechanisms exist. Recently (Elosegui-Artola et al., 2017) showed that a stiff ECM causes actomyosin fibers to pull the nucleus membrane, thus leading to nucleus flattening and opening of the nuclear pore, favoring the nuclear import of YAP/TAZ without affecting their export rates (Figure 31).

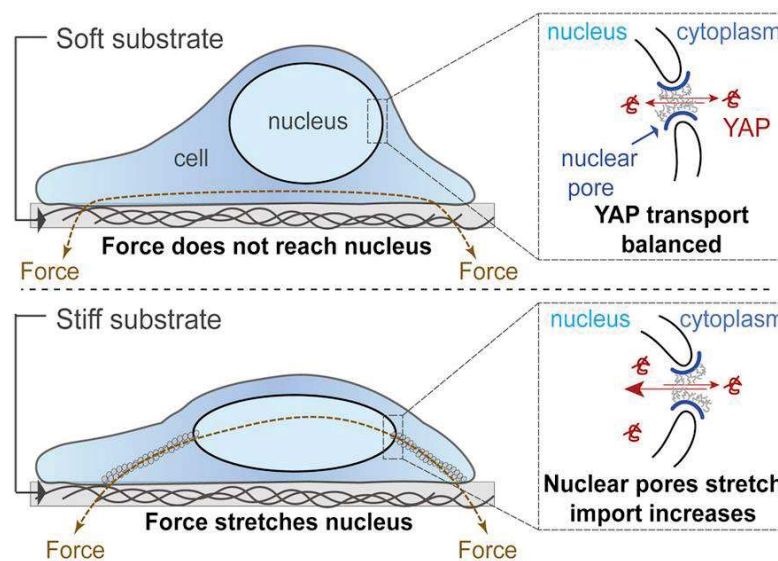


Figure 31: Schematic representation the effect of ECM stiffness on YAP/TAZ nuclear localization independently from the Hippo pathway components.

When cells are cultivated on soft substrate, they are round relaxed with no cytoskeleton tension thus no YAP import in the nucleus. When the cells are grown on stiff matrix, they are flattened and spread, actin fibers are under tension pulling toward the nucleus enhancing thereby the nuclear pores stretching and the entry of YAP in the nucleus. Taken from Elosegui-Artola et al, 2017.

Based on Figure 4 from the article presented above, I observed elevated levels of phosphorylated YAP accompanied by a downregulation of its transcriptional targets such as CTGF, CYR61, BIRC2 and AREG upon downregulation of *MAGI1* in MCF7 cells.

Knowing that the Hippo pathway and YAP activity are highly modulated by the ECM stiffness, I wanted to check if plating MCF7 cells on a soft matrix (Elastic Modulus of 0.5KPa) would modify the phenotype of MAGI1 loss on YAP activity and localization.

Western blot and qPCR analysis were performed on MCF7shluc (ctrl) and shMAGI1. I observed an accumulation of p-YAP (Figure 32A) with a downregulation of one of the main YAP transcription targets CYR61 (Figure 32B). Even though, I could not observe a change in the activation state of canonical Hippo signaling on hard/plastic plates, I then decided to check whether a similar situation was occurring on soft matrix. Giving that MOB1 is a LATS kinase scaffold important for its activity within the canonical Hippo pathway, I checked for the status of MOB1 in the cell. Elevated ratio of pMOB1/MOB1 in the cell upon MAGI1 KD (Figure 32C) shows that the canonical Hippo pathway is activated and that the effect observed on YAP are potentially mediated by canonical Hippo in MCF7 cells cultured on soft matrix. Thus whether on soft or hard matrix, MAGI1 KD leads to YAP inhibition, even though the mechanistic details (canonical vs non-canonical respectively) might differ.

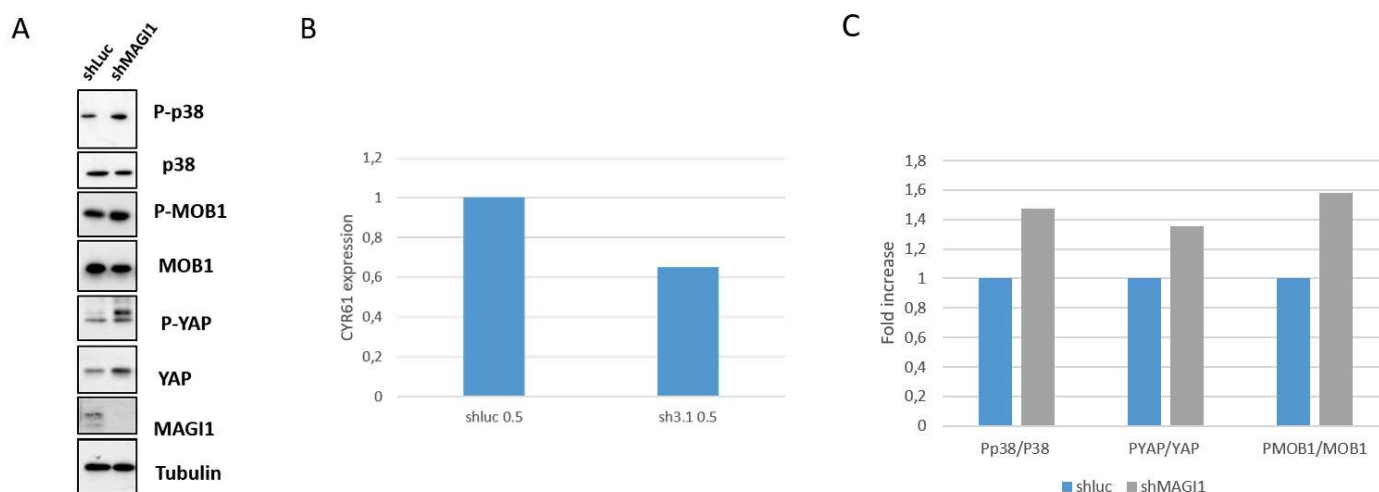


Figure 32: Effect of shRNA MAGI1 on MCF7 cells cultivated on soft matrix (0.5 KPa).

- A) Western blot analysis of MCF7 shluc and MCF7 shMAGI1 showing more p-P38 levels, more p-MOB1 and more p-YAP in the cells after MAGI1 KD. MAGI1 is used as a control of the shRNA efficacy. Tubulin is a loading control.
- B) qPCR analysis showing a downregulation of CYR61, one of known YAP target genes after MAGI1 KD.
- C) Quantification of the western blot analysis presented in panel A. these quantification show up regulation of p-P38, p-YAP and p-MOB1 in the cells upon removal of MAGI1.

Moreover, the level of p-P38 is elevated in MCF7shMAGI1 as compared to MCF7shLuc suggesting that the same signaling events as those described on hard matrices in the article above are also taking place on soft extracellular matrix.

On hard matrix / plastic plates, elevated levels of p-YAP could be explained by the increased levels of AMOTL2 observed upon MAGI1 loss. Indeed, AMOTL2 is a known negative regulator of YAP activity (B. Zhao et al., 2011), which by homology with AMOT could act either by trapping YAP in the cytoplasm or by activating indirectly LATS1 (through complex interactions between F-actin, NF2, and LATS). Thus one would expect that the downregulation of AMOTL2 would restore YAP activity in MCF7 cells. Using siRNA against AMOTL2 followed by qPCR analysis, transfected cells were not able to rescue the transcription levels of the different YAP target genes (CYR61 is shown as an example in *Figure 33A*). Even though the levels of the different transcription targets were not rescued upon AMOTL2 knockdown, p-YAP levels were lowered (data not shown), and immunofluorescence analysis showed a re-localization of YAP in the nucleus (*Figure 33B*).

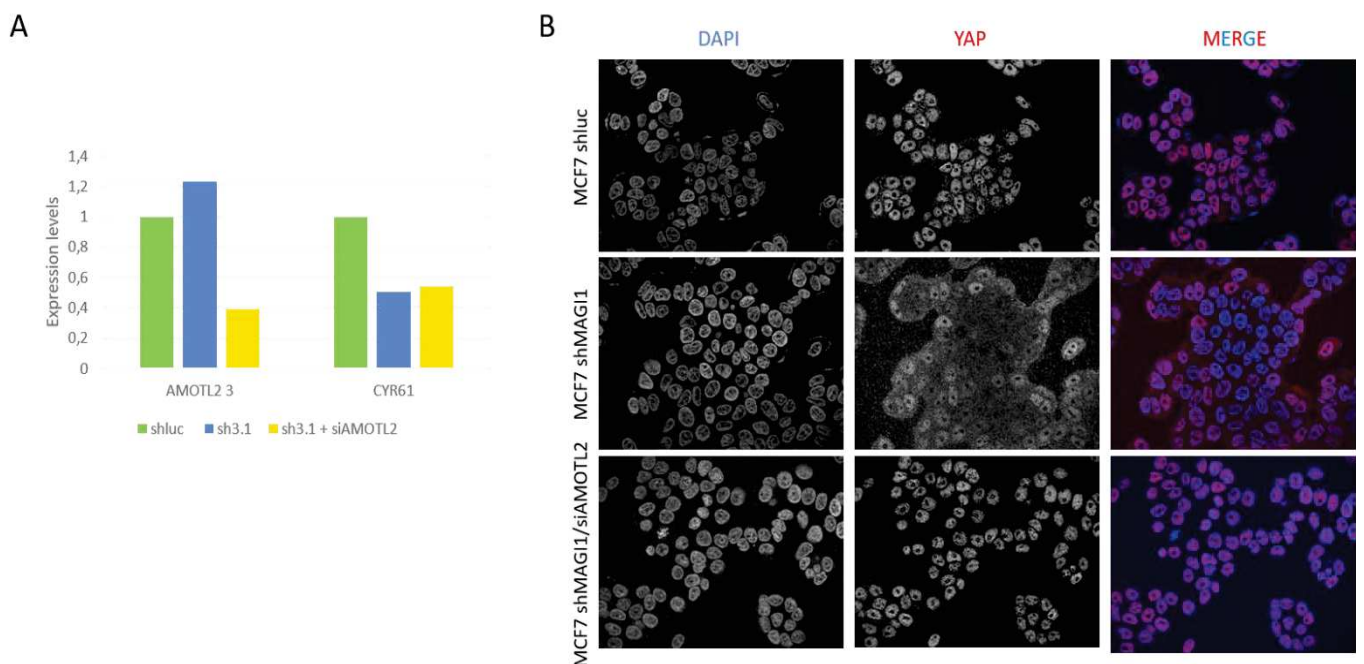


Figure 33: Analysis of the effect of siRNA AMOTL2.

A) qPCR on MCF7shluc as control in green, MCF7 shMAGI1 (3.1) in blue and MCF7 cells with shRNA MAGI1 and transfected with siRNA AMOTL2 in yellow, showing that siRNA AMOTL2 does not rescue the effect of the shRNA MAGI1 on CYR61, one of YAP targets. This is a representation of the $\Delta\Delta CT$ normalized over GAPDH. B) Immunofluorescence of MCF7 cells. The second panel correspond to YAP (in red) and the first panel shows the nucleus (stained with DAPI in blue). This figure shows that upon downregulation of MAGI1 in MCF7 cells YAP is exported from the nucleus to the cytoplasm. This phenotype is rescued by knocking down AMOTL2 in these cells. Cells were imaged using Zeiss apotome with 40X objective.

It appears thus, that MAGI1 acts on two different levels of YAP activity. MAGI1 promotes YAP nuclear localization, a process that is dependent on AMOTL2 and on YAP phosphorylation on Ser127, but also on YAP efficient transcriptional activity, a process that appears independent of AMOTL2. Interestingly, when doing a confluence-course study of the effect of shMAGI1 on YAP localization, it should be noted that at low confluence, YAP is strongly nuclear in Ctrl and

shMAGI1. It appears thus that shMAGI1 is shifting YAP nuclear exclusion earlier on hard matrices, as if cells were sensitized to confluence inhibition, an interpretation that correlates with the harder membrane and compressive forces experienced by MAGI1 KD cells. This process, appears thus dependent on AMOTL2. It should be noticed that siRNA AMOTL2 was able to alleviate the activation p-P38 levels on plastic (stiff) observed after shMAGI1 (as mentioned in the article) also on soft matrix, and that knocking down AMOTL2 rescued the effect of the loss of MAGI1 on 2D cell and anchorage-independent cell growth. These results suggest that the phenotypes obtained upon MAGI1 loss are mediated by AMOTL2 but interestingly that MAGI1 also controls the transcriptional activity of YAP/TAZ independently of AMOTL2. One attractive hypothesis is that MAGI1 could affect the Y-phosphorylation of YAP, since the phosphorylation of YAP on Yxxx by YES/SRC or by FAK was shown to control directly its activity. These results will need further investigation.

Upon the loss of MAGI1 in MCF7 cell lines, we reported the phosphorylation (and thus activation) of the myosin light chain (MLC). This activation is coupled with an elevated cellular membrane stiffness measured by scan atomic force microscopy (AFM). When myosin is activated, it starts to pull on the actin filaments generating tension inside the cell. The main kinase of MLC is ROCK, and inhibitors of ROCK activity prevented several effects of MAGI1 KD, suggesting that ROCK is indeed activated. The next step is thus to understand how the ROCK kinase is activated upon the loss of MAGI1. Increased RhoA activity could activate ROCK by phosphorylation. RhoA is a small GTPase part of the Rho family of small GTPases along with CDC42 and RAC1 (summarized in (Hoon et al., 2016)). They are well known for their role in the modulation of the cytoskeleton upon a wide variety of extracellular stimuli. CDC42 and Rac1 are also known to activate the formation of lamellipodia and filopodia respectively (cf chapter 2 section 3 of the introduction). When introduced in epithelial cells, RhoA enables the formation of stress fibers and enhances Focal Adhesion formation / stability.

The regulation of RhoA is very complex, covered by a vast literature and numerous studies. Interestingly, a recent article published by (Meng et al., 2018) suggested that RAPGEF6 (a.k.a. PDZ-GEF2 in the article), a RAP guanine nucleotide exchange factor 6 is able to regulate RhoA through the activation of RAP2, another small GTPase. RAPGEF6 is an especially interesting lead to look at since proteomic analyses that we have performed in MCF7 cells overexpressing MAGI1 identified RAPGEF6 as a strong potential binding partner for MAGI1. *RAPGEF6* loss of function experiments as well as drug inhibition of RhoA are currently being performed in the lab and will

be followed by western blot analysis and phenotypic studies to determine a potential implication of RAPGEF6 in our model.

3. Characterization of the mechanism of action of the Oxaliplatin treatment in colorectal cancer cells (CCR).

Oxaliplatin treatment is considered as a first line chemotherapy treatment for CRC patients. Oxaliplatin belongs to the platinum compound based chemotherapies; it forms inter and intra strands cross link (called adducts) within the DNA molecules inhibiting replication and transcription and thus leading to damage-induced cell death. Used along with 5FU (FOLFOX), it has greater effect than used alone (Graham et al., 2004).

Because of the big interest of our lab in the Hippo pathway and based on omics approaches done in collaboration with the lab of Dr Céline Gongora, we investigated the effect of Oxaliplatin treatment on the Hippo pathway and its effectors YAP and TAZ in HCT116 cell line. This work was done in collaboration with Dr Vera Slaninova, a former post doc in the lab.

After establishing the IC₅₀ (the half maximal inhibitory concentration required to kill 50% of the cells after 4 days of treatment) of Oxaliplatin in HCT116 at 0.5 μ M, it was used to treat the cells during all the experiments that I will describe below.

a) Oxaliplatin activates YAP/TAZ activity in HCT116:

To check for the Hippo pathway status after Oxaliplatin treatment, HCT116 were incubated with 0,5 μ M of drug for 24h and 48h and then analyzed by western blot to check the different components of the pathway and qPCR to check the transcription levels of YAP/TAZ targets.

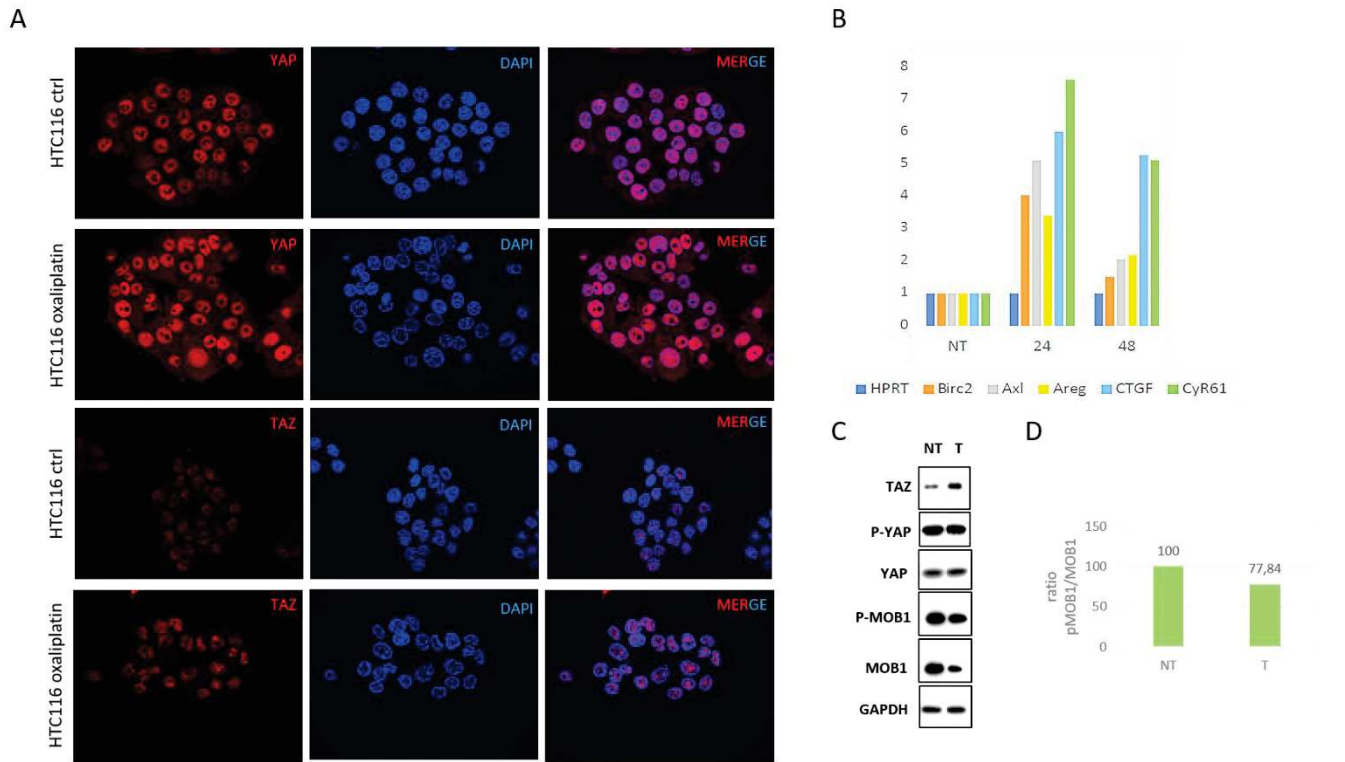


Figure 34: Analysis of HCT116 cells after Oxaliplatin treatment.

A) Immunofluorescence analysis of YAP (the first and second line) and TAZ (third and fourth line) both in red after 48h of Oxaliplatin treatment. After the treatment, we see a clear accumulation of both YAP and TAZ in the nucleus presented in blue. These images were acquired using a ZEISS apotome microscope at 40X objective. B) The expression of the different targets of YAP/TAZ: BIRC2, AXL, AREG, CTGF and CYR61 analysed by qPCR. After 24h and 48h of treatment, the transcription levels of the different targets are elevated compared to the control. This graph is a representation of the $2^{-\Delta\Delta C_t}$ of each gene normalized over the expression of HPRT (Hypoxanthine-guanine phosphoribosyl transferase). A stronger expression of the different genes is observed at 24h compared to 48h of treatment. C) Western blot analysis showing the levels of YAP and its phosphorylated form, TAZ, MOB1 and p-MOB1 in the cells after 24h of treatment. GAPDH (Glyceraldehyde 3-phosphate dehydrogenase) is used as a loading control. More TAZ in the cells is observed after the treatment while YAP and p-YAP levels do not move. MOB1 and p-MOB1 are used to check the status of the Hippo pathway. D) quantification of pMOB1/MOB1 signals obtained in C using ImageJ. The fact that we do not see 22% less p-MOB1/MOB1 in the treated cells implies that an inhibition of the Hippo pathway might be triggering this accumulation of TAZ in the cell.

Even though Oxaliplatin treatment causes an accumulation of YAP and TAZ in the nucleus, seen in immunofluorescence analysis using HCT116 cells treated with $0.5\mu\text{M}$ of Oxaliplatin during 48 hours (Figure 34A), WB analysis shows elevated levels of TAZ only whereas the levels of YAP do not change (Figure 34C). This effect is observed at 24 hours, same results were obtained after 48 hours of treatment. The accumulation in the nucleus is accompanied by higher levels of the transcription targets CTGF, CYR61, BIRC2, AXL and AREG (Figure 34B). To assess the status of the Hippo pathway in cells, I tried to detect several components of this pathway: LATS1 and its activated phosphorylated form and MOB1 and its activated phosphorylated form. As a reminder, when the components of the Hippo pathway get phosphorylated the pathway is activated and YAP/TAZ are phosphorylated and trapped in the cytoplasm. What we expect is low levels of activation of the different components. The Figure 34C-D show the results of MOB1 and p-MOB1 because our p-LATS1 did not give us interpretable results. This experiment was done once and

needs further validation but as preliminary data, we can say that we have a slight decrease of the p-MOB1/MOB1 ratio after Oxaliplatin treatment implying that the accumulation of TAZ in the nucleus might be due to the inhibition of the activity of the Hippo pathway.

Apart from canonical Hippo signaling, the localization and the activity of YAP and TAZ could also be regulated by actin reorganization. Thus I looked at the actin organization by immunofluorescence analysis. Strikingly, we can observe an accumulation of cortical F-actin at the leading edge of the cells after 48h of treatment with Oxaliplatin (*Figure 35* in Red). Whether such re-organisation is only at the cortex, or also affects FA and stress fibers will need to be explored further with higher magnification. This actin re-organization, might thus also play a part in the activation of YAP/TAZ (in parallel to canonical Hippo).

Alternatively, actin re-organization, instead of actin upstream of YAP/TAZ, could be a consequence of YAP/TAZ activation following treatment, or could represent a completely independent response of the treated cells. These different hypotheses needs further investigation; for instance experiments of tension disturbance and actin cytoskeleton disorganization should be performed to evaluate whether actin tension participates in YAP/TAZ activation.

b) Characterization of the mechanism of action of Oxaliplatin on Hippo pathway and TAZ:

We wanted to better characterize the effects of Oxaliplatin treatment on the activation of the transcription of the different targets of YAP/TAZ. To do so, I monitored TEAD4 levels and localization in the cells; TEAD4 is the main transcription factor to which YAP/TAZ bind in the nucleus to activate the different target genes in colon cells. This experiment should allow us to understand if the activation of transcription upon oxaliplatin treatment could be due in part to increased TEAD4 presence. Immunofluorescence analyses of TEAD4 in cells after 48h of Oxaliplatin treatment (*Figure 35* in Green) shows that the levels and localization of TEAD4 are not affected by the treatment. This suggests that the elevated levels of TAZ in the cell and its accumulation in the nucleus are likely causing the increased transcriptional activity.

The question that remains to be answered is that, even though we still have the same amount of TEAD4 in the cell after the treatment, did the binding sites of this transcription factor change as a result of the treatment? Are we facing a change in the transcriptional program of TAZ? To answer this question chromatin immunoprecipitation analysis (chIP) of TEAD4 in Oxaliplatin treated cells needs to be done.

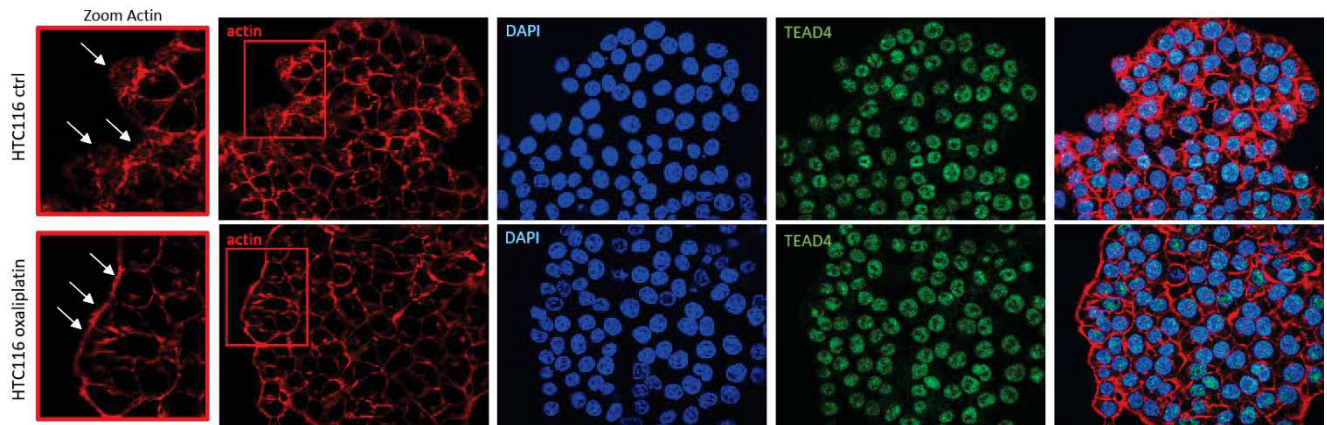


Figure 35: Immunofluorescence of HCT116 cells after 48h of Oxaliplatin treatment. Phalloidin was used to visualize actin (in red), DAPI staining for the nucleus and TEAD4 is in green. The first column represents a zoom of the red squared regions in the actin panel. The TEAD4 is the transcription factor that YAP/TAZ bind in the nucleus to activate the different targets. The no changing in the staining of TEAD4 after Oxaliplatin treatment shows that we do not have more binding sites of TAZ at the levels of the DNA but the effect is directly linked to the levels of TAZ in the cell. The actin staining show an accumulation of cortical actin at the leading edges of the cells treated with Oxaliplatin shown with the white arrows. This shows that the treatment is affecting the actin organization inside the cell. These images were acquired using ZEISS apotome Microscope at 40X objective.

c) Wider look at the effect of Oxaliplatin in HCT116:

To better characterize the effect of Oxaliplatin treatment on HCT116 and try to understand which part of the response could be controlled by the increased YAP/TAZ activity, we decided to realize transcriptomic analysis on cells treated with Oxaliplatin for 24h and 48h. This approach consists on sequencing the whole set of RNAs present in the cells and perform differential expression analyses to identify the gene expression changes after treatment. HCT116 cells are Oxaliplatin sensitive cells activating cell death upon treatment.

Interestingly, cells treated with Oxaliplatin have higher YAP/TAZ activity. This can be counter-intuitive since a vast literature supports a role for YAP/TAZ as oncogenic drivers and as promoting resistance, even though YAP/TAZ are also involved in differentiation or stemness depending on cell type. Our results suggest that HCT116 cells treated with oxaliplatin might activate an oncogenic response when dying. Alternatively, it could be that in this context, YAP/TAZ might control a completely different program, not involved in cell proliferation or migration. Therefore, the main goal of the RNA sequence approach is to understand this unusual phenomenon. Moreover, this approach will allow us to understand the effect of Oxaliplatin of sensitive cells independently from its known role in inducing DNA double strand breaks.

Following differential expression analysis (tuxedo algorithm implemented by the RNA-Seq facility

at fold-change 1.5 and FDR 5%) 288 genes were upregulated after 24h of treatment and 1311 genes after 48h. Most importantly, almost all the genes up-regulated at 24h were also up-regulated at 48h, suggesting that these two time points capture a similar transcriptional phase, which gets amplified and broader with time. Obviously, not all the genes affected (up-regulated) are direct targets of YAP/TA. In order to identify the TEAD4/YAP/TAZ program, we crossed the lists of up-regulated genes with published TEAD4 ChIP-Seq data in untreated HCT116 cells from the lab of Junhao Mao (Liu et al., 2016). The intersect identifies upregulated genes with TEAD4 binding in the vicinity that represent genes potentially directly regulated by YAP/TAZ activity. Based on Figure 36, the YAP/TAZ activity is progressively going up through time suggested and the number of potential direct targets is increasing from 60 at 24h to 200 genes at 48h. The canonical targets of YAP/TAZ are upregulated at 48h such as CTGF, CYR61 and AREG.

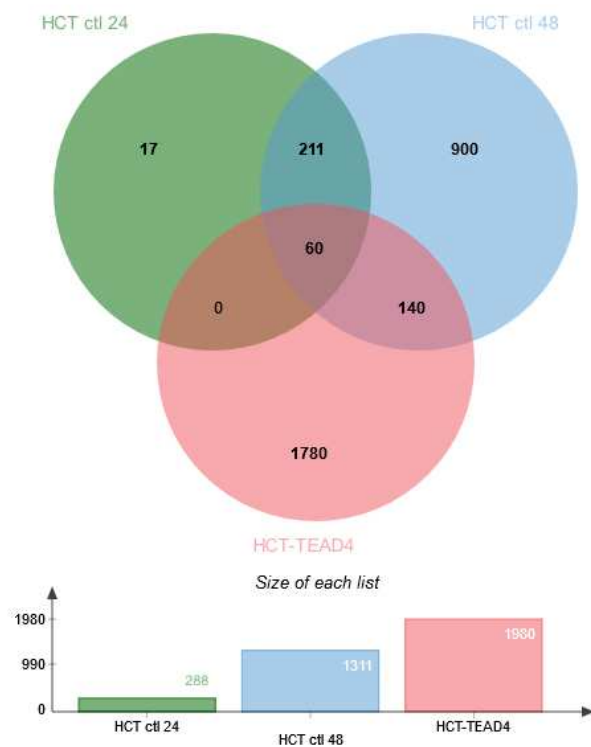


Figure 36: Venn diagram showing the intersection between the upregulated genes obtained by RNAseq at different time point in Oxaliplatin treated HCT116 cells and the chipseq list of gene of TEAD4 taken from Liu et al, 2016.

24h of treatment (in green), 48h of treatment (in blue) and the chipseq list of gene of TEAD4 taken from Liu et al, 2016 (in pink).

60 different genes are common between the three lists, whereas 211 genes are common between the 24 and the 48 hours of treatment and 140 are common between 48 and HCT TEAD4. It is clear that YAP/TAZ activity is progressively going up showing by the progressive up regulation of its target genes.

The analysis of the genes family of the different targets of YAP/TAZ in GSEA revealed the activation of 20 different transcription factors, 6 oncogenes and 3 tumor suppressors (Table 6). From the 20 different transcription factors activated, I found some interesting genes worth mentioning and commenting. JUN and FOSL2 are two important subunits of the AP1 complex. This complex regulates expression genes in response to stress and other stimuli. Oxaliplatin treated cells are clearly experiencing cellular stress, and several studies have reported a strong overlap between TEAD and AP-1 responses.

	cytokines and growth factors	transcription factors	homeodomain proteins	cell differentiation markers	protein kinases	translocated cancer genes	oncogenes	tumor suppressors
tumor suppressors	0	1	0	0	0	0	0	3
oncogenes	0	3	0	0	0	5	6	
translocated cancer genes	0	2	0	0	0	5		
protein kinases	0	0	0	0	10			
cell differentiation markers	1	0	0	7				
homeodomain proteins	0	0	0					
transcription factors	0	20						
cytokines and growth factors	14							

Table 6: Gene family analysis of the 200 genes of YAP/TAZ targets observed at the different Oxaliplatin treatment time points.

Other interesting genes are those associated with cytoskeleton remodeling such as SNAI2, a transcription factor linked to EMT (Epithelial to mesenchymal transition), ARC (Activity regulated cytoskeleton associated protein), or TRIP6 (thyroid hormone receptor interactor 6) responsible for the transmission of signals from cell surface to nucleus promoting the weakening of AJs and actin cytoskeleton reorganization. NF2 (Merlin) is also found in this cytoskeleton regulators list; it is a negative regulator of YAP/TAZ activity suggesting the presence of a probable negative feedback loop.

Basic regulatory elements analyses on the lists of upregulated genes at 24h and 48h of Oxaliplatin treatment, and looking for enrichment with predefined Transcription Factor targets database (composed of 958 gene sets), identified the major TF that potentially control the response to oxaliplatin. For 24h the most significant enrichment is an AP1 signature (meaning genes having at least one occurrence of the highly conserved motif for AP1 fixation of DNA), further demonstrating that treated cells experience cellular stress.

For the 48 hours up regulated gene list, the best hit is for genes with binding domain for TEAD2 in their promoter. This result suggests an implication of YAP/TAZ mediated transcription at 48 hours and validate our initial hypothesis and observations. Moreover, the AP1 signature remains at 48 hours, along with other transcription factors such DIDO1 (Death inducer obliterator 1), a tumor

suppressor implicated in activating pro-apoptotic genes, NFE2L1 (endoplasmic reticulum membrane sensor) able to translocate to the nucleus upon stress stimuli in the cell.

In conclusion, after 48h of Oxaliplatin treatment, HCT116 cells exhibit a transcriptional response which resemble a TEAD4/YAP/TAZ program as well as an AP1 program. Interestingly, (Liu et al., 2016) suggested that TEAD4 cooperated with AP1 transcription factors and they co-occupy cis regulatory regions. The same conclusion was drawn in breast cell lines in (Zanconato et al., 2015). In addition, cells starts to activate whole programs able to detect and respond to the stress stimulus caused by the Oxaliplatin treatment.

These results are still preliminary and need further bioinformatics analysis and in cellulo validation, but they strongly suggest that Oxaliplatin treatment triggers a YAP/TAZ early response. Whether this response participates in the cell sensitivity to oxaliplatin, or represents early phase of resistance acquisition remain to be established, but preliminary results impairing YAP/TAZ suggest that higher YAP/TAZ activity sensitizes HCT116 cells to oxaliplatin.

- What is the role of YAP/TAZ activity in Oxaliplatin treated cells?
- Is the remodeling of the actin cytoskeleton observed in *Figure 35*, a cause or a consequence of YAP TAZ activity?
- Even though YAP/TAZ activity is high after the treatment, it just consists of 20% of the total genes upregulated at the different time point, is there any other transcription programs activated in these cells and being the main output, in spite of YAP/TAZ, that are shadowing the effect caused by YAP/TAZ activity?
- Is YAP/TAZ working in concert with other transcription factors?

Many question remain to be answered and analysis of the different list of RNA seq results will allow that.

Materials and Methods

Cell culture: MCF7 and HCT116 cell lines were grown in DMEM/F12 glutamax (Dulbecco's Modified Eagle Medium: Nutrient Mixture F12) and RPMI 1640 glutamax respectively, supplemented with 10% fetal bovine serum and 1% de pencillin/Streptomycin. Grown at 37°C with 5% CO₂. shRNA infected cell lines were cultured in the presence of 1ug/ml puromycin for selection.

Plasmids, mutant constructs and shRNA cloning: All expression plasmids were generated with the Gateway system (Invitrogen). The Entry vector pDONR223-MAGI1 was a gift from William Hahn (Addgene plasmid #23523) and it was used to introduce the different point mutations in MAGI1 by mutagenesis PCR using PfuTurbo (Agilent). All the Gateway destination vectors that were generated are listed as follows: pCMV10 3xFlag RfB-MAGI1, pCMV10 3xFlag RfB-MAGI1 P331A, pCMV10 3xFlag RfB-MAGI1 P390A and pCMV10 3xFlag RfB-MAGI1-P331/390A. pEZY-EGFP-MAGI1 was constructed by Gateway recombination between the pDONR223-MAGI1 and the pEZY-EGFP destination vector that was a gift from Zu-Zhu Zhang (Addgene plasmid #18671). pcDNA3 HA-AMOT, pcDNA3 HA-AMOT Y242A, pcDNA3 HA-AMOT Y287A and pcDNA3 HA-AMOT Y242/287A were gifts from Kunliang Guan (Addgene plasmids #32821, #32823, #32824 and #32822 respectively).

shRNA directed against human MAGI1 and AMOTL2 were constructed and cloned in the pSIREN-RetroQ vector (TaKaRa) according to the manufacturer's conditions between BamHI and EcoRI cloning sites. Targeted sequences were:

shRNA-MAGI1(3-1): GATCTCATAGTGGAAGTTAA

shRNA-AMOTL2(1416): GGAACAAGATGGACAGTGA

shRNA-AMOTL2(3667): GAGATGTCTTGTTAGCATA

All hairpins were validated (<http://cancan.cshl.edu/cgi-bin/Codex/Codex.cgi>). The shRNA targeting Luciferase as a control was kindly provided by Celine Gongora (IRCM). Retroviral particles were produced in HEK293 cells and used to infect MCF7, T47D, and HCT116 cell lines.

Western blotting: Cells were lysated using a 1ml syringe-needle 25G after adding a home made laemelli 1X supplemented with 100 mM DTT. Proteins were separated by SDS-PAGE and transferred on nitrocellulose membranes. After incubating 1h with 10% TBS-milk, membranes

were incubated overnight at 4°C with primary antibodies (*Table 7*) . Antibodies used are listed in *Table 7*. The Next day membrane are washed three times with PBS 1X/0.1 Tween and incubated for one hour at room temperature with the secondary antibodies: HRP coupled Goat anti Mouse (1/15000) or Goat anti-Rabbit (1/15000). After incubation, the membrane are washed three times with PBS 1X/0.1 Tween and revealed using SuperSignal West Pico PLUS Chemiluminescent Substrate (Thermofisher Scientific #34580).

Quantitative Real Time PCR: Total RNA extraction was performed using the RNeasy extraction kit (QIAGEN), according to the manufacturer instructions. 1 μ g to total RNA was subjected to reverse transcription using the SuperScript III (Thermofisher) and random primers (Invitrogen). Gene expression was monitored by quantitative qPCR using the SYBR Green I Mastermix (Roche) according to the manufacturer instructions, on Light Cycler 480 device (Roche). Transcript expression levels were calculated as mean normalized expression ratios referred to housekeeping gene using the $\Delta\Delta$ CT method. Three different housekeeping genes were used each time. The primers used for analysis are summarized in *Table 9*.

Immunofluorescence: MCF7 and HCT116 cells were fixed with 4% PFA for 10 minutes, permeabilized with 0.5% PBS1X/Triton X-100, and subsequently blocked with 0.5% PBS1X/BSA before incubation with specific primary antibodies at 4°C overnight. Antibodies used are listed in *Table 8*. Secondary Alexa Fluor Antibodies (1/200; Invitrogen) were used as described previously for 1 hour at room temperature before mounting the coverslips with Vectashield (Vector Laboratories #H1200) and imaging on a Zeiss Apotome microscope.

Cells transfection: Transfection with siRNA AMOTL2, siRNA RAPGEF6 and siRNA P38 α (HorizonDiscovery/Dharmacon) or the different plasmids was performed using lipofectamin 2000 according to the manufacturer instructions, and kept for 48 or 24 hours respectively prior to subsequent assays.

ROCK inhibitors treatment: The treatments of MCF7shRNA cell lines with either Blebbistatin (Selleckchem #7099) or Y-27632 (Selleckchem #S1049) were both performed at a final concentration of 10 μ M and cells were treated during 2 hours before being lysed for Western blot analyses.

p38 MAPK inhibitor treatment: The different MCF7shRNA cell lines were plated at 3×10^6 cells per 60mm plates. The day after, 10 μ M of Ralimetinib (LY2228020; Selleckchem #S1494) was added and 24 h later cells were collected and counted to be plated for the different experiments (Ralimetinib treatment is maintained throughout the experiments). The same experiments were conducted with another p38 inhibitor using 10 μ M of Pexmetinib (ARRY-614; Selleckchem #S7799).

Oxaliplatin Treatments: HCT116 cells were plated at a density of 125000 cells/ well in a 6 wells plate. The next day cells were treated or not with 0.5 μ M of oxaliplatin (the IC50 dose) for 24 and 48 hours. After 48h, cells were collected for RNA and protein extractions. For Immunofluorescence, the protocol is described above, the antibodies used for staining are listed in Table 8.

Cell viability assay: MCF7 shRNA cell lines were plated at a density of 3000 cells/well in a 96wells plate. Depending on the experiments two growth assay were conducted:

- MTT (3-(4,5-dimethylthiazol-2-yl)-2,5-diphenyltetrazolium bromide (Sigma Aldrich #M2128)). Cells were stopped at day 0 till day 7 by incubation with MTT solution (0.5 mg/mL final concentration) during 4 hours at 37 °C. Before reading OD at 570 nm, DMSO was added to solubilize the formazan crystals formed in the presence of MTT.
- Sulforhodamin B (Sigma Aldrich #230162) assay. Plates were fixed using 10 % of Trichloroacetic acid (TCA; Sigma Aldrich #T4885) for 10 min, then washed 3 times with PBS and stored at 4°C until the end of the experiment (Day 8). Once the experiment is finished, 50 μ l of Sulforhodamine B (SRB; 0.04% diluted in acetic acid 1%) were added for 30 min before extensive washes with acetic acid 1% and drying step overnight at room temperature. Before reading OD at 540 nm, cells were incubated with Tris 10 mM pH 10.5.

Soft Agar assay: To assess anchorage independent growth, a first layer of 0.8% Noble agar (Sigma Aldrich #A5431) was prepared in 12-well plates and left at 4°C during 1 hour for the agar to polymerize gently. The plate was kept at 37°C before the cell-containing agar layer was prepared. 5,000 or 10,000 cells were imbedded in the second layer containing 0.4% Noble agar on top of the first layer. When the second layer was polymerized, fresh medium was added on top of the cells. MCF7 cell lines were cultured during 14 to 21 days before Crystal violet coloration (0.01% final concentration; Sigma Aldrich #C0775) or MTT coloration (1 mg/mL final concentration).

Subcellular fractionation - Isolation of cytoplasmic, nuclear and membrane protein fractions:

Subcellular fractionation of cultured human cell lines was performed as previously described; samples, buffers and centrifugations were kept and performed at 4°C at all time. For more details, the protocol is available on-line (<http://www.bio-protocol.org/e754>).

Cell cycle analysis: MCF7 shRNA cell lines were trypsinized and fixed at a density of 10⁶ cells using Ethanol 70% overnight at -20°C. The Next day cells were centrifuged washed once with PBS 1X and incubated with Propidium iodide for 5 hours. Analysis were performed on Gallios Flow Cytometer (Beckman Coulter).

Immunoprecipitation and co-immunoprecipitation: Protein extracts were prepared in lysis buffer (NaCl 150 mM, Tris pH 7.4 10 mM, EDTA 1 mM, Triton X-100 1%, NP-40 0.5%, cOmplete, EDTA-free protease inhibitors (Roche #11873580001) for 30 min on ice before centrifugation. Immunoprecipitations were performed overnight at 4°C on a rocking wheel using either mouse anti-MAGI1 antibody for endogenous immunoprecipitations or anti-HA antibody and EZview Red anti-FLAG M2 affinity gel (Sigma-Aldrich #F1804) for co-immunoprecipitations. Protein G sepharose was then added to the MAGI1- or HA- immunoprecipitates for 1 hour at 4°C before extensive washes. Concerning the FLAG immunoprecipitation, washes were performed followed by protein elution by competition with 3XFLAG peptide (150 ng/μL final concentration) during 1 hour at 4°C. The different immunoprecipitates were then submitted to Western blotting for detection of protein complexes.

Cytosoft: Cytosoft® plates of 0.5KPa (Sigma-Aldrich #5140) and 32KPa (Sigma-Aldrich #5144) were prepared in advance by coating them with 100 μg/μl collagen (Sigma-Aldrich #C3867) and left at room temperature to polymerize. After one hour, the exceeding collagen was removed and the wells were washed twice with medium. Meanwhile, cells were trypsinized, counted and seeded at a density of 3x10⁶ cells/well. The next day, cells were collected for RNA and protein extractions.

Boyden chamber assays: In Transwell permeable supports, 6.5mm Insert with 8μm polycarbonate membrane, 24 wells plate (Costar, #3422) 100 μl of matrigel (AMSBIO, #3433-010-01) at final concentration of 300 μg/ml was deposited. These plates are incubated at 37°C for one hour for the

matrigel to polymerize. Meanwhile, MCF7 cells were trypsinized, counted and seeded at a density of 50000 cells/insert in 1% FBS medium. Under the insert, medium with 10% FBS was added. As a control, wells without inserts were seeded at the same cell density to assess the proliferation rate. The plates were kept for 48h in the incubator before analyses. After 48h, cells in the inserts are aspirated and the inside of the insert is cleaned with a cotton swab. The media below the insert is aspirated and MTT solution was added and the plates are incubated for 4h at 37°C. Before reading OD at 570 nm, DMSO was added to solubilize the formazan crystals formed in the presence of MTT.

Antibodies:

Table 7: List of antibodies used for western blots analysis.

For Western blot			
Antigen	Specie	Dilution	Manufacturer
<i>MAG11</i>	<i>mouse</i>	<i>1/250</i>	Santa Cruz #sc100326
<i>MAG11</i>	<i>Rabbit</i>	<i>1/1000</i>	Sigma #HPA031853
<i>MAG12</i>	<i>Rabbit</i>	<i>1/250</i>	Santa Cruz #sc25664
<i>MAG13</i>	<i>Rabbit</i>	<i>1/250</i>	Santa Cruz discontinued
<i>tubulin</i>	<i>Mouse</i>	<i>1/20000</i>	Sigma-Aldrich #T6074
<i>AMOT</i>	<i>Mouse</i>	<i>1/250</i>	Santa Cruz #sc166924
<i>AMOTL2</i>	<i>Rabbit</i>	<i>1/2000</i>	Atlas Antibodies #HPA063027
<i>M2 FLAG</i>	<i>Mouse</i>	<i>1/2000</i>	Sigma-Aldrich #F1804
<i>HA</i>	<i>Mouse</i>	<i>1/2000</i>	BioLegend #901501
<i>GFP</i>	<i>Rabbit</i>	<i>1/2000</i>	Torrey Pines Laboratories #TP401
<i>YAP/TAZ</i>	<i>Rabbit</i>	<i>1/1000</i>	Cell Signaling Technology #8418
<i>YAP</i>	<i>Rabbit</i>	<i>1/1000</i>	Cell Signaling Technology #14074S
<i>TAZ</i>	<i>Rabbit</i>	<i>1/1000</i>	Cell Signaling Technology #4883S
<i>p-YAP(S127)</i>	<i>Rabbit</i>	<i>1/1000</i>	Cell Signaling Technology #13008
<i>p-YAP(S397)</i>	<i>Rabbit</i>	<i>1/1000</i>	Cell Signaling Technology #13619
<i>LATS1</i>	<i>Rabbit</i>	<i>1/1000</i>	Cell Signaling Technology #3477
<i>p-LATS1</i>	<i>Rabbit</i>	<i>1/1000</i>	Cell Signaling Technology #8654
<i>MOB1</i>	<i>Rabbit</i>	<i>1/1000</i>	Cell Signaling Technology #13730P
<i>p-MOB1</i>	<i>Rabbit</i>	<i>1/1000</i>	Cell Signaling Technology #8699
<i>Actin</i>	<i>Mouse</i>	<i>1/250</i>	Hybridoma Bank #JLA20
<i>GAPDH</i>	<i>Mouse</i>	<i>1/20000</i>	Proteintech #60004-1-Ig
<i>Claudin1</i>	<i>Rabbit</i>	<i>1/1000</i>	Cell Signaling Technology #13255
<i>ZO1</i>	<i>Rabbit</i>	<i>1/1000</i>	Cell Signaling Technology #8193
<i>B-catenin</i>	<i>Rabbit</i>	<i>1/1000</i>	Cell Signaling Technology #8480
<i>PARD3</i>	<i>Rabbit</i>	<i>1/1000</i>	Millipore #07-330
<i>E-cadherin</i>	<i>Rabbit</i>	<i>1/1000</i>	Cell Signaling Technology #3195
<i>P38</i>	<i>Rabbit</i>	<i>1/1000</i>	Cell Signaling Technology #8690
<i>p-P38</i>	<i>Rabbit</i>	<i>1/1000</i>	Cell Signaling Technology #4511

Table 8: List of antibodies used for Immunofluorescence analysis.

For Immunofluorescence			
Antigen	Specie	Dilution	Manufacturer
<i>MAG11</i>	<i>Mouse</i>	<i>1/100</i>	<i>Sigma Aldrich #HPA031853</i>
<i>AMOT</i>	<i>Rabbit</i>	<i>1/100</i>	<i>Proteintech #24550-I-AP</i>
<i>AMOTL2</i>	<i>Rabbit</i>	<i>1/100</i>	<i>Atlas Antibodies #HPA063027</i>
<i>YAP</i>	<i>Rabbit</i>	<i>1/50</i>	<i>Santa Cruz #15407 discontinued</i>
<i>YAP</i>	<i>Rabbit</i>	<i>1/100</i>	<i>Cell Signaling Technology #14074S</i>
<i>E-cadherin</i>	<i>Rabbit</i>	<i>1/200</i>	<i>Cell Signaling Technology #3195</i>
<i>E-cadherin</i>	<i>Mouse</i>	<i>1/200</i>	<i>BD Transduction Lab #610182</i>
<i>Phalloidin</i>	<i>x</i>	<i>1/200</i>	<i>Sigma-Aldrich #HP1951</i>
<i>Claudin-3</i>	<i>Rabbit</i>	<i>1/100</i>	<i>Genetex #GTX15102</i>
<i>ZO-1</i>	<i>Rabbit</i>	<i>1/100</i>	<i>Cell Signaling Technology #8193</i>
<i>TAZ</i>	<i>Rabbit</i>	<i>1/50</i>	<i>Santa Cruz #SC-48805</i>
<i>TEAD4</i>	<i>Mouse</i>	<i>1/50</i>	<i>Santa Cruz sc-101184</i>

Table 9: List of primers used for qPCR analysis

Gene	Sequence 5'→3'
HPRT F	CTGACCTGCTGGATTACA
HPRT R	GCGACCTTGACCATCTTT
28S F	CGATCCATCATCCGCAATG
28S R	AGCCAAGCTCAGCGCAAC
GAPDH F	TCTATAAATTGAGCCCAGCC
GAPDH R	AGTTAAAAGCAGCCCTGGTGA
MAGI1 F	CGTAAAGTGGTTTTTGC GG TGC
MAGI1 R	TCTCCACGTCGTAGGGCTGC
MAGI2 F	ATCATTGGTGGAGACGAGCC
MAGI2 R	TAGCCACGACACAACACCAG
MAGI3 F	CTGCACTTTTCAGTCTTCTTTTGAC
MAGI3 R	CTGAACCAAATTACGTGGCCC
AMOTL2 F	CCAAGTCGGTGCCATCTGTT
AMOTL2 R	CCATCTCTGCTCCCGTGTTT
CYR61 F	ACCAAGAAATCCCCGAACC
CYR61 R	CGGGCAGTTGTAGTTGCATT
CTGF F	TTCCAAGACCTGTGGGAT
CTGF R	GTGCAGCCAGAAAGCTC
AREG F	CGAAGGACCAATGAGAGCCC
AREG R	AGGCATTTCACTCACAGGGG
BIRC2 F	GTCAGAACACCGGAGGCATT
BIRC2 R	TGACATCATCATTGCGACCCA
TAZ F	CTGGGGTTAGGGTGCTACAG
TAZ R	TCATTGAAGAGGGGGATCAG
AXIN2 F	GGGGTTGTGTTGGATGGGAT
AXIN2 R	ATTTCCACGAAAGCACAGCG
CCND1 F	TGGCTGAAGTCACCTCTTGG
CCND1 R	AGCGTATCGTAGGAGTGGGA
RUNX2 F	GGAGATCATCGCCGACCAC
RUNX2 R	CATCGTTACCCGCCATGACA

CRELD2 F	CTGCTCTCCAGGAACCTACG
CRELD2 R	GAGCTGAAGTAGCCGTCCAT
CHOP F	AGTCTAAGGCACTGAGCGTATC
CHOP R	TCTGTTTCCGTTTCCTGGTT
CHAK1 F	GAA CCC TGG TTA CCT GGG C
CHAK1 R	CGC AGC AAG TAT TCA AGG TTG
ASNS F	GGA AGA CAG CCC CGA TTT ACT
ASNS R	AGC ACG AAC TGT TGT AAT GTC
ATF3 F	CCT CTG CGC TGG AAT CAG TC
ATF3 R	TTC TTT CTC GTC GCC TCT TTT T
ATF4 F	TTCTCCAGCGACAAGGCTAAGG
ATF4 R	CTCCAACATCCAATCTGTCCCG
SLC6A9 F	GATCAGCCCCATGTTCAAAGG
SLC6A9 R	GTTGGAGGCGTCCAGTACAC
MYC F	CAGCGACTCTGAGGAGGAAC
MYC R	GCTGCGTAGTTGTGCTGATG

Discussion and perspectives

What we demonstrated so far is that MAGI1 has the same tumor suppressive role in luminal A BC as in HCC (Zhang and Wang, 2011), ALL (Kuang et al., 2008), CRC (Zaric et al., 2012), GC (Jia et al., 2017), Renal carcinoma (Wang et al., 2019) and in gliomas (Li et al., 2019).

Recently, (Alday-Parejo et al., 2020) described similarly to our findings, a cancer opposing role of MAGI1 in ER positive breast cancer cells. Using MCF7 cells as model for Luminal A breast cancer cells, they claim that MAGI1 knock-down promotes AKT phosphorylation and propose (without testing it formally) that this increased AKT signaling mediates the pro-tumoral effect of MAGI1 loss. My results do not support such claims. Furthermore, AKT phosphorylation is triggered by PI3K, and MCF7 cells are known to harbor an activating mutation in the PI3K enzyme rendering it constitutively active. “Normal” MCF7 cells have thus very high levels of activated AKT, and it appears highly unlikely that the knock-down of 50% in MAGI1 expression they obtained could trigger an even higher AKT activation. Actually, I have many concerns regarding the “MCF7” cells they have used in their study, since they reported N-Cadherin expression in MCF7, a claim that has never been observed and/or reported in the numerous research papers that have used MCF7 cells. In all likelihood, the cells they have used either derived or were simply not epithelial MCF7 cells, casting serious doubt about their findings and conclusions. Our results, based on signaling pathways profiling, tightly controlled experiments, and more importantly “rescue” experiments to validate functionally our observations, do not support AKT modulation, but show that MAGI1 is controlling AMOTL2 (a protein located at the junctions) and is preventing the excessive activation of the p38 stress MAPK pathway in cells. In the absence of MAGI1, p38 is activated and supports increased tumorigenic behaviors.

MAGI1 is part of the AJs and the TJs and its knock-down would affect the stoichiometry of the junctions. We never saw an activation of EMT in MAGI1 depleted cells (no expression of mesenchymal cell markers such as vimentin, or the transcription factors Snail, Slug and Twist). On the contrary, the levels of E-cadh (a main protein of the AJs and a marker of epithelial cells) were higher upon the removal of MAGI1 (cf. Figure 2 in the paper).

How to explain this correlation between high levels of E-cadherin and elevated tumorigenic traits of MAGI1 depleted cells?

Carcinogenesis is composed of many steps: initiation, promotion and progression and the loss of E-cadherin has been associated with tumor progression and metastasis. Many evidence exist to support this theory. Reviewed in (Mendonsa et al., 2018), E-cadherin is an important regulator of contact inhibition. When cells multiply under space constraints, they reach a point at which maximum confluency is sensed and relayed by components of the cellular junctions leading to inhibitory signals inside the cells to stop proliferation. When E-cadherin is deregulated or absent these inhibitory signals are not sent anymore which lead to an over proliferation and an uncontrolled growth (Figure 37). Moreover, E-cadherin is a marker of epithelial cells and its loss leads to a detachment form the epithelial sheet, which can lead to epithelial to mesenchymal transition or EMT, where cells acquire a migratory behavior (single cell mesenchymal migration). Many TFs responsible of EMT are known to inhibit the expression of E-cadherin in the cells. It is clear that at primary tumor sites, cells get rid of this tumor suppressor to grow and progress and to migrate, but once arrived to distant sites there are evidence suggesting that cells re-express E-cadherin. (Harigopal et al., 2005) show that distant metastatic sites tumors have increased levels of E-cadherin. Metastatic cells, once they have reached their distant sites, need to anchor tightly together and to the ECM to promote their survival.

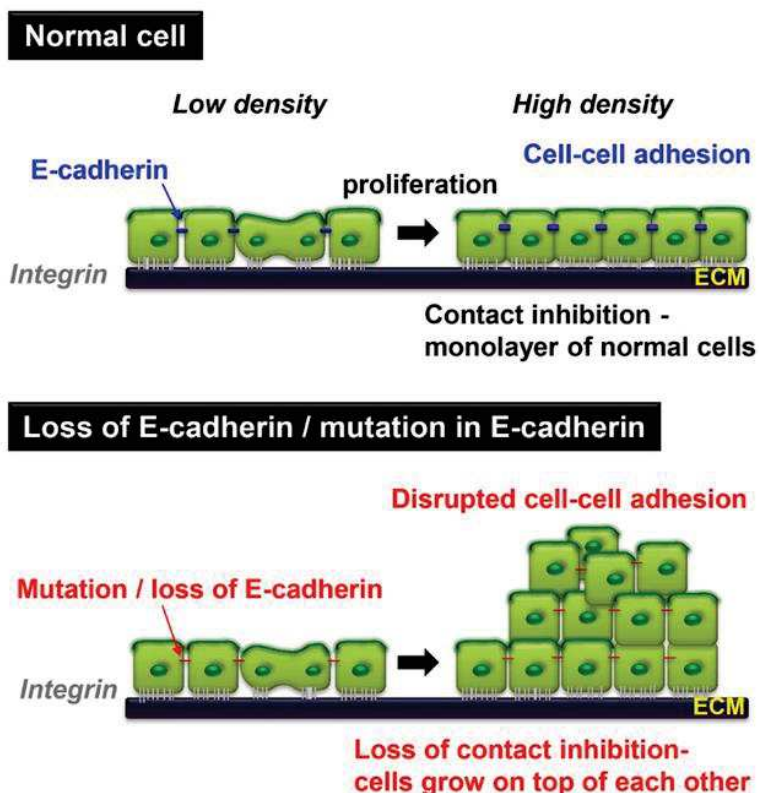


Figure 37: E-cadherin and contact inhibition. In normal cells, E-cadherin senses the high density of cells causing an inhibition of proliferation and this called contact inhibition. When E-cadherin is lost, cells grow even when they reach high density because the sensor is absent leading to high proliferation and overgrowth. Taken from Mendonsa et al. 2018.

However, cell migration in cancer is not restricted to sparse cell migration, and many examples of collective cell invasion and migration have been reported. In this case, coordinated E-cad changes within the migrating cell clusters support migration. It appears therefore that E-cad loss is not that

simple or straightforward in cancers. In a recent study, (Padmanaban et al., 2019) shows that E-cadherin is required for cancer cells survival and metastasis. They show that even though loss of E-cadherin promote invasion it promotes also apoptosis and reduction of metastases formation. E-cadherin protect the cell from Reactive Oxygen species (ROS), and thus promotes their survival during early phases of tumorigenesis. More studies are emerging with this novel role of E-cadherin in promoting cancer cell survival. In our study, we showed that upon MAGI1 loss more E-cad was accumulating in the cells. We observed increase cell numbers, and better mammosphere formation and soft agar growth. However we did not observe any increase 2D cell migration (collective migration) and MCF7 cells remained as low migratory cells as commonly observed, nor did we observe any increase in invasion (Boyden chamber assay). Together, these results would suggest that MAGI1 loss increases the cells ability to initiate tumors, to resist anoikis, and to overcome contact inhibition. All these steps, could be considered as early steps before tumor spreading, where according to the study of (Padmanaban et al., 2019) increased E-cad levels could actually be beneficial. It is possible that later transient modulations of E-cad could help spreading, but we have not directly assayed that.

It should be noticed that so far, I have just observed a correlation, and I have not directly tested whether the increased E-cad levels are functionally important and required for the effects of MAGI1 knock-down. To assess the function of E-cadherin in our cells it would thus be interesting to follow the status of the ROS inside the cells and study whether modulating E-cadherin levels would activate or not apoptosis and render the cells less fit and less tumorigenic.

But E-cad was not the only accumulating junctional protein, and we observed high levels of AMOTL2 in the cells upon MAGI1 KD.

How these elevated levels of AMOTL2 could be explained?

AMOTL2 like AMOT, are regulated by many processes inside the cell. AMOT is documented to be highly expressed in breast cancer tissues and cell lines. (Lv et al., 2015) show that MCF7 cells lacking AMOT are less invasive and have reduced proliferation, supporting our observation that AMOT family members increase expression is associated with increased tumorigenicity, contrary to what is currently assumed from the YAP sequestering function (anti-YAP basically) of AMOTs (B. Zhao et al., 2011)

After using an shRNA targeting MAGI1 in MCF7 cells we observed increased levels of AMOTL2 in qPCR, in western blot (cf. Figure 2B in the paper) and also in immunofluorescence analyses. The

increased expression levels are a bit unexpected since AMOTL2 is a known YAP targets, and we clearly show that YAP signaling is down in MAGI1-depleted cells, as evidenced by YAP nuclear exclusion and a robust decrease in classic YAP transcriptional targets (CYR61, BIRC2, AREG, CTGF...). One possibility is that AMOTL2 transcription is activated by other signaling pathways activated upon MAGI1 loss. One obvious candidate is P38 signaling, even though I have not formally tested that hypothesis.

But the increased level of AMOTL2 is unlikely only due to increased mRNA expression. Indeed when using expression vectors with CMV strong promoters to transiently express MAGI1 and AMOTs, we consistently observed lower AMOTs protein levels when MAGI1 was co-expressed, suggesting that MAGI1, somehow decreases AMOTs stability. The mechanisms of this potential MAGI1-dependent protein degradation remain unknown.

The Tankyrase (TNKS1, TNKS2) is known to regulate the stability of AMOT/AMOTL2 in the cell (Wang et al., 2015). This enzyme is a member of the poly (ADP-ribose) polymerase family (PARP) that are known to poly ADP ribosylate (PARsylate) their substrate leading to their degradation or changes in their localization. AMOT is parysated by TNKS and thus recognized by the E3 ubiquitin ligase RNF146 (Ring Finger Protein 146) ubiquitinated and degraded. One would think that the removal of MAGI1 destabilizes the TNKS activity on AMOTL2, and it would be interesting to study AMOTL2 PARsylation and Ubiquitination status with and without MAGI1, and whether MAGI1 directs TNKS towards AMOTL2, for instance by stabilizing an AMOTL2 TNKS interaction. A schematic summary of the hypothesis supporting AMOTL2 accumulation is represented in *Figure 38*.

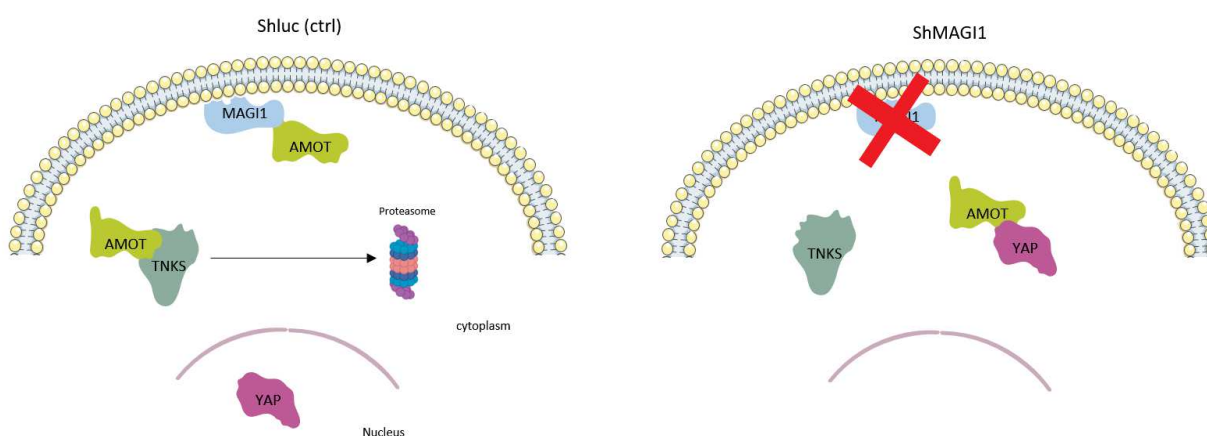


Figure 38: representation explaining the hypothesis supporting AMOTL2 accumulation in MCF7 cells upon MAGI1 removal.

Another important mechanism to regulate AMOT stability is its phosphorylation by LATS1, and phosphomimetic forms of AMOT S175D are more stable and accumulate in the cell (Adler et al., 2013). We have been able in the lab to confirm that at equivalent quantity of transfected plasmidic DNA, more AMOT S175D is detected in the cells than wild-type AMOT. A similar regulation for AMOTL2 has not been demonstrated, but it would be interesting to

- Test whether similar mutations cause AMOTL2 stability
- Monitor the +P status of AMOTL2 in the absence of MAGI1
- Whether the AMOTL2 accumulation in MAGI1 knock-down could be reversed by simultaneous knock-down of LATS1 (even though that experiment might turn out difficult to interpret since AMOTL2 is a YAP direct target and that LATS1 knock down should potentiate YAP transcriptional activity).

Alternatively, it is possible that AMOTL2 is stabilized by another phosphorylation. One attractive candidate is ROCK (or any kinase activated downstream of ROCK), since we were able to document an increased ROCK activity upon MAGI1 loss. Indeed my preliminary results suggest that AMOTL2 depletion, can rescue all MAGI1 KD associated phenotypes but the increased phosphorylation of MLC, suggesting that AMOTL2 might be acting downstream of ROCK.

Interestingly, AMOTL2 is an F-actin binding protein and it was shown to couple adhesion complexes to actin and allow actin tension (Hildebrand et al., 2017). KD of MAGI1 in MCF7 cells caused elevated intracellular stiffness and/or membrane strength as observed by AFM measurements. As previously shown and reproduced by us, relaxing the F-actin tension by inhibiting ROCK activity (using Y-27632) or by inhibiting the Myosin II (using blebbistatin) mimic the siRNA AMOTL2 phenotype linking thus AMOTL2 to cellular tension via F-actin contractility.

How are AMOTL2 and cellular tension linked?

(Hildebrand et al., 2017) demonstrated that E-cadherin, AMOTL2 and MAGI1 form a ternary complex that could be responsible for actin cytoskeleton tension observed during egg hatching in Zebrafish embryos. They verified the function of this complex by depleting AMOTL2 and they saw that siRNA AMOTL2 and F-actin relaxing by drug usage had the same effect. They thus suggested that E-cad, AMOTL2, and MAGI1 work together to promote actin tension, a process necessary for correct embryo morphogenesis. However, it should be noticed that they never formally checked for role of MAGI1 in

this process, and just extended the role of AMOTL2 to the whole complex based on the physical interaction of AMOTs with MAGI1, and with the assumption that protein that interact must work together. However, there are abundant examples of inhibitory/antagonistic physical interactions. Indeed, after KD MAGI1 in MCF7 cells we observed increased level of AMOTL2 and increased cytoskeleton contractility as monitored by the high levels of activated Myosin Light Chain (cf. Figure 3E-F of the paper). These results would suggest that MAGI1 in the complex acts as a regulatory inhibitory component, probably ensuring that the actin cytoskeleton is not put under too much contraction and tension.

But how could MAGI1 regulate ROCK activity and Myosin? Mass spectrometry analysis done on overexpressed Flag tagged MAGI1 immunoprecipitates in MCF7 cells (but also in HCT116) show that peptides corresponding to RAPGEF6 are amongst the most abundantly recovered. RAPGEF6 is a RAP guanine nucleotide exchange factor, interacting with and activating the RAP2 small GTPase which in return activates RhoA by activating the Rho GTPases activating protein 29 (ARHGAP29) (Meng et al., 2018). RhoA is one of the main activator of ROCK, the kinase phosphorylating and activating MLC, thus promoting F-actin contractility (tension). One hypothesis would be that the KD of MAGI1 unleashes a higher activity of RAPGEF6, thus promoting increased F-actin tension. Preliminary results supporting our hypothesis show that shRNA MAGI1 cells have more ARHGAP29 protein levels compared to Ctrl.

To verify this hypothesis, we would need to perform loss of function analyses of RAPGEF6 and test whether it could rescue the phenotypes caused by the loss of MAGI1 (2D proliferation, 3D soft agar, ROCK activity by monitoring the levels of MLC/p-MLC, AMOTL2 and E-cad accumulation, P38 phosphorylation). Moreover, RhoA is a druggable molecule and it would be interesting to try blocking its activity to restore MAGI1 KD phenotypes, even though such experiments might reveal to be challenging for long time exposures (2D proliferation, soft agar, AMOTL2 accumulation...) as RhoA represents a pleiotropic protein.

Another potential player is Syx (synectin-binding guanine exchange factor), a protein belonging to the RhoGEF family. It is involved in vasculature sprouting in Zebrafish and in Mice (Garnaas et al., 2008) and was characterized as a binding partner of AMOT (but also AMOTL1 and AMOTL2) in endothelial cells (Ernkvist et al., 2009). It is involved in the migration of polarized breast tumor cells by activating Diaphanous 1 (DIA1), an enzyme involved in F-actin cables bundle polymerization, and a RhoA downstream effector (Dachsel et al., 2013). One potential model could be that when SYX is bound to AMOTL2 in epithelial cells, it would promote the activation of RhoA that will activate in return ROCK activating thus MLC and enabling tension of the cytoskeleton. However, preliminary experiment using AMOTL2 knock-down shows that the pMLC increase after MAGI KD (ROCK activity) is not suppressed, suggesting that ROCK activation occurs upstream or in parallel to AMOTL2 accumulation (and thus the potential activation of SYX). Schematic representation of RhoA signaling to regulate actin dynamic is represented in *Figure 39* (Bros et al., 2019).

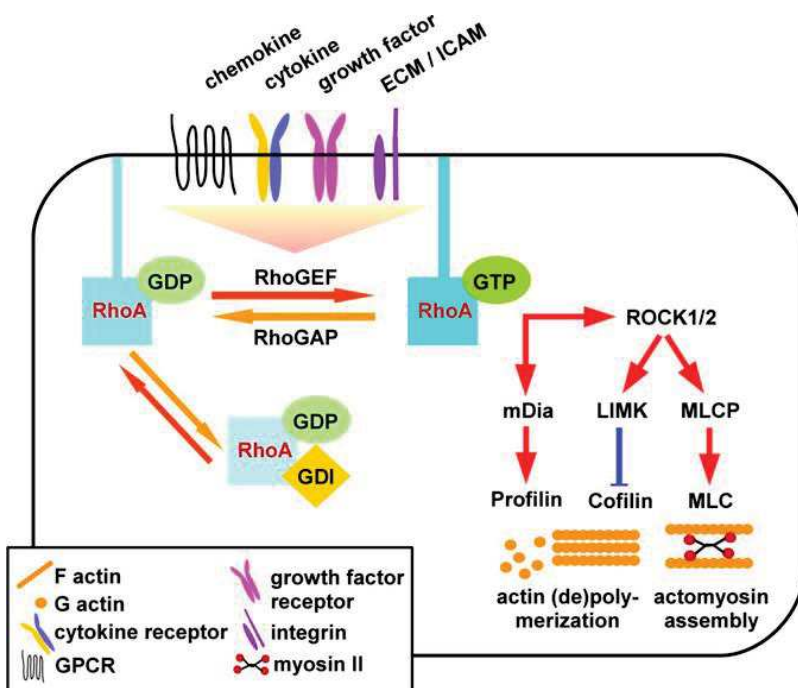


Figure 39: Scheme of RhoA signaling. Binding of exogenous ligands via different types of receptors as well as intracellular events trigger activation of RhoA GEF which, in turn, engage membrane-bound RhoA and mediate the exchange of GDP by GTP mediated by RhoGEF resulting in RhoA activation. GAP elevate the GTPase activity of RhoA, thereby promoting its inactivation. GDI translocate RhoA from the membrane and keep it in an inactive state. Active RhoA via protein kinases regulates cytoskeletal rearrangements. Active RhoA via ROCK/LIMK negatively regulates cofilin, which is required for F-actin turnover. Additionally, ROCK via inhibition of MLCP confers activation of MLC promoting actomyosin assembly. Active RhoA also promotes mDia activity, which in turn, activates profilin that is also involved in actin remodeling. Taken from Bros et al. 2019.

Another intriguing aspect of MAGI1 KD cells is the increased phosphorylated (activated levels) of p38 MAPK (cf. Figure 5A of the paper).

By which mechanism cells are activating the p38 MPAK pathway?

MAGI1 KD cells experience a high intracellular pressure and/or increased membrane strength. One would think that high pressure inside the cell would be translated into a stress stimulus, mimicking the confluency states in epithelial cells, Mechanical strain on MDCK cells could indeed lead to E-cad

junctions sensing and Yap translocation in the nucleus leading to cell cycle re-entry (Benham-Pyle et al., 2015). This process probably mediated by transverse stress fibers tension, is not the only one occurring in epithelial cells. Indeed, here the key actin structure is not the transverse stretch fibers, but the cortical actin belt encircling the TJs and AJs. When epithelial cells become more confluent, junctional engagement promotes the positive re-enforcement of actin/myosin cortical tension leading to clustering of junctional material. However, as compression continues, cells might then experience increased cellular pressure, which could be sensed as a stress

Molecularly, p38 kinases belong to the MAPK family and they are classically activated by a cascade of kinases. In the upstream steps, specific MAPKKKK (MAP4K) exhibit some degrees of specificity towards one or the other of the different MAPK cascades (ERK, JNK, p38...). For p38, Ste-20 family kinases like MAP4K4 (aka Misshapen MSN), MAP4K6 (aka Misshapen like kinase 1 or MINK1), or SLK have been shown to activate the p38 cascade (Nicke et al., 2005).

Interestingly, in *Drosophila* Msn has also been linked to the activation of Moesin an ERM (Ezrin Radixin Moesin) protein regulating cortical actin cytoskeleton which when activated promotes apical membrane strength (a phenotype reminiscent to the increased membrane strength seen upon MAGI1 KD) (Plutoni et al., 2019). It is thus possible that MSN is activated upon MAGI1 KD leading both to ERM activation (membrane strength) and p38 activation (MAP4K cascade activation). Such hypothesis could be validated by following ERM activation (phospho ERM) and MSN inactivation by si/sh RNA strategies.

As mentioned previously, and supported by the interaction seen between MAGI1 and RAPGEF6 in our proteomic data, (Meng et al., 2018) have shown that RAPGEF6 activation leads to ARHGAP29 activation which could then activate amongst others the p38 upstream MAP4K MINK1 (Nicke et al., 2005). It is thus attractive to speculate that upon MAGI1 depletion, the activation of RAPGEF6/RAP2/ARHGAP29 would lead to MINK1 activation and thus p38 activation. To test this model, we would need to invalidate MINK1 by si/shRNA in the context of MAGI1 KD and check whether p38 activation could be reverted.

What is the role of p38 α in this phenotype?

Normally acute stress kinase activation should lead to cell cycle arrest and be detrimental to cell fitness or survival, and ultimately lead to cell death. However, at low or intermediate levels, stress kinase activation could help protect cells against aggressions and prepare for mitigation of the initiating stress. As such, there is wide literature demonstrating the rewiring or hijack of stress pathway responses, including p38, by cancer cells to fuel their growth and aggressiveness (Martínez-Limón et al., 2020). We demonstrated that the inhibition of p38 α activation is able to rescue the phenotype of over-proliferation observed upon MAGI1 KD. Even though p38 α is described to be a tumor suppressor recently emerging evidence have been linking it to tumor promotion functions (reviewed in (Igea and Nebreda, 2015) (Figure 40).

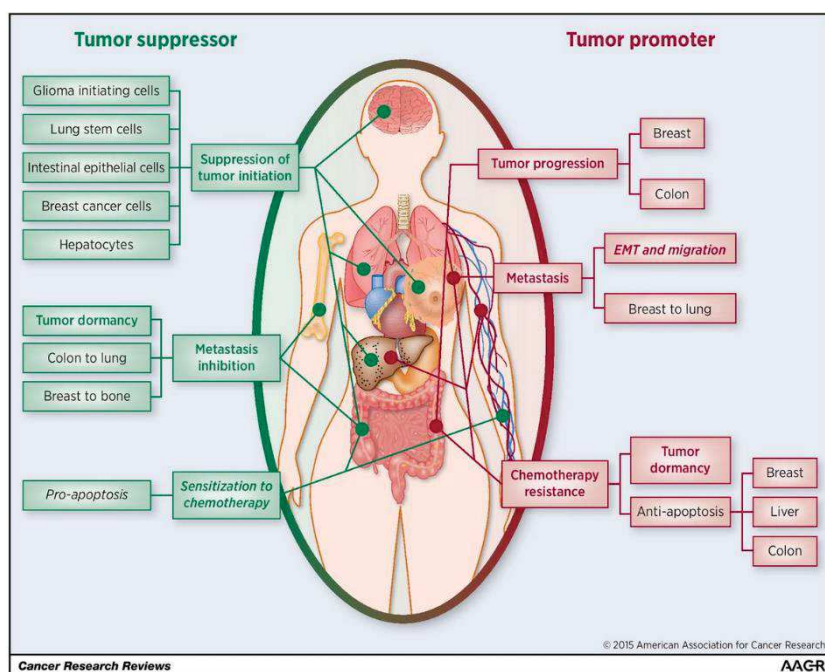


Figure 40: Role of p38 α in tumorigenesis based on mouse models.

Its tumor suppressive functions are shown in green. In red, we can see its tumor promoting functions. Taken from Igea and Nebreda, 2015.

Many mechanisms could explain how p38 is promoting this tumorigenic phenotype in MAGI1 KD MCF7 cells. P38 α could act in synergy with its downstream target ATF2 to control cell cycle progression. Enhancement of proliferation by ATF2 is well documented in many cancers such as skin adenocarcinomas (Zoumpourlis et al., 2000), melanomas (Recio and Merlino, 2003) and in prostate cancer (Ricote et al., 2006), and it would thus be interesting to monitor the levels of ATF2 and to assay directly its function (by si/shRNA invalidation).

Another p38 target is the MK2 (MAP kinase activated protein kinase 2) it is phosphorylated and activated by p38 and known for its positive contribution in tumor progression (Soni et al., 2019). The Ralimetinib (LY2228820), a drug used to block the p38 pathway is known to inhibit the activation of

MK2. Using Ralimetinib in the paper, we proved that inhibiting the p38 α pathway was able to attenuate the tumorigenesis phenotype caused by the loss of MAGI1 in MCF7 cells. Therefore, it would be interesting to check if p38 acts through MK2 in our cells to promote tumorigenesis.

Moreover, (Cánovas et al., 2018, p. 38) showed that p38 α is required for a correct progression through the cell cycle and to prevent cell death in mice. After depletion of p38 α using CRE/LOX experiments they documented high levels of DNA damage caused by an impairment of the DNA single strand break machinery mostly done by ATR and CHK1. In addition, in tumor epithelial cells they observed high levels of chromosome instability upon KO of p38 after treatment. Among the most prevalent features of cancer cells are uncontrolled proliferation, reduced apoptosis and genomic instability. Perhaps activation of p38 upon MAGI1 KD could represent a sign the cells are fighting against excessive DNA damage and chromosome instability that would be deleterious.

Besides p38 activation, we demonstrated that KD of MAGI1 is accompanied by retained p-YAP in the cytoplasm and reduction of YAP activity seen by monitoring its different transcription targets. This is counter-intuitive especially that YAP is a known oncogene and we observe higher oncogenic traits upon removal of MAGI1.

How to explain the retention of YAP in the cytoplasm?

(Furukawa et al., 2017) demonstrated in MDCK cells that at high density, AJs components are able to sense the tension of the apical actin belt. When this belts is under tension YAP and TAZ are translocated to the cytoplasm. They support these findings by treating cells at high density with blebbistatin, and this treatment causes the import of YAP/TAZ in the nucleus even at high cell density levels. This key paper support our findings regarding YAP localization upon MAGI1 removal in cells with increased AJ material and which experience increase in Actin contractility (pMLC increase). The mechanisms by which YAP is then excluded involve the mechano-sensing properties of a-catenin and NF2 (Furukawa et al., 2017)..

Another mechanism, by which MAGI1 KD could induce YAP nuclear exclusion, is through AMOTL2. Indeed, AMOTL2 is a known negative regulator of the YAP activity in the cells. It is well document that AMOTL2 is able to trap YAP in the cytoplasm and inhibit its translocation to the nucleus. Since we have high levels of AMOTL2, this could explain the retention of YAP. This theory was confirmed by using siRNA AMOTL2 (cf. *Figure 33B*). We see increased nuclear YAP after the removal of

AMOTL2 in MCF7 cell with a shRNA MAGI1. However, it should be noted that this effect is only seen at circa 70%-80% confluency. Indeed, at low confluency, YAP is nuclear even in shMAGI1 MCF7 cells, and the removal of AMOTL2 at low confluency (50%) has thus no effect. The YAP exclusion occurs “faster” in shMAGI1 MCF7 cells and at 70% confluency YAP is excluded for the nucleus while it remains nuclear in Ctrl cells. Surprisingly, after AMOTL2 removal, even though YAP stayed nuclear at 70% confluency, its transcriptional activity was not restored. That would suggest that MAGI1 is also required for YAP activity somehow.

1. It is reported that YAP full activity requires the phosphorylation of key Y residues on its C-terminal part by SRC family of kinases or by FAK (reviewed in (Dasgupta and McCollum, 2019)) Whether MAGI1 could control the action of these kinase on YAP independently of its action on localization, is an interesting prospect that needs further investigation.
2. In our Mass spectrometry analysis performed on MAGI1, we see that NF2/Merlin is able to bind MAGI1. NF2 is a known regulator of YAP. In (Furukawa et al., 2017), they show that Merlin is able to bind YAP and translocate with it in the nucleus. This interaction inhibit the binding of YAP to the TEAD transcription factors thus inhibiting the transcription of its target genes. This would be an interesting theory to test especially if we hypothesize that the loss of MAGI1 would release NF2 in the cytoplasm to be able to bind YAP. First, we need to verify the interaction between YAP and NF2 in our cells by performing a co-IP then we need to do some loss of function experiments of NF2 and monitor the transcription activity of YAP/TEAD.

The Hippo pathway is a mechanosensitive pathway remodeled by intercellular junctional engagement, Actin cytoskeletal tension (stress fibers and cortical actin tension with opposing effects), but also by the stiffness of the ECM. It was interesting to monitor the effect of the ECM on the phenotype caused by the loss of MAGI1.

How to explain the different phenotype regarding the Hippo pathway obtained on stiff and soft matrices?

We used commercially available Cytosoft plates with different ECM stiffness (soft 0.5KPa and stiff the plastic plate). Comparison between the two conditions made us realize that in both cases the shRNA MAGI1 causes an accumulation of p-YAP in the cells. An interesting observation was the effect of the core components of the Hippo pathway. On plastic dishes, MCF7 shMAGI1 cells did not harbor an

activation of LATS1 nor MOB1, core components of the Hippo pathway which made us conclude that, even though LATS1 is probably mediated the phosphorylation, the accumulation of p-YAP is not due to an increase in Hippo/LATS1 activity, but rather by increased cytoplasmic retention (AMOTL2 ...). On the other hand, on soft matrix we observed elevated levels of phosphorylated MOB1 suggesting an activation of the canonical Hippo pathway. This activation could be the cause of the accumulation of the p-YAP.

We hypothesize that depending on the stiffness of the matrix MAGI1 binding partners could change. Preliminary results show that MAGI1 could bind to LATS in cells plated on soft matrix. Whether this interaction is controlling the activity of LATS toward YAP, and that upon MAGI1 KD LATS would be released to phosphorylate YAP and inhibit its translocation to the nucleus, is an attractive model that needs further investigation.

It is interesting though to see that on soft and on stiff ECM these luminal A breast cancer cell do not depend on YAP activity to promote their tumorigenic traits.

REFERENCES

- Abe, J., Ko, K.A., Kotla, S., Wang, Y., Paez-Mayorga, J., Shin, I.J., Imanishi, M., Vu, H.T., Tao, Y., Leiva-Juarez, M.M., Thomas, T.N., Medina, J.L., Won, J.H., Fujii, Y., Giancursio, C.J., McBeath, E., Shin, J.-H., Guzman, L., Abe, R.J., Taunton, J., Mochizuki, N., Faubion, W., Cooke, J.P., Fujiwara, K., Evans, S.E., Le, N.-T., 2019. MAGI1 as a link between endothelial activation and ER stress drives atherosclerosis. *JCI Insight* 4. <https://doi.org/10.1172/jci.insight.125570>
- Adams, R.H., Porras, A., Alonso, G., Jones, M., Vintersten, K., Panelli, S., Valladares, A., Perez, L., Klein, R., Nebreda, A.R., 2000. Essential role of p38alpha MAP kinase in placental but not embryonic cardiovascular development. *Mol. Cell* 6, 109–116.
- Adler, J.J., Johnson, D.E., Heller, B.L., Bringman, L.R., Ranahan, W.P., Conwell, M.D., Sun, Y., Hudmon, A., Wells, C.D., 2013. Serum deprivation inhibits the transcriptional co-activator YAP and cell growth via phosphorylation of the 130-kDa isoform of Angiomin by the LATS1/2 protein kinases. *PNAS* 110, 17368–17373. <https://doi.org/10.1073/pnas.1308236110>
- Ahuja, R., Pinyol, R., Reichenbach, N., Custer, L., Klingensmith, J., Kessels, M.M., Qualmann, B., 2007. Cordon-bleu is an actin nucleation factor and controls neuronal morphology. *Cell* 131, 337–350. <https://doi.org/10.1016/j.cell.2007.08.030>
- Alday-Parejo, B., Richard, F., Wörthmüller, J., Rau, T., Galván, J.A., Desmedt, C., Santamaria-Martinez, A., Rüegg, C., 2020. MAGI1, a New Potential Tumor Suppressor Gene in Estrogen Receptor Positive Breast Cancer. *Cancers (Basel)* 12. <https://doi.org/10.3390/cancers12010223>
- Alonso, A., Domènech, E., Julià, A., Panés, J., García-Sánchez, V., Mateu, P.N., Gutiérrez, A., Gomollón, F., Mendoza, J.L., Garcia-Planella, E., Barreiro-de Acosta, M., Muñoz, F., Vera, M., Saro, C., Esteve, M., Andreu, M., Chaparro, M., Manyé, J., Cabré, E., López-Lasanta, M., Tortosa, R., Gelpí, J.L., García-Montero, A.C., Bertranpetit, J., Absher, D., Myers, R.M., Marsal, S., Gisbert, J.P., 2015. Identification of risk loci for Crohn's disease phenotypes using a genome-wide association study. *Gastroenterology* 148, 794–805. <https://doi.org/10.1053/j.gastro.2014.12.030>
- Al-Sadi, R., Khatib, K., Guo, S., Ye, D., Youssef, M., Ma, T., 2011. Occludin regulates macromolecule flux across the intestinal epithelial tight junction barrier. *Am. J. Physiol. Gastrointest. Liver Physiol.* 300, G1054-1064. <https://doi.org/10.1152/ajpgi.00055.2011>
- Anatomy of the Female Breast [WWW Document], n.d. URL http://www.breastcancertreatment.in/breast_anatomy.htm
- Angelow, S., Ahlstrom, R., Yu, A.S.L., 2008. Biology of claudins. *American Journal of Physiology-Renal Physiology* 295, F867–F876. <https://doi.org/10.1152/ajprenal.90264.2008>
- Arteaga, C.L., Engelman, J.A., 2014. ERBB receptors: from oncogene discovery to basic science to mechanism-based cancer therapeutics. *Cancer Cell* 25, 282–303. <https://doi.org/10.1016/j.ccr.2014.02.025>
- Assémat, E., Bazellières, E., Pallesi-Pocachard, E., Le Bivic, A., Massey-Harroche, D., 2008. Polarity complex proteins. *Biochimica et Biophysica Acta (BBA) - Biomembranes, Apical Junctional Complexes Part I* 1778, 614–630. <https://doi.org/10.1016/j.bbamem.2007.08.029>
- Azzolin, L., Panciera, T., Soligo, S., Enzo, E., Bicciato, S., Dupont, S., Bresolin, S., Frasson, C., Basso, G., Guzzardo, V., Fassina, A., Cordenonsi, M., Piccolo, S., 2014. YAP/TAZ Incorporation in the β -Catenin Destruction Complex Orchestrates the Wnt Response. *Cell* 158, 157–170. <https://doi.org/10.1016/j.cell.2014.06.013>
- Badouel, C., Gardano, L., Amin, N., Garg, A., Rosenfeld, R., Le Bihan, T., McNeill, H., 2009. The FERM-Domain Protein Expanded Regulates Hippo Pathway Activity via Direct Interactions with the Transcriptional Activator Yorkie. *Developmental Cell* 16, 411–420. <https://doi.org/10.1016/j.devcel.2009.01.010>

- Bailey, M.J., Prehoda, K.E., 2015. Establishment of Par-Polarized Cortical Domains via Phosphoregulated Membrane Motifs. *Developmental Cell* 35, 199–210. <https://doi.org/10.1016/j.devcel.2015.09.016>
- Balda, M.S., Whitney, J.A., Flores, C., González, S., Cereijido, M., Matter, K., 1996. Functional dissociation of paracellular permeability and transepithelial electrical resistance and disruption of the apical-basolateral intramembrane diffusion barrier by expression of a mutant tight junction membrane protein. *J. Cell Biol.* 134, 1031–1049. <https://doi.org/10.1083/jcb.134.4.1031>
- Barmchi, M.P., Samarasekera, G., Gilbert, M., Auld, V.J., Zhang, B., 2016. Magi Is Associated with the Par Complex and Functions Antagonistically with Bazooka to Regulate the Apical Polarity Complex. *PLOS ONE* 11, e0153259. <https://doi.org/10.1371/journal.pone.0153259>
- Basu, S., Totty, N.F., Irwin, M.S., Sudol, M., Downward, J., 2003. Akt Phosphorylates the Yes-Associated Protein, YAP, to Induce Interaction with 14-3-3 and Attenuation of p73-Mediated Apoptosis. *Molecular Cell* 11, 11–23. [https://doi.org/10.1016/S1097-2765\(02\)00776-1](https://doi.org/10.1016/S1097-2765(02)00776-1)
- Basuroy, S., Sheth, P., Kuppaswamy, D., Balasubramanian, S., Ray, R.M., Rao, R.K., 2003. Expression of kinase-inactive c-Src delays oxidative stress-induced disassembly and accelerates calcium-mediated reassembly of tight junctions in the Caco-2 cell monolayer. *J. Biol. Chem.* 278, 11916–11924. <https://doi.org/10.1074/jbc.M211710200>
- Bazellières, E., Aksenova, V., Barthélémy-Requin, M., Massey-Harroche, D., Le Bivic, A., 2018. Role of the Crumbs proteins in ciliogenesis, cell migration and actin organization. *Seminars in Cell & Developmental Biology* 81, 13–20. <https://doi.org/10.1016/j.semcd.2017.10.018>
- Benham-Pyle, B.W., Pruitt, B.L., Nelson, W.J., 2015. Mechanical strain induces E-cadherin-dependent Yap1 and β -catenin activation to drive cell cycle entry. *Science* 348, 1024–1027. <https://doi.org/10.1126/science.aaa4559>
- Benton, R., Johnston, D.S., 2003. Drosophila PAR-1 and 14-3-3 Inhibit Bazooka/PAR-3 to Establish Complementary Cortical Domains in Polarized Cells. *Cell* 115, 691–704. [https://doi.org/10.1016/S0092-8674\(03\)00938-3](https://doi.org/10.1016/S0092-8674(03)00938-3)
- Berger, M.F., Lawrence, M.S., Demichelis, F., Drier, Y., Cibulskis, K., Sivachenko, A.Y., Sboner, A., Esgueva, R., Pflueger, D., Sougnez, C., Onofrio, R., Carter, S.L., Park, K., Habegger, L., Ambrogio, L., Fennell, T., Parkin, M., Saksena, G., Voet, D., Ramos, A.H., Pugh, T.J., Wilkinson, J., Fisher, S., Winckler, W., Mahan, S., Ardlie, K., Baldwin, J., Simons, J.W., Kitabayashi, N., MacDonald, T.Y., Kantoff, P.W., Chin, L., Gabriel, S.B., Gerstein, M.B., Golub, T.R., Meyerson, M., Tewari, A., Lander, E.S., Getz, G., Rubin, M.A., Garraway, L.A., 2011. The genomic complexity of primary human prostate cancer. *Nature* 470, 214–220. <https://doi.org/10.1038/nature09744>
- Bertocchi, C., Vaman Rao, M., Zaidel-Bar, R., 2012. Regulation of Adherens Junction Dynamics by Phosphorylation Switches. *J Signal Transduct* 2012. <https://doi.org/10.1155/2012/125295>
- Bienz, M., 2005. β -Catenin: A Pivot between Cell Adhesion and Wnt Signalling. *Current Biology* 15, R64–R67. <https://doi.org/10.1016/j.cub.2004.12.058>
- Bilder, D., 2004. Epithelial polarity and proliferation control: links from the Drosophila neoplastic tumor suppressors. *Genes Dev.* 18, 1909–1925. <https://doi.org/10.1101/gad.1211604>
- Bilder, D., Birnbaum, D., Borg, J.-P., Bryant, P., Huigbretse, J., Jansen, E., Kennedy, M.B., Labouesse, M., Legouis, R., Mechler, B., Perrimon, N., Petit, M., Sinha, P., 2000. Collective nomenclature for LAP proteins. *Nature Cell Biology* 2, E114–E114. <https://doi.org/10.1038/35017119>
- Bilder, D., Perrimon, N., 2000. Localization of apical epithelial determinants by the basolateral PDZ protein Scribble. *Nature* 403, 676–680. <https://doi.org/10.1038/35001108>
- Blanchoin, L., Boujemaa-Paterski, R., Sykes, C., Plastino, J., 2014. Actin Dynamics, Architecture, and Mechanics in Cell Motility. *Physiological Reviews* 94, 235–263. <https://doi.org/10.1152/physrev.00018.2013>

- Bollaert, E., de Rocca Serra, A., Demoulin, J.-B., 2019. The HMG box transcription factor HBP1: a cell cycle inhibitor at the crossroads of cancer signaling pathways. *Cell. Mol. Life Sci.* 76, 1529–1539. <https://doi.org/10.1007/s00018-019-03012-9>
- Bonello, T.T., Peifer, M., 2019. Scribble: A master scaffold in polarity, adhesion, synaptogenesis, and proliferation. *J Cell Biol* 218, 742–756. <https://doi.org/10.1083/jcb.201810103>
- Boulton, T.G., Yancopoulos, G.D., Gregory, J.S., Slaughter, C., Moomaw, C., Hsu, J., Cobb, M.H., 1990. An insulin-stimulated protein kinase similar to yeast kinases involved in cell cycle control. *Science* 249, 64–67. <https://doi.org/10.1126/science.2164259>
- Bouwmeester, T., Kim, S.-H., Sasai, Y., Lu, B., Robertis, E.M.D., 1996. Cerberus is a head-inducing secreted factor expressed in the anterior endoderm of Spemann's organizer. *Nature* 382, 595–601. <https://doi.org/10.1038/382595a0>
- Breast Development and Anatomy : Clinical Obstetrics and Gynecology [WWW Document], n.d. URL https://journals.lww.com/clinicalobgyn/Abstract/2011/03000/Breast_Development_and_Anatomy.14.aspx
- Brembeck, F.H., Schwarz-Romond, T., Bakkers, J., Wilhelm, S., Hammerschmidt, M., Birchmeier, W., 2004. Essential role of BCL9-2 in the switch between β -catenin's adhesive and transcriptional functions. *Genes Dev.* 18, 2225–2230. <https://doi.org/10.1101/gad.317604>
- Bros, M., Haas, K., Moll, L., Grabbe, S., 2019. RhoA as a Key Regulator of Innate and Adaptive Immunity. *Cells* 8, 733. <https://doi.org/10.3390/cells8070733>
- Bryant, D.M., Mostov, K.E., 2008. From cells to organs: building polarized tissue. *Nat Rev Mol Cell Biol* 9, 887–901. <https://doi.org/10.1038/nrm2523>
- Camilleri, M., Carlson, P., Valentin, N., Acosta, A., O'Neill, J., Eckert, D., Dyer, R., Na, J., Klee, E.W., Murray, J.A., 2016. Pilot study of small bowel mucosal gene expression in patients with irritable bowel syndrome with diarrhea. *Am. J. Physiol. Gastrointest. Liver Physiol.* 311, G365-376. <https://doi.org/10.1152/ajpgi.00037.2016>
- Campbell, H.K., Maiers, J.L., DeMali, K.A., 2017. Interplay between tight junctions & adherens junctions. *Experimental Cell Research, Cell Sensing and Signaling via Cell-Cell Adhesion* 358, 39–44. <https://doi.org/10.1016/j.yexcr.2017.03.061>
- Campbell, R.M., Anderson, B.D., Brooks, N.A., Brooks, H.B., Chan, E.M., Dios, A.D., Gilmour, R., Graff, J.R., Jambrina, E., Mader, M., McCann, D., Na, S., Parsons, S.H., Pratt, S.E., Shih, C., Stancato, L.F., Starling, J.J., Tate, C., Velasco, J.A., Wang, Y., Ye, X.S., 2014. Characterization of LY2228820 Dimesylate, a Potent and Selective Inhibitor of p38 MAPK with Antitumor Activity. *Mol Cancer Ther* 13, 364–374. <https://doi.org/10.1158/1535-7163.MCT-13-0513>
- Cánovas, B., Igea, A., Sartori, A.A., Gomis, R.R., Paull, T.T., Isoda, M., Pérez-Montoyo, H., Serra, V., González-Suárez, E., Stracker, T.H., Nebreda, A.R., 2018. Targeting p38 α Increases DNA Damage, Chromosome Instability, and the Anti-tumoral Response to Taxanes in Breast Cancer Cells. *Cancer Cell* 33, 1094-1110.e8. <https://doi.org/10.1016/j.ccell.2018.04.010>
- Cao, F., Miao, Y., Xu, K., Liu, P., 2015. Lethal (2) Giant Larvae: An Indispensable Regulator of Cell Polarity and Cancer Development. *Int. J. Biol. Sci.* 11, 380–389. <https://doi.org/10.7150/ijbs.11243>
- Cargnello, M., Roux, P.P., 2011. Activation and Function of the MAPKs and Their Substrates, the MAPK-Activated Protein Kinases. *Microbiol Mol Biol Rev* 75, 50–83. <https://doi.org/10.1128/MMBR.00031-10>
- CBFB Mutations and MAGI3–AKT3 Fusions Recur In Breast Cancer, 2012. . *Cancer Discovery* 2, OF10–OF10. <https://doi.org/10.1158/2159-8290.CD-RW2012-092>
- Chalmers, A.D., Whitley, P., Elsum, I., Yates, L., Humbert, P.O., Richardson, H.E., 2012. The Scribble–Dlg–Lgl polarity module in development and cancer: from flies to man. *Essays Biochem* 53, 141–168. <https://doi.org/10.1042/bse0530141>
- Chao, Y.L., Shepard, C.R., Wells, A., 2010. Breast carcinoma cells re-express E-cadherin during mesenchymal to epithelial reverting transition. *Mol Cancer* 9, 179. <https://doi.org/10.1186/1476-4598-9-179>

- Chen, G., Hitomi, M., Han, J., Stacey, D.W., 2000. The p38 Pathway Provides Negative Feedback for Ras Proliferative Signaling. *J. Biol. Chem.* 275, 38973–38980. <https://doi.org/10.1074/jbc.M002856200>
- Chen, L., Mayer, J.A., Krisko, T.I., Speers, C.W., Wang, T., Hilsenbeck, S.G., Brown, P.H., 2009. Inhibition of the p38 Kinase Suppresses the Proliferation of Human ER-Negative Breast Cancer Cells. *Cancer Res* 69, 8853–8861. <https://doi.org/10.1158/0008-5472.CAN-09-1636>
- Chen, Y.-H., Lu, Q., Goodenough, D.A., Jeansonne, B., 2002. Nonreceptor tyrosine kinase c-Yes interacts with occludin during tight junction formation in canine kidney epithelial cells. *Mol. Biol. Cell* 13, 1227–1237. <https://doi.org/10.1091/mbc.01-08-0423>
- Chereau, D., Boczkowska, M., Skwarek-Maruszewska, A., Fujiwara, I., Hayes, D.B., Rebowski, G., Lappalainen, P., Pollard, T.D., Dominguez, R., 2008. Leiomodin is an actin filament nucleator in muscle cells. *Science* 320, 239–243. <https://doi.org/10.1126/science.1155313>
- Chesarone, M.A., Goode, B.L., 2009. Actin nucleation and elongation factors: mechanisms and interplay. *Current Opinion in Cell Biology, Cell structure and dynamics* 21, 28–37. <https://doi.org/10.1016/j.ceb.2008.12.001>
- Chiasson, C.M., Wittich, K.B., Vincent, P.A., Faundez, V., Kowalczyk, A.P., 2009. p120-catenin inhibits VE-cadherin internalization through a Rho-independent mechanism. *Mol. Biol. Cell* 20, 1970–1980. <https://doi.org/10.1091/mbc.e08-07-0735>
- Citi, S., Guerrero, D., Spadaro, D., Shah, J., 2014. Epithelial junctions and Rho family GTPases: the zonular signalosome. *Small GTPases* 5, 1–15. <https://doi.org/10.4161/21541248.2014.973760>
- Claude, P., Goodenough, D.A., 1973. FRACTURE FACES OF ZONULAE OCCLUDENTES FROM TIGHT AND LEAKY EPITHELIA. *J Cell Biol* 58, 390–400. <https://doi.org/10.1083/jcb.58.2.390>
- Colegio, O.R., Van Itallie, C., Rahner, C., Anderson, J.M., 2003. Claudin extracellular domains determine paracellular charge selectivity and resistance but not tight junction fibril architecture. *Am. J. Physiol., Cell Physiol.* 284, C1346-1354. <https://doi.org/10.1152/ajpcell.00547.2002>
- Colegio, O.R., Van Itallie, C.M., McCrea, H.J., Rahner, C., Anderson, J.M., 2002. Claudins create charge-selective channels in the paracellular pathway between epithelial cells. *Am. J. Physiol., Cell Physiol.* 283, C142-147. <https://doi.org/10.1152/ajpcell.00038.2002>
- Collinet, C., Lecuit, T., 2013. Chapter Two - Stability and Dynamics of Cell–Cell Junctions, in: van Roy, F. (Ed.), *Progress in Molecular Biology and Translational Science, The Molecular Biology of Cadherins*. Academic Press, pp. 25–47. <https://doi.org/10.1016/B978-0-12-394311-8.00002-9>
- Cooper, G.M., 2000. *Structure and Organization of Actin Filaments*. The Cell: A Molecular Approach. 2nd edition.
- Coopman, P., Djiane, A., 2016. Adherens Junction and E-Cadherin complex regulation by epithelial polarity. *Cell. Mol. Life Sci.* 73, 3535–3553. <https://doi.org/10.1007/s00018-016-2260-8>
- Cording, J., Berg, J., Käding, N., Bellmann, C., Tscheik, C., Westphal, J.K., Milatz, S., Günzel, D., Wolburg, H., Piontek, J., Huber, O., Blasig, I.E., 2013. In tight junctions, claudins regulate the interactions between occludin, tricellulin and marvelD3, which, inversely, modulate claudin oligomerization. *J. Cell. Sci.* 126, 554–564. <https://doi.org/10.1242/jcs.114306>
- Costa, R.L.B., Han, H.S., Gradishar, W.J., 2018. Targeting the PI3K/AKT/mTOR pathway in triple-negative breast cancer: a review. *Breast Cancer Res. Treat.* 169, 397–406. <https://doi.org/10.1007/s10549-018-4697-y>
- Cselenyi, C.S., Jernigan, K.K., Tahinci, E., Thorne, C.A., Lee, L.A., Lee, E., 2008. LRP6 transduces a canonical Wnt signal independently of Axin degradation by inhibiting GSK3's phosphorylation of β -catenin. *PNAS* 105, 8032–8037. <https://doi.org/10.1073/pnas.0803025105>
- Cuadrado, A., Nebreda, A.R., 2010. Mechanisms and functions of p38 MAPK signalling. *Biochem. J.* 429, 403–417. <https://doi.org/10.1042/BJ20100323>

- Cuenda, A., Rousseau, S., 2007. p38 MAP-Kinases pathway regulation, function and role in human diseases. *Biochimica et Biophysica Acta (BBA) - Molecular Cell Research, Mitogen-Activated Protein Kinases: New Insights on Regulation, Function and Role in Human Disease* 1773, 1358–1375. <https://doi.org/10.1016/j.bbamcr.2007.03.010>
- Dachsel, J.C., Ngok, S.P., Lewis-Tuffin, L.J., Kourtidis, A., Geyer, R., Johnston, L., Feathers, R., Anastasiadis, P.Z., 2013. The Rho Guanine Nucleotide Exchange Factor Syx Regulates the Balance of Dia and ROCK Activities To Promote Polarized-Cancer-Cell Migration. *Molecular and Cellular Biology* 33, 4909–4918. <https://doi.org/10.1128/MCB.00565-13>
- Dang, I., 2014. Migration cellulaire: identification d'Arpin, un nouvel inhibiteur du complexe Arp2/3, et mécanismes moléculaires de sa régulation (phdthesis). Université Paris Sud.
- Dasgupta, I., McCollum, D., 2019. Control of cellular responses to mechanical cues through YAP/TAZ regulation. *J. Biol. Chem.* 294, 17693–17706. <https://doi.org/10.1074/jbc.REV119.007963>
- Davis, J.R., Tapon, N., 2019. Hippo signalling during development. *Development* 146. <https://doi.org/10.1242/dev.167106>
- Davis, M.A., Ireton, R.C., Reynolds, A.B., 2003. A core function for p120-catenin in cadherin turnover. *J. Cell Biol.* 163, 525–534. <https://doi.org/10.1083/jcb.200307111>
- Dawson, S.-J., Rueda, O.M., Aparicio, S., Caldas, C., 2013. A new genome-driven integrated classification of breast cancer and its implications. *EMBO J* 32, 617–628. <https://doi.org/10.1038/emboj.2013.19>
- de Azambuja, E., Cardoso, F., de Castro, G., Colozza, M., Mano, M.S., Durbecq, V., Sotiriou, C., Larsimont, D., Piccart-Gebhart, M.J., Paesmans, M., 2007. Ki-67 as prognostic marker in early breast cancer: a meta-analysis of published studies involving 12 155 patients. *British Journal of Cancer* 96, 1504–1513. <https://doi.org/10.1038/sj.bjc.6603756>
- de Kruijf, E.M., Dekker, T.J.A., Hawinkels, L.J. a. C., Putter, H., Smit, V.T.H.B.M., Kroep, J.R., Kuppen, P.J.K., van de Velde, C.J.H., ten Dijke, P., Tollenaar, R. a. E.M., Mesker, W.E., 2013. The prognostic role of TGF- β signaling pathway in breast cancer patients. *Ann. Oncol.* 24, 384–390. <https://doi.org/10.1093/annonc/mds333>
- Dhawan, P., Singh, A.B., Deane, N.G., No, Y., Shiou, S.-R., Schmidt, C., Neff, J., Washington, M.K., Beauchamp, R.D., 2005. Claudin-1 regulates cellular transformation and metastatic behavior in colon cancer. *J. Clin. Invest.* 115, 1765–1776. <https://doi.org/10.1172/JCI24543>
- Djiane, A., Yogev, S., Mlodzik, M., 2005. The Apical Determinants aPKC and dPatj Regulate Frizzled-Dependent Planar Cell Polarity in the Drosophila Eye. *Cell* 121, 621–631. <https://doi.org/10.1016/j.cell.2005.03.014>
- Dobrosotskaya, I.Y., James, G.L., 2000. MAGI-1 Interacts with β -Catenin and Is Associated with Cell-Cell Adhesion Structures. *Biochemical and Biophysical Research Communications* 270, 903–909. <https://doi.org/10.1006/bbrc.2000.2471>
- Dolado, I., Swat, A., Ajenjo, N., De Vita, G., Cuadrado, A., Nebreda, A.R., 2007. p38alpha MAP kinase as a sensor of reactive oxygen species in tumorigenesis. *Cancer Cell* 11, 191–205. <https://doi.org/10.1016/j.ccr.2006.12.013>
- Dupont, S., Morsut, L., Aragona, M., Enzo, E., Giulitti, S., Cordenonsi, M., Zanconato, F., Le Digabel, J., Forcato, M., Bicciato, S., Elvassore, N., Piccolo, S., 2011. Role of YAP/TAZ in mechanotransduction. *Nature* 474, 179–183. <https://doi.org/10.1038/nature10137>
- Ebnet, K., 2013. JAM-A and aPKC. *Tissue Barriers* 1, e22993. <https://doi.org/10.4161/tisb.22993>
- Edwards, M., Zwolak, A., Schafer, D.A., Sept, D., Dominguez, R., Cooper, J.A., 2014. Capping protein regulators fine-tune actin assembly dynamics. *Nature Reviews Molecular Cell Biology* 15, 677–689. <https://doi.org/10.1038/nrm3869>
- Elosegui-Artola, A., Andreu, I., Beedle, A.E.M., Lezamiz, A., Uroz, M., Kosmalka, A.J., Oriá, R., Kechagia, J.Z., Rico-Lastres, P., Le Roux, A.-L., Shanahan, C.M., Trepát, X., Navajas, D., Garcia-Manyes, S., Roca-Cusachs, P., 2017. Force Triggers YAP Nuclear Entry by Regulating Transport across Nuclear Pores. *Cell* 171, 1397–1410.e14. <https://doi.org/10.1016/j.cell.2017.10.008>

- Ernkvist, M., Persson, N.L., Audebert, S., Lecine, P., Sinha, I., Liu, M., Schlueter, M., Horowitz, A., Aase, K., Weide, T., Borg, J.-P., Majumdar, A., Holmgren, L., 2009. The Amot/Patj/Syx signaling complex spatially controls RhoA GTPase activity in migrating endothelial cells. *Blood* 113, 244–253. <https://doi.org/10.1182/blood-2008-04-153874>
- Farquhar, M.G., Palade, G.E., 1963. JUNCTIONAL COMPLEXES IN VARIOUS EPITHELIA. *The Journal of Cell Biology* 17, 375–412. <https://doi.org/10.1083/jcb.17.2.375>
- Feldman, G.J., Mullin, J.M., Ryan, M.P., 2005. Occludin: Structure, function and regulation. *Advanced Drug Delivery Reviews, Adhesion Proteins in Cellular Tight Junctions: Critical Components in the Modulation of Paracellular Permeability* 57, 883–917. <https://doi.org/10.1016/j.addr.2005.01.009>
- Feng, X., Jia, S., Martin, T.A., Jiang, W.G., 2014. Regulation and Involvement in Cancer and Pathological Conditions of MAGI1, a Tight Junction Protein. *Anticancer Research* 34, 3251–3256.
- Feng, Y., Spezia, M., Huang, S., Yuan, C., Zeng, Z., Zhang, L., Ji, X., Liu, W., Huang, B., Luo, W., Liu, B., Lei, Y., Du, S., Vuppapapati, A., Luu, H.H., Haydon, R.C., He, T.-C., Ren, G., 2018. Breast cancer development and progression: Risk factors, cancer stem cells, signaling pathways, genomics, and molecular pathogenesis. *Genes Dis* 5, 77–106. <https://doi.org/10.1016/j.gendis.2018.05.001>
- Ferreiro, I., Joaquin, M., Islam, A., Gomez-Lopez, G., Barragan, M., Lombardía, L., Domínguez, O., Pisano, D.G., Lopez-Bigas, N., Nebreda, A.R., Posas, F., 2010. Whole genome analysis of p38 SAPK-mediated gene expression upon stress. *BMC Genomics* 11, 144. <https://doi.org/10.1186/1471-2164-11-144>
- Fre, S., Huyghe, M., Mourikis, P., Robine, S., Louvard, D., Artavanis-Tsakonas, S., 2005. Notch signals control the fate of immature progenitor cells in the intestine. *Nature* 435, 964–968. <https://doi.org/10.1038/nature03589>
- Frömter, E., Diamond, J., 1972. Route of passive ion permeation in epithelia. *Nature New Biol.* 235, 9–13. <https://doi.org/10.1038/newbio235009a0>
- Fujita, Y., Krause, G., Scheffner, M., Zechner, D., Leddy, H.E.M., Behrens, J., Sommer, T., Birchmeier, W., 2002. Hakai, a c-Cbl-like protein, ubiquitinates and induces endocytosis of the E-cadherin complex. *Nat. Cell Biol.* 4, 222–231. <https://doi.org/10.1038/ncb758>
- Furukawa, K.T., Yamashita, K., Sakurai, N., Ohno, S., 2017. The Epithelial Circumferential Actin Belt Regulates YAP/TAZ through Nucleocytoplasmic Shuttling of Merlin. *Cell Rep* 20, 1435–1447. <https://doi.org/10.1016/j.celrep.2017.07.032>
- Furuse, M., Hirase, T., Itoh, M., Nagafuchi, A., Yonemura, S., Tsukita, S., Tsukita, S., 1993. Occludin: a novel integral membrane protein localizing at tight junctions. *The Journal of Cell Biology* 123, 1777–1788. <https://doi.org/10.1083/jcb.123.6.1777>
- Furuse, M., Izumi, Y., Oda, Y., Higashi, T., Iwamoto, N., 2014. Molecular organization of tricellular tight junctions. *Tissue Barriers* 2, e28960. <https://doi.org/10.4161/tisb.28960>
- Furuse, M., Sasaki, H., Fujimoto, K., Tsukita, S., 1998. A Single Gene Product, Claudin-1 or -2, Reconstitutes Tight Junction Strands and Recruits Occludin in Fibroblasts. *Journal of Cell Biology* 143, 391–401. <https://doi.org/10.1083/jcb.143.2.391>
- Furuse, M., Sasaki, H., Tsukita, S., 1999. Manner of Interaction of Heterogeneous Claudin Species within and between Tight Junction Strands. *J Cell Biol* 147, 891–903. <https://doi.org/10.1083/jcb.147.4.891>
- Gao, L., Joberty, G., Macara, I.G., 2002. Assembly of epithelial tight junctions is negatively regulated by Par6. *Curr. Biol.* 12, 221–225. [https://doi.org/10.1016/s0960-9822\(01\)00663-7](https://doi.org/10.1016/s0960-9822(01)00663-7)
- Garnaas, M.K., Moodie, K.L., Liu, M., Samant, G.V., Li, K., Marx, R., Baraban, J.M., Horowitz, A., Ramchandran, R., 2008. Syx, a RhoA guanine exchange factor, is essential for angiogenesis in Vivo. *Circ. Res.* 103, 710–716. <https://doi.org/10.1161/CIRCRESAHA.108.181388>
- Ghimire, K., Zaric, J., Alday-Parejo, B., Seebach, J., Bousquenaud, M., Stalin, J., Bieler, G., Schnittler, H.-J., Rüegg, C., 2019. MAGI1 Mediates eNOS Activation and NO Production in Endothelial Cells in Response to Fluid Shear Stress. *Cells* 8. <https://doi.org/10.3390/cells8050388>

- Gillett, C.E., Miles, D.W., Ryder, K., Skilton, D., Liebman, R.D., Springall, R.J., Barnes, D.M., Hanby, A.M., 2001. Retention of the expression of E-cadherin and catenins is associated with shorter survival in grade III ductal carcinoma of the breast. *J. Pathol.* 193, 433–441. <https://doi.org/10.1002/path.831>
- Glaunsinger, B.A., Lee, S.S., Thomas, M., Banks, L., Javier, R., 2000. Interactions of the PDZ-protein MAGI-1 with adenovirus E4-ORF1 and high-risk papillomavirus E6 oncoproteins. *Oncogene* 19, 5270–5280. <https://doi.org/10.1038/sj.onc.1203906>
- Glinka, A., Wu, W., Delius, H., Monaghan, A.P., Blumenstock, C., Niehrs, C., 1998. Dickkopf-1 is a member of a new family of secreted proteins and functions in head induction. *Nature* 391, 357–362. <https://doi.org/10.1038/34848>
- Goldstein, J., Borowsky, A.D., Goyal, R., Roland, J.T., Arnold, S.A., Gellert, L.L., Clark, P.E., Hameed, O., Giannico, G.A., 2016. MAGI-2 in prostate cancer: an immunohistochemical study. *Human Pathology* 52, 83–91. <https://doi.org/10.1016/j.humpath.2016.01.003>
- González-Mariscal, L., Betanzos, A., Nava, P., Jaramillo, B.E., 2003. Tight junction proteins. *Progress in Biophysics and Molecular Biology* 81, 1–44. [https://doi.org/10.1016/S0079-6107\(02\)00037-8](https://doi.org/10.1016/S0079-6107(02)00037-8)
- Gonzalez-Mariscal, L., Miranda, J., Ortega-Olvera, J.M., Gallego-Gutierrez, H., Raya-Sandino, A., Vargas-Sierra, O., 2016. Involvement of Tight Junction Plaque Proteins in Cancer. *Curr Pathobiol Rep* 4, 117–133. <https://doi.org/10.1007/s40139-016-0108-4>
- Good, M.C., Zalatan, J.G., Lim, W.A., 2011. Scaffold proteins: hubs for controlling the flow of cellular information. *Science* 332, 680–686. <https://doi.org/10.1126/science.1198701>
- Gotoh, Y., Nishida, E., 1995. Activation mechanism and function of the MAP kinase cascade. *Mol. Reprod. Dev.* 42, 486–492. <https://doi.org/10.1002/mrd.1080420417>
- Graff, J.R., Herman, J.G., Lapidus, R.G., Chopra, H., Xu, R., Jarrard, D.F., Isaacs, W.B., Pitha, P.M., Davidson, N.E., Baylin, S.B., 1995. E-cadherin expression is silenced by DNA hypermethylation in human breast and prostate carcinomas. *Cancer Res.* 55, 5195–5199.
- Graham, J., Muhsin, M., Kirkpatrick, P., 2004. Fresh from the pipeline: Oxaliplatin. *Nature Reviews drug discovery* 3, 11–12. <https://doi.org/10.1038/nrd1287>
- Gravdal, K., Halvorsen, O.J., Haukaas, S.A., Akslen, L.A., 2007. A switch from E-cadherin to N-cadherin expression indicates epithelial to mesenchymal transition and is of strong and independent importance for the progress of prostate cancer. *Clin. Cancer Res.* 13, 7003–7011. <https://doi.org/10.1158/1078-0432.CCR-07-1263>
- Greenberg, A.K., Basu, S., Hu, J., Yie, T., Tchou-Wong, K.M., Rom, W.N., Lee, T.C., 2002. Selective p38 activation in human non-small cell lung cancer. *Am. J. Respir. Cell Mol. Biol.* 26, 558–564. <https://doi.org/10.1165/ajrcmb.26.5.4689>
- Gressin, L., 2016. Désassemblage de réseaux de filaments d’actine : rôle de l’architecture et du confinement (phdthesis). Université Grenoble Alpes.
- Guillemot, L., Hammar, E., Kaister, C., Ritz, J., Caille, D., Jond, L., Bauer, C., Meda, P., Citi, S., 2004. Disruption of the cingulin gene does not prevent tight junction formation but alters gene expression. *J. Cell. Sci.* 117, 5245–5256. <https://doi.org/10.1242/jcs.01399>
- Guillemot, L., Paschoud, S., Pulimeno, P., Foglia, A., Citi, S., 2008. The cytoplasmic plaque of tight junctions: A scaffolding and signalling center. *Biochimica et Biophysica Acta (BBA) - Biomembranes, Apical Junctional Complexes Part I* 1778, 601–613. <https://doi.org/10.1016/j.bbamem.2007.09.032>
- Guo, T., Lu, Y., Li, P., Yin, M.-X., Lv, D., Zhang, W., Wang, H., Zhou, Z., Ji, H., Zhao, Y., Zhang, L., 2013. A novel partner of Scalloped regulates Hippo signaling via antagonizing Scalloped-Yorkie activity. *Cell Res.* 23, 1201–1214. <https://doi.org/10.1038/cr.2013.120>
- Guo, Y.-J., Pan, W.-W., Liu, S.-B., Shen, Z.-F., Xu, Y., Hu, L.-L., 2020. ERK/MAPK signalling pathway and tumorigenesis. *Exp Ther Med* 19, 1997–2007. <https://doi.org/10.3892/etm.2020.8454>
- Hagen, S.J., 2017. Non-canonical functions of claudin proteins: Beyond the regulation of cell-cell adhesions. *Tissue Barriers* 5. <https://doi.org/10.1080/21688370.2017.1327839>

- Halaoui, R., McCaffrey, L., 2015. Rewiring cell polarity signaling in cancer. *Oncogene* 34, 939–950. <https://doi.org/10.1038/onc.2014.59>
- Hamaratoglu, F., Willecke, M., Kango-Singh, M., Nolo, R., Hyun, E., Tao, C., Jafar-Nejad, H., Halder, G., 2006. The tumour-suppressor genes NF2/Merlin and Expanded act through Hippo signalling to regulate cell proliferation and apoptosis. *Nat. Cell Biol.* 8, 27–36. <https://doi.org/10.1038/ncb1339>
- Hamazaki, Y., Itoh, M., Sasaki, H., Furuse, M., Tsukita, S., 2002. Multi-PDZ Domain Protein 1 (MUPP1) Is Concentrated at Tight Junctions through Its Possible Interaction with Claudin-1 and Junctional Adhesion Molecule. *J. Biol. Chem.* 277, 455–461. <https://doi.org/10.1074/jbc.M109005200>
- Hammad, M.M., Dunn, H.A., Ferguson, S.S.G., 2016. MAGI Proteins Regulate the Trafficking and Signaling of Corticotropin-Releasing Factor Receptor 1 via a Compensatory Mechanism. *J Mol Signal* 11. <https://doi.org/10.5334/1750-2187-11-5>
- Han, J., Lee, J.D., Bibbs, L., Ulevitch, R.J., 1994. A MAP kinase targeted by endotoxin and hyperosmolarity in mammalian cells. *Science* 265, 808–811. <https://doi.org/10.1126/science.7914033>
- Hanahan, D., Weinberg, R.A., 2000. The hallmarks of cancer. *Cell* 100, 57–70. [https://doi.org/10.1016/s0092-8674\(00\)81683-9](https://doi.org/10.1016/s0092-8674(00)81683-9)
- Harbeck, N., Penault-Llorca, F., Cortes, J., Gnant, M., Houssami, N., Poortmans, P., Ruddy, K., Tsang, J., Cardoso, F., 2019. Breast cancer. *Nature Reviews Disease Primers* 5, 1–31. <https://doi.org/10.1038/s41572-019-0111-2>
- Harigopal, M., Berger, A.J., Camp, R.L., Rimm, D.L., Kluger, H.M., 2005. Automated Quantitative Analysis of E-Cadherin Expression in Lymph Node Metastases Is Predictive of Survival in Invasive Ductal Breast Cancer. *Clin Cancer Res* 11, 4083–4089. <https://doi.org/10.1158/1078-0432.CCR-04-2191>
- Hartsock, A., Nelson, W.J., 2008. Adherens and tight junctions: Structure, function and connections to the actin cytoskeleton. *Biochimica et Biophysica Acta (BBA) - Biomembranes, Apical Junctional Complexes Part I* 1778, 660–669. <https://doi.org/10.1016/j.bbamem.2007.07.012>
- Hildebrand, S., Hultin, S., Subramani, A., Petropoulos, S., Zhang, Y., Cao, X., Mpindi, J., Kalloniemi, O., Johansson, S., Majumdar, A., Lanner, F., Holmgren, L., 2017. The E-cadherin/AmotL2 complex organizes actin filaments required for epithelial hexagonal packing and blastocyst hatching. *Scientific Reports* 7, 1–17. <https://doi.org/10.1038/s41598-017-10102-w>
- Hirose, T., Izumi, Y., Nagashima, Y., Tamai-Nagai, Y., Kurihara, H., Sakai, T., Suzuki, Y., Yamanaka, T., Suzuki, A., Mizuno, K., Ohno, S., 2002. Involvement of ASIP/PAR-3 in the promotion of epithelial tight junction formation. *Journal of Cell Science* 115, 2485–2495.
- Hoang, B.H., Thomas, J.T., Abdul-Karim, F.W., Correia, K.M., Conlon, R.A., Luyten, F.P., Ballock, R.T., 1998. Expression pattern of two Frizzled-related genes, Frzb-1 and Sfrp-1, during mouse embryogenesis suggests a role for modulating action of Wnt family members. *Dev. Dyn.* 212, 364–372. [https://doi.org/10.1002/\(SICI\)1097-0177\(199807\)212:3<364::AID-AJA4>3.0.CO;2-F](https://doi.org/10.1002/(SICI)1097-0177(199807)212:3<364::AID-AJA4>3.0.CO;2-F)
- Hoffman, M., MD, n.d. The Colon (Human Anatomy): Picture, Function, Definition, Problems [WWW Document]. WebMD. URL <https://www.webmd.com/digestive-disorders/picture-of-the-colon>
- Hoon, J.L., Tan, M.H., Koh, C.-G., 2016. The Regulation of Cellular Responses to Mechanical Cues by Rho GTPases. *Cells* 5. <https://doi.org/10.3390/cells5020017>
- Hsieh, J.-C., Kodjabachian, L., Rebbert, M.L., Rattner, A., Smallwood, P.M., Samos, C.H., Nusse, R., Dawid, I.B., Nathans, J., 1999. A new secreted protein that binds to Wnt proteins and inhibits their activities. *Nature* 398, 431–436. <https://doi.org/10.1038/18899>
- Hu, Y., Li, Z., Guo, L., Wang, L., Zhang, L., Cai, X., Zhao, H., Zha, X., 2007. MAGI-2 Inhibits cell migration and proliferation via PTEN in human hepatocarcinoma cells. *Archives of Biochemistry and Biophysics* 467, 1–9. <https://doi.org/10.1016/j.abb.2007.07.027>

- Huang, R.Y.-J., Guilford, P., Thiery, J.P., 2012. Early events in cell adhesion and polarity during epithelial-mesenchymal transition. *J Cell Sci* 125, 4417–4422. <https://doi.org/10.1242/jcs.099697>
- Huelsken, J., Vogel, R., Brinkmann, V., Erdmann, B., Birchmeier, C., Birchmeier, W., 2000. Requirement for beta-catenin in anterior-posterior axis formation in mice. *J. Cell Biol.* 148, 567–578. <https://doi.org/10.1083/jcb.148.3.567>
- Hurov, J., Piwnica-Worms, H., 2007. The Par-1/MARK Family of Protein Kinases: From Polarity to Metabolism. *Cell Cycle* 6, 1966–1969. <https://doi.org/10.4161/cc.6.16.4576>
- Ibar, C., Kirichenko, E., Keepers, B., Enners, E., Fleisch, K., Irvine, K.D., 2018. Tension-dependent regulation of mammalian Hippo signaling through LIMD1. *J Cell Sci* 131. <https://doi.org/10.1242/jcs.214700>
- Ide, N., Hata, Y., Nishioka, H., Hirao, K., Yao, I., Deguchi, M., Mizoguchi, A., Nishimori, H., Tokino, T., Nakamura, Y., Takai, Y., 1999. Localization of membrane-associated guanylate kinase (MAGI)-1/BAI-associated protein (BAP) 1 at tight junctions of epithelial cells. *Oncogene* 18, 7810–7815. <https://doi.org/10.1038/sj.onc.1203153>
- Igea, A., Nebreda, A.R., 2015. The Stress Kinase p38 α as a Target for Cancer Therapy. *Cancer Res.* 75, 3997–4002. <https://doi.org/10.1158/0008-5472.CAN-15-0173>
- Ikenouchi, J., Furuse, M., Furuse, K., Sasaki, H., Tsukita, Sachiko, Tsukita, Shoichiro, 2005. Tricellulin constitutes a novel barrier at tricellular contacts of epithelial cells. *J. Cell Biol.* 171, 939–945. <https://doi.org/10.1083/jcb.200510043>
- Ikenouchi, J., Matsuda, M., Furuse, M., Tsukita, S., 2003. Regulation of tight junctions during the epithelium-mesenchyme transition: direct repression of the gene expression of claudins/occludin by Snail. *J. Cell. Sci.* 116, 1959–1967. <https://doi.org/10.1242/jcs.00389>
- Ikenouchi, J., Sasaki, H., Tsukita, Sachiko, Furuse, M., Tsukita, Shoichiro, 2008. Loss of Occludin Affects Tricellular Localization of Tricellulin. *MBoC* 19, 4687–4693. <https://doi.org/10.1091/mbc.e08-05-0530>
- Illina, O., Bakker, G.-J., Vasaturo, A., Hofmann, R.M., Friedl, P., 2011. Two-photon laser-generated microtracks in 3D collagen lattices: principles of MMP-dependent and -independent collective cancer cell invasion. *Phys Biol* 8, 015010. <https://doi.org/10.1088/1478-3975/8/1/015010>
- Itoh, M., Furuse, M., Morita, K., Kubota, K., Saitou, M., Tsukita, S., 1999. Direct Binding of Three Tight Junction-Associated Maguks, Zo-1, Zo-2, and Zo-3, with the CooH Termini of Claudins. *J Cell Biol* 147, 1351–1363. <https://doi.org/10.1083/jcb.147.6.1351>
- Itoh, M., Sasaki, H., Furuse, M., Ozaki, H., Kita, T., Tsukita, S., 2001. Junctional adhesion molecule (JAM) binds to PAR-3. *J Cell Biol* 154, 491–498. <https://doi.org/10.1083/jcb.200103047>
- Izumi, Y., Hirose, T., Tamai, Y., Hirai, S., Nagashima, Y., Fujimoto, T., Tabuse, Y., Kempthues, K.J., Ohno, S., 1998. An Atypical PKC Directly Associates and Colocalizes at the Epithelial Tight Junction with ASIP, a Mammalian Homologue of *Caenorhabditis elegans* Polarity Protein PAR-3. *J Cell Biol* 143, 95–106. <https://doi.org/10.1083/jcb.143.1.95>
- Jaggi, M., Johansson, S.L., Baker, J.J., Smith, L.M., Galich, A., Balaji, K.C., 2005. Aberrant expression of E-cadherin and beta-catenin in human prostate cancer. *Urol. Oncol.* 23, 402–406. <https://doi.org/10.1016/j.urolonc.2005.03.024>
- Jia, S., Lu, J., Qu, T., Feng, Y., Wang, X., Liu, C., Ji, J., 2017. MAGI1 inhibits migration and invasion via blocking MAPK/ERK signaling pathway in gastric cancer. *Chin. J. Cancer Res.* 29, 25–35. <https://doi.org/10.21147/j.issn.1000-9604.2017.01.04>
- Joaquin, M., de Nadal, E., Posas, F., 2017. An RB insensitive to CDK regulation. *Mol Cell Oncol* 4, e1268242. <https://doi.org/10.1080/23723556.2016.1268242>
- Joberty, G., Petersen, C., Gao, L., Macara, I.G., 2000. The cell-polarity protein Par6 links Par3 and atypical protein kinase C to Cdc42. *Nature Cell Biology* 2, 531–539. <https://doi.org/10.1038/35019573>

- Jones, J.C.R., Kam, C.Y., Harmon, R.M., Woychek, A.V., Hopkinson, S.B., Green, K.J., 2017. Intermediate Filaments and the Plasma Membrane. *Cold Spring Harb Perspect Biol* 9, a025866. <https://doi.org/10.1101/cshperspect.a025866>
- Jou, T.S., Schneeberger, E.E., Nelson, W.J., 1998. Structural and functional regulation of tight junctions by RhoA and Rac1 small GTPases. *J. Cell Biol.* 142, 101–115. <https://doi.org/10.1083/jcb.142.1.101>
- Julià, A., Pinto, J.A., Gratacós, J., Queiró, R., Ferrándiz, C., Fonseca, E., Montilla, C., Torre-Alonso, J.C., Puig, L., Pérez Venegas, J.J., Fernández Nebro, A., Fernández, E., Muñoz-Fernández, S., Daudén, E., González, C., Roig, D., Sánchez Carazo, J.L., Zarco, P., Erra, A., López Esteban, J.L., Rodríguez, J., Ramírez, D.M., de la Cueva, P., Vanaclocha, F., Herrera, E., Castañeda, S., Rubio, E., Salvador, G., Díaz-Torné, C., Blanco, R., Willis Domínguez, A., Mosquera, J.A., Vela, P., Tornero, J., Sánchez-Fernández, S., Corominas, H., Ramírez, J., López-Lasanta, M., Tortosa, R., Palau, N., Alonso, A., García-Montero, A.C., Gelpí, J.L., Codó, L., Day, K., Absher, D., Myers, R.M., Cañete, J.D., Marsal, S., 2015. A deletion at ADAMTS9-MAGI1 locus is associated with psoriatic arthritis risk. *Ann. Rheum. Dis.* 74, 1875–1881. <https://doi.org/10.1136/annrheumdis-2014-207190>
- Kawauchi, T., 2012. Cell adhesion and its endocytic regulation in cell migration during neural development and cancer metastasis. *Int J Mol Sci* 13, 4564–4590. <https://doi.org/10.3390/ijms13044564>
- Kemler, R., 1993. From cadherins to catenins: cytoplasmic protein interactions and regulation of cell adhesion. *Trends in Genetics* 9, 317–321. [https://doi.org/10.1016/0168-9525\(93\)90250-L](https://doi.org/10.1016/0168-9525(93)90250-L)
- Kemphues, K.J., Priess, J.R., Morton, D.G., Cheng, N., 1988. Identification of genes required for cytoplasmic localization in early *C. elegans* embryos. *Cell* 52, 311–320. [https://doi.org/10.1016/S0092-8674\(88\)80024-2](https://doi.org/10.1016/S0092-8674(88)80024-2)
- Khramtsov, A.I., Khramtsova, G.F., Tretiakova, M., Huo, D., Olopade, O.I., Goss, K.H., 2010. Wnt/beta-catenin pathway activation is enriched in basal-like breast cancers and predicts poor outcome. *Am. J. Pathol.* 176, 2911–2920. <https://doi.org/10.2353/ajpath.2010.091125>
- Kim, N.-G., Koh, E., Chen, X., Gumbiner, B.M., 2011. E-cadherin mediates contact inhibition of proliferation through Hippo signaling-pathway components. *Proceedings of the National Academy of Sciences* 108, 11930–11935. <https://doi.org/10.1073/pnas.1103345108>
- Kinugasa, T., Akagi, Y., Ochi, T., Tanaka, N., Kawahara, A., Ishibashi, Y., Gotanda, Y., Yamaguchi, K., Shiratuchi, I., Oka, Y., Kage, M., Shirouzu, K., 2012. Increased claudin-1 protein expression in hepatic metastatic lesions of colorectal cancer. *Anticancer Res.* 32, 2309–2314.
- Kiyono, T., Hiraiwa, A., Fujita, M., Hayashi, Y., Akiyama, T., Ishibashi, M., 1997. Binding of high-risk human papillomavirus E6 oncoproteins to the human homologue of the *Drosophila* discs large tumor suppressor protein. *Proc. Natl. Acad. Sci. U.S.A.* 94, 11612–11616. <https://doi.org/10.1073/pnas.94.21.11612>
- Klebes, A., Knust, E., 2000. A conserved motif in Crumbs is required for E-cadherin localisation and zonula adherens formation in *Drosophila*. *Current Biology* 10, 76–85. [https://doi.org/10.1016/S0960-9822\(99\)00277-8](https://doi.org/10.1016/S0960-9822(99)00277-8)
- Klezovitch, O., Fernandez, T.E., Tapscott, S.J., Vasioukhin, V., 2004. Loss of cell polarity causes severe brain dysplasia in Lgl1 knockout mice. *Genes Dev.* 18, 559–571. <https://doi.org/10.1101/gad.1178004>
- Knights, A.J., Funnell, A.P.W., Crossley, M., Pearson, R.C.M., 2012. Holding Tight: Cell Junctions and Cancer Spread. *Trends Cancer Res* 8, 61–69.
- Knust, E., Bossinger, O., 2002. Composition and Formation of Intercellular Junctions in Epithelial Cells. *Science* 298, 1955–1959. <https://doi.org/10.1126/science.1072161>
- Kobayashi, J., Inai, T., Shibata, Y., 2002. Formation of tight junction strands by expression of claudin-1 mutants in their ZO-1 binding site in MDCK cells. *Histochem. Cell Biol.* 117, 29–39. <https://doi.org/10.1007/s00418-001-0359-x>
- Kobielak, A., Fuchs, E., 2004. α -CATENIN: AT THE JUNCTION OF INTERCELLULAR ADHESION AND ACTIN DYNAMICS. *Nat Rev Mol Cell Biol* 5, 614–625.

- Komiya, Y., Habas, R., 2008. Wnt signal transduction pathways. *Organogenesis* 4, 68–75.
- Kotelevets, L., van Hengel, J., Bruyneel, E., Mareel, M., van Roy, F., Chastre, E., 2005. Implication of the MAGI-1b/PTEN signalosome in stabilization of adherens junctions and suppression of invasiveness. *FASEB J.* 19, 115–117. <https://doi.org/10.1096/fj.04-1942fje>
- Kouchi, Z., Barthet, G., Serban, G., Georgakopoulos, A., Shioi, J., Robakis, N.K., 2009. p120 Catenin Recruits Cadherins to γ -Secretase and Inhibits Production of A β Peptide. *J. Biol. Chem.* 284, 1954–1961. <https://doi.org/10.1074/jbc.M806250200>
- Kourtidis, A., Ngok, S.P., Anastasiadis, P.Z., 2013. Chapter Eighteen - p120 Catenin: An Essential Regulator of Cadherin Stability, Adhesion-Induced Signaling, and Cancer Progression, in: van Roy, F. (Ed.), *Progress in Molecular Biology and Translational Science, The Molecular Biology of Cadherins*. Academic Press, pp. 409–432. <https://doi.org/10.1016/B978-0-12-394311-8.00018-2>
- Kranjec, C., Banks, L., 2011. A systematic analysis of human papillomavirus (HPV) E6 PDZ substrates identifies MAGI-1 as a major target of HPV type 16 (HPV-16) and HPV-18 whose loss accompanies disruption of tight junctions. *J. Virol.* 85, 1757–1764. <https://doi.org/10.1128/JVI.01756-10>
- Krisanaprakornkit, S., Iamaroon, A., 2012. Epithelial-mesenchymal transition in oral squamous cell carcinoma. *ISRN Oncol* 2012, 681469. <https://doi.org/10.5402/2012/681469>
- Kuang, S.-Q., Tong, W.-G., Yang, H., Lin, W., Lee, M.K., Fang, Z.H., Wei, Y., Jelinek, J., Issa, J.-P., Garcia-Manero, G., 2008. Genome-wide identification of aberrantly methylated promoter associated CpG islands in acute lymphocytic leukemia. *Leukemia* 22, 1529–1538. <https://doi.org/10.1038/leu.2008.130>
- Kuipers, E.J., Grady, W.M., Lieberman, D., Seufferlein, T., Sung, J.J., Boelens, P.G., van de Velde, C.J.H., Watanabe, T., 2015. Colorectal cancer. *Nature Reviews Disease Primers* 1, 1–25. <https://doi.org/10.1038/nrdp.2015.65>
- Kurrey, N.K., K, A., Bapat, S.A., 2005. Snail and Slug are major determinants of ovarian cancer invasiveness at the transcription level. *Gynecol. Oncol.* 97, 155–165. <https://doi.org/10.1016/j.ygyno.2004.12.043>
- Lanigan, F., McKiernan, E., Brennan, D.J., Hegarty, S., Millikan, R.C., McBryan, J., Jirstrom, K., Landberg, G., Martin, F., Duffy, M.J., Gallagher, W.M., 2009. Increased claudin-4 expression is associated with poor prognosis and high tumour grade in breast cancer. *Int. J. Cancer* 124, 2088–2097. <https://doi.org/10.1002/ijc.24159>
- Lapierre, L.A., Tuma, P.L., Navarre, J., Goldenring, J.R., Anderson, J.M., 1999. VAP-33 localizes to both an intracellular vesicle population and with occludin at the tight junction. *J. Cell. Sci.* 112 (Pt 21), 3723–3732.
- Laprise, P., Tepass, U., 2011. Novel insights into epithelial polarity proteins in *Drosophila*. *Trends in Cell Biology* 21, 401–408. <https://doi.org/10.1016/j.tcb.2011.03.005>
- Larue, L., Ohsugi, M., Hirchenhain, J., Kemler, R., 1994. E-cadherin null mutant embryos fail to form a trophectoderm epithelium. *PNAS* 91, 8263–8267. <https://doi.org/10.1073/pnas.91.17.8263>
- Laura, R.P., Ross, S., Koeppen, H., Lasky, L.A., 2002. MAGI-1: A Widely Expressed, Alternatively Spliced Tight Junction Protein. *Experimental Cell Research* 275, 155–170. <https://doi.org/10.1006/excr.2002.5475>
- Lechner, J., Krall, M., Netzer, A., Radmayr, C., Ryan, M.P., Pfaller, W., 1999. Effects of interferon alpha-2b on barrier function and junctional complexes of renal proximal tubular LLC-PK1 cells. *Kidney Int.* 55, 2178–2191. <https://doi.org/10.1046/j.1523-1755.1999.00487.x>
- Lee, J.C., Laydon, J.T., McDonnell, P.C., Gallagher, T.F., Kumar, S., Green, D., McNulty, D., Blumenthal, M.J., Heys, J.R., Landvatter, S.W., Strickler, J.E., McLaughlin, M.M., Siemens, I.R., Fisher, S.M., Livi, G.P., White, J.R., Adams, J.L., Young, P.R., 1994. A protein kinase involved in the regulation of inflammatory cytokine biosynthesis. *Nature* 372, 739–746. <https://doi.org/10.1038/372739a0>

- Lee, M., Vasioukhin, V., 2008. Cell polarity and cancer – cell and tissue polarity as a non-canonical tumor suppressor. *Journal of Cell Science* 121, 1141–1150. <https://doi.org/10.1242/jcs.016634>
- Lee, S.S., Weiss, R.S., Javier, R.T., 1997. Binding of human virus oncoproteins to hDlg/SAP97, a mammalian homolog of the *Drosophila* discs large tumor suppressor protein. *Proc. Natl. Acad. Sci. U.S.A.* 94, 6670–6675. <https://doi.org/10.1073/pnas.94.13.6670>
- Legouis, R., Jaulin-Bastard, F., Schott, S., Navarro, C., Borg, J.-P., Labouesse, M., 2003. Basolateral targeting by leucine-rich repeat domains in epithelial cells. *EMBO reports* 4, 1096–1100. <https://doi.org/10.1038/sj.embor.7400006>
- Lemmers, C., Michel, D., Lane-Guermonprez, L., Delgrossi, M.-H., Médina, E., Arsanto, J.-P., Le Bivic, A., 2004. CRB3 Binds Directly to Par6 and Regulates the Morphogenesis of the Tight Junctions in Mammalian Epithelial Cells. *MBoC* 15, 1324–1333. <https://doi.org/10.1091/mbc.e03-04-0235>
- Li, D., Mrsny, R.J., 2000. Oncogenic Raf-1 disrupts epithelial tight junctions via downregulation of occludin. *J. Cell Biol.* 148, 791–800. <https://doi.org/10.1083/jcb.148.4.791>
- Li, Y., Zhou, H., Li, F., Chan, S.W., Lin, Z., Wei, Z., Yang, Z., Guo, F., Lim, C.J., Xing, W., Shen, Y., Hong, W., Long, J., Zhang, M., 2015. Angiotensin binding-induced activation of Merlin/NF2 in the Hippo pathway. *Cell Res.* 25, 801–817. <https://doi.org/10.1038/cr.2015.69>
- Li, Z.-Y., Li, X.-H., Tian, G.-W., Zhang, D.-Y., Gao, H., Wang, Z.-Y., 2019. <p>MAGI1 Inhibits the Proliferation, Migration and Invasion of Glioma Cells</p> [WWW Document]. *OncoTargets and Therapy*. <https://doi.org/10.2147/OTT.S230236>
- Lin, D., Edwards, A.S., Fawcett, J.P., Mbamalu, G., Scott, J.D., Pawson, T., 2000. A mammalian PAR-3–PAR-6 complex implicated in Cdc42/Rac1 and aPKC signalling and cell polarity. *Nature Cell Biology* 2, 540–547. <https://doi.org/10.1038/35019582>
- Lin, S.Y., Xia, W., Wang, J.C., Kwong, K.Y., Spohn, B., Wen, Y., Pestell, R.G., Hung, M.C., 2000. Beta-catenin, a novel prognostic marker for breast cancer: its roles in cyclin D1 expression and cancer progression. *Proc. Natl. Acad. Sci. U.S.A.* 97, 4262–4266. <https://doi.org/10.1073/pnas.060025397>
- Liu, X., Li, H., Rajurkar, M., Li, Q., Cotton, J.L., Ou, J., Zhu, L.J., Goel, H.L., Mercurio, A.M., Park, J.-S., Davis, R.J., Mao, J., 2016. Tead and AP1 Coordinate Transcription and Motility. *Cell Reports* 14, 1169–1180. <https://doi.org/10.1016/j.celrep.2015.12.104>
- Lu, Y., Sun, W., Zhang, L., Li, J., 2019. Silencing Of MAGI1 Promotes The Proliferation And Inhibits Apoptosis Of Glioma Cells Via The Wnt/β-Catenin And PTEN/AKT Signaling Pathways. *Onco Targets Ther* 12, 9639–9650. <https://doi.org/10.2147/OTT.S215400>
- Luissint, A.-C., Nusrat, A., Parkos, C.A., 2014. JAM-related proteins in mucosal homeostasis and inflammation. *Semin Immunopathol* 36, 211–226. <https://doi.org/10.1007/s00281-014-0421-0>
- Lv, Meng, Lv, Meng, Lv, Meiling, Lv, Meiling, Chen, L., Chen, L., Qin, T., Qin, T., Zhang, X., Zhang, X., Liu, P., Liu, P., Yang, J., Yang, J., 2015. Angiotensin promotes breast cancer cell proliferation and invasion. *Oncology Reports* 33, 1938–1946. <https://doi.org/10.3892/or.2015.3780>
- Lynch, A.M., Grana, T., Cox-Paulson, E., Couthier, A., Cameron, M., Chin-Sang, I., Pettitt, J., Hardin, J., 2012. A Genome-wide Functional Screen Shows MAGI-1 Is an L1CAM-Dependent Stabilizer of Apical Junctions in *C. elegans*. *Current Biology* 22, 1891–1899. <https://doi.org/10.1016/j.cub.2012.08.024>
- Makarova, O., Roh, M.H., Liu, C.-J., Laurinec, S., Margolis, B., 2003. Mammalian Crumbs3 is a small transmembrane protein linked to protein associated with Lin-7 (Pals1). *Gene* 302, 21–29. <https://doi.org/10.1016/S0378111902010843>
- Markov, A.G., Aschenbach, J.R., Amasheh, S., 2015. Claudin clusters as determinants of epithelial barrier function. *IUBMB Life* 67, 29–35. <https://doi.org/10.1002/iub.1347>
- Martin, T.A., Mansel, R.E., Jiang, W.G., 2010. Loss of occludin leads to the progression of human breast cancer. *Int. J. Mol. Med.* 26, 723–734. https://doi.org/10.3892/ijmm_00000519

- Martínez-Estrada, O.M., Cullerés, A., Soriano, F.X., Peinado, H., Bolós, V., Martínez, F.O., Reina, M., Cano, A., Fabre, M., Vilaró, S., 2006. The transcription factors Slug and Snail act as repressors of Claudin-1 expression in epithelial cells. *Biochem. J.* 394, 449–457. <https://doi.org/10.1042/BJ20050591>
- Martínez-Limón, A., Joaquin, M., Caballero, M., Posas, F., de Nadal, E., 2020. The p38 Pathway: From Biology to Cancer Therapy. *International Journal of Molecular Sciences* 21, 1913. <https://doi.org/10.3390/ijms21061913>
- Martinez-Palomo, A., Erij, D., 1975. Structure of tight junctions in epithelia with different permeability. *Proceedings of the National Academy of Sciences* 72, 4487–4491. <https://doi.org/10.1073/pnas.72.11.4487>
- Martín-Padura, I., Lostaglio, S., Schneemann, M., Williams, L., Romano, M., Fruscella, P., Panzeri, C., Stoppacciaro, A., Ruco, L., Villa, A., Simmons, D., Dejana, E., 1998. Junctional Adhesion Molecule, a Novel Member of the Immunoglobulin Superfamily That Distributes at Intercellular Junctions and Modulates Monocyte Transmigration. *Journal of Cell Biology* 142, 117–127. <https://doi.org/10.1083/jcb.142.1.117>
- Masuda, S., Oda, Y., Sasaki, H., Ikenouchi, J., Higashi, T., Akashi, M., Nishi, E., Furuse, M., 2011. LSR defines cell corners for tricellular tight junction formation in epithelial cells. *J. Cell. Sci.* 124, 548–555. <https://doi.org/10.1242/jcs.072058>
- McCarthy, K.M., Francis, S.A., McCormack, J.M., Lai, J., Rogers, R.A., Skare, I.B., Lynch, R.D., Schneeberger, E.E., 2000. Inducible expression of claudin-1-myc but not occludin-VSV-G results in aberrant tight junction strand formation in MDCK cells. *J. Cell. Sci.* 113 Pt 19, 3387–3398.
- Medema, J.P., Vermeulen, L., 2011. Microenvironmental regulation of stem cells in intestinal homeostasis and cancer. *Nature* 474, 318–326. <https://doi.org/10.1038/nature10212>
- Medina, R., Rahner, C., Mitic, L.L., Anderson, J.M., Van Itallie, C.M., 2000. Occludin localization at the tight junction requires the second extracellular loop. *J. Membr. Biol.* 178, 235–247. <https://doi.org/10.1007/s002320010031>
- Meloche, S., Pouyssegur, J., 2007. The ERK1/2 mitogen-activated protein kinase pathway as a master regulator of the G1- to S-phase transition. *Oncogene* 26, 3227–3239. <https://doi.org/10.1038/sj.onc.1210414>
- Mendonça, A., Na, T.-Y., Gumbiner, B.M., 2018. E-cadherin in Contact Inhibition and Cancer. *Oncogene* 37, 4769–4780. <https://doi.org/10.1038/s41388-018-0304-2>
- Meng, Z., Moroishi, T., Guan, K.-L., 2016. Mechanisms of Hippo pathway regulation. *Genes Dev.* 30, 1–17. <https://doi.org/10.1101/gad.274027.115>
- Meng, Z., Moroishi, T., Mottier-Pavie, V., Plouffe, S.W., Hansen, C.G., Hong, A.W., Park, H.W., Mo, J.-S., Lu, W., Lu, S., Flores, F., Yu, F.-X., Halder, G., Guan, K.-L., 2015. MAP4K family kinases act in parallel to MST1/2 to activate LATS1/2 in the Hippo pathway. *Nat Commun* 6. <https://doi.org/10.1038/ncomms9357>
- Meng, Z., Qiu, Y., Lin, K.C., Kumar, A., Placone, J.K., Fang, C., Wang, K.-C., Lu, S., Pan, M., Hong, A.W., Moroishi, T., Luo, M., Plouffe, S.W., Diao, Y., Ye, Z., Park, H.W., Wang, X., Yu, F.-X., Chien, S., Wang, C.-Y., Ren, B., Engler, A.J., Guan, K.-L., 2018. RAP2 Mediates Mechano-responses of Hippo Pathway. *Nature* 560, 655–660. <https://doi.org/10.1038/s41586-018-0444-0>
- Mizuhara, E., Nakatani, T., Minaki, Y., Sakamoto, Y., Ono, Y., Takai, Y., 2005. MAGI1 recruits Dll1 to cadherin-based adherens junctions and stabilizes it on the cell surface. *J. Biol. Chem.* 280, 26499–26507. <https://doi.org/10.1074/jbc.M500375200>
- Møllgård, K., Malinowska, D.H., Saunders, N.R., 1976. Lack of correlation between tight junction morphology and permeability properties in developing choroid plexus. *Nature* 264, 293–294. <https://doi.org/10.1038/264293a0>
- Morris, M.A., Young, L.S., Dawson, C.W., 2008. DNA tumour viruses promote tumour cell invasion and metastasis by deregulating the normal processes of cell adhesion and motility.

- European Journal of Cell Biology, FEBS Workshop: Invadopodia, Podosomes and Focal Adhesions in Tissue Invasion 87, 677–697. <https://doi.org/10.1016/j.ejcb.2008.03.005>
- Morrison, D.K., 2012. MAP Kinase Pathways. *Cold Spring Harb Perspect Biol* 4. <https://doi.org/10.1101/cshperspect.a011254>
- Mu–sch, A., Cohen, D., Yeaman, C., Nelson, W.J., Rodriguez-Boulan, E., Brennwald, P.J., 2002. Mammalian Homolog of *Drosophila* Tumor Suppressor Lethal (2) Giant Larvae Interacts with Basolateral Exocytic Machinery in Madin-Darby Canine Kidney Cells. *MBoC* 13, 158–168. <https://doi.org/10.1091/mbc.01-10-0496>
- Mudgett, J.S., Ding, J., Guh-Siesel, L., Chartrain, N.A., Yang, L., Gopal, S., Shen, M.M., 2000. Essential role for p38alpha mitogen-activated protein kinase in placental angiogenesis. *Proc. Natl. Acad. Sci. U.S.A.* 97, 10454–10459. <https://doi.org/10.1073/pnas.180316397>
- Müller, D., Kausalya, P.J., Claverie-Martin, F., Meij, I.C., Eggert, P., Garcia-Nieto, V., Hunziker, W., 2003. A Novel Claudin 16 Mutation Associated with Childhood Hypercalciuria Abolishes Binding to ZO-1 and Results in Lysosomal Mistargeting. *The American Journal of Human Genetics* 73, 1293–1301. <https://doi.org/10.1086/380418>
- Müller, H.A., Wieschaus, E., 1996. armadillo, bazooka, and stardust are critical for early stages in formation of the zonula adherens and maintenance of the polarized blastoderm epithelium in *Drosophila*. *J Cell Biol* 134, 149–163. <https://doi.org/10.1083/jcb.134.1.149>
- Nagai-Tamai, Y., Mizuno, K., Hirose, T., Suzuki, A., Ohno, S., 2002. Regulated protein–protein interaction between aPKC and PAR-3 plays an essential role in the polarization of epithelial cells. *Genes to Cells* 7, 1161–1171. <https://doi.org/10.1046/j.1365-2443.2002.00590.x>
- Nagasaka, K., Nakagawa, S., Yano, T., Takizawa, S., Matsumoto, Y., Tsuruga, T., Nakagawa, K., Minaguchi, T., Oda, K., Hiraike-Wada, O., Ooishi, H., Yasugi, T., Taketani, Y., 2006. Human homolog of *Drosophila* tumor suppressor Scribble negatively regulates cell-cycle progression from G1 to S phase by localizing at the basolateral membrane in epithelial cells. *Cancer Science* 97, 1217–1225. <https://doi.org/10.1111/j.1349-7006.2006.00315.x>
- Nava, P., López, S., Arias, C.F., Islas, S., González-Mariscal, L., 2004. The rotavirus surface protein VP8 modulates the gate and fence function of tight junctions in epithelial cells. *J. Cell. Sci.* 117, 5509–5519. <https://doi.org/10.1242/jcs.01425>
- Navarro, C., Nola, S., Audebert, S., Santoni, M.-J., Arsanto, J.-P., Ginestier, C., Marchetto, S., Jacquemier, J., Isnardon, D., Le Bivic, A., Birnbaum, D., Borg, J.-P., 2005. Junctional recruitment of mammalian Scribble relies on E-cadherin engagement. *Oncogene* 24, 4330–4339. <https://doi.org/10.1038/sj.onc.1208632>
- Nelson, W.J., Nusse, R., 2004. Convergence of Wnt, β -Catenin, and Cadherin Pathways. *Science* 303, 1483–1487. <https://doi.org/10.1126/science.1094291>
- Ni, J., Bao, S., Johnson, R.I., Zhu, B., Li, J., Vadaparampil, J., Smith, C.M., Campbell, K.N., Grahammer, F., Huber, T.B., He, J.C., D’Agati, V.D., Chan, A., Kaufman, L., 2016. MAGI-1 Interacts with Nephrin to Maintain Slit Diaphragm Structure through Enhanced Rap1 Activation in Podocytes. *J. Biol. Chem.* 291, 24406–24417. <https://doi.org/10.1074/jbc.M116.745026>
- Nicke, B., Bastien, J., Khanna, S.J., Warne, P.H., Cowling, V., Cook, S.J., Peters, G., Delpuech, O., Schulze, A., Berns, K., Mullenders, J., Beijersbergen, R.L., Bernards, R., Ganesan, T.S., Downward, J., Hancock, D.C., 2005. Involvement of MINK, a Ste20 family kinase, in Ras oncogene-induced growth arrest in human ovarian surface epithelial cells. *Mol. Cell* 20, 673–685. <https://doi.org/10.1016/j.molcel.2005.10.038>
- Nunbhakdi-Craig, V., Machleidt, T., Ogris, E., Bellotto, D., White, C.L., Sontag, E., 2002. Protein phosphatase 2A associates with and regulates atypical PKC and the epithelial tight junction complex. *J. Cell Biol.* 158, 967–978. <https://doi.org/10.1083/jcb.200206114>
- Ohnishi, H., Nakahara, T., Furuse, K., Sasaki, H., Tsukita, S., Furuse, M., 2004. JACOP, a novel plaque protein localizing at the apical junctional complex with sequence similarity to cingulin. *J. Biol. Chem.* 279, 46014–46022. <https://doi.org/10.1074/jbc.M402616200>
- OpenStax, 2013a. 4.2 Epithelial Tissue, in: *Anatomy and Physiology*. OpenStax.

- OpenStax, 2013b. 23.5 The Small and Large Intestines, in: Anatomy and Physiology. OpenStax.
- Orbán, E., Szabó, E., Lotz, G., Kupcsulik, P., Páska, C., Schaff, Z., Kiss, A., 2008. Different expression of occludin and ZO-1 in primary and metastatic liver tumors. *Pathol. Oncol. Res.* 14, 299–306. <https://doi.org/10.1007/s12253-008-9031-2>
- Padmanaban, V., Krol, I., Suhail, Y., Szczerba, B.M., Aceto, N., Bader, J.S., Ewald, A.J., 2019. E-cadherin is required for metastasis in multiple models of breast cancer. *Nature* 573, 439–444. <https://doi.org/10.1038/s41586-019-1526-3>
- Pearson, H.B., Perez-Mancera, P.A., Dow, L.E., Ryan, A., Tennstedt, P., Bogani, D., Elsum, I., Greenfield, A., Tuveson, D.A., Simon, R., Humbert, P.O., 2011. SCRIB expression is deregulated in human prostate cancer, and its deficiency in mice promotes prostate neoplasia. *J Clin Invest* 121, 4257–4267. <https://doi.org/10.1172/JCI58509>
- Piao, S., Lee, S.-H., Kim, H., Yum, S., Stamos, J.L., Xu, Y., Lee, S.-J., Lee, J., Oh, S., Han, J.-K., Park, B.-J., Weis, W.I., Ha, N.-C., 2008. Direct Inhibition of GSK3 β by the Phosphorylated Cytoplasmic Domain of LRP6 in Wnt/ β -Catenin Signaling. *PLOS ONE* 3, e4046. <https://doi.org/10.1371/journal.pone.0004046>
- Piccolo, S., Dupont, S., Cordenonsi, M., 2014. The biology of YAP/TAZ: Hippo signaling and beyond. <https://doi.org/10.1152/physrev.00005.2014>
- Pichaud, F., 2018. PAR-Complex and Crumbs Function During Photoreceptor Morphogenesis and Retinal Degeneration. *Front. Cell. Neurosci.* 12. <https://doi.org/10.3389/fncel.2018.00090>
- Plant, P.J., Fawcett, J.P., Lin, D.C.C., Holdorf, A.D., Binns, K., Kulkarni, S., Pawson, T., 2003. A polarity complex of mPar-6 and atypical PKC binds, phosphorylates and regulates mammalian Lgl. *Nature Cell Biology* 5, 301–308. <https://doi.org/10.1038/ncb948>
- Plouffe, S.W., Meng, Z., Lin, K.C., Lin, B., Hong, A.W., Chun, J.V., Guan, K.-L., 2016. Characterization of Hippo Pathway Components by Gene Inactivation. *Mol. Cell* 64, 993–1008. <https://doi.org/10.1016/j.molcel.2016.10.034>
- Plutoni, C., Keil, S., Zeledon, C., Delsin, L.E.A., Decelle, B., Roux, P.P., Carréno, S., Emery, G., 2019. Misshapen coordinates protrusion restriction and actomyosin contractility during collective cell migration. *Nature Communications* 10, 3940. <https://doi.org/10.1038/s41467-019-11963-7>
- Pocaterra, A., Romani, P., Dupont, S., 2020. YAP/TAZ functions and their regulation at a glance. *J Cell Sci* 133. <https://doi.org/10.1242/jcs.230425>
- Pollard, T.D., 2016. Actin and Actin-Binding Proteins. *Cold Spring Harb Perspect Biol* 8, a018226. <https://doi.org/10.1101/cshperspect.a018226>
- Pollard, T.D., Goldman, R.D., 2018. Overview of the Cytoskeleton from an Evolutionary Perspective. *Cold Spring Harb Perspect Biol* 10, a030288. <https://doi.org/10.1101/cshperspect.a030288>
- Qi, M., Elion, E.A., 2005. MAP kinase pathways. *J Cell Sci* 118, 3569–3572. <https://doi.org/10.1242/jcs.02470>
- Qin, Y., Capaldo, C., Gumbiner, B.M., Macara, I.G., 2005. The mammalian Scribble polarity protein regulates epithelial cell adhesion and migration through E-cadherin. *J Cell Biol* 171, 1061–1071. <https://doi.org/10.1083/jcb.200506094>
- Quinlan, M.E., Heuser, J.E., Kerkhoff, E., Mullins, R.D., 2005. Drosophila Spire is an actin nucleation factor. *Nature* 433, 382–388. <https://doi.org/10.1038/nature03241>
- Raleigh, D.R., Marchiando, A.M., Zhang, Y., Shen, L., Sasaki, H., Wang, Y., Long, M., Turner, J.R., 2010. Tight Junction-associated MARVEL Proteins MarvelD3, Tricellulin, and Occludin Have Distinct but Overlapping Functions. *MBoC* 21, 1200–1213. <https://doi.org/10.1091/mbc.e09-08-0734>
- Raman, M., Chen, W., Cobb, M.H., 2007. Differential regulation and properties of MAPKs. *Oncogene* 26, 3100–3112. <https://doi.org/10.1038/sj.onc.1210392>
- Rao, R.K., Basuroy, S., Rao, V.U., Karnaky, K.J., Gupta, A., 2002. Tyrosine phosphorylation and dissociation of occludin-ZO-1 and E-cadherin-beta-catenin complexes from the cytoskeleton by oxidative stress. *Biochem. J.* 368, 471–481. <https://doi.org/10.1042/BJ20011804>

- Rauskolb, C., Sun, S., Sun, G., Pan, Y., Irvine, K.D., 2014. Cytoskeletal Tension Inhibits Hippo Signaling through an Ajuba-Warts Complex. *Cell* 158, 143–156. <https://doi.org/10.1016/j.cell.2014.05.035>
- Recio, J.A., Merlino, G., 2003. Hepatocyte growth factor/scatter factor induces feedback up-regulation of CD44v6 in melanoma cells through Egr-1. *Cancer Res.* 63, 1576–1582.
- Reedijk, M., Odorcic, S., Chang, L., Zhang, H., Miller, N., McCready, D.R., Lockwood, G., Egan, S.E., 2005. High-level coexpression of JAG1 and NOTCH1 is observed in human breast cancer and is associated with poor overall survival. *Cancer Res.* 65, 8530–8537. <https://doi.org/10.1158/0008-5472.CAN-05-1069>
- Rehder, D., Iden, S., Nasdala, I., Wegener, J., Brickwedde, M.-K.M.Z., Vestweber, D., Ebnet, K., 2006. Junctional adhesion molecule-A participates in the formation of apico-basal polarity through different domains. *Experimental Cell Research* 312, 3389–3403. <https://doi.org/10.1016/j.yexcr.2006.07.004>
- Reynolds, A.B., Roesel, D.J., Kanner, S.B., Parsons, J.T., 1989. Transformation-specific tyrosine phosphorylation of a novel cellular protein in chicken cells expressing oncogenic variants of the avian cellular src gene. *Molecular and Cellular Biology* 9, 629–638. <https://doi.org/10.1128/MCB.9.2.629>
- Riazuddin, Saima, Ahmed, Z.M., Fanning, A.S., Lagziel, A., Kitajiri, S., Ramzan, K., Khan, S.N., Chattaraj, P., Friedman, P.L., Anderson, J.M., Belyantseva, I.A., Forge, A., Riazuddin, Sheikh, Friedman, T.B., 2006. Tricellulin is a tight-junction protein necessary for hearing. *Am. J. Hum. Genet.* 79, 1040–1051. <https://doi.org/10.1086/510022>
- Ricote, M., García-Tuñón, I., Bethencourt, F., Fraile, B., Onsurbe, P., Paniagua, R., Royuela, M., 2006. The p38 transduction pathway in prostatic neoplasia. *The Journal of Pathology* 208, 401–407. <https://doi.org/10.1002/path.1910>
- Roberts, S., Delury, C., Marsh, E., 2012. The PDZ protein discs-large (DLG): the ‘Jekyll and Hyde’ of the epithelial polarity proteins. *The FEBS Journal* 279, 3549–3558. <https://doi.org/10.1111/j.1742-4658.2012.08729.x>
- Rogers, S.L., Wiedemann, U., Stuurman, N., Vale, R.D., 2003. Molecular requirements for actin-based lamella formation in *Drosophila* S2 cells. *J. Cell Biol.* 162, 1079–1088. <https://doi.org/10.1083/jcb.200303023>
- Roh, M.H., Liu, C.-J., Laurinec, S., Margolis, B., 2002. The Carboxyl Terminus of Zona Occludens-3 Binds and Recruits a Mammalian Homologue of Discs Lost to Tight Junctions. *J. Biol. Chem.* 277, 27501–27509. <https://doi.org/10.1074/jbc.M201177200>
- Rouse, J., Cohen, P., Trigon, S., Morange, M., Alonso-Llamazares, A., Zamanillo, D., Hunt, T., Nebreda, A.R., 1994. A novel kinase cascade triggered by stress and heat shock that stimulates MAPKAP kinase-2 and phosphorylation of the small heat shock proteins. *Cell* 78, 1027–1037. [https://doi.org/10.1016/0092-8674\(94\)90277-1](https://doi.org/10.1016/0092-8674(94)90277-1)
- Said, T.K., Conneely, O.M., Medina, D., O’Malley, B.W., Lydon, J.P., 1997. Progesterone, in addition to estrogen, induces cyclin D1 expression in the murine mammary epithelial cell, in vivo. *Endocrinology* 138, 3933–3939. <https://doi.org/10.1210/endo.138.9.5436>
- Saitou, M., Furuse, M., Sasaki, H., Schulzke, J.D., Fromm, M., Takano, H., Noda, T., Tsukita, S., 2000. Complex phenotype of mice lacking occludin, a component of tight junction strands. *Mol. Biol. Cell* 11, 4131–4142. <https://doi.org/10.1091/mbc.11.12.4131>
- Salmeron, A., Ahmad, T.B., Carlile, G.W., Pappin, D., Narsimhan, R.P., Ley, S.C., 1996. Activation of MEK-1 and SEK-1 by Tpl-2 proto-oncoprotein, a novel MAP kinase kinase kinase. *EMBO J.* 15, 817–826.
- Salvador, J.M., Mittelstadt, P.R., Guszczynski, T., Copeland, T.D., Yamaguchi, H., Appella, E., Fornace, A.J., Ashwell, J.D., 2005. Alternative p38 activation pathway mediated by T cell receptor-proximal tyrosine kinases. *Nat. Immunol.* 6, 390–395. <https://doi.org/10.1038/ni1177>
- Sawada, N., 2013. Tight junction-related human diseases. *Pathology International* 63, 1–12. <https://doi.org/10.1111/pin.12021>

- Schneeberger, E.E., Lynch, R.D., 2004. The tight junction: a multifunctional complex. *American Journal of Physiology-Cell Physiology* 286, C1213–C1228. <https://doi.org/10.1152/ajpcell.00558.2003>
- Schulzke, J.D., Gitter, A.H., Mankertz, J., Spiegel, S., Seidler, U., Amasheh, S., Saitou, M., Tsukita, S., Fromm, M., 2005. Epithelial transport and barrier function in occludin-deficient mice. *Biochim. Biophys. Acta* 1669, 34–42. <https://doi.org/10.1016/j.bbame.2005.01.008>
- Schulzke, J.-D., Günzel, D., John, L.J., Fromm, M., 2012. Perspectives on tight junction research. *Annals of the New York Academy of Sciences* 1257, 1–19. <https://doi.org/10.1111/j.1749-6632.2012.06485.x>
- Seth, A., Sheth, P., Elias, B.C., Rao, R., 2007. Protein phosphatases 2A and 1 interact with occludin and negatively regulate the assembly of tight junctions in the CACO-2 cell monolayer. *J. Biol. Chem.* 282, 11487–11498. <https://doi.org/10.1074/jbc.M610597200>
- Shen, L., Weber, C.R., Raleigh, D.R., Yu, D., Turner, J.R., 2011. Tight junction pore and leak pathways: a dynamic duo. *Annu. Rev. Physiol.* 73, 283–309. <https://doi.org/10.1146/annurev-physiol-012110-142150>
- Sheth, P., Basuroy, S., Li, C., Naren, A.P., Rao, R.K., 2003. Role of phosphatidylinositol 3-kinase in oxidative stress-induced disruption of tight junctions. *J. Biol. Chem.* 278, 49239–49245. <https://doi.org/10.1074/jbc.M305654200>
- Shiratsuchi, T., Futamura, M., Oda, K., Nishimori, H., Nakamura, Y., Tokino, T., 1998. Cloning and characterization of BAI-associated protein 1: a PDZ domain-containing protein that interacts with BAI1. *Biochem. Biophys. Res. Commun.* 247, 597–604. <https://doi.org/10.1006/bbrc.1998.8603>
- Skehel, P.A., Martin, K.C., Kandel, E.R., Bartsch, D., 1995. A VAMP-binding protein from *Aplysia* required for neurotransmitter release. *Science* 269, 1580–1583. <https://doi.org/10.1126/science.7667638>
- Soini, Y., 2012. Tight junctions in lung cancer and lung metastasis: a review. *Int J Clin Exp Pathol* 5, 126–136.
- Soni, S., Anand, P., Padwad, Y.S., 2019. MAPKAPK2: the master regulator of RNA-binding proteins modulates transcript stability and tumor progression. *J. Exp. Clin. Cancer Res.* 38, 121. <https://doi.org/10.1186/s13046-019-1115-1>
- Stamos, J.L., Chu, M.L.-H., Enos, M.D., Shah, N., Weis, W.I., 2014. Structural basis of GSK-3 inhibition by N-terminal phosphorylation and by the Wnt receptor LRP6. *eLife* 3, e01998. <https://doi.org/10.7554/eLife.01998>
- Steinhart, Z., Angers, S., 2018. Wnt signaling in development and tissue homeostasis. *Development* 145. <https://doi.org/10.1242/dev.146589>
- Stetak, A., Hajnal, A., 2011. The *C. elegans* MAGI-1 protein is a novel component of cell junctions that is required for junctional compartmentalization. *Dev. Biol.* 350, 24–31. <https://doi.org/10.1016/j.ydbio.2010.10.026>
- Stevenson, B.R., Siliciano, J.D., Mooseker, M.S., Goodenough, D.A., 1986. Identification of ZO-1: a high molecular weight polypeptide associated with the tight junction (zonula occludens) in a variety of epithelia. *The Journal of Cell Biology* 103, 755–766. <https://doi.org/10.1083/jcb.103.3.755>
- Straight, S.W., Shin, K., Fogg, V.C., Fan, S., Liu, C.-J., Roh, M., Margolis, B., 2004. Loss of PALS1 Expression Leads to Tight Junction and Polarity Defects. *MBoC* 15, 1981–1990. <https://doi.org/10.1091/mbc.e03-08-0620>
- Strathdee, G., 2002. Epigenetic versus genetic alterations in the inactivation of E-cadherin. *Semin. Cancer Biol.* 12, 373–379. [https://doi.org/10.1016/s1044-579x\(02\)00057-3](https://doi.org/10.1016/s1044-579x(02)00057-3)
- Suzuki, A., Ishiyama, C., Hashiba, K., Shimizu, M., Ebnet, K., Ohno, S., 2002. aPKC kinase activity is required for the asymmetric differentiation of the premature junctional complex during epithelial cell polarization. *Journal of Cell Science* 115, 3565–3573. <https://doi.org/10.1242/jcs.00032>

- Suzuki, A., Yamanaka, T., Hirose, T., Manabe, N., Mizuno, K., Shimizu, M., Akimoto, K., Izumi, Y., Ohnishi, T., Ohno, S., 2001. Atypical Protein Kinase C Is Involved in the Evolutionarily Conserved Par Protein Complex and Plays a Critical Role in Establishing Epithelia-Specific Junctional Structures. *J Cell Biol* 152, 1183–1196. <https://doi.org/10.1083/jcb.152.6.1183>
- Svitkina, T., 2018. The Actin Cytoskeleton and Actin-Based Motility. *Cold Spring Harb Perspect Biol* 10, a018267. <https://doi.org/10.1101/cshperspect.a018267>
- Takeichi, M., 2018. Multiple functions of α -catenin beyond cell adhesion regulation. *Current Opinion in Cell Biology, Cell Dynamics* 54, 24–29. <https://doi.org/10.1016/j.ceb.2018.02.014>
- Takeichi, M., 2014. Dynamic contacts: rearranging adherens junctions to drive epithelial remodelling. *Nature Reviews Molecular Cell Biology* 15, 397–410. <https://doi.org/10.1038/nrm3802>
- Takeichi, M., 1977. Functional correlation between cell adhesive properties and some cell surface proteins. *J. Cell Biol.* 75, 464–474. <https://doi.org/10.1083/jcb.75.2.464>
- Takekawa, M., Adachi, M., Nakahata, A., Nakayama, I., Itoh, F., Tsukuda, H., Taya, Y., Imai, K., 2000. p53-inducible wip1 phosphatase mediates a negative feedback regulation of p38 MAPK-p53 signaling in response to UV radiation. *EMBO J.* 19, 6517–6526. <https://doi.org/10.1093/emboj/19.23.6517>
- Talbot, L.J., Bhattacharya, S.D., Kuo, P.C., 2012. Epithelial-mesenchymal transition, the tumor microenvironment, and metastatic behavior of epithelial malignancies. *Int J Biochem Mol Biol* 3, 117–136.
- Tanemoto, M., Toyohara, T., Abe, T., Ito, S., 2008. MAGI-1a Functions as a Scaffolding Protein for the Distal Renal Tubular Basolateral K⁺ Channels. *J. Biol. Chem.* 283, 12241–12247. <https://doi.org/10.1074/jbc.M707738200>
- Taylor, A., Brady, A.F., Frayling, I.M., Hanson, H., Tischkowitz, M., Turnbull, C., Side, L., UK Cancer Genetics Group (UK-CGG), 2018. Consensus for genes to be included on cancer panel tests offered by UK genetics services: guidelines of the UK Cancer Genetics Group. *J. Med. Genet.* 55, 372–377. <https://doi.org/10.1136/jmedgenet-2017-105188>
- Tepass, U., Theres, C., Knust, E., 1990. crumbs encodes an EGF-like protein expressed on apical membranes of Drosophila epithelial cells and required for organization of epithelia. *Cell* 61, 787–799. [https://doi.org/10.1016/0092-8674\(90\)90189-L](https://doi.org/10.1016/0092-8674(90)90189-L)
- The Large Intestine | Boundless Anatomy and Physiology [WWW Document], n.d. URL <https://courses.lumenlearning.com/boundless-ap/chapter/the-large-intestine/>
- Thoreson, M.A., Anastasiadis, P.Z., Daniel, J.M., Ireton, R.C., Wheelock, M.J., Johnson, K.R., Hummingbird, D.K., Reynolds, A.B., 2000. Selective uncoupling of p120(ctn) from E-cadherin disrupts strong adhesion. *J. Cell Biol.* 148, 189–202. <https://doi.org/10.1083/jcb.148.1.189>
- Tobioka, H., Isomura, H., Kokai, Y., Tokunaga, Y., Yamaguchi, J., Sawada, N., 2004. Occludin expression decreases with the progression of human endometrial carcinoma. *Hum. Pathol.* 35, 159–164. <https://doi.org/10.1016/j.humpath.2003.09.013>
- Tolwinski, N.S., Wieschaus, E., 2004. Rethinking WNT signaling. *Trends Genet.* 20, 177–181. <https://doi.org/10.1016/j.tig.2004.02.003>
- Tsukita, S., Furuse, M., Itoh, M., 2001. Multifunctional strands in tight junctions. *Nat Rev Mol Cell Biol* 2, 285–293. <https://doi.org/10.1038/35067088>
- Tsukita, S., Tanaka, H., Tamura, A., 2019. The Claudins: From Tight Junctions to Biological Systems. *Trends in Biochemical Sciences* 44, 141–152. <https://doi.org/10.1016/j.tibs.2018.09.008>
- Tunggal, J.A., Helfrich, I., Schmitz, A., Schwarz, H., Günzel, D., Fromm, M., Kemler, R., Krieg, T., Niessen, C.M., 2005. E-cadherin is essential for in vivo epidermal barrier function by regulating tight junctions. *EMBO J.* 24, 1146–1156. <https://doi.org/10.1038/sj.emboj.7600605>
- Umeda, K., Ikenouchi, J., Katahira-Tayama, S., Furuse, K., Sasaki, H., Nakayama, M., Matsui, T., Tsukita, Sachiko, Furuse, M., Tsukita, Shoichiro, 2006. ZO-1 and ZO-2 independently

- determine where claudins are polymerized in tight-junction strand formation. *Cell* 126, 741–754. <https://doi.org/10.1016/j.cell.2006.06.043>
- Valenta, T., Hausmann, G., Basler, K., 2012. The many faces and functions of β -catenin. *EMBO J.* 31, 2714–2736. <https://doi.org/10.1038/emboj.2012.150>
- van Dop, W.A., Uhmman, A., Wijgerde, M., Sleddens–Linkels, E., Heijmans, J., Offerhaus, G.J., van den Bergh Weerman, M.A., Boeckxstaens, G.E., Hommes, D.W., Hardwick, J.C., Hahn, H., van den Brink, G.R., 2009. Depletion of the Colonic Epithelial Precursor Cell Compartment Upon Conditional Activation of the Hedgehog Pathway. *Gastroenterology* 136, 2195–2203.e7. <https://doi.org/10.1053/j.gastro.2009.02.068>
- van Es, J.H., de Geest, N., van de Born, M., Clevers, H., Hassan, B.A., 2010. Intestinal stem cells lacking the Math1 tumour suppressor are refractory to Notch inhibitors. *Nat Commun* 1, 18. <https://doi.org/10.1038/ncomms1017>
- van Es, J.H., van Gijn, M.E., Riccio, O., van den Born, M., Vooijs, M., Begthel, H., Cozijnsen, M., Robine, S., Winton, D.J., Radtke, F., Clevers, H., 2005. Notch/gamma-secretase inhibition turns proliferative cells in intestinal crypts and adenomas into goblet cells. *Nature* 435, 959–963. <https://doi.org/10.1038/nature03659>
- Van Itallie, C.M., Gambling, T.M., Carson, J.L., Anderson, J.M., 2005. Palmitoylation of claudins is required for efficient tight-junction localization. *J. Cell. Sci.* 118, 1427–1436. <https://doi.org/10.1242/jcs.01735>
- Varelas, X., Samavarchi-Tehrani, P., Narimatsu, M., Weiss, A., Cockburn, K., Larsen, B.G., Rossant, J., Wrana, J.L., 2010. The Crumbs Complex Couples Cell Density Sensing to Hippo-Dependent Control of the TGF- β -SMAD Pathway. *Developmental Cell* 19, 831–844. <https://doi.org/10.1016/j.devcel.2010.11.012>
- Vlahopoulos, S.A., 2017. Aberrant control of NF- κ B in cancer permits transcriptional and phenotypic plasticity, to curtail dependence on host tissue: molecular mode. *Cancer Biol Med* 14, 254–270. <https://doi.org/10.20892/j.issn.2095-3941.2017.0029>
- von Burstin, J., Eser, S., Paul, M.C., Seidler, B., Brandl, M., Messer, M., von Werder, A., Schmidt, A., Mages, J., Pagel, P., Schnieke, A., Schmid, R.M., Schneider, G., Saur, D., 2009. E-cadherin regulates metastasis of pancreatic cancer in vivo and is suppressed by a SNAIL/HDAC1/HDAC2 repressor complex. *Gastroenterology* 137, 361–371, 371.e1–5. <https://doi.org/10.1053/j.gastro.2009.04.004>
- Vreede, G. de, Schoenfeld, J.D., Windler, S.L., Morrison, H., Lu, H., Bilder, D., 2014. The Scribble module regulates retromer-dependent endocytic trafficking during epithelial polarization. *Development* 141, 2796–2802. <https://doi.org/10.1242/dev.105403>
- Vuong, D., Simpson, P.T., Green, B., Cummings, M.C., Lakhani, S.R., 2014. Molecular classification of breast cancer. *Virchows Arch* 465, 1–14. <https://doi.org/10.1007/s00428-014-1593-7>
- Wada, K.-I., Itoga, K., Okano, T., Yonemura, S., Sasaki, H., 2011. Hippo pathway regulation by cell morphology and stress fibers. *Development* 138, 3907–3914. <https://doi.org/10.1242/dev.070987>
- Wagner, E.F., Nebreda, Á.R., 2009. Signal integration by JNK and p38 MAPK pathways in cancer development. *Nat Rev Cancer* 9, 537–549. <https://doi.org/10.1038/nrc2694>
- Wang, Q., Chen, X.-W., Margolis, B., 2006. PALS1 Regulates E-Cadherin Trafficking in Mammalian Epithelial Cells. *MBoC* 18, 874–885. <https://doi.org/10.1091/mbc.e06-07-0651>
- Wang, W., Li, N., Li, X., Tran, M.K., Han, X., Chen, J., 2015. Tankyrase inhibitors target YAP by stabilizing angiomin family proteins. *Cell Rep* 13, 524–532. <https://doi.org/10.1016/j.celrep.2015.09.014>
- Wang, W., Yang, Y., Chen, X., Shao, S., Hu, S., Zhang, T., 2019. MAGI1 mediates tumor metastasis through c-Myb/miR-520h/MAGI1 signaling pathway in renal cell carcinoma. *Apoptosis* 24, 837–848. <https://doi.org/10.1007/s10495-019-01562-8>
- Weitz, J., Koch, M., Debus, J., Höhler, T., Galle, P.R., Büchler, M.W., 2005. Colorectal cancer. *The Lancet* 365, 153–165. [https://doi.org/10.1016/S0140-6736\(05\)17706-X](https://doi.org/10.1016/S0140-6736(05)17706-X)

- Wong, V., 1997. Phosphorylation of occludin correlates with occludin localization and function at the tight junction. *Am. J. Physiol.* 273, C1859-1867.
<https://doi.org/10.1152/ajpcell.1997.273.6.C1859>
- Wright, G.J., Leslie, J.D., Ariza-McNaughton, L., Lewis, J., 2004. Delta proteins and MAGI proteins: an interaction of Notch ligands with intracellular scaffolding molecules and its significance for zebrafish development. *Development* 131, 5659–5669. <https://doi.org/10.1242/dev.01417>
- Wu, Q., Wu, W., Fu, B., Shi, L., Wang, X., Kuca, K., 2019. JNK signaling in cancer cell survival. *Medicinal Research Reviews* 39, 2082–2104. <https://doi.org/10.1002/med.21574>
- Wu, Z., Nybom, P., Magnusson, K.E., 2000. Distinct effects of *Vibrio cholerae* haemagglutinin/protease on the structure and localization of the tight junction-associated proteins occludin and ZO-1. *Cell. Microbiol.* 2, 11–17. <https://doi.org/10.1046/j.1462-5822.2000.00025.x>
- Xiao, K., Oas, R.G., Chiasson, C.M., Kowalczyk, A.P., 2007. Role of p120-catenin in cadherin trafficking. *Biochimica et Biophysica Acta (BBA) - Molecular Cell Research*, The p120-catenin protein family 1773, 8–16. <https://doi.org/10.1016/j.bbamcr.2006.07.005>
- Xue, L., Williamson, A., Gaines, S., Andolfi, C., Paul-Olson, T., Neerukonda, A., Steinhagen, E., Smith, R., Cannon, L.M., Polite, B., Umanskiy, K., Hyman, N., 2018. An Update on Colorectal Cancer. *Current Problems in Surgery* 55, 76–116.
<https://doi.org/10.1067/j.cpsurg.2018.02.003>
- Yang, L., Chen, Y., Cui, T., Knösel, T., Zhang, Q., Albring, K.F., Huber, O., Petersen, I., 2012. Desmoplakin acts as a tumor suppressor by inhibition of the Wnt/ β -catenin signaling pathway in human lung cancer. *Carcinogenesis* 33, 1863–1870.
<https://doi.org/10.1093/carcin/bgs226>
- Yonemura, S., Wada, Y., Watanabe, T., Nagafuchi, A., Shibata, M., 2010. α -Catenin as a tension transducer that induces adherens junction development. *Nat. Cell Biol.* 12, 533–542.
<https://doi.org/10.1038/ncb2055>
- Yoon, S., Seger, R., 2006. The extracellular signal-regulated kinase: Multiple substrates regulate diverse cellular functions. *Growth Factors* 24, 21–44.
<https://doi.org/10.1080/02699050500284218>
- Yu, J., Zheng, Y., Dong, J., Klusza, S., Deng, W.-M., Pan, D., 2010. Kibra Functions as a Tumor Suppressor Protein that Regulates Hippo Signaling in Conjunction with Merlin and Expanded. *Developmental Cell* 18, 288–299. <https://doi.org/10.1016/j.devcel.2009.12.012>
- Zaessinger, S., Zhou, Y., Bray, S.J., Tapon, N., Djiane, A., 2015. *Drosophila* MAGI interacts with RASSF8 to regulate E-Cadherin-based adherens junctions in the developing eye. *Development* 142, 1102–1112. <https://doi.org/10.1242/dev.116277>
- Zanconato, F., Forcato, M., Battilana, G., Azzolin, L., Quaranta, E., Bodega, B., Rosato, A., Bicciato, S., Cordenonsi, M., Piccolo, S., 2015. Genome-wide association between YAP/TAZ/TEAD and AP-1 at enhancers drives oncogenic growth. *Nat Cell Biol* 17, 1218–1227.
<https://doi.org/10.1038/ncb3216>
- Zaric, J., Joseph, J.-M., Tercier, S., Sengstag, T., Ponsonnet, L., Delorenzi, M., Rüegg, C., 2012. Identification of MAGI1 as a tumor-suppressor protein induced by cyclooxygenase-2 inhibitors in colorectal cancer cells. *Oncogene* 31, 48–59.
<https://doi.org/10.1038/onc.2011.218>
- Zeitler, J., Hsu, C.P., Dionne, H., Bilder, D., 2004. Domains controlling cell polarity and proliferation in the *Drosophila* tumor suppressor Scribble. *J Cell Biol* 167, 1137–1146.
<https://doi.org/10.1083/jcb.200407158>
- Zeke, A., Misheva, M., Reményi, A., Bogoyevitch, M.A., 2016. JNK Signaling: Regulation and Functions Based on Complex Protein-Protein Partnerships. *Microbiol Mol Biol Rev* 80, 793–835. <https://doi.org/10.1128/MMBR.00043-14>
- Zekri, A.-R.N., Hafez, M.M., Bahnassy, A.A., Hassan, Z.K., Mansour, T., Kamal, M.M., Khaled, H.M., 2008. Genetic profile of Egyptian hepatocellular-carcinoma associated with hepatitis C virus

- Genotype 4 by 15 K cDNA microarray: preliminary study. *BMC Res Notes* 1, 106.
<https://doi.org/10.1186/1756-0500-1-106>
- Zhang, G., Liu, T., Wang, Z., 2012. Downregulation of MAGI1 Associates with Poor Prognosis of Hepatocellular Carcinoma. *Journal of Investigative Surgery* 25, 93–99.
<https://doi.org/10.3109/08941939.2011.606875>
- Zhang, G., Wang, Z., 2011. MAGI1 inhibits cancer cell migration and invasion of hepatocellular carcinoma via regulating PTEN. *Zhong Nan Da Xue Xue Bao Yi Xue Ban* 36, 381–385.
<https://doi.org/10.3969/j.issn.1672-7347.2011.05.002>
- Zhang, N., Bai, H., David, K.K., Dong, J., Zheng, Y., Cai, J., Giovannini, M., Liu, P., Anders, R.A., Pan, D., 2010. The Merlin/NF2 tumor suppressor functions through the YAP oncoprotein to regulate tissue homeostasis in mammals. *Dev. Cell* 19, 27–38.
<https://doi.org/10.1016/j.devcel.2010.06.015>
- Zhang, W., Liu, H.T., 2002. MAPK signal pathways in the regulation of cell proliferation in mammalian cells. *Cell Research* 12, 9–18. <https://doi.org/10.1038/sj.cr.7290105>
- Zhao, Bin, Li, L., Lei, Q., Guan, K.-L., 2010. The Hippo–YAP pathway in organ size control and tumorigenesis: an updated version. *Genes Dev* 24, 862–874.
<https://doi.org/10.1101/gad.1909210>
- Zhao, B., Li, L., Lu, Q., Wang, L.H., Liu, C.-Y., Lei, Q., Guan, K.-L., 2011. Angiomotin is a novel Hippo pathway component that inhibits YAP oncoprotein. *Genes & Development* 25, 51–63.
<https://doi.org/10.1101/gad.2000111>
- Zhao, Bin, Li, L., Lu, Q., Wang, L.H., Liu, C.-Y., Lei, Q., Guan, K.-L., 2011a. Angiomotin is a novel Hippo pathway component that inhibits YAP oncoprotein. *Genes Dev.* 25, 51–63.
<https://doi.org/10.1101/gad.2000111>
- Zhao, Bin, Li, L., Lu, Q., Wang, L.H., Liu, C.-Y., Lei, Q., Guan, K.-L., 2011b. Angiomotin is a novel Hippo pathway component that inhibits YAP oncoprotein. *Genes Dev.* 25, 51–63.
<https://doi.org/10.1101/gad.2000111>
- Zhao, B., Li, L., Tumaneng, K., Wang, C.-Y., Guan, K.-L., 2010. A coordinated phosphorylation by Lats and CK1 regulates YAP stability through SCF -TRCP. *Genes & Development* 24, 72–85.
<https://doi.org/10.1101/gad.1843810>
- Zou, S., Pita-Almenar, J.D., Eskin, A., 2011. Regulation of glutamate transporter GLT-1 by MAGI-1. *Journal of Neurochemistry* 117, 833–840. <https://doi.org/10.1111/j.1471-4159.2011.07250.x>
- Zoumpourlis, V., Papassava, P., Linardopoulos, S., Gillespie, D., Balmain, A., Pintzas, A., 2000. High levels of phosphorylated c-Jun, Fra-1, Fra-2 and ATF-2 proteins correlate with malignant phenotypes in the multistage mouse skin carcinogenesis model. *Oncogene* 19, 4011–4021.
<https://doi.org/10.1038/sj.onc.1203732>

The apical scaffold big bang binds to spectrins and regulates the growth of *Drosophila melanogaster* wing discs

Elodie Forest, Rémi Logeay, Charles Géminard, Diala Kantar, Florence Frayssinoux, Lisa Heron-Milhavet, and Alexandre Djiane

IRCM, Inserm, University of Montpellier, ICM, Montpellier, France

During development, cell numbers are tightly regulated, ensuring that tissues and organs reach their correct size and shape. Recent evidence has highlighted the intricate connections between the cytoskeleton and the regulation of the key growth control Hippo pathway. Looking for apical scaffolds regulating tissue growth, we describe that *Drosophila melanogaster* big bang (Bbg), a poorly characterized multi-PDZ scaffold, controls epithelial tissue growth without affecting epithelial polarity and architecture. *bbg*-mutant tissues are smaller, with fewer cells that are less apically constricted than normal. We show that Bbg binds to and colocalizes tightly with the β -heavy-Spectrin/Kst subunit at the apical cortex and promotes Yki activity, F-actin enrichment, and the phosphorylation of the myosin II regulatory light chain Spaghetti squash. We propose a model in which the spectrin cytoskeleton recruits Bbg to the cortex, where Bbg promotes actomyosin contractility to regulate epithelial tissue growth.

Introduction

In animals, the fine regulation of cell numbers and cell size ensures that tissues and organs reach their correct size and shape to fulfill their function. Intercellular signaling pathways, and in particular their effects on the cell cycle and cell death programs, are key mediators to coordinate this harmonious growth. Hippo signaling represents one key pathway regulating tissue size and cell proliferation, in particular for epithelial tissues. First identified using genetic screens in *Drosophila melanogaster*, the core Hippo pathway is composed of two cytoplasmic kinases, Hippo (MST1/2 in humans; Harvey et al., 2003; Wu et al., 2003) and Warts (Wts; LATS1/2), which act to phosphorylate and exclude out of the nucleus the transcription coactivator Yorkie (Yki; YAP and TAZ). Mutations in *hippo* or *warts* lead to a stabilization of unphosphorylated Yki in the nucleus and overproliferation. Recent evidence points to a major role of the Hippo pathway in the biology of stem cells and as a tumor suppressor in many cancers (Halder and Johnson, 2011; Yu and Guan, 2013; Meng et al., 2016).

This core Hippo pathway integrates many upstream inputs, in particular from the apical scaffolds Expanded (Ex; FRMD6), Merlin (Mer; NF2; Hamaratoglu et al., 2006; Badouel et al., 2009; Yin et al., 2013), and Kibra (Kib; KIBRA; Baumgartner et al., 2010; Genevet et al., 2010; Yu et al., 2010) acting redundantly to recruit and activate the core kinases and to trap Yki in an inactive cortical compartment. Among the many other upstream activators of the Hippo pathway, the cell architecture and cytoskeletal tension have recently emerged as a key,

but still poorly understood, regulator. Indeed, in epithelial cells, different members of the apical-basal polarity machinery such as Crumbs (Crb; Chen et al., 2010; Grzeschik et al., 2010; Ling et al., 2010; Robinson et al., 2010) modulate the activity and localization of the upstream scaffolds Ex, Mer, and Kib or directly impinge on Wts/LATS activity on Yki/YAP/TAZ (Schroeder and Halder, 2012; Yu and Guan, 2013). Different studies have highlighted the role of the actin cytoskeleton. Capped or destabilized actin filaments promote the sequestration of Yki/YAP/TAZ out of the nucleus, whereas filamentous actin polymerization and contractile actin networks favor Yki/YAP/TAZ activity (Dupont et al., 2011; Fernández et al., 2011; Sansores-Garcia et al., 2011; Gaspar and Tapon, 2014). Although the level of activated phosphorylated nonmuscle myosin II light chain (MLC; p-MLC) is critical for this effect of the actin cytoskeleton on Yki/YAP/TAZ activity, it is, however, not clear to what extent the core Hippo kinases cassette mediate this effect (Dupont et al., 2011; Codelia et al., 2014; Gaspar and Tapon, 2014).

Recent studies have described the negative role on Yki/YAP/TAZ activity of the spectrin-based cytoskeleton both in *Drosophila* and in human cell lines. *Spectrin* mutant cells accumulate Yki/YAP/TAZ in the nucleus and slightly overproliferate (Deng et al., 2015; Fletcher et al., 2015; Wong et al., 2015). Even though conserved across evolution, this role of spectrins

© 2018 Forest et al. This article is distributed under the terms of an Attribution–Noncommercial–Share Alike–No Mirror Sites license for the first six months after the publication date (see <http://www.rupress.org/terms/>). After six months it is available under a Creative Commons license (Attribution–Noncommercial–Share Alike 4.0 International license, as described at <https://creativecommons.org/licenses/by-nc-sa/4.0/>).

Correspondence to Alexandre Djiane: alexandre.djiane@inserm.fr



must be tissue specific because not all *spectrin* mutant tissues in *Drosophila* show enhanced proliferation (Ng et al., 2016). Spectrins form an elastic submembranous network of heterotetramers of α and β subunits, which cross-links actin fibers (Bennett and Baines, 2001; Baines, 2009; Stabach et al., 2009). In *Drosophila*, there is one α and two β isoforms: β and β -heavy (β H; also known as karst [Kst]). In epithelial cells, α/β dimers are found basolaterally, whereas α/β H dimers are localized apically (Thomas and Kiehart, 1994; Lee et al., 1997; Thomas et al., 1998; Thomas and Williams, 1999; Zarnescu and Thomas, 1999). Spectrins prevent Yki activity in the eye and wing epithelial tissues, but the exact mechanism is still unclear and has been proposed to involve either the clustering and activation of the upstream Hippo activators as well as spectrin-binding partners Crb and Ex (Fletcher et al., 2015) or alternatively, the relaxation of the contractile actomyosin network and down-regulation of active p-MLC (Deng et al., 2015).

To better understand the regulation of epithelial cell numbers and proliferation, we have been interested in the role of apical scaffolds and, in particular, of PDZ domains containing scaffolds, as they represent attractive candidates to link apical-basal polarity cues, adhesion, and the cytoskeleton to integrate numerous stimuli. In this study, we report that *Drosophila* big bang (Bbg), a poorly characterized multi-PDZ scaffold (Kim et al., 2006) that had previously been linked to midgut homeostasis (Bonnay et al., 2013) and border cell migration in the adult *Drosophila* female egg chamber (Aranjuez et al., 2012), controls epithelial tissue growth without affecting epithelial polarity and architecture and that *bbg* mutant tissues are smaller with fewer cells. We show that Bbg binds to and colocalizes tightly with β H-Spectrin/Kst at the apical cortex, but contrary to spectrins, Bbg promotes Yki activity. Unlike spectrins, Bbg promotes the accumulation of a dense apical F-actin network and of activated p-MLC. We propose a model in which, through its stabilization of a contractile-prone actin cytoskeleton, Bbg positively regulates Yki activity and epithelial tissue growth.

Results

Bbg is an apical scaffold regulating epithelial cell numbers

Bbg encodes for a large protein with two or three PDZ domains depending on isoform: a long isoform encoding a 2,637-aa-long protein with three PDZs, referred to as Bbg-L (Fig. 1 B) or short and intermediate isoforms coding for 1,033-aa-long and 1,842-aa-long proteins with only two PDZs, which are referred to as Bbg-S and Bbg-M, respectively (Fig. 1 B). PDZ domains are protein-protein interaction domains, suggesting that Bbg could act as a large protein scaffold. To study the function of *bbg*, we first raised an antibody directed at the last two PDZ domains shared by all Bbg isoforms (anti-Bbg). Bbg was expressed ubiquitously at the level of the apical cortex of epithelial cells. In third instar larval wing imaginal discs in particular, Bbg was expressed in all cells with a strong enrichment at the level of the dorsoventral boundary in the central wing pouch region. This staining was completely lost in clones of cells mutant for the transposable P element *P{EPgy2|EY02818}*, inserted in a common exon to all *bbg* isoforms (Fig. 1 A), validating both the specificity of the anti-Bbg antibody and suggesting that the *bbg*^{EY02818} mutation is a protein null (Fig. 1 C). Western blot analysis on whole larval head extracts highlighted a specific

band at ~120 kD corresponding with the predicted size of the Bbg-S isoform (Fig. 1 D; note that this antibody also recognized a 60-, a 95-, and a 180-kD band, all of which were not specific).

After genetic background cleaning, the *bbg*^{EY02818} mutation was viable and fertile, but homozygous individuals exhibited smaller adult external structures such as wings or legs; *bbg*^{EY02818} mutant wings were ~15% smaller than WT controls (Fig. 1, E–H). This effect was almost as strong as that of *bbg*^{EY02818} put over *Df(3L)Exel6123*, a genetically mapped deficiency covering the *bbg* locus (18% reduction), suggesting that *bbg*^{EY02818} behaved genetically as a strong hypomorph. Importantly, this was efficiently rescued by transgenes driving ubiquitously WT forms of Bbg (*bbg-S*-rescued wings were only 2% smaller than controls, and *bbg-M*- and *bbg-L*-rescued wings only 6% smaller; Fig. 1 H), showing that the small wing phenotype was indeed caused by mutations in the *bbg* gene. It is noteworthy that *Df(3L)Exel6123* gave a dominant small wing phenotype of ~8%, opening the possibility that the stronger phenotype of *bbg*^{EY02818} when put over the deficiency could be caused by additional haploinsufficient mutations.

Despite not being detected by Western blots, we tested whether the Bbg-M and Bbg-L isoforms could be implicated in *bbg* function. We therefore generated isoform-specific mutations using recombinase-mediated cassette exchange (Venken et al., 2011). We replaced the two *MiMIC* insertions flanking two large exons found only in the *bbg-M* and *bbg-L* isoforms (Fig. 1 A) with cassettes carrying a *mini-white* gene (for easier selection) and a loxP site. When put in trans together with a source of Cre recombinase, the two loxP sites recombined, generating a precise deletion of these two exons at high frequency (Fig. S1). However, the *bbg* mutant generated, called *bbg*³⁴, appeared completely normal and fertile with no discernable external phenotype, suggesting that neither the *bbg-L* nor the *bbg-M* isoform had any noticeable role, at least on the viability or external morphology of *Drosophila*. Furthermore, when put over the *Df(3L)Exel6123* deficiency, *bbg*³⁴ did not produce smaller wings (Fig. 1 H), further validating that the *bbg-L* and *bbg-M* isoforms did not affect wing size. However, even though *bbg-L* and *bbg-M* are not necessary for the control of wing size, they appear sufficient because the Bbg-L and Bbg-M isoforms were still able to rescue the *bbg*^{EY02818} mutant small wing phenotype. Indeed, Bbg-M and Bbg-L contain all of the domains of Bbg-S and therefore likely could compensate for its absence.

Collectively, these results show that Bbg-S (referred simply as Bbg hereafter) is ubiquitously expressed in imaginal discs and controls the growth of wing tissues. To investigate whether these smaller adult wings could be reflecting fewer cells in the tissue, we estimated the number of cells along a line between the L3 and L4 veins above the posterior cross-vein. As each adult wing cell normally produces a single distally pointing wing hair, wing hair numbers can be used as a proxy to wing cell numbers. Along this fixed landmark, *bbg* mutant wings had fewer cells (16.1 on average) than controls (19.1). This was rescued by a WT *bbg-S* transgene (17.9; Fig. 1 I), suggesting that the *bbg* mutant small adult wings were at least in part a result of fewer cells being produced or retained.

Using mitotic clonal analysis, we then investigated in the central pouch region of third instar wing discs whether at this early stage, *bbg* mutant clones had fewer cells than control (Fig. 2, A and B). *Bbg* mutant clones were on average 18% smaller than their WT twin spots when total area was considered (control empty clones revealed no difference with their

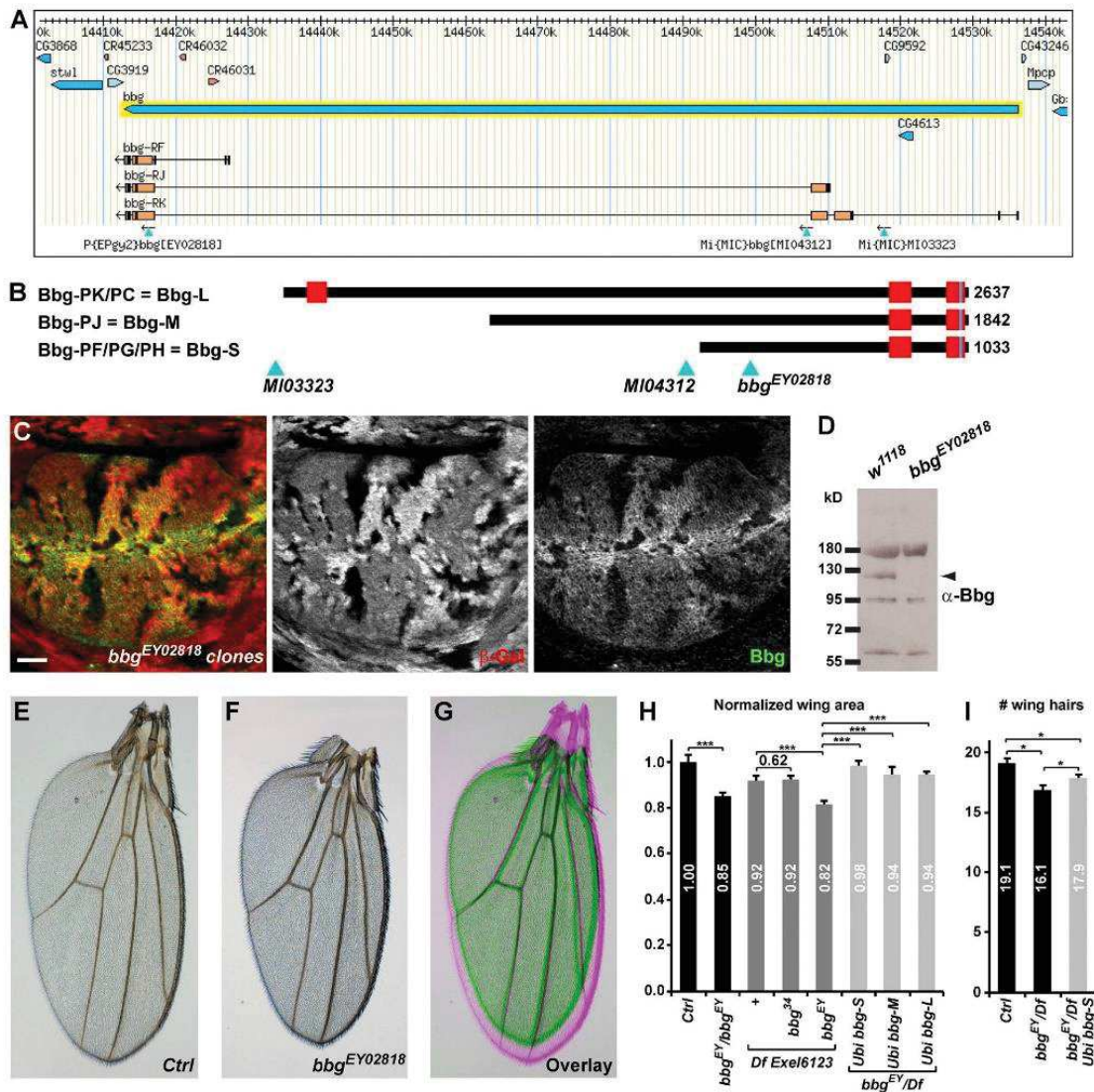


Figure 1. *bbg* controls adult *Drosophila* wing size. (A) A *bbg* locus (adapted from Flybase GBrowse) showing the main *bbg* transcript isoforms and the transposable elements used in this study. (B) Diagram representation of the main three Bbg protein isoforms. Red boxes represent PDZ domains. Light blue triangles indicate the localization of the transposable elements used with respect to the translated Bbg proteins. (C) *bbg^{EY02818}* mutant clones in the larval wing disc marked by the absence of β -galactosidase (red, middle). In mutant cells, Bbg protein was totally absent (green, right). Bar, 25 μ m. (D) Western blot of cleared lysates from third instar larval heads of control (*w¹¹¹⁸*; left) and *bbg^{EY02818}* (right) reveals a specific band at ~120 kD for Bbg. (E–G) Effect of the *bbg* mutations on adult wing size. *bbg^{EY02818}* homozygous wings (F and green in G) were misshapen and smaller than controls (E and pink in G). (H) Quantifications of the *bbg* small wing phenotype expressed as ratios compared with the mean sizes (area) of the control (Ctrl) wings. The *bbg³⁴* allele had no effect. Providing ubiquitously expressed *bbg* transgenes (*bbg-S*, *bbg-M*, and *bbg-L*) in the *bbg^{EY02818}* mutant background significantly rescued the adult small wing phenotype. SD is shown; $n = 18$ –20 independent female wings. (I) Quantification of wing cell numbers. Cells were estimated by counting the number of wing hairs along a vertical above the posterior cross vein between the L3 and L4 veins. SEM is shown; unpaired two-tailed Student's *t* test; *, $P < 0.05$; ***, $P < 0.001$; $n = 19$ independent female wings.

twin spots; Fig. 2 C) and had ~30% fewer cells (Fig. 2 D). The small size effect of *bbg* mutants appeared therefore more pronounced at earlier stages than in adult wings, suggesting that compensatory mechanisms could be playing after larval stages. Alternatively, this difference could also reflect the difference in the experimental systems used: whole mutant wing in the adult measurement, compared with small mutant clones competing with WT cells in the larval setup. *Bbg* mutant clones had fewer cells, but *bbg* mutant cells were wider and more apically relaxed than controls as their mean apical size (total clone area

divided by number of cells) was ~21% bigger (Fig. 2 E). Given that the apical size of cells varies widely in the larval wing disc depending on their position (more packed at the center and more stretched at the periphery), we always compared the size of equivalently located clones (*bbg* mutant with their twin spots) to eliminate this position bias.

Bbg regulates cortical actin

The size of the apical surface is controlled by the network of actin cables that belt the apical cortex. Strikingly, in *bbg*-

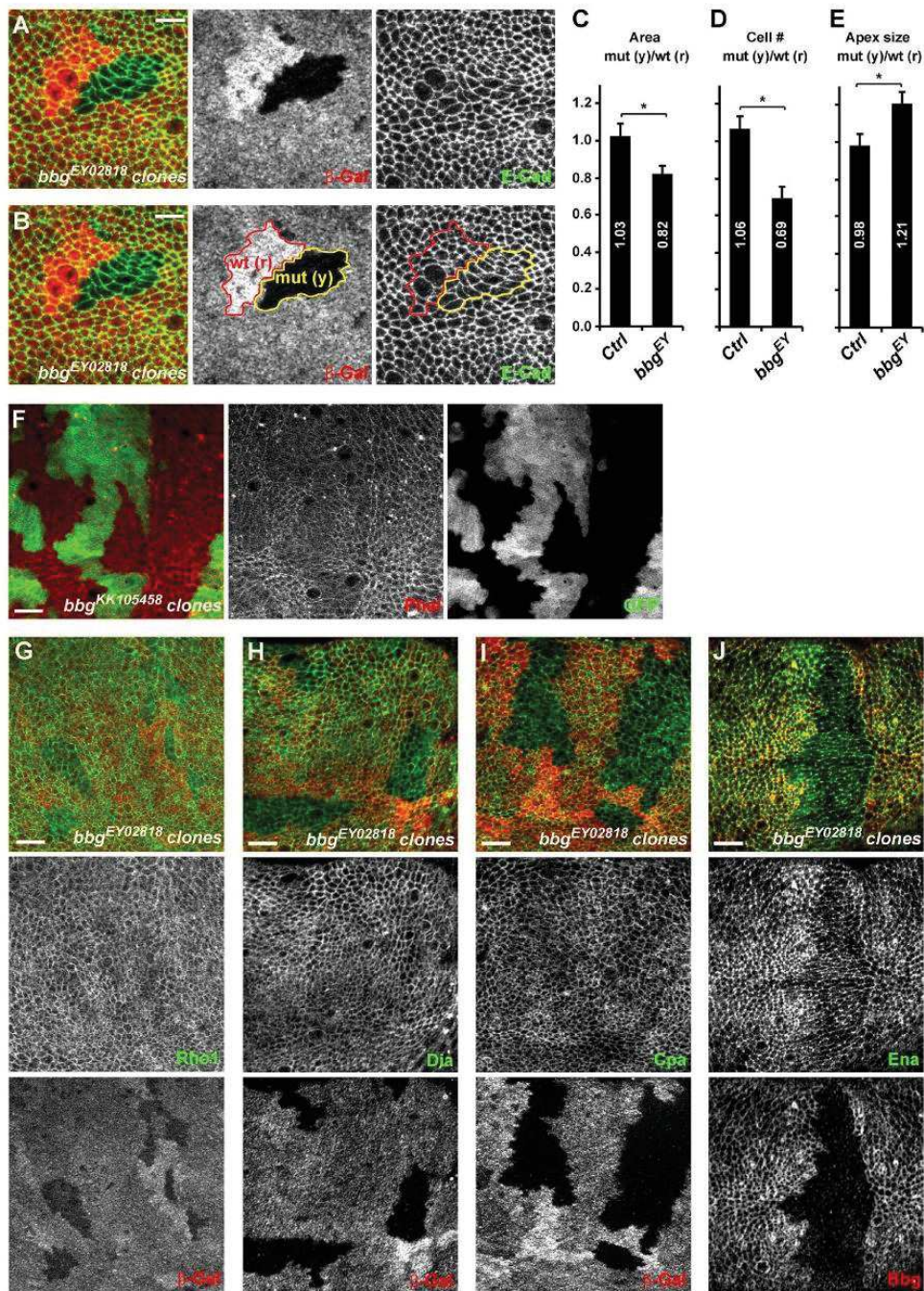


Figure 2. ***bbg* controls cell number and cell size.** (A and B) Mitotic clones for *bbg^{EY02818}* in the central region of third instar wing imaginal discs. Homozygous mutant clones are marked by the absence of β -galactosidase (β -Gal; red; middle panels) and highlighted by the yellow outline (mut (y)) in the right two panels in B. Twin spots, which were fully WT for *bbg* and arose at the same time as the *bbg* mutant clones, are marked by the bright β -Gal staining (two copies), and are highlighted by the red outline (wt (r)) in the middle and right panels in B. Apical cell outlines are revealed by E-Cad staining (green; right). Bars, 5 μ m. (C–E) Quantification of the mean *FRT80B* *bbg^{EY02818}* mutant clone total area (C), cell number (D), and apical cell size (E) and shown as the mean ratio between individual mutant tissue clones (yellow) and their corresponding WT twin spots (red). Controls were “empty” clones performed with *FRT80B*. SEM is shown; unpaired two-tailed student *t* test; *, $P < 0.05$; $n = 10$ clone pairs from independent discs. (F) Overexpression clones marked by GFP (green, right) leading to the depletion of *bbg* and showing the organization of the cortical apical F-actin (red, middle). A strong decrease of apical F-actin was seen in *bbg*-depleted cells. (G–J) *bbg^{EY02818}* mutant clones in the larval wing disc marked by the absence of β -galactosidase (red, bottom) and marked for the actin regulators Rho1 (G; green, middle), Dia (H; green, middle), Cpa (I; green, middle), and Ena (J; green, middle). Cpa and Ena cortical levels were reduced in *bbg* mutant cells. Bars, 10 μ m.

depleted cells (using the strong *bbg*^{KK105458} RNAi line), less filamentous cortical actin was detected, as shown by phalloidin staining (Fig. 2 F), suggesting that the defects in apical constriction could be a consequence of an impaired apical cortical actin cytoskeleton. We therefore investigated whether Bbg could be regulating the localization and levels of different actin regulators, focusing on the key actin cytoskeleton regulator and small GTPase Rho1 (Settleman, 2001), on the actin filament nucleators responsible for actin cables growth such as the formin diaphanous (Dia; Afshar et al., 2000), on the destabilizing factors such as capping protein α (Cpa; Fernández et al., 2011), which through their occupancy of the barbed end of actin cables prevent their further growth and ultimately lead to actin cable destruction, and on the capping protein inhibitor Ena (Ena; VASP in mammals; Bear and Gertler, 2009). All were localized at the apical cortex of wing imaginal disc cells. In *bbg* mutant cells, the level and localization of Rho1 were unaffected, suggesting that the actin filament defects are not a consequence of weakened or altered Rho1 recruitment at the cortex (Fig. 2 G). Similarly, in *bbg* mutant cells, the level and localization of Dia remained unaffected (Fig. 2 H), suggesting that the effects of *bbg* mutants on cortical F-actin accumulation are unlikely to be a consequence of a reduced Dia-mediated F-actin nucleation. A weak reduction in Cpa cortical levels could be observed in *bbg* mutant cells (Fig. 2 I). Because *cpa* loss leads to F-actin accumulation (Fernández et al., 2011; Sansores-Garcia et al., 2011), the F-actin reduction observed in *bbg* mutant cells cannot be explained by this weaker Cpa recruitment. However, even though not grossly affected by *bbg* mutations, more subtle interactions between *cpa* and *bbg* could be taking place. We thus tested whether the effects of *cpa* loss could be modified by *bbg* mutants. In the wing pouch of third instar larvae, *cpa*-depleted cells (through the use of the strong *cpa*^{KK108554} or *cpa*^{HMS02249} RNAi lines) transiently accumulated actin (increased phalloidin staining; Fig. S2 A) and were extruded basally out of the epithelia (Fernández et al., 2011). The further depletion of *bbg* imposed its phenotype on cortical actin, and instead of accumulating actin, *cpa bbg* double mutant cells showed less cortical actin (Fig. S2 B). However, similarly to *cpa* mutant cells, *cpa bbg* double mutant cells were also extruded out of the epithelia, and very few mutant cells were recovered in the wing pouch. Among the actin regulators tested, only Ena was affected, and *bbg* mutant cells had lower levels of cortical Ena (Fig. 2 J). Ena has been shown to regulate F-actin elongation in several *Drosophila* epithelia (Grevengoed et al., 2003; Gates et al., 2007), and it is tantalizing to propose that the effects of Bbg on cortical actin are mediated at least in part through Ena. However, we did not observe any obvious cortical F-actin alterations similar to those seen in *bbg* mutants by modulating Ena levels either through overexpression or RNAi-mediated knockdown (Fig. S2, C and D). These results, even though obtained with RNAi-hypomorphic combinations, suggest that the cortical F-actin fibers in *bbg* mutant cells are insensitive to Cpa or to the inhibitory role Ena plays on acting capping proteins (Bear and Gertler, 2009), suggesting that the F-actin stabilization by Bbg is likely mediated by other mechanisms than the modulation of the Cpa–Ena complex.

Bbg associates with the spectrin cytoskeleton

To identify the mechanisms by which *bbg* could be acting, we sought to identify the Bbg protein partners by performing

whole-genome yeast two-hybrid (Y2H) screens using the Bbg-S isoform as a bait. Among the 177 Bbg-interacting clones recovered, 58 corresponded with β H-Spectrin, also known as Kst in *Drosophila*, and three clones corresponded with β -Spectrin. The spectrin cytoskeleton is made of tetramers of two α and two β spectrin chains that arrange in a lattice all around the cell cortex (Bennett and Baines, 2001; Baines, 2009; Stabach et al., 2009). In imaginal disc epithelial cells, there are two types of β chains: the basolateral β -Spectrin and the apical β H-Spectrin Kst (Thomas and Kiehart, 1994; Thomas and Williams, 1999; Zarnescu and Thomas, 1999). Kst was the top Bbg interactor in terms of number of prey clones recovered.

To validate these Y2H results, we performed coimmunoprecipitation (coIP) experiments in cultured *Drosophila* S2 cells. Kst is a huge 4,097-aa-long protein which is too big to work with in coIPs. The sequence shared by all the isolated Kst prey clones defined a potential minimal necessary interacting fragment or selected interaction domain (SID) spanning aa 1,833–2,056, centered around the spectrin/ α -actinin repeat 15 (Fig. 3 A). We therefore generated a Flag-tagged Kst fragment encompassing the SID Kst-BC (aa 1,650–2,600; Fig. 3 A). In coIPs, Flag–Kst-BC was detected in the GFP immunoprecipitate only in the presence of GFP–Bbg, showing that Kst and Bbg interacted physically (Fig. 3 B).

One possible role of this binding is that Bbg and Kst could regulate each other's localization. In wing disc epithelial cells, Bbg accumulated as an apical cortical ring. In particular, along the dorsoventral midline, Bbg was found in a very thick submembranous compartment (Fig. 3 C) colocalizing very intimately with Kst, as indicated by the Kst–YFP fusion protein at the level of the adherens junctions (AJs; marked by E-cadherin [E-Cad]; Fig. 3 G), and apically of the septate junctions (marked by discs-large [Dlg]; Fig. 3 H). Given this colocalization, we then tested whether Kst and Bbg control each other's localization. In *bbg*-depleted cells (using the strong *bbg*^{KK105458} RNAi line driven in all dorsal cells by *apterous-Gal4*), Kst localization and levels were normal or very subtly lowered (Fig. 3 D). Similarly, in *bbg* mutant cells, the levels and localization of apical markers and scaffolds such as aPKC (subapical compartment), E-Cad, Arm, Pyd (AJs), or Dlg (septate junctions) were not affected (Fig. S3), indicating that the overall polarity of *bbg* mutant cells was not affected. In *kst* mutant cells, however, Bbg cortical localization was strongly reduced, even though it was not completely abolished, and low levels of Bbg were retained at the cortex (Fig. 3 E). α -Spec-depleted cells showed similar effects (Fig. 3 F), showing that not only Kst but the spectrin cytoskeleton was required for Bbg apical cortical localization. The residual cortical Bbg, observed even when the core α -Spectrin subunit was absent (Fig. 3 F), suggests that two pools of cortical Bbg exist: a pool associated with the spectrin cytoskeleton and a smaller pool of Bbg more tightly associated with the membrane and which might be recruited through alternative mechanisms such as interaction with other binding partners or with lipids (Bbg presents a putative palmitoylation site at its C terminus).

However, we note that despite its binding and its action to stabilize Bbg in a broad subcortical domain, Kst is unlikely to mediate the effect of Bbg on F-actin. Indeed, in contrast to *bbg*-mutant cells, *kst* mutant tissues had no changes in cortical F-actin (Fig. S2 E) as reported previously (Deng et al., 2015). Strikingly, in tissues mutant for *kst* and *bbg*, less cortical actin was detected (Fig. S2 F), further showing that even though

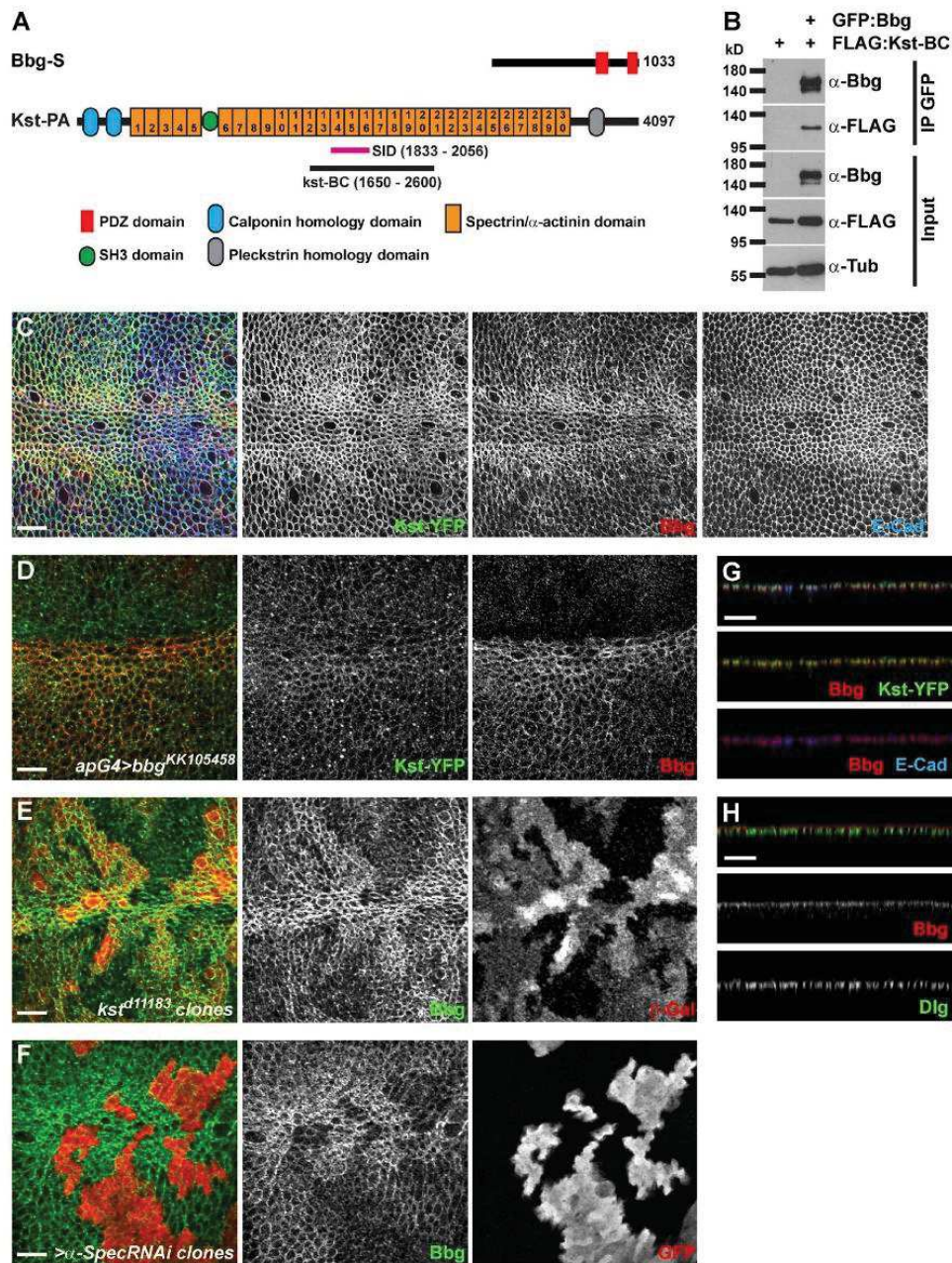


Figure 3. **Bbg binds to the spectrin cytoskeleton.** (A) Schematic diagrams of Bbg and the β H-Spectrin Kst structures. In pink is shown the minimal overlap of the Kst Y2H prey clones interacting with Bbg (SID). In black is shown the newly generated Kst-BC fragment used in colP experiments in B. (B) The Kst-BC fragment coimmunoprecipitates with Bbg. Bottom: Western blot of cleared lysates from cells expressing either FLAG alone (negative control) or FLAG-tagged Kst-BC with GFP-tagged Bbg. Top: Western blot after immunoprecipitation (IP) with anti-GFP. FLAG-tagged Kst-BC was detected only when GFP-Bbg was present. (C) In larval wing imaginal disc epithelial cells, Bbg (red) colocalized with Kst (green). Apical cell junctions were revealed by E-Cad (blue). Note that both Bbg and Kst were found in a cortical ring just inside the membrane-bound belt of E-Cad. (D) The RNAi-mediated depletion of *bbg* in dorsal wing disc cells using the *apterous-Gal4* driver (*apG4*; top part of the image) did not affect the localization of Kst (Kst-YFP; green, middle), whereas Bbg (red, right) was completely absent. (E and F) In *kst* mutant clones marked by the absence of β -Gal (E; red, right) or in clones expressing an α -Spec RNAi transgene marked by the presence of GFP (F; red, right), Bbg (green, middle) was only weakly recruited to the cortex. (G) Z section corresponding with the image in C and showing the overlap between Bbg (red, middle and bottom) and Kst-YFP (green, middle) or E-Cad (blue, bottom). (H) Z section showing that Bbg (red, middle) was localized apically to the septate junctions marker Dlg (green, bottom). Bars, 10 μ m.

Bbg and β H-Spectrin form a complex, the effect of Bbg on cortical F-actin is independent of Kst. Our observations do not rule out, however, that possible redundant mechanisms might

account for the lack of effect of Kst on F-actin, but if they do, they are unlikely to be mediated by an effect on Rho1 or Cpa, because similarly to what we observed for *bbg*, in *kst* mutant

cells, the levels and localization of Rho1 and Cpa were unaffected (Fig. S2, G and H).

Collectively, these results show that Kst and Bbg interact physically and that this interaction is responsible for the cortical apical ring accumulation of Bbg in *Drosophila* wing disc epithelial cells, but they suggest that the cortical Kst-independent pool of Bbg is the active pool controlling cortical actin accumulation.

Bbg, spectrins, and the Hippo pathway

Apart from stabilizing apical cortical F-actin, Bbg also regulates wing tissue growth. We first sought to study the relationship between Bbg and spectrins in the control of wing growth. We thus recombined the two strong *kst*^{d11183} and *bbg*^{EY02818} mutations, which are both located on chromosome 3L. The strong hypomorph *kst*^{d11183} is pupal lethal, reflecting the pleiotropic role of the spectrin cytoskeleton. Unfortunately, the double mutant *kst*^{d11183} *bbg*^{EY02818} did not produce viable adults, and the relationship between Bbg and Kst on adult wing growth could only be studied using inducible localized RNAi-mediated knockdown, in this case in the whole wing pouch territory, with the *nubbin-Gal4* driver. Similarly to *bbg*^{EY02818} mutations, *bbg*^{RNAi} wings were smaller than controls (~5% smaller; Fig. 4, A, B, and G). In contrast and as previously reported (Deng et al., 2015; Fletcher et al., 2015), *kst* or α -*Spec* RNAi-mediated knockdown generated bigger wings than controls (14–18% bigger; Fig. 4, A, C, E, and G). The roles of *bbg* and *spectrins* are therefore opposite. These 5–15% effects on wing growth by RNAi of *bbg* and *spectrins* are within the range of weak mutations in the Hippo pathway such as *kibra* (Fig. S4 A). We then investigated whether any of the effects would impose on the others and generated double RNAi lines. Lowering the dose of *bbg* in the context of impaired *spectrin* levels led to wing tissues that were smaller than *spectrin*^{RNAi} alone but still bigger than *bbg*^{RNAi} alone (Fig. 4, D, F, and G). Even though RNAi-based interactions could be difficult to interpret as they usually reflect partial knockdowns, these results suggest that *bbg* and *spectrins* act either at the same level or independently in the control of wing tissue growth.

But although the *kst*^{d11183} *bbg*^{EY02818} double mutant chromosome could not be used to monitor adult wing size and morphology, we could recover double mutant clones in third instar wing discs. Although *bbg* mutant clones were smaller and possessed fewer cells than their twin spots, *kst* mutant clones were slightly larger and possessed slightly more cells, even though this failed to reach statistical significance (Fig. 4, H and I). Interestingly, double mutant clones were also slightly larger, with slightly more cells. Finally, we did not detect any difference in the apical size of *kst* mutant cells (Fig. 4 J), suggesting that Kst does not control apical constriction. This is reminiscent of the normal apical cortical F-actin belt seen in *kst* mutant cells (Fig. S2 E). Strikingly, in *kst* *bbg* double mutant cells, the apex was enlarged, reminiscent of the *bbg* phenotype and of the impaired cortical actin of *kst* *bbg* double mutant cells (Fig. S2 F).

Collectively, these results suggest that even though spectrins (Kst and α -Spec) are required for the apical cortical enrichment of Bbg, Kst and Bbg have separable functions regarding cortical actin enrichment and apical constriction. Furthermore, Kst and Bbg have opposite effects on wing tissue growth and appear to act either independently or at the same level, converging on a common growth regulator. Recent studies demonstrated that in *Drosophila* and in human cell lines, the spectrin cytoskeleton controls epithelial growth by antag-

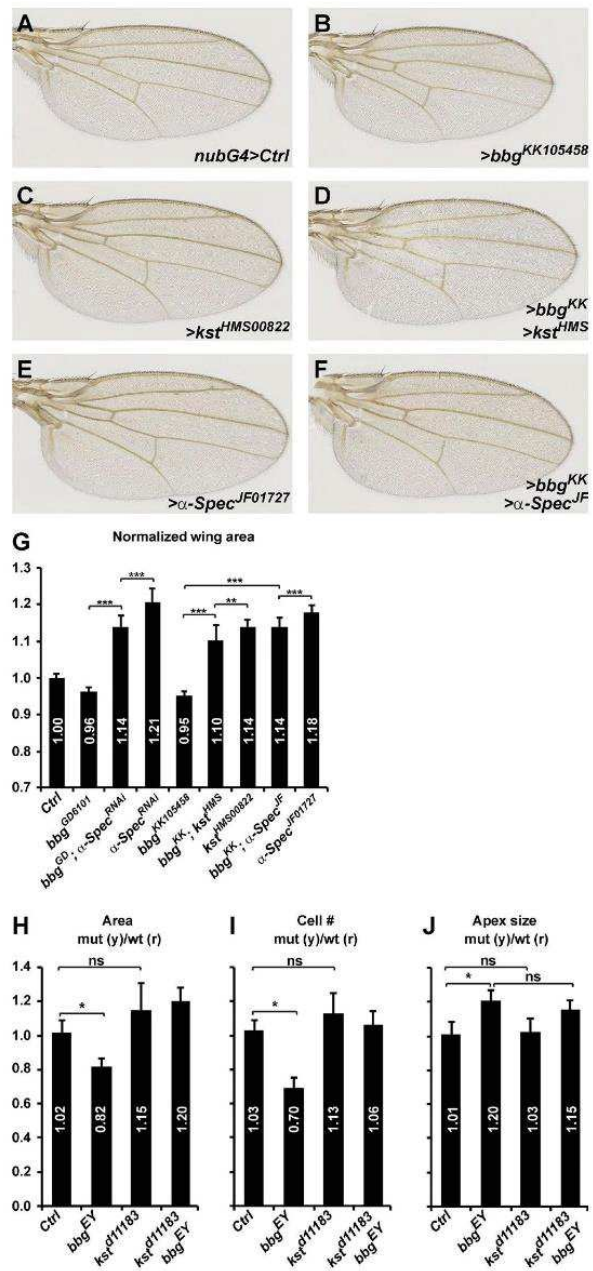


Figure 4. *bbg* can modify the overgrowth of *spectrin* mutants. (A–F) Representative adult female *Drosophila* wings after *nubbin-Gal4* (*nubG4*)-driven RNAi knockdown of the indicated genotypes. Lowering *bbg* dosage can modify (reduce) the overgrowth induced by *kst* or α -*Spec* RNAi. (G) Quantification of the effects shown in A–F. The wing area for each genotype is expressed as a ratio compared with the mean wing area of the *nubG4*>UAS *GFP* controls [Ctrl]. SD is shown; unpaired two-tailed Student's *t* test on raw data; **, $P < 0.01$; ***, $P < 0.001$; $n = 17$ –22 independent female wings. (H–J) Quantification of the mean *FRT80B* mutant clone total areas (H), cell numbers (I), and apical cell sizes (J) of the indicated genotypes shown as the mean ratio between individual mutant tissue clones and their corresponding WT twin spots as shown in Fig. 2. Controls are “empty” clones performed with *FRT80B*. SEM is shown; unpaired two-tailed Student's *t* test; *, $P < 0.05$; $n = 10$ clone pairs from independent discs.

onizing the activity of the proliferation and antiapoptosis transcription coactivators Yki and YAP (Deng et al., 2015; Fletcher et al., 2015; Wong et al., 2015). In *Drosophila*, mutant wing tissues for *α -Spec* or for *β H-Spectrin* exhibit an elevated Yki activity and grow larger than controls. Similarly, human cell lines with impaired *SPECTRINS* exhibit reduced inactive phosphorylated YAP levels.

We thus investigated whether the spectrin-binding Bbg could also be controlling Yki activity and whether *bbg* and *spectrins* have opposite effects as suggested by their adult wing phenotypes (smaller and bigger than WT, respectively; Fig. 1, E and F; Deng et al., 2015; Fletcher et al., 2015). When driven in the posterior part of the wing disc (under the control of the *hh-Gal4* driver), the RNAi-mediated knockdown of *bbg* (Fig. 5, A and F) led to a subtle decreased expression of the Yki activity reporter *ex-LacZ* (Harvey and Tapon, 2007). Conversely, a slight increase in *ex-LacZ* reporter activity was observed when *kst* was impaired (Fig. 5, B and F). These effects were subtle and could not be observed for *Diap1-LacZ*, another Yki activity reporter (Wu et al., 2008). Although the effects observed were very modest, these results suggest that *bbg* acts positively on Yki activity. To better monitor the effects of *bbg* on these Yki-activity reporters, we used two sensitized backgrounds in which Yki-activity was enhanced, thus allowing for a better detection of a putative decreased activity as predicted by the *bbg* adult wing phenotype. Such sensitized backgrounds have been helpful in revealing the role of other Hippo pathway regulators such as *crumbs* or *spectrins* on *ex-LacZ* levels (in combination with *kibra*; Ling et al., 2010; Fletcher et al., 2015).

Indeed and as reported previously (Fletcher et al., 2015), in a *kibra^{RNAi}*-sensitized background, the RNAi-mediated knockdown of *kst* promoted a robust increase in the expression of both *ex-LacZ* and *Diap1-LacZ* reporters (note that in the conditions used, *kibra^{RNAi}* alone did not have any significant effect; Fig. 5, C, D, I, and J). Interestingly, this effect of the double *kst^{RNAi} kibra^{RNAi}* was suppressed by coexpressing an RNAi construct for *bbg* (Fig. 5, E, F, K, and L), further showing that *bbg* acts positively on Yki activity either downstream or in parallel with *kst*. Importantly, even if the spectrin cytoskeleton stabilized a large pool of Bbg in an apical cortical ring, a small pool of Bbg remained tightly associated with the plasma membrane in *spectrins* mutants, which was further affected by *bbg^{RNAi}* in these experiments. However, *bbg* knockdown did not have any effect on the up-regulation of both *ex-LacZ* and *Diap1-LacZ* reporters induced by the knockdown of the core kinase *hippo* (*hpo^{RNAi}*; Fig. 5, F and L; and Fig. S4, B–E). These results therefore suggest that Bbg promotes Yki activity during the growth of larval wing discs but that its action lies at the level of the upstream regulators of the Hippo pathway such as Kib or spectrins and not downstream of the core kinases.

Bbg does not affect upstream Hippo pathway scaffolds

Even though the effects of *bbg* mutations or knockdown on total wing size were modest, they were nevertheless within the range of weak mutations in the Hippo pathway such as *kibra* (see Fig. 5 [C and I] on *ex-LacZ* and *Diap1-LacZ* expressions; see also overall wing size in Fig. S4 A). Collectively, these results suggest that Bbg, contrary to spectrins, promotes Yki activity and wing growth. We thus sought to identify by which mechanisms Bbg could be acting. Given that Bbg is an apical cortical scaffold affected in *kst* mutant tissues, we first investigated

whether the localization of the two β H-Spectrin binding partners and Hippo pathway apical regulators Crb (Thomas et al., 1998; Zarnescu and Thomas, 1999; Médina et al., 2002; Pellicka et al., 2002) and Ex (Hamaratoglu et al., 2006; Maitra et al., 2006; Badouel et al., 2009; Fletcher et al., 2015) could be affected in *bbg* mutant tissues. In *bbg* mutant clones, the correct apical localization of neither Crb nor Ex was affected (Fig. 6, A and B). If anything, we could only detect in a few clones a very subtle down-regulation of Crb or Ex (compare stars and arrowheads in Fig. 6, A and B). However, this is not consistent with the positive role of Bbg on Yki because such a role predicts that *bbg* mutant tissues should exhibit an accumulation of upstream Hippo pathway activators. It appears therefore that Bbg does not control the localization of upstream Hippo pathway activators such as Crb or Ex. Furthermore, if the role of Bbg was to inhibit the activity rather than the localization of apical scaffolds, one would predict that a potent overexpression of these scaffolds would bypass this inhibition and that reducing *bbg* expression would not have any effect on wing size. Using genetic interactions, we could show that although *nubbin-Gal4*-driven overexpressed *ex* led to very reduced adult wings (33% reduction compared with controls; Fig. 6, C and G), the loss of *bbg* by RNAi produced only slightly reduced wings (4% reduction; Fig. 6 G). Strikingly, combining both led to even smaller wings in an additive fashion (Fig. 6, D and G), suggesting that *ex* and *bbg* act either independently or at the same epistatic level to control growth. We then investigated whether *bbg* could be branching on the Hippo pathway further downstream at the level of the core kinases. Although the loss of the *hippo* kinase by RNAi produced enlarged wings (21% increase compared with controls; Fig. 6, E and G), this effect could not be modified by combining it with *bbg^{RNAi}*, reminiscent to what was seen with the Yki activity reporters *ex-LacZ* and *Diap1-LacZ* (Figs. 5 F and S4, B–E), further confirming that Bbg acts in parallel or downstream of the Hippo pathway upstream regulators (such as Kib, Ex, or Kst) but upstream of the core kinase Hippo to regulate wing tissue growth.

Bbg controls MLC phosphorylation

Besides apical scaffolds, the actin cytoskeleton, and in particular its tension, has recently been implicated in the control of Yki activity in growing epithelial tissues, and spectrins have been proposed to inhibit Yki activity by preventing the phosphorylation of the nonmuscle MLC (also known as Spaghetti squash; Sqh), the major regulator of actin cytoskeleton contractility (Rauskolb et al., 2014; Deng et al., 2015). In *bbg* mutant tissue, less filamentous cortical actin was detected, as shown by phalloidin staining (Fig. 2 F). We thus monitored the levels and activity of MLC in *Drosophila* wing discs using a Sqh-GFP fusion protein driven by the endogenous *sqh* promoter because there are no good antibodies to follow the endogenous Sqh protein (*sqh>sqh-GFP*; Martin et al., 2009). In *bbg* mutant cells, there was no gross effect on Sqh-GFP (Fig. 7 A; the weak reduction of apical Sqh-GFP that could be seen in *bbg* clones could reflect that *bbg* mutant cells were apically larger). As previously reported, we could not detect any changes in Sqh-GFP recruitment in *kst* mutant cells (Fig. 7 B; Deng et al., 2015). The activity of MLC is controlled by phosphorylation by a range of kinases including Rho-kinase (ROK), and p-MLC promotes contractility of the actin cytoskeleton (Rauskolb et al., 2014). We therefore also monitored the activity level of MLC using an anti-p-MLC antibody that cross-reacts in *Drosophila* on whole-disc protein

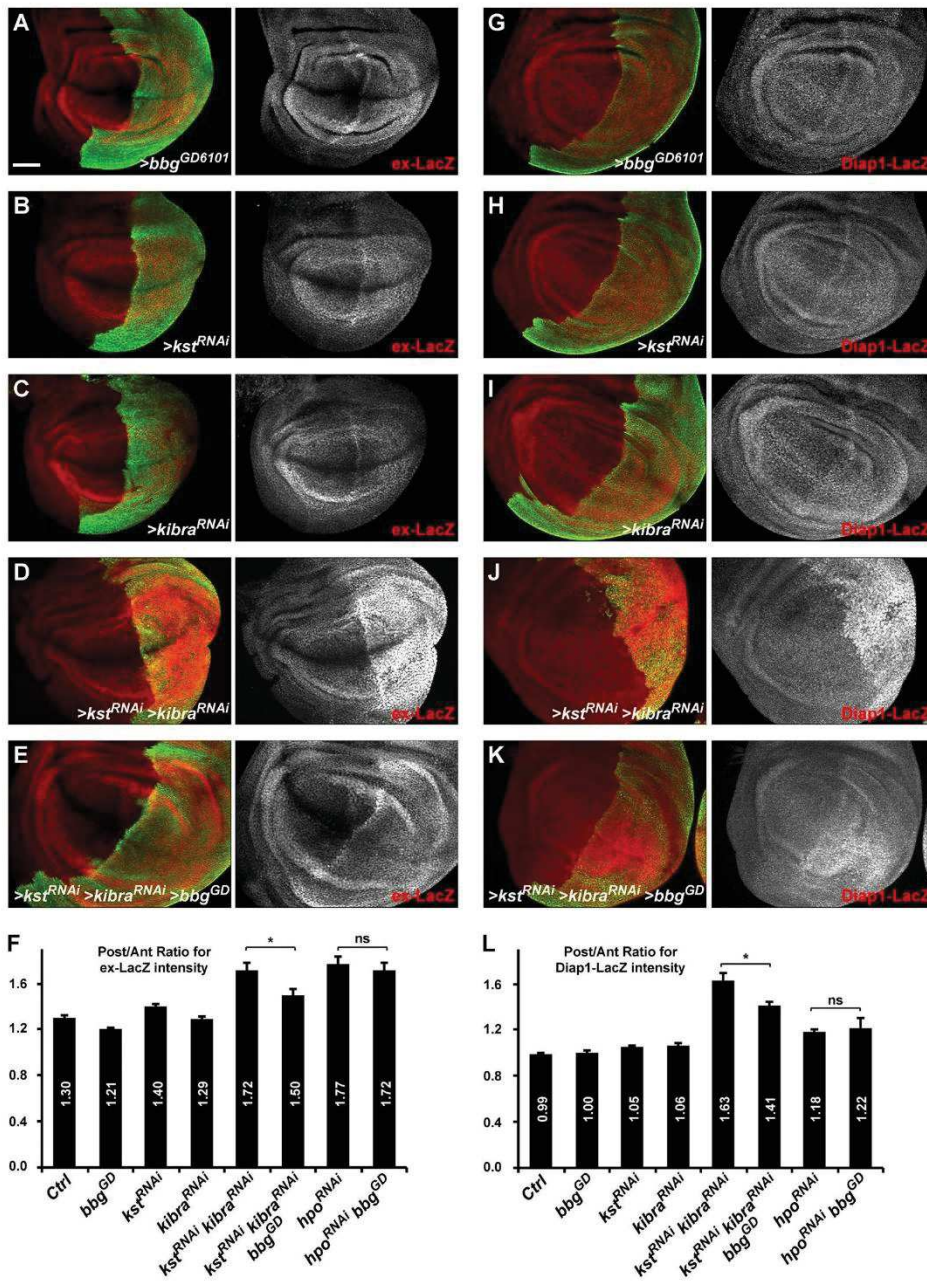


Figure 5. *bbg* controls Yki activity. (A–E and G–K) Pouch region of third instar larva wing imaginal discs. Effects of *hh-Gal4*-driven RNAi knockdown in the posterior compartment marked by GFP (green) on the expression of the Yki activity reporters *ex-LacZ* (A–E, red) and *Diap1-LacZ* (G–K, red). The expression of *ex-LacZ* or *Diap1-LacZ* was almost not affected when *bbg* (A and G), *kst* (B and H), or *kibra* (C and I) are knocked down individually. Although a strong Yki activity was detected after double RNAi for *kst* and *kibra* (D and J), this was partially suppressed by *bbg* RNAi (E and K). Bar, 50 μ m. (F and L) Quantifications of the effects presented in A–E for *ex-LacZ* (F) and in G–K for *Diap1-LacZ* (L). Results are presented as means of ratios calculated for each experimental disc between the mean gray intensity (reflecting reporter expression) of the posterior compartment (GFP positive) and the mean gray intensity of the corresponding anterior compartment. Note that in control discs, the expression of *ex-LacZ* was stronger in the posterior compared with the anterior. SEM is shown; unpaired two-tailed Student's *t* test; *, $P < 0.05$; $n = 10$ –13 independent discs.

extracts. Consistent with previously published results, p-MLC levels were increased in *kst* mutants (Fig. 7 C; Deng et al., 2015). Opposite to *kst*, in *bbg* mutant discs, p-MLC levels were decreased compared with WT controls. Strikingly, in *kst bbg* double mutant discs, p-MLC levels were also slightly increased,

mimicking what was seen in single *kst* mutants (Fig. 7 C). These results show that Bbg promotes p-MLC accumulation and suggest that Kst might be acting downstream of Bbg, compatible with a model where Bbg prevents the destabilizing effect of Kst. These results suggest that the sparse actomyosin network

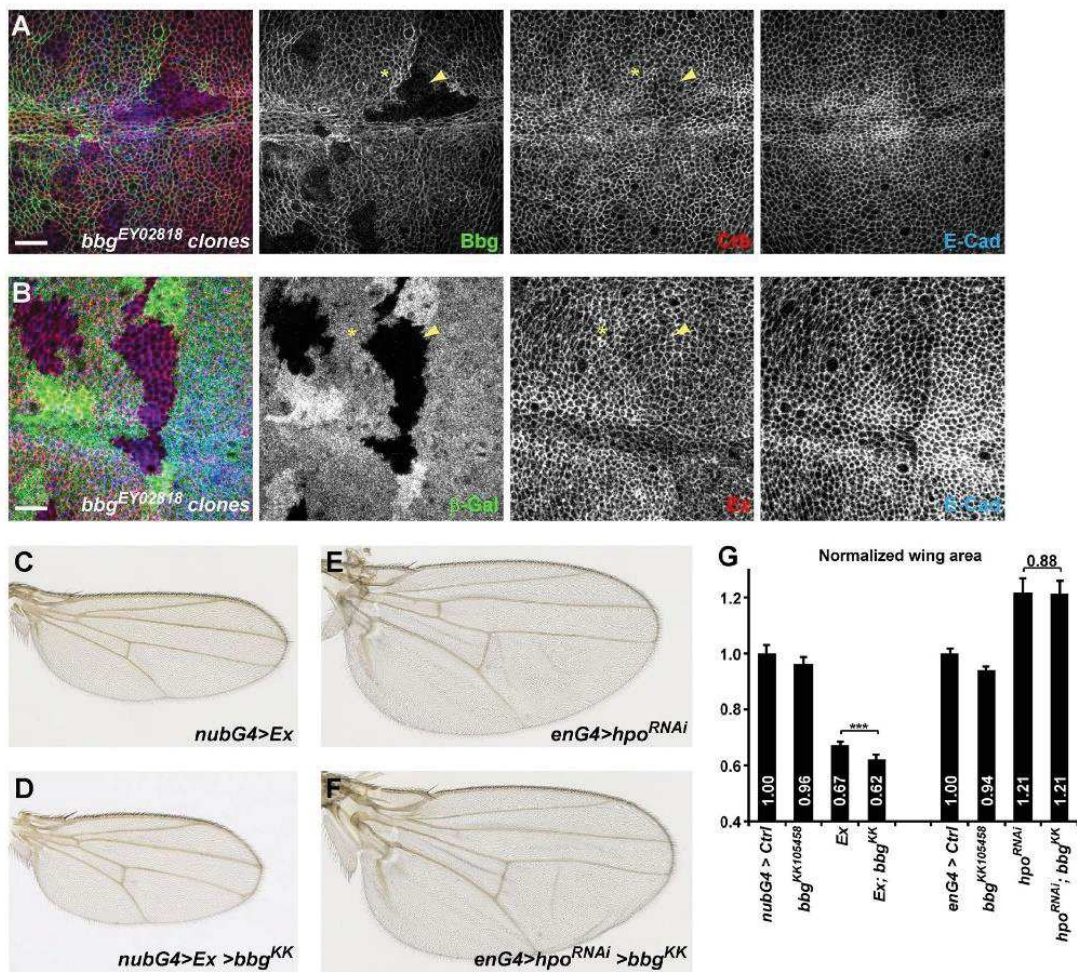


Figure 6. The upstream Yki negative regulators Crb and Ex are not affected in *bbg* mutants. (A and B) In *bbg* mutant clones stained for E-Cad (blue) and marked by the absence of Bbg (A, red) or β -Gal (B, red), the localization and levels of Crb (A, green) or Ex (B, green) were not affected or weakly reduced (compare yellow arrowheads [mutant] with yellow asterisks [WT]). Bars, 10 μ m. (C and D) Genetic interaction between *bbg* and *ex*. Although overexpressed *ex* under the control of the *nubG4* driver led to strongly reduced wings (C), this effect was further enhanced when *bbg* was knocked down by RNAi (D). (E and F) Genetic interaction between *bbg* and *hpo*. Although the knockdown of *hippo* by RNAi under the control of the *engrailed-Gal4* (*enG4*) driver led to strongly enlarged wings (E), this effect could not be modified by further impairing *bbg* (F). (G) Quantification of the effects shown in C–F. The wing area for each genotype was expressed as a ratio compared with the mean wing area of controls (*nubG4>UAS GFP* controls on the left, and *enG4>UAS GFP* controls on the right). SD is shown; unpaired two-tailed Student's *t* test on raw data; ***, $P < 0.001$; $n = 17$ –22 independent female wings.

in *bbg* mutants could be less amenable to contractile behavior. Indeed, when providing a constitutively activated version of Sqh (SqhEE, mimicking the activating phosphorylation of Sqh by ROK), *bbg* mutant cells were able to apically constrict again (Fig. 7 D), and the overall undergrowth effect of *bbg* knockdown on the adult wing size was suppressed (Fig. 7 E).

These results support a model in which Bbg promotes a contractile actomyosin network at the cortex of wing epithelial cells through the stabilization of cortical F-actin and activated p-MLC. However, because *kst bbg* double mutant cells are still as apically relaxed as *bbg* mutant cells (Fig. 4 J) even though they appear to have higher p-MLC levels, the simple enrichment in activated Sqh is not the only factor controlling apical cell size. The architecture and levels of F-actin might also be critical. More studies are needed to better understand the respective contributions of F-actin,

of p-MLC, and of their localization within epithelial cells on apical constriction.

Recently, a tensile actin–myosin network has been shown to promote the recruitment of the Hippo pathway–negative regulator and LIM domain–containing scaffold Ajuba (Jub). This actin-dependent Jub accumulation has been proposed to inhibit the Hippo pathway and increase Yki activity (Rauskolb et al., 2014) at least in part through the binding and inhibition of Wts (Das Thakur et al., 2010). We therefore investigated whether the positive effect of Bbg on Yki could be mediated through Jub relocation. Indeed, the RNAi-mediated knockdown of *bbg* in the posterior wing compartment (using the *engrailed-Gal4* driver) led to a reduction of Jub cortical recruitment in the posterior cells as evidenced using a Jub-GFP fusion protein (Fig. 7 F). This effect was suppressed by providing a constitutively active Sqh (SqhEE; Fig. 7 G), showing

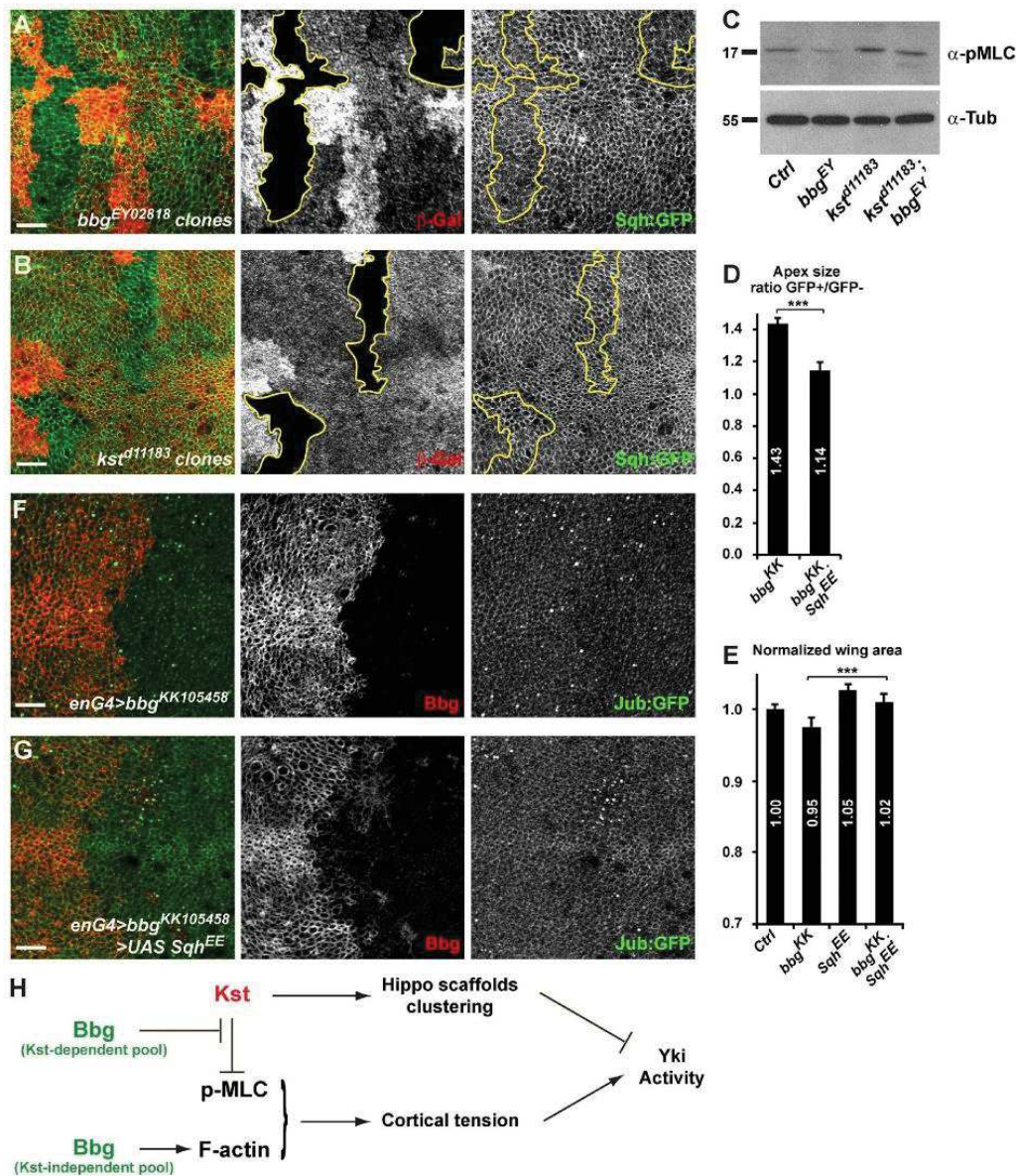


Figure 7. Bbg controls p-Sqh levels and Jub cortical recruitment. (A and B) *bbg* (A) or *kst* (B) mutant clones (outlined in yellow) marked by the absence of the β -Gal marker (red) and the apical accumulation of the MLC regulatory subunit Sqh (Sqh-GFP; green). (C) Western blot of cleared lysates from third instar larval homozygous mutant wing discs reveals a decrease in p-Sqh (anti-pMLC) levels in *bbg* mutants (0.76 ± 0.20 times), whereas the levels were up-regulated in *kst* (1.44 ± 0.24) and *kst bbg* double mutants (1.51 ± 0.23). Tubulin (anti-Tub) was used as a loading control and for normalization. Molecular masses are given in kilodaltons. (D) Quantification of the mean apical cell size in overexpression clones for *bbg^{RNAi}* (left) and for *bbg^{RNAi}* with a constitutively active form of Sqh (SqhEE; right) and shown as the mean ratio between GFP-positive tissues (overexpressing) and GFP-negative tissues (non-expressing controls) in individual experimental wing discs (see the Cell numbers and apical cell size section of Materials and methods). SEM is shown; unpaired two-tailed Student's *t* test; $n = 12$ area pairs from independent discs. (E) Quantification of the wing area after SqhEE overexpression. Each genotype is expressed as a ratio compared with the mean wing area of the *nubG4>UAS GFP* controls (Ctrl). SD is shown; unpaired two-tailed Student's *t* test based on raw data; ***, $P < 0.001$; $n = 17$ –20 independent female wings. (F and G) Effect of *bbg* depletion marked by the absence of Bbg (red) on the apical recruitment of the Hippo-negative regulator Jub (Jub-GFP; green). Cells depleted for *bbg* (F) had slightly lower levels of Jub-GFP. This effect was suppressed when an activated form of Sqh (SqhEE) was coexpressed (G). Bars, 10 μ m. (H) Model for the action of Bbg on the regulation of actin and growth in the *Drosophila* wing imaginal discs. Bbg bound to the spectrin cytoskeleton (Kst) accumulates at the cortex of epithelial cells, where it opposes the effect of Kst on MLC phosphorylation. Bbg, through its role on the actin cytoskeleton, promotes cortical tension and Jub recruitment, negatively impinging on the Hippo signaling pathway to promote proper growth of the tissue.

that experimentally promoting a more contractile actomyosin network in *bbg*-depleted cells is sufficient to restore Jub-GFP recruitment. Therefore, we propose that by stabilizing F-actin

and phosphorylated active Sqh at the apical cortex, Bbg promotes Yki activity in wing discs at least in part through the local recruitment of Jub (Fig. 7 H) to sustain correct tissue growth.

Furthermore, our results highlight a critical role for Bbg in controlling F-actin apical enrichment independently of Kst or of the Cpa–Ena capping complex and support a model where the pool of Bbg that is apically recruited by Kst acts there to inhibit the destabilizing role of Kst on p-MLC (Fig. 7 H).

Discussion

Investigating the role of PDZ-containing protein scaffolds, we describe in this study a new role for the previously reported *bbg* gene in regulating epithelial wing disc cell numbers. Even though our studies were primarily focused on wing imaginal discs, *bbg* must exert its role in other epithelial tissues such as imaginal leg discs because *bbg* mutant legs are ~10% shorter than WT controls. Performing an unbiased Y2H screen, we show that the spectrin cytoskeleton, and in particular the β H-Spectrin subunit Kst, binds and stabilizes Bbg at the apical cortex. But even though spectrins recruit Bbg, Bbg plays an opposite role to that of spectrins on tissue growth and cell number control, and contrary to spectrins, Bbg promotes p-MLC enrichment and Yki activity. Based on detailed phenotypic analysis of *bbg* mutant cells, our work supports a role for Bbg independent of spectrins to stabilize a dense actomyosin network, promoting the recruitment of the Hippo pathway–negative regulator Jub, which was shown to then inhibit Wts activity (Rauskolb et al., 2014). Given the emerging link between actin dynamics and contractility and the regulation of the Hippo pathway (Dupont et al., 2011; Fernández et al., 2011; Sansores-Garcia et al., 2011; Yu and Guan, 2013; Gaspar and Tapon, 2014), we propose that through its role on the actomyosin cytoskeleton, *bbg* ultimately impinges on the activity of the terminal Hippo effector Yki to fine-tune epithelial cell numbers.

Spectrins and Bbg

The relationship between Kst and Bbg appears therefore complex. Kst binds and helps to recruit Bbg at the apical cortex, suggesting that Bbg could be acting downstream of the spectrin cytoskeleton. But even though spectrins stabilize Bbg at the cortex, Bbg and spectrins have opposite roles on overall wing growth and cell number. Furthermore, despite their physical association, Bbg acts independently of Kst to promote the apical enrichment of F-actin and more modestly of the myosin II regulatory subunit Sqh.

However, although Kst and Bbg have different roles on cortical actin, they converge to control the phosphorylation and activity of Sqh, albeit in opposite ways. Indeed, our study shows that Bbg promotes p-Sqh accumulation (Fig. 7 C), and previous research has shown that Kst prevents p-Sqh upstream of ROK (Deng et al., 2015). These opposite effects on p-Sqh are reminiscent to the opposite phenotypes of *bbg* and *kst* mutations on adult wing size (smaller and bigger, respectively). Given the one-way link between Kst and Bbg, namely that Kst controls Bbg accumulation, whereas Bbg has no effect on Kst (Fig. 3 E), one possible model is that through its binding and recruitment in a broad cortical ring, the Kst-trapped Bbg inhibits the negative role of Kst on p-Sqh. Indeed, we note that in *kst* or α -*Spec* mutant cells, some Bbg protein is still present at the cortex, suggesting that at least two pools of Bbg exist and that other mechanisms act in parallel with spectrins to promote Bbg cortical localization. Alternatively, the effect of Kst on Bbg localization could be completely independent from the action of Kst on tissue growth, and despite

their physical interaction, Kst and Bbg could be acting through independent mechanisms converging on Sqh phosphorylation.

It appears therefore that the opposite effects of Bbg and Kst could be explained, at least in part, by their opposite effects on p-Sqh accumulation and contractility of the apical cortical actin network and their final effect on Yki activity: positive for Bbg and negative for Kst. We propose that the modification of Yki activity in *kst* mutants by the *bbg* mutation as reported by the *ex-LacZ* and *Diap1-LacZ* reporters reflects a modulation of the actin contractility (total F-actin levels and p-Sqh) by combining these two mutations.

Bbg stabilizes both apical F-actin and total p-Sqh levels, promoting a more contractile actomyosin cytoskeleton, a more constricted cellular apex, and the recruitment of the Wts inhibitor Jub. It is noteworthy that, even though Kst has been proposed to regulate Sqh activity, Kst does not appear to control Yki activity through Jub and Wts membrane recruitment (Deng et al., 2015) as would be predicted if Kst were indeed modifying actin cytoskeleton tension (Rauskolb et al., 2014). Alternatively, Kst has been proposed to prevent Yki function independently of actin regulation through the clustering of Hippo pathway upstream activators such as Crb (Fletcher et al., 2015). Future studies will help clarify some of these seemingly contradictory observations arising in part from the high degree of functional redundancy of the Hippo pathway upstream activators and the modular nature of the scaffolds involved. We note here that *bbg* cannot modify the *hpo* mutants, which could suggest that the actin-mediated regulation of Yki activity could be independent of the core Hippo pathway. Indeed, the role of the core Hippo and Wts kinases in response to mechanical stress or cytoskeletal changes is still unclear (Gaspar and Tapon, 2014). Alternatively, it could reflect the fact that core Hippo pathway members exhibit effects that are too strong to be modified. Future studies will help clarify whether the actin cytoskeleton influence on Yki is independent or not of the core Hippo pathway.

Bbg and cortical actin regulation

Even though regulating actin, Bbg does not have any obvious actin-binding domain. However, spectrins can bind to F-actin (Baines, 2009), but the role of Bbg on actin is unlikely mediated by the apical spectrin cytoskeleton because the organization or stability of F-actin fibers were unaffected in *kst* mutants even though Bbg levels and localization were strongly reduced (Thomas et al., 1998; Deng et al., 2015; this study). We observed, however, that a small fraction of Bbg was still present just under the membrane, suggesting that this small fraction of Bbg, which localizes independently of spectrins, is sufficient for Bbg-mediated cortical actin organization.

Among the different actin organizers that we could test, we could only detect a weak down-regulation of Ena in *bbg* mutant cells, suggesting that the capping protein inhibitor Ena/VASP could be implicated. During border cell migration, cortical Wts has been shown to phosphorylate and inhibit Ena activity, leading to a polarized and functional actin cytoskeleton (Lucas et al., 2013). It is therefore possible that through the recruitment of Jub and cortical inhibition of Wts (Rauskolb et al., 2014), Bbg promotes Ena enrichment. However, modulating Ena levels did not produce F-actin disruptions similar to those observed in *bbg* mutant cells, and the effect of Ena on cortical F-actin in wing disc cells must be more subtle. Furthermore, the enrichment in F-actin observed in *cpa*-deficient cells was completely suppressed by mutations in *bbg*. These striking observations suggest that the elongated actin filaments in

cpa mutants require an intact *bbg* function to accumulate apically in epithelial cells. Further studies are therefore required to clarify the complex link between Bbg, spectrins, and cortical F-actin stabilization along with how this fine-tunes Yki activity.

A general role for Bbg

bbg mutants were originally described as more sensitive to knocking disturbances (“bang;” Kim et al., 2006), suggesting that they could have neuronal functions in sensing or responding to that stimulus. Bbg has also been implicated in gut immune tolerance, and *bbg* mutant flies die prematurely in cases of bacterial infection with signs of weakened gut epithelial barrier (Bonney et al., 2013). Finally, a targeted RNAi screen identified *bbg* as a key regulator of border cell migration in the adult female egg chamber, with *bbg*-knockdown cells migrating slower than WT (Aranjuez et al., 2012). All these different phenotypes could be explained by subtle defects in the actin cytoskeleton, and it would be interesting to revisit these earlier studies in light of our results. In particular, both the spectrin cytoskeleton (Lee et al., 1997; Zarnescu and Thomas, 1999) and the Hippo pathway (Lucas et al., 2013) have been implicated in the regulation of border cell migration, which could represent a suitable system to study further the complex regulations between spectrins, actin dynamics, apical scaffolds, and the Hippo pathway.

Materials and methods

Drosophila genetics

The viable *bbg*³⁴ allele was generated by exchanging the MiMIC cassettes to introduce loxP sites in the same orientation in the two MiMIC lines *Mi[MIC]MI0323* and *Mi[MIC]MI04312* that flank the two large 5' exons coding for specific regions for the long (*bbg*-RC and *bbg*-RK) and medium (*bbg*-RJ) *bbg* isoforms. After providing a pulse of Cre recombinase, the precise deletion of these two exons was followed by PCR on genomic DNA (see Fig. S1).

The viable *bbg*^{EY02818} allele is a *P*-transposable element *P{EPgy2}* *bbg*^{EY02818} and was cleaned of an unrelated lethal mutation by six rounds of back crossing to a WT stock. Mapping of this *P*-element insertion was then confirmed by PCR on genomic DNA to disrupt the large 3' exon common to all *bbg* isoforms.

All *bbg* alleles (*bbg*³⁴ and *bbg*^{EY02818}) were then recombined on *FRT80B* chromosomes to perform mitotic clonal analysis. The *bbg* loss-of-function phenotype was obtained either as *bbg*^{EY02818} homozygous or by crossing *bbg*^{EY02818} with the *Df(3L)Exel6123* spanning the *bbg* locus.

The full-length *bbg* coding sequence corresponding with the long (*bbg*-RK), medium (*bbg*-RJ), or short (*bbg*-RF) isoforms were amplified by PCR as four different fragments and later reassembled by using conveniently located unique restriction sites using as template either the partial cDNA RE18302, newly generated random primed cDNAs from wing discs, or the BACPAC clones CH322-2L24 and CH322-132B5. These *bbg* isoforms were then cloned in the pKC26w-pUbiq rescue plasmid that allows expression of the cloned fragments under the ubiquitous ubiquitin promoter. All transgenes were inserted at the same chromosomal location (51C) using phiC31-mediated integration on the *M{3xP3-RFP.attP}ZH-51C* landing platform.

RNAi-mediated knockdown experiments were performed using the *nubbin-Gal4* (all cells in the pouch central region of third instar wing discs), *hedgehog-Gal4* or *engrailed[e16E]-Gal4* (posterior compartment of the wing disc), *apterous-Gal4* (dorsal wing disc), or randomly generated flip-out clones (using the γ -, *hsFLP122*; *Act FRT* γ + *FRT Gal4*, *UAS* *GFP* line) to drive the expression of differ-

ent RNAi-containing transgenes under upstream activation sequence (UAS) control. Crosses were usually cultivated at 30°C to allow maximum RNAi activity. The *bbg* RNAi lines used were the *bbg*^{GD6101} and *bbg*^{KK105458} from the Vienna Drosophila Research Centre, which were shown previously to promote very efficient *bbg* knockdown (Aranjuez et al., 2012). Genomic PCR following published guidelines (Vissers et al., 2016) showed that the *bbg*^{KK105458} contained only one insertion on platform 30B, and therefore was devoid of the reported “*tiptop* effect.”

Mutant clones were generated at high frequency in the wing using *abxUbxFLPase* in combination with *FRT80B bbg*³⁴, *FRT80B bbg*^{EY02818}, or *FRT80B kst*^{d11183}.

Bbg antibody generation

The sequences corresponding with aa 2,317–2,637 of the Bbg-PK protein (IVEEADPP...GPVKICFA) were cloned in frame with the glutathione S-transferase (GST) gene in the pGEX-6P-1 expression vector. The GST fusion protein was produced in *Escherichia coli* bacteria grown at 30°C after induction with 1 mM IPTG and purified on glutathione agarose beads (Thermo Fisher Scientific) before being eluted with an excess of free reduced glutathione (50 mM NaH₂PO₄, 300 mM NaCl, 1 mM DTT, 50 mM glutathione reduced, 1× cOmplete protease inhibitors [Roche], and 0.1% Triton X-100, pH 8). Rabbits were immunized with the purified protein (four rounds of injection with 200 μ g each over a 3-mo period; Eurogentec). The best animal responder was then selected, and the serum was collected to produce the polyclonal rabbit anti-Bbg antibody.

Wing measurements

15–20 wings from independent females were mounted, imaged using NDP.view, and measured using ImageJ (National Institutes of Health). For quantification of RNAi effects, the ratio between the area of each experimental wing and the mean area of control wings (Gal4 driving a UAS GFP transgene) was calculated. Statistical significance was determined using unpaired, two-tailed Student's *t* tests on raw wing measurements.

Cell numbers and apical cell size

In Figs. 2 and 4, mutant clones were generated by flippase-mediated FRT chromosome exchange. In this experimental setup, mutant clones and their twin spots originated from the same parental cell and should be of the same size and have the same number of cells. The apical size of cells was obtained by dividing clone area by the number of cells.

In Fig. 7, the mutant clones were generated by the overexpression of RNAi or UAS constructs. They were marked by GFP. In this setup, the size of the mutant GFP-positive tissue could not be compared with any WT counterpart, and we could not assess differences in clone size or cell numbers. Counting cells between equivalent area within each disc, the change in apical size of cells between control (GFP⁻) and mutant cells (GFP⁺) was evaluated.

Y2H screen

The Bbg-S Y2H screen was performed by Hybrigenics SA. Full-length Bbg-S (lacking its last 4 aa, which represent a potential palmitoylation site that could have interfered with the yeast nucleus targeting of the Bbg bait fusion) was cloned as an N-terminal LexA fusion in pB27 and used as a bait against a *Drosophila* whole embryo (0–24 h) cDNA library (RP2) in 0.0 mM 3-amino triazole. 7.39×10^7 clones were screened, from which 177 positive clones were recovered and retested under the same conditions as the screen. Putative positive hits such as Kst were confirmed by coIP in S2 cells.

Plasmids for cell culture

In *Drosophila* S2 cells, genes were expressed either by cotransfecting an Act5C-Gal4 plasmid (gift from B. Shilo, Weizmann Institute of

Science, Rehovot, Israel) with UAS plasmids for the genes of interest or by using the Act5C promoter driven gateway destination vectors from the Drosophila Gateway Vector collection (<http://emb.carnegiescience.edu/drosophila-gateway-vector-collection>). The Kst fragments (Kst-A^{1-1,632}, Kst-B^{1,633-1,903}, Kst-C^{1,904-2,632}, and Kst-D^{2,594-4,097}) were described previously (Fletcher et al., 2015) and were used to generate the pAWF-Kst-BC^{1,650-2,600} construct by PCR using linker primers spanning over the codons corresponding with the Kst aa 1,898 and 1,909. Primers used were sense, 5'-GAAGCGACAGGAACAAC CAGAATTCTCTGGGAGAAC-3', and anti-sense, 5'-GTTCTCCCA GGAAGTTCGAGTTGTCTCTGTCGCTTC-3'.

Western blotting and immunoprecipitation

All immunoprecipitations were done in lysates from S2 cells grown in Schneider's *Drosophila* medium (Gibco) supplemented with 10% FCS (Sigma-Aldrich), 100 U/ml penicillin, and 100 µg/ml streptomycin. 3.10⁶ S2 cells were transfected using Effectene (QIAGEN). 48 h after transfection, S2 cells were lysed with Hepes lysis buffer (50 mM Hepes NaOH, pH 7.5, 150 mM NaCl, and 0.5% Triton X-100) supplemented with 1 mM DTT and cOmplete protease inhibitor cocktail. Half of the lysate was incubated with Sepharose beads with 3 µl of rabbit anti-GFP antibody (TP401; Torrey Pines Biolabs) for 1 h at 4°C. The beads were washed with Hepes lysis buffer four times.

After SDS-PAGE protein gel separation, proteins were visualized by immunoblotting using rabbit anti-GFP (1:2,000; TP401; Torrey Pines Biolabs), mouse anti-FLAG (1:5,000; F1804; Sigma-Aldrich), rabbit anti-pMLC2 (1:500; 3671; Cell Signaling Technology), and mouse antitubulin (1:10,000; DM1A; Sigma-Aldrich) antibodies.

Immunocytochemistry

Antibody staining of wing imaginal discs were performed using standard protocols. In short, larval heads containing the brain and imaginal discs were dissected in PBS, fixed for 20 min at RT in PBS with 4% formaldehyde, washed 3× for 10 min in PBS with 0.2% Triton X-100 (PBX), and blocked for 30 min in PBX with 0.1% BSA. Primary antibodies were then incubated overnight at 4°C under gentle agitation in PBX and 0.1% BSA at the indicated dilutions (see next paragraph). Samples were then washed 3× for 15 min in PBX, and fluorescent dye-coupled secondary antibodies were incubated for 90 min in PBX and 1% BSA at RT. After several washes in PBX, the stained tissues were then transferred to CitiFluor AFI (Agar) mounting media for overnight equilibration. Individual discs were then dissected and mounted in CitiFluor. Images were acquired with an SP2-405 confocal microscope (Leica Microsystems) or an Apotome2 microscope (ZEISS) and processed using ImageJ.

Primary antibodies used were: mouse anti-Arm (1:25; N2 7A1; Developmental Studies Hybridoma Bank [DSHB]), mouse anti-β-galactosidase (1:25; 40-1a; DSHB), mouse anti-Crb (1:25; Cq4; DSHB), mouse anti-Dlg (1:25; 4F3; DSHB), mouse anti-Ena (1:200; 5G2; DSHB), mouse anti-Rho1 (1:25; p1D9; DSHB), rabbit anti-aPKC (1:500; anti-PKCz C-20; Santa Cruz Biotechnology, Inc.), rabbit anti-Bbg (1:5,000; polyclonal directed against Bbg aa 2,317–2,637 generated for this study), rabbit anti-Cpa (1:200; a gift from F. Janody; Amândio et al., 2014), rabbit anti-Dia (1:500; a gift from S. Wasserman; Afshar et al., 2000), rabbit anti-Ex (1:1,000; a gift from R. Fehon; Maitra et al., 2006), rabbit anti-GFP (1:200; TP401; Torrey Pines Biolabs), rabbit anti-Pyd (1:2,000; Djiane et al., 2011), and rat anti-E-Cad (1:25; DCAD2; DSHB). Actin fibers were visualized using TRITC-phalloidin (1:500; P1951; Sigma-Aldrich). Secondary antibodies used were conjugated to the Alexa Fluor 350, Alexa Fluor 488, Cy3, or Alexa Fluor 647 fluorochromes (1:500; Jackson ImmunoResearch Laboratories, Inc.).

Diap1-LacZ and ex-LacZ quantifications

Quantifications were performed as described previously (Djiane et al., 2014). In brief, in each wing disc, the mean level of gray was measured by ImageJ in an equivalent area in the anterior (non-GFP) and posterior (GFP) of the wing pouch, excluding the anterior/posterior and dorsal/ventral boundaries, which show discontinuities.

Online supplemental material

Four supplemental figures are provided, detailing the generation of the *bbg*³⁴ mutant affecting specifically the *bbg-M* and *bbg-L* isoforms (Fig. S1), the effects of *cpa*, *enabled*, and *karst* on cortical F-actin in third instar wing discs (Fig. S2), the effects of *bbg* mutants on apico-basal markers (Fig. S3), and the relationship between *bbg* and the core Hippo pathway (Fig. S4).

Acknowledgments

We thank Amel Zouaz for help with *Drosophila* S2 cell cultures and François Schweisguth for discussions. We thank Richard Fehon, Georgina Fletcher, Florence Janody, Duoqia Pan, Nic Tapon, Barry Thompson, Mirka Uhlirva, Koen Venken, Xiabao Wang, and Steven Wasserman for sharing flies, constructs, and antibodies. We acknowledge the Bloomington Drosophila Stock Center, the Vienna Drosophila Stock Center, the DGRC Kyoto Stock Center, and the Developmental Studies Hybridoma Bank for flies and antibodies.

This work was supported by grants from the Fondation ARC pour la Recherche sur le Cancer (PJA 20141201630), the Ligue Nationale Contre le Cancer (9F112549ROSA), a European Commission Marie Curie Career Integration Grant (PCIG13-GA-2013-618371), and the ATIP/Avenir Programme.

The authors declare no competing financial interests.

Author contributions: conceived and analyzed experiments: E. Forest, L. Heron-Milhavet, and A. Djiane. Performed experiments: E. Forest, R. Logeay, C. Géminard, D. Kantar, L. Heron-Milhavet, F. Frayssinoux, and A. Djiane. Wrote the manuscript: A. Djiane.

Submitted: 16 May 2017

Revised: 22 October 2017

Accepted: 2 January 2018

References

- Afshar, K., B. Stuart, and S.A. Wasserman. 2000. Functional analysis of the *Drosophila* diaphanous FH protein in early embryonic development. *Development*. 127:1887–1897.
- Amândio, A.R., P. Gaspar, J.L. Whited, and F. Janody. 2014. Subunits of the *Drosophila* actin-capping protein heterodimer regulate each other at multiple levels. *PLoS One*. 9:e96326. <https://doi.org/10.1371/journal.pone.0096326>
- Aranjuez, G., E. Kudlaty, M.S. Longworth, and J.A. McDonald. 2012. On the role of PDZ domain-encoding genes in *Drosophila* border cell migration. *G3 (Bethesda)*. 2:1379–1391. <https://doi.org/10.1534/g3.112.004093>
- Badouel, C., L. Gardano, N. Amin, A. Garg, R. Rosenfeld, T. Le Bihan, and H. McNeill. 2009. The FERM-domain protein Expanded regulates Hippo pathway activity via direct interactions with the transcriptional activator Yorkie. *Dev. Cell*. 16:411–420. <https://doi.org/10.1016/j.devcel.2009.01.010>
- Baines, A.J. 2009. Evolution of spectrin function in cytoskeletal and membrane networks. *Biochem. Soc. Trans.* 37:796–803. <https://doi.org/10.1042/BST0370796>
- Baumgartner, R., I. Poembacher, N. Buser, E. Hafen, and H. Stocker. 2010. The WW domain protein Kibra acts upstream of Hippo in *Drosophila*. *Dev. Cell*. 18:309–316. <https://doi.org/10.1016/j.devcel.2009.12.013>
- Bear, J.E., and F.B. Gertler. 2009. Ena/VASP: towards resolving a pointed controversy at the barbed end. *J. Cell Sci.* 122:1947–1953. <https://doi.org/10.1242/jcs.038125>

- Bennett, V., and A.J. Baines. 2001. Spectrin and ankyrin-based pathways: metazoan inventions for integrating cells into tissues. *Physiol. Rev.* 81:1353–1392. <https://doi.org/10.1152/physrev.2001.81.3.1353>
- Bonnay, F., E. Cohen-Berros, M. Hoffmann, S.Y. Kim, G.L. Boulianne, J.A. Hoffmann, N. Matt, and J.-M. Reichhart. 2013. big bang gene modulates gut immune tolerance in *Drosophila*. *Proc. Natl. Acad. Sci. USA.* 110:2957–2962. <https://doi.org/10.1073/pnas.1221910110>
- Chen, C.-L., K.M. Gajewski, F. Hamaratoglu, W. Bossuyt, L. Sansores-Garcia, C. Tao, and G. Halder. 2010. The apical-basal cell polarity determinant Crumbs regulates Hippo signaling in *Drosophila*. *Proc. Natl. Acad. Sci. USA.* 107:15810–15815. <https://doi.org/10.1073/pnas.1004060107>
- Codelia, V.A., G. Sun, and K.D. Irvine. 2014. Regulation of YAP by mechanical strain through Jnk and Hippo signaling. *Curr. Biol.* 24:2012–2017. <https://doi.org/10.1016/j.cub.2014.07.034>
- Das Thakur, M., Y. Feng, R. Jagannathan, M.J. Seppa, J.B. Skeath, and G.D. Longmore. 2010. Ajuba LIM proteins are negative regulators of the Hippo signaling pathway. *Curr. Biol.* 20:657–662. <https://doi.org/10.1016/j.cub.2010.02.035>
- Deng, H., W. Wang, J. Yu, Y. Zheng, Y. Qing, and D. Pan. 2015. Spectrin regulates Hippo signaling by modulating cortical actomyosin activity. *eLife.* 4:e06567. <https://doi.org/10.7554/eLife.06567>
- Djiane, A., H. Shimizu, M. Wilkin, S. Mazleyrat, M.D. Jennings, J. Avis, S. Bray, and M. Baron. 2011. Su(dx) E3 ubiquitin ligase-dependent and -independent functions of polychaetoid, the *Drosophila* ZO-1 homologue. *J. Cell Biol.* 192:189–200. <https://doi.org/10.1083/jcb.201007023>
- Djiane, A., S. Zaessinger, A.B. Babaoğlu, and S.J. Bray. 2014. Notch inhibits Yorkie activity in *Drosophila* wing discs. *PLoS One.* 9:e106211. <https://doi.org/10.1371/journal.pone.0106211>
- Dupont, S., L. Morsut, M. Aragona, E. Enzo, S. Giulitti, M. Cordenonsi, F. Zanconato, J. Le Dégabel, M. Forcato, S. Bicciato, et al. 2011. Role of YAP/TAZ in mechanotransduction. *Nature.* 474:179–183. <https://doi.org/10.1038/nature10137>
- Fernández, B.G., P. Gaspar, C. Brás-Pereira, B. Jezowska, S.R. Rebelo, and F. Janody. 2011. Actin-Capping Protein and the Hippo pathway regulate F-actin and tissue growth in *Drosophila*. *Development.* 138:2337–2346. <https://doi.org/10.1242/dev.063545>
- Fletcher, G.C., A. Elbediwy, I. Khanal, P.S. Ribeiro, N. Tapon, and B.J. Thompson. 2015. The Spectrin cytoskeleton regulates the Hippo signalling pathway. *EMBO J.* 34:940–954. <https://doi.org/10.15252/emboj.201489642>
- Gaspar, P., and N. Tapon. 2014. Sensing the local environment: actin architecture and Hippo signalling. *Curr. Opin. Cell Biol.* 31:74–83. <https://doi.org/10.1016/j.cob.2014.09.003>
- Gates, J., J.P. Mahaffey, S.L. Rogers, M. Emerson, E.M. Rogers, S.L. Sottile, D. Van Vactor, F.B. Gertler, and M. Peifer. 2007. Enabled plays key roles in embryonic epithelial morphogenesis in *Drosophila*. *Development.* 134:2027–2039. <https://doi.org/10.1242/dev.02849>
- Genevet, A., M.C. Wehr, R. Brain, B.J. Thompson, and N. Tapon. 2010. Kibra is a regulator of the Salvador/Warts/Hippo signaling network. *Dev. Cell.* 18:300–308. <https://doi.org/10.1016/j.devcel.2009.12.011>
- Grevengeod, E.E., D.T. Fox, J. Gates, and M. Peifer. 2003. Balancing different types of actin polymerization at distinct sites. *J. Cell Biol.* 163:1267–1279. <https://doi.org/10.1083/jcb.200307026>
- Grzeschik, N.A., L.M. Parsons, M.L. Allott, K.F. Harvey, and H.E. Richardson. 2010. Lgl, aPKC, and Crumbs regulate the Salvador/Warts/Hippo pathway through two distinct mechanisms. *Curr. Biol.* 20:573–581. <https://doi.org/10.1016/j.cub.2010.01.055>
- Halder, G., and R.L. Johnson. 2011. Hippo signaling: growth control and beyond. *Development.* 138:9–22. <https://doi.org/10.1242/dev.045500>
- Hamaratoglu, F., M. Willecke, M. Kango-Singh, R. Nolo, E. Hyun, C. Tao, H. Jafar-Nejad, and G. Halder. 2006. The tumour-suppressor genes NF2/Merlin and Expanded act through Hippo signalling to regulate cell proliferation and apoptosis. *Nat. Cell Biol.* 8:27–36. <https://doi.org/10.1038/ncb1339>
- Harvey, K., and N. Tapon. 2007. The Salvador-Warts-Hippo pathway - an emerging tumour-suppressor network. *Nat. Rev. Cancer.* 7:182–191. <https://doi.org/10.1038/nrc2070>
- Harvey, K.F., C.M. Pfeifer, and I.K. Hariharan. 2003. The *Drosophila* Mst ortholog, hippo, restricts growth and cell proliferation and promotes apoptosis. *Cell.* 114:457–467. [https://doi.org/10.1016/S0092-8674\(03\)00557-9](https://doi.org/10.1016/S0092-8674(03)00557-9)
- Kim, S.Y., M.K. Renihan, and G.L. Boulianne. 2006. Characterization of big bang, a novel gene encoding for PDZ domain-containing proteins that are dynamically expressed throughout *Drosophila* development. *Gene Expr. Patterns.* 6:504–518. <https://doi.org/10.1016/j.modgep.2005.10.009>
- Lee, J.K., E. Brandin, D. Branton, and L.S. Goldstein. 1997. alpha-Spectrin is required for ovarian follicle monolayer integrity in *Drosophila* melanogaster. *Development.* 124:353–362.
- Ling, C., Y. Zheng, F. Yin, J. Yu, J. Huang, Y. Hong, S. Wu, and D. Pan. 2010. The apical transmembrane protein Crumbs functions as a tumor suppressor that regulates Hippo signaling by binding to Expanded. *Proc. Natl. Acad. Sci. USA.* 107:10532–10537. <https://doi.org/10.1073/pnas.1004279107>
- Lucas, E.P., I. Khanal, P. Gaspar, G.C. Fletcher, C. Polesello, N. Tapon, and B.J. Thompson. 2013. The Hippo pathway polarizes the actin cytoskeleton during collective migration of *Drosophila* border cells. *J. Cell Biol.* 201:875–885. <https://doi.org/10.1083/jcb.201210073>
- Maitra, S., R.M. Kulikauskas, H. Gavilan, and R.G. Fehon. 2006. The tumor suppressors Merlin and Expanded function cooperatively to modulate receptor endocytosis and signaling. *Curr. Biol.* 16:702–709. <https://doi.org/10.1016/j.cub.2006.02.063>
- Martin, A.C., M. Kaschube, and E.F. Wieschaus. 2009. Pulsed contractions of an actin-myosin network drive apical constriction. *Nature.* 457:495–499. <https://doi.org/10.1038/nature07522>
- Médina, E., J. Williams, E. Klipfell, D. Zarnescu, G. Thomas, and A. Le Bivic. 2002. Crumbs interacts with moesin and beta(Heavy)-spectrin in the apical membrane skeleton of *Drosophila*. *J. Cell Biol.* 158:941–951. <https://doi.org/10.1083/jcb.200203080>
- Meng, Z., T. Moroishi, and K.-L. Guan. 2016. Mechanisms of Hippo pathway regulation. *Genes Dev.* 30:1–17. <https://doi.org/10.1101/gad.274027.115>
- Ng, B.F., G.K. Selvaraj, C. Santa-Cruz Mateos, I. Grosheva, I. Alvarez-Garcia, M.D. Martín-Bermudo, and I.M. Palacios. 2016. α -Spectrin and integrins act together to regulate actomyosin and columnarization, and to maintain a monolayered follicular epithelium. *Development.* 143:1388–1399. <https://doi.org/10.1242/dev.130070>
- Pellikka, M., G. Tanentzapf, M. Pinto, C. Smith, C.J. McGlade, D.F. Ready, and U. Tepass. 2002. Crumbs, the *Drosophila* homologue of human CRB1/RP12, is essential for photoreceptor morphogenesis. *Nature.* 416:143–149. <https://doi.org/10.1038/nature721>
- Rauskolb, C., S. Sun, G. Sun, Y. Pan, and K.D. Irvine. 2014. Cytoskeletal tension inhibits Hippo signaling through an Ajuba-Warts complex. *Cell.* 158:143–156. <https://doi.org/10.1016/j.cell.2014.05.035>
- Robinson, B.S., J. Huang, Y. Hong, and K.H. Moberg. 2010. Crumbs regulates Salvador/Warts/Hippo signaling in *Drosophila* via the FERM-domain protein Expanded. *Curr. Biol.* 20:582–590. <https://doi.org/10.1016/j.cub.2010.03.019>
- Sansores-Garcia, L., W. Bossuyt, K. Wada, S. Yonemura, C. Tao, H. Sasaki, and G. Halder. 2011. Modulating F-actin organization induces organ growth by affecting the Hippo pathway. *EMBO J.* 30:2325–2335. <https://doi.org/10.1038/emboj.2011.157>
- Schroeder, M.C., and G. Halder. 2012. Regulation of the Hippo pathway by cell architecture and mechanical signals. *Semin. Cell Dev. Biol.* 23:803–811. <https://doi.org/10.1016/j.semcdb.2012.06.001>
- Settleman, J. 2001. Rac 'n Rho: the music that shapes a developing embryo. *Dev. Cell.* 1:321–331. [https://doi.org/10.1016/S1534-5807\(01\)00053-3](https://doi.org/10.1016/S1534-5807(01)00053-3)
- Stabach, P.R., I. Simonović, M.A. Ranieri, M.S. Aboodi, T.A. Steitz, M. Simonović, and J.S. Morrow. 2009. The structure of the ankyrin-binding site of beta-spectrin reveals how tandem spectrin-repeats generate unique ligand-binding properties. *Blood.* 113:5377–5384. <https://doi.org/10.1182/blood-2008-10-184291>
- Thomas, G.H., and D.P. Kiehart. 1994. Beta heavy-spectrin has a restricted tissue and subcellular distribution during *Drosophila* embryogenesis. *Development.* 120:2039–2050.
- Thomas, G.H., and J.A. Williams. 1999. Dynamic rearrangement of the spectrin membrane skeleton during the generation of epithelial polarity in *Drosophila*. *J. Cell Sci.* 112:2843–2852.
- Thomas, G.H., D.C. Zarnescu, A.E. Juedes, M.A. Bales, A. Londergan, C.C. Korte, and D.P. Kiehart. 1998. *Drosophila* betaHeavy-spectrin is essential for development and contributes to specific cell fates in the eye. *Development.* 125:2125–2134.
- Venken, K.J.T., K.L. Schulze, N.A. Haelterman, H. Pan, Y. He, M. Evans-Holm, J.W. Carlson, R.W. Levis, A.C. Spradling, R.A. Hoskins, and H.J. Bellen. 2011. MiMIC: a highly versatile transposon insertion resource for engineering *Drosophila melanogaster* genes. *Nat. Methods.* 8:737–743. <https://doi.org/10.1038/nmeth.1662>
- Vissers, J.H.A., S.A. Manning, A. Kulkarni, and K.F. Harvey. 2016. A *Drosophila* RNAi library modulates Hippo pathway-dependent tissue growth. *Nat. Commun.* 7:10368. <https://doi.org/10.1038/ncomms10368>
- Wong, K.K.L., W. Li, Y. An, Y. Duan, Z. Li, Y. Kang, and Y. Yan. 2015. β -Spectrin regulates the hippo signaling pathway and modulates the basal actin network. *J. Biol. Chem.* 290:6397–6407. <https://doi.org/10.1074/jbc.M114.629493>
- Wu, S., J. Huang, J. Dong, and D. Pan. 2003. hippo encodes a Ste-20 family protein kinase that restricts cell proliferation and promotes apoptosis in conjunction with salvador and warts. *Cell.* 114:445–456. [https://doi.org/10.1016/S0092-8674\(03\)00549-X](https://doi.org/10.1016/S0092-8674(03)00549-X)

- Wu, S., Y. Liu, Y. Zheng, J. Dong, and D. Pan. 2008. The TEAD/TEF family protein Scalloped mediates transcriptional output of the Hippo growth-regulatory pathway. *Dev. Cell.* 14:388–398. <https://doi.org/10.1016/j.devcel.2008.01.007>
- Yin, F., J. Yu, Y. Zheng, Q. Chen, N. Zhang, and D. Pan. 2013. Spatial organization of Hippo signaling at the plasma membrane mediated by the tumor suppressor Merlin/NF2. *Cell.* 154:1342–1355. <https://doi.org/10.1016/j.cell.2013.08.025>
- Yu, F.-X., and K.-L. Guan. 2013. The Hippo pathway: regulators and regulations. *Genes Dev.* 27:355–371. <https://doi.org/10.1101/gad.210773.112>
- Yu, J., Y. Zheng, J. Dong, S. Klusza, W.-M. Deng, and D. Pan. 2010. Kibra functions as a tumor suppressor protein that regulates Hippo signaling in conjunction with Merlin and Expanded. *Dev. Cell.* 18:288–299. <https://doi.org/10.1016/j.devcel.2009.12.012>
- Zarnescu, D.C., and G.H. Thomas. 1999. Apical spectrin is essential for epithelial morphogenesis but not apicobasal polarity in *Drosophila*. *J. Cell Biol.* 146:1075–1086. <https://doi.org/10.1083/jcb.146.5.1075>

Résumé:

Au cours du développement, le comportement des cellules est étroitement régulé, ce qui assure un fonctionnement optimal des tissus épithéliaux sains. Les cellules épithéliales établissent ainsi des jonctions intercellulaires bien organisées, une polarité apico/basale, une architecture de la cytosquelette et intègrent des entrées régulatrices et homéostatiques relayées par des voies de signalisation dédiées. Les altérations de ces processus sont le plus souvent associées au cancer.

Mon laboratoire s'intéresse au décryptage des mécanismes par lesquels les altérations de jonctions et de polarité sont capables d'induire une tumorigenèse. Les protéines d'échafaudage représentent des régulateurs importants de ces différents processus, et les altérations de plusieurs échafaudages épithéliaux clés ont été liées au cancer. Des travaux récents de l'équipe ont identifié Magi, un membre de la famille MAGUK, comme un régulateur des jonctions adhérentes à base d'E-Cadherin pendant le développement de l'œil chez la drosophile. Le but principal de ma thèse était d'étudier la fonction de MAGI1, le membre le plus abondant de la famille MAGI dans les tissus humains, pendant le cancer, et plus spécifiquement ses rôles dans les cellules luminales A du cancer du sein. En utilisant principalement des approches de perte de fonction, nous avons pu identifier une fonction de suppression de tumeur de MAGI1 dans les cellules BCa luminales, aussi bien par des essais cellulaires *in vitro* que sur des souris nues xénotransplantées. De plus, ces travaux ont révélé que MAGI1 inhibe un axe de signalisation AMOTL2/P38 qui est activé lors de la perte de MAGI1 et qui est ensuite responsable du phénotype de tumorigénicité accrue obtenu. Il est intéressant de noter que la perte de MAGI1 a induit une augmentation de l'activité de la myosine, des comportements de compression amplifiés et une tension élevée de la membrane plasmique associée, que nous proposons d'être l'un des activateurs de P38 en aval de la perte de MAGI1. Il est frappant de constater que, même si les cellules dépourvues de MAGI1 présentent une tumorigénicité élevée, l'activité de l'onco-protéine YAP est réduite dans les cellules du cancer du sein luminal dépourvues de MAGI1, ce qui suggère que la relation entre YAP et la tumorigenèse pourrait être plus complexe qu'on ne le pense généralement.

L'étude de la régulation de la voie d'Hippo est en effet un axe majeur de l'équipe. Un objectif secondaire de ma thèse était donc d'explorer l'implication de YAP/TAZ et de la voie Hippo lors de l'exposition à l'oxaliplatine dans les cellules cancéreuses du côlon. En tant que chimiothérapie de première ligne avec le 5 Fluorouracil, il est important de comprendre le mécanisme d'action de l'Oxaliplatine au-delà de son rôle majeur d'inducteur de cassures délétères des doubles brins d'ADN. Les cellules cancéreuses du côlon HCT116 traitées avec des doses relativement modestes d'oxaliplatine (à la IC50) ont présenté une translocation de YAP/TAZ vers le noyau accompagnée d'une augmentation de la transcription médiée par YAP/TAZ, comme en témoignent la RTqPCR et l'ARN-Seq. Cet effet a été couplé à une réorganisation du cytosquelette d'actine à l'intérieur de la cellule lors du traitement, et de nombreux gènes affectés par le traitement à l'oxaliplatine étaient des régulateurs d'actine (dont plusieurs qui sont également des cibles potentielles de YAP/TAZ). Cette étude implique YAP/TAZ dans la réponse HCT116 au traitement à l'oxaliplatine, et nous proposons qu'elle conduise à une réorganisation de l'actine.

Abstract:

During development, the behaviour of cells is tightly regulated ensuring optimal functioning of healthy epithelial tissues. Epithelial cells thus establish well organized intercellular junctions, apico/basal polarity, cytoskeletal architecture, and integrate regulatory and homeostatic inputs relayed by dedicated signalling pathways. Alterations in these processes are most often associated with cancer.

My lab is interested in deciphering the mechanisms in which junctional and polarity alterations are able to induce tumorigenesis. Scaffold proteins represent important regulators of these different processes, and alterations to several key epithelial scaffolds have been linked to cancer. Recent work in the team identified Magi, a member of the MAGUK family, as a regulator of E-Cadherin-based Adherens Junctions during eye development in *Drosophila*. The main goal of my thesis was to study the function of MAGI1, the most abundant MAGI family member in human tissues, during cancer, and more specifically its roles in luminal A Breast Cancer cells. Using mainly loss-of-function approaches, we were able to identify a tumour suppressive function of MAGI1 in luminal BCa cells both *in vitro* cellular assays as well as in xenografted nude mice. Moreover, this work revealed that MAGI1 inhibits an AMOTL2/P38 signalling axis that is activated upon *MAGI1* loss and then responsible for the enhanced tumorigenicity phenotype obtained. Interestingly, the loss of MAGI1 induced increased myosin activity, increased compressive behaviours, and associated elevated plasma membrane tension, which we propose to be one of the activator of P38 downstream of MAGI1 loss. Strikingly, even though cells lacking MAGI1 showed increased tumorigenicity, the activity of the YAP onco-protein is lowered in MAGI1-deficient luminal breast cancer cells, suggesting that the relationship between YAP and tumorigenesis could be more complex than commonly assumed.

The study of Hippo pathway regulations is indeed a major axis of the team. A secondary objective of my thesis was thus to explore the involvement of YAP/TAZ and of the Hippo pathway during Oxaliplatin exposure in colon cancer cells. As first line chemotherapy along with 5 Fluorouracil, it is important to understand the mechanism of action of Oxaliplatin beyond its major role as inducer of deleterious DNA double strand breaks. HCT116 colon cancer cells treated with relatively modest doses of Oxaliplatin (at IC50), featured a translocation of YAP/TAZ to the nucleus accompanied with increased YAP/TAZ-mediated transcription, as judged by qPCR and RNA-Seq. This effect was coupled with a re-organization of the actin cytoskeleton inside the cell upon the treatment, and many genes affected by oxaliplatin treatment were actin regulators (including several that are also potential YAP/TAZ targets). This study involves YAP/TAZ in HCT116 response to Oxaliplatin treatment, and we propose that it leads to actin re-organization.